Empire State Electric
Energy Research Corporation
and
Electric Power
Research Institute

Topics:
Soils
Testing
Foundations
Transmission towers
Transmission lines
Design

EPRI EL-6965
Project 1493-4
Final Report
August 1990

Field Evaluation of Grillage Foundation Uplift Capacity

Prepared by
Cornell University
Ithaca, New York

REPORT SUMMARY

SUBJECTS: Overhead structures and foundations / Overhead transmission

TOPICS: Soils; Testing; Foundations; Transmission towers; Transmission lines; Design

AUDIENCE: Transmission managers and engineers

Field Evaluation of Grillage Foundation Uplift Capacity

This report presents the results of eight comprehensive full-scale field uplift tests on steel grillage foundations. At two field sites in New York, a test of three grillage types produced detailed geotechnical evaluations. Detailed comparisons of capacity and load-displacement behavior with the modern analytic model in the CUFAD code showed good agreement.

BACKGROUND

Although grillages compose a substantial fraction of the in-place foundations for lattice transmission line towers, much of their behavior under load is not known. Before the evolution of modern principles of soil behavior, purely empirical rules governed the design of most grillages. Highway relocations and a severe wind storm created the opportunity to test the foundations of three lattice towers, in place since 1929, 1947, and 1958.

OBJECTIVES

To document field uplift test results on steel grillage foundations, including detailed geotechnical evaluation of the test sites; to evaluate modern analytic models for predicting grillage behavior.

APPROACH

Researchers performed geotechnical characterizations of the sites using a variety of in situ methods, including standard penetration, cone penetration, pressuremeter, borehole shear, drive cone, and dilatometer tests. They also performed laboratory classification and strength tests. Load testing followed the general guidelines given in EPRI report EL-5915 to evaluate both foundation and soil mass response. Modern geotechnical practice governed the interpretation of all test results, including the model in the TLWorkstation™ task module CUFAD code (EPRI report EL-6420, volume 15).

RESULTS

The field test results, for D/B ratios from 1 to 3, indicate side resistance determines roughly 55 to 80% of uplift capacity, whereas soil weight determines 20 to 45%. The overall load test results show that rational predictions of the uplift capacity of grillage foundations can be made. The importance of good geotechnical documentation and the relative importance of geotechnical parameters is illustrated. These results suggest a modest improvement upon existing procedures for evaluating the load-displacement behavior of grillages in granular soils.

EPRI PERSPECTIVE

This report will aid in evaluating the capacity and load-displacement behavior of grillage foundations. The study, cosponsored by ESEERCO, shows conclusively that grillage behavior can be predicted by rational geotechnical methods, such as those in the CUFAD code, instead of empirical rules of thumb. The results also suggest that conservative design methods were probably used for most existing grillage installations. This may eliminate the need for extensive foundation upgrades or replacements to accommodate line upgradings—a significant economic factor for future work. Related work is described in reports EL-2870, *Transmission Line Structure Foundations for Uplift-Compression Loading;* EL-6583-CCML, *CUFAD+TM: Compression/Uplift Foundation Analysis and Design with Expert System Data Advisor;* and EL-6800, *Manual on Estimating Soil Properties for Foundation Design.*

PROJECT

RP1493-4
EPRI Project Manager: Vito J. Longo
Electrical Systems Division
Contractor: Cornell University

For further information on EPRI research programs, call EPRI Technical Information Specialists (415) 855-2411.

Field Evaluation of Grillage Foundation Uplift Capacity

EL-6965
Research Project 1493-4

Final Report, August 1990

Prepared by

CORNELL UNIVERSITY
Geotechnical Engineering Group
Hollister Hall
Ithaca, New York 14853-3501

Authors and Principal Investigators
H. E. Stewart
F. H. Kulhawy

Prepared for

Empire State Electric Energy Research Corporation
1155 Avenue of the Americas
New York, New York 10036

and

Electric Power Research Institute
3412 Hillview Avenue
Palo Alto, California 94304

EPRI Project Manager
V. J. Longo

Overhead Transmission Lines Program
Electrical Systems Division

ORDERING INFORMATION

Requests for copies of this report should be directed to Research Reports Center (RRC), Box 50490, Palo Alto, CA 94303, (415) 965-4081. There is no charge for reports requested by EPRI member utilities and affiliates, U.S. utility associations, U.S. government agencies (federal, state, and local), media, and foreign organizations with which EPRI has an information exchange agreement. On request, RRC will send a catalog of EPRI reports.

NOTICE

Prepared by
Cornell University
Ithaca, New York

ABSTRACT

This study presents the results of eight full-scale field uplift tests on steel grillage foundations. The two field sites where the tests were conducted in New York State are described, along with the three grillage types found at these sites. Structural and construction details of the grillages are given.

Soil characterization of the sites was conducted using a variety of in-situ test methods including the standard penetration, cone penetration, pressuremeter, borehole shear, drive cone, and dilatometer tests. Laboratory classification and strength tests also were performed to aid in the characterizations.

The field testing equipment and the test procedures used for the uplift tests are described. The load-displacement results are given, as well as the ground movements in the zones above the grillages. The vertical shear model reported in EPRI EL-2870 is used to predict the uplift capacities, and comparisons are made with the field measurements.

The vertical shear model, coupled with well-documented geotechnical properties, can be used to predict accurately the uplift capacity of grillage foundations. For grillages in granular soils, the incorporation of side shearing resistance is important. The field test results indicated that, for D/B ratios from 1 to 3, roughly 55 to 80 percent of the uplift capacity is attributable to side resistance, with only 20 to 45 percent of the capacity resulting from soil weight. This result is important when deciding on the allowable loadings that may be imposed from line upgradings and increased tower heights. The use of existing foundations may result in substantial cost savings over new foundations, provided that adequate subsurface exploration and geotechnical data are incorporated into the planning and design stages.

ACKNOWLEDGMENTS

The authors appreciate the assistance of numerous people during the field testing. The Cornell field test crew consisted of K. George, K. L. Gunsallus, M. F. Kleinmann, C. A. Reyes, W. F. Sangrey, and the authors. The in-situ field testing was performed by A. J. Lutenegger, with the support of Buffalo Drilling Company. The rigging for the tests was supplied by Malcon Developers, Inc. The support and participation of all those involved is greatly appreciated. The assistance of P. W. Mayne with the interpretation of the in-situ data is acknowledged, as are the detailed review comments made by Cornell staff members B. Birgisson, P. W. Mayne, and C. H. Trautmann.

Several colleagues graciously responded to a request for review and evaluation of this report. These included: J. I. Adams, Consultant; J. C. Burton, San Diego Gas & Electric; A. M. DiGioia, Jr., GAI Consultants; E. B. Lawless, III, Potomac Electric Power Company; A. J. Lutenegger, University of Massachusetts; F. G. Picciano, New York State Electric & Gas Corporation; F. E. Porretto, ESEERCO; H. S. Radhakrishna, Ontario Hydro; T. E. Rodgers, Jr., Virginia Power; J. W. Rustvold, Bonneville Power Administration; and J. J. Wolf, Western Area Power Administration.

The support of the Empire State Electric Energy Research Corporation (ESEERCO) and the Electric Power Research Institute (EPRI) is appreciated. Special thanks are due to F. G. Picciano from the Transmission Engineering Division of New York State Electric & Gas Corporation (NYSEG) for his encouragement and support.

K. J. Stewart prepared the manuscript and A. Avcisoy drafted the figures with their usual style and attention.

CONTENTS

ILLUSTRATIONS

TABLES

SYMBOLS

ENGLISH LETTERS - UPPER CASE

A - cross-sectional area; DMT reading

A_f - foundation area

B - base width; DMT reading

C_A - correction factor for aging

C_B - correction factor for borehole diameter

C_c - coefficient of curvature

C_{ER} - correction factor for energy ratio

C_N - overburden correction factor

C_{OCR} - correction factor for overconsolidation ratio

COV - coefficient of variation

C_P - correction factor for particle size

C_R - correction factor for rod length

C_S - correction factor for sampling method

C_u - coefficient of uniformity

D - depth

D_{max} - maximum grain size

D_r - relative density

D_{ref} - reference depth

D_{10} - grain size at 10 percent passing

D_{30} - grain size at 30 percent passing

D_{50} - grain size at 50 percent passing

D_{60} - grain size at 60 percent passing

E - Young's modulus

E_b - Young's modulus of backfill

E_D - dilatometer modulus from DMT

E_f - Young's modulus of structural element

E_m - Young's modulus in pseudo-elastic range from PMT

E_r - Young's modulus for unload-reload from PMT

E_{sn} - Young's modulus of native soil

E_t - Young's modulus of backfill-foundation combination

F - uplift load

F_u - uplift capacity factor

G - shear modulus

I_D - material index from DMT

I.D. - inside diameter

I_r - soil rigidity index

K - operative horizontal stress

K_a - coefficient of minimum active soil stress

K_b - horizontal stress coefficient developed by backfilling

K_e - horizontal stress coefficient developed from excavation

K_D - horizontal stress index from DMT

K_o - coefficient of horizontal soil stress

K_{onc} - K_o for normally consolidated soil

K_p - coefficient of maximum passive soil stress

L - length

M - constrained modulus

N - blow count or measured SPT value

NC - normally consolidated

N_q - bearing capacity factor

N_{60} - corrected N value for 60 percent efficiency

$(N_1)_{60}$ - corrected N value to one atmospheric pressure

OCR - overconsolidation ratio

OCR_{max} - maximum overconsolidation ratio

O.D. - outside diameter

P - foundation perimeter

PI - plasticity index

Q - load

Q_{su} - side resistance in uplift

Q_{tu} - tip resistance in uplift

Q_u - interpreted failure load in uplift

Q_u^* - computed failure load in uplift at other K/K_o value

Q_{um} - maximum load in uplift

Q_u (measured) - measured interpreted failure load in uplift

RC - relative compaction

R_Q - ratio of computed to measured uplift load

S_r - saturation

W - weight

W_f - weight of foundation

$\bar{W}_f$ - effective weight of foundation

W_{ref} - reference weight

W_u - uplift weight factor

Z_m - gage deviation from DMT

ENGLISH LETTERS - LOWER CASE

a - hyperbolic curve constant

b - hyperbolic curve constant

n - number of observations

$\bar{p}$ - mean effective stress

p_a - atmospheric pressure

p_c - transition stress

$\bar{p}_f$ - mean effective stress at failure

p_ℓ - limit stress

p_o - expansion stress from PMT

$p_{o,1}$ - stress readings from DMT

$\bar{p}_o$ - initial mean effective stress

q - one-half of deviator stress

q_c - cone tip resistance from CPT

$\bar{q}_{i,q}$ - effective surcharge

s - geometric standard deviation

t_α - one-sided Student's t distribution

u_o - initial pore water pressure

w - water content

w_L - liquid limit

w_P - plastic limit

z - displacement

z_f - displacement at interpreted failure load

z_{50} - displacement at one-half interpreted failure load

GREEK LETTERS

α - Mohr-Coulomb parameter in p-q space

α_1 - hyperbolic curve constant

β - reduced lateral stress

β_1 - hyperbolic curve constant

γ - unit weight

$\bar{\gamma}$ - effective unit weight

γ_d - dry unit weight

γ_{dmax} - maximum dry unit weight

$\bar{\gamma}_{ref}$ - reference unit weight

γ_t - total unit weight

γ_w - unit weight of water

ΔA - calibration reading from DMT

ΔB - calibration reading from DMT

ΔK - change in horizontal soil stress coefficient

δ - interface/soil friction angle

δ_h - hub vertical displacement

δ_s - stub vertical displacement

ϵ_a - axial strain

ϵ_f - axial strain at failure

ϵ_s - steel stub strain

ζ_{qd} - modification factor for anchor depth

ζ_{qr} - modification factor for soil rigidity

ζ_{qs} - modification factor for anchor shape

θ - stub inclination angle

ν - Poisson's ratio

σ - standard deviation or normal stress

$\bar{\sigma}_c$ - effective confining stress

$\bar{\sigma}_{hb}$ - backfill horizontal stress

$\bar{\sigma}_{hn}$ - native soil horizontal stress

$\bar{\sigma}_{ho}$ - horizontal effective stress

$\bar{\sigma}_v$ - vertical effective stress

$\bar{\sigma}_{vo}$ - initial vertical effective stress

σ_1 - major principal stress

σ_3 - minor principal stress

$\bar{\sigma}_1$ - effective major principal stress

$\bar{\sigma}_3$ - effective minor principal stress

τ - shear stress

$\bar{\phi}$ - friction angle

ϕ_{rel} - relative friction angle

$\bar{\phi}_{sp}$ - secant friction angle

Section 1

INTRODUCTION

Grillage foundations have been used extensively since the early 1900s for electrical transmission line structures. In the United States and elsewhere, grillages have been and are used most commonly as foundations for lattice steel towers.

However, full-scale field test data on these foundation types are limited in both number and documentation (e.g., 1). The overwhelming majority of the available tests have been conducted to answer specific design and construction questions for a particular line construction, and therefore detailed geotechnical, construction, and performance measurements were not obtained. Unfortunately, without these field measurements, general verification of analysis and design methods is not possible.

In this study, the results of eight full-scale field uplift tests are presented for three sizes of grillage foundations, tested at two sites in New York State. The sites were evaluated in detail using a variety of in-situ testing methods and laboratory testing of field samples. The uplift tests were documented extensively, and these test results are presented herein. This study was co-funded by the Empire State Electric Energy Research Corporation (ESEERCO) and the Electric Power Research Institute (EPRI).

SCOPE OF STUDY

This research study included testing of several types of grillage foundations commonly used in New York State and elsewhere to determine their uplift capacities and load-displacement responses. In-situ and laboratory soil tests were made to determine the physical states of both the native and backfill materials at each grillage site. The results of these tests were used to identify the effect of soil type and properties on the grillage capacities. The results of eight full-scale uplift tests, the identification of the in-situ soil conditions, and the results of in-situ and laboratory soil tests were used to evaluate recommended methods used to evaluate uplift behavior (2, 3, 4).

The grillages tested were of varying dimensions and depths. Two types of grillage foundations were located near the New York State Electric & Gas Corporation (NYSEG) Hickling Generating Station, east of Corning in Big Flats, NY. At this site, there were two tower foundation systems left in place following a highway relocation project. Each tower system had four individual grillage foundations. The towers at these sites included a Lehigh dead-end structure and a BA dead-end American Bridge Company tower. The Lehigh tower was installed in 1947, while the BA tower was installed in 1958.

The second test site was north of the village of Chemung, NY, southeast of Elmira, NY. A windstorm during a tornado in 1983 sheared all 32 bolts on the leg splices at the top of the 10 ft (3.05 m) leg extensions on a Lehigh X-tower supporting a double circuit 115 kV tangent line. This tower was installed in 1929. The leg extensions, stub angles, and grillages were left in place. There was, however, no visual evidence of foundation displacements prior to conducting the field tests.

The results of the eight field load tests and the in-situ geotechnical investigations, as well as detailed analyses of the test results, are presented in this report.

ORGANIZATION OF REPORT

The methods used to conduct the field tests and analyze the results are presented in this report. General descriptions of the two grillage sites and structural details of the three grillage types are presented in Section 2. The results of in-situ field tests performed at the sites, along with interpretation of the derived properties, are given in Section 3. Soil samples recovered from the sites were tested in the laboratory for basic index properties and strengths. The results of these laboratory tests are summarized in Section 4. The field test equipment and procedures used are presented in Section 5. Section 6 evaluates the uplift test results in terms of load-displacement response, ground surface movements, and an interpretation of maximum loads and displacements. Section 7 presents comparisons between the measured field test results and results obtained using the vertical shear model given in EPRI EL-2870 (2). Section 8 summarizes and concludes this study. Appendices A through D report the in-situ measurements, load-displacement data, ground movement data, and photographs of the testing program. Unit conversions are given in Appendix E.

REFERENCES

1. Kulhawy, F. H., O'Rourke, T. D., Stewart, J. P., and Beech, J. F., "Transmission Line Structure Foundations for Uplift-Compression Loading: Load Test Summaries", Report EL-3160, Electric Power Research Institute, Palo Alto, June 1983, 729 p.

2. Kulhawy, F. H., Trautmann, C. H., Beech, J. F., O'Rourke, T. D., McGuire, W., Wood, W. A., and Capano, C., "Transmission Line Structure Foundations for Uplift-Compression Loading", Report EL-2870, Electric Power Research Institute, Palo Alto, Feb. 1983, 412 p.

3. Kulhawy, F. H., Trautmann, C. H., and Nicolaides, C. N., "Spread Foundations in Uplift: Experimental Study", Foundations for Transmission Line Towers (GSP 8), Ed. J. L. Briaud, ASCE, New York, Apr. 1987, pp. 96-109.

4. Trautmann, C. H. and Kulhawy, F. H., "Uplift Load-Displacement Behavior of Spread Foundations", Journal of Geotechnical Engineering (ASCE), Vol. 114, No. 2, Feb. 1988, pp. 168-184.

Section 2

SITE DESCRIPTIONS

Two geographical locations were included in the field testing. Both are in New York State, as shown in Figure 2-1, within the service area of the New York State Electric & Gas Corporation (NYSEG). This section describes the two test sites and the structural details of the grillages present at these sites.

HICKLING STATION SITE

The Hickling Station site is located in Steuben County, a few miles east of Corning, NY, as shown in Figure 2-1. In 1983, a highway relocation program was initiated for portions of New York State Route 17, which passes by the Hickling Generating Station. This relocation required the removal of several steel lattice towers and their replacement with single steel poles to support the conductors over a higher embankment for the new highway. Figure 2-2 shows the Hickling Station sites, including the locations of the steel lattice towers that were removed and the new structures that were used as replacements. Two types of towers were removed, leaving two sets of grillage foundations in place. These foundations are referred to as grillage sets No. 4 and No. 84.

Grillage Set No. 4

The grillages used with structure No. 4 at the Hickling Station site were installed in December, 1958. The tower types are referred to as "BA" towers, and they were designed by the American Bridge Division of United States Steel Corporation. During field testing, W. G. Armstrong, the original construction superintendent for NYSEG at the time the steel tower was erected, visited the site. He recalled that the grillages were installed just prior to Christmas, 1958. The typical installation procedure for these grillage types consisted of stripping the topsoil and making a 10 ft x 10 ft (3.05 m x 3.05 m) surface plan excavation that tapered downward to the neat footing dimension at the bottom of the excavation. No problems with excavation support were encountered, and no water was found during installation. The tower stubs had to be timbered for support during installation. The foundation was backfilled a foot or so above each

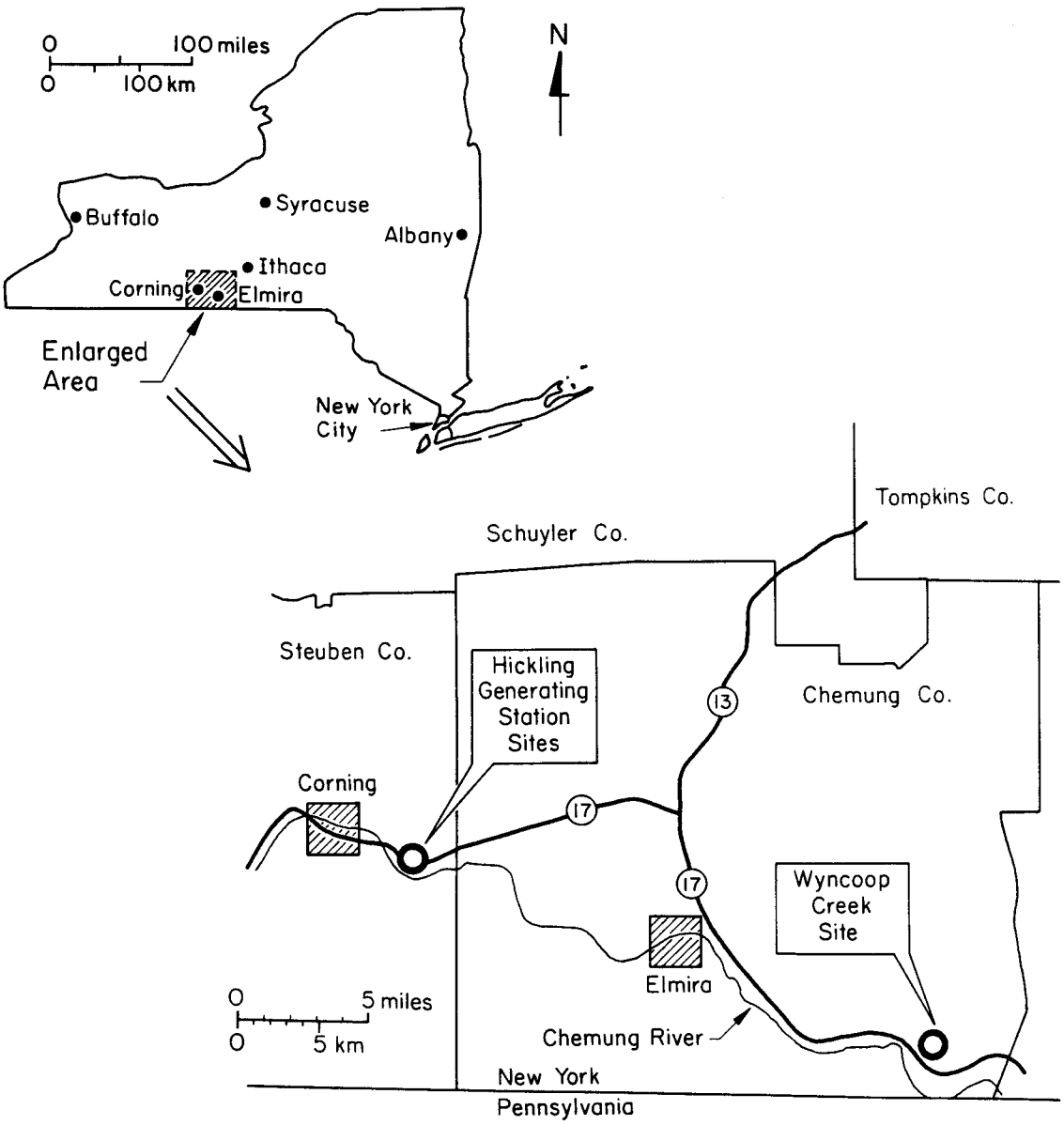

Figure 2-1. Grillage Field Test Locations

grillage base, and then the first steel lift was placed to stabilize all the grillages. The excavated, native, coarse granular soil was used as backfill. A "pogo" compactor was used only around the grillage itself. No tests were done following compaction to evaluate the effectiveness of this compactor. At the time, W. G. Armstrong reported that a typical production rate for this type of tower was about two complete towers per week on flat ground and one tower per

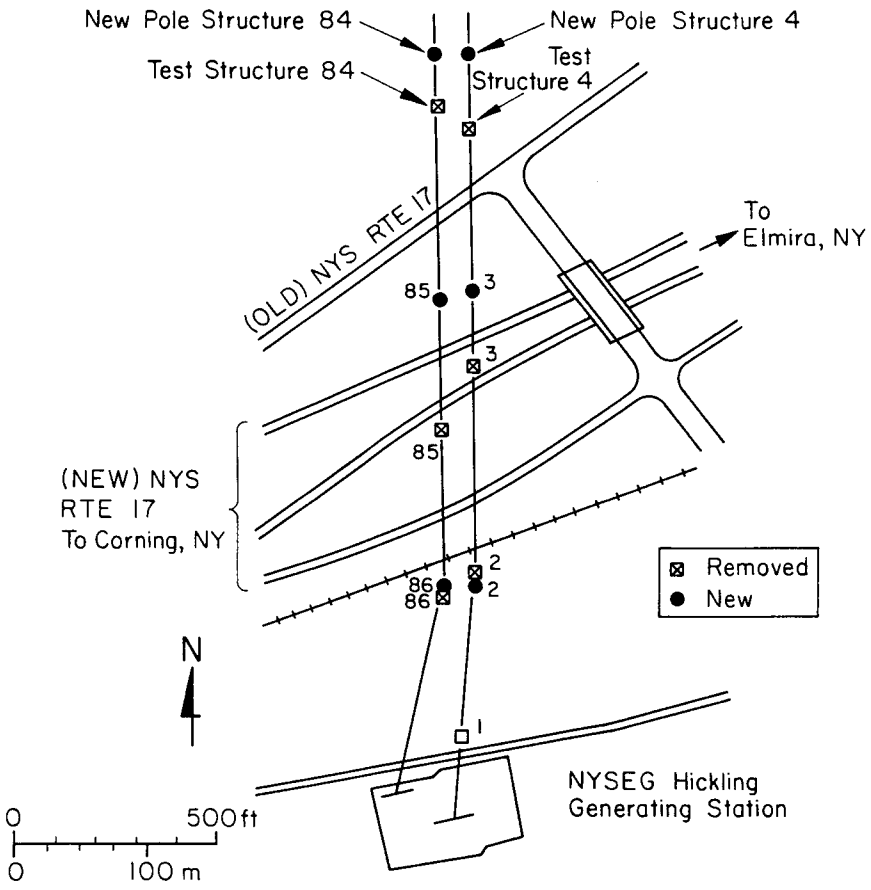

Figure 2-2. Hickling Station Sites

two weeks on the adjacent hills.

Figure 2-3 shows details of the galvanized steel members used for the grillages. Figure 2-3a shows the stub sections, consisting of 8 in. x 8 in. x 1/2 in. (203 mm x 203 mm x 12.7 mm) angles having a total length of 13.9 ft (4.24 m). The base sections of the grillages had overall dimensions of 4.75 ft x 5 ft (1.45 m x 1.52 m), as shown in Figure 2-3b. Additional steel sections, shown in Figure 2-3c, were used to connect the stub to the base of the grillage. Figure 2-3d shows the central portion of the base and the connection arrangements for the components. The inclinations from vertical of the stubs toward the towers was approximately 12 degrees.

The nominal embedment from ground line to the foundation base was 11 ft (3.35 m), with approximately 2.8 ft (0.87 m) of the stub exposed above the ground

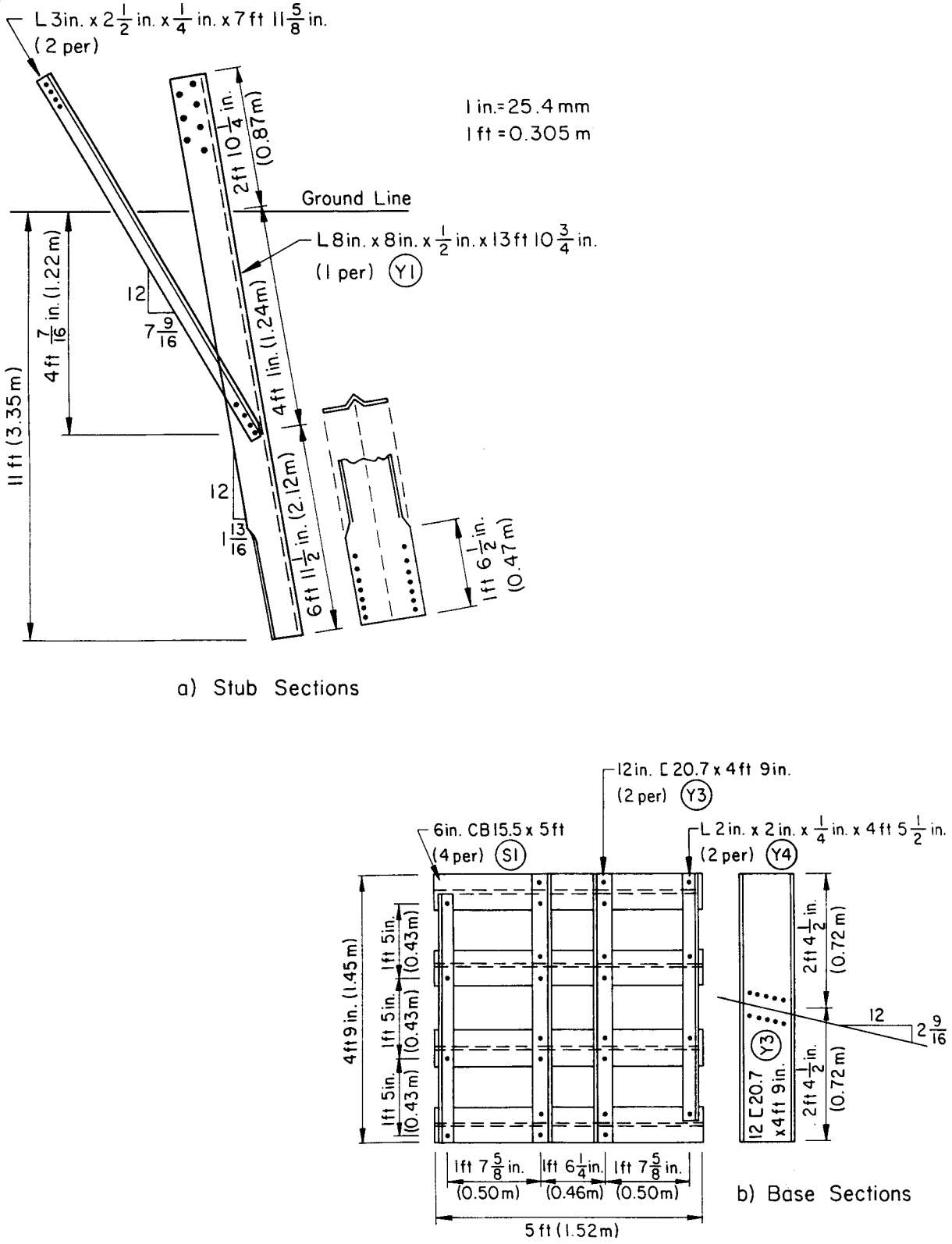

Figure 2-3. Structural Details of Hickling Station No. 4 (BA) Grillages

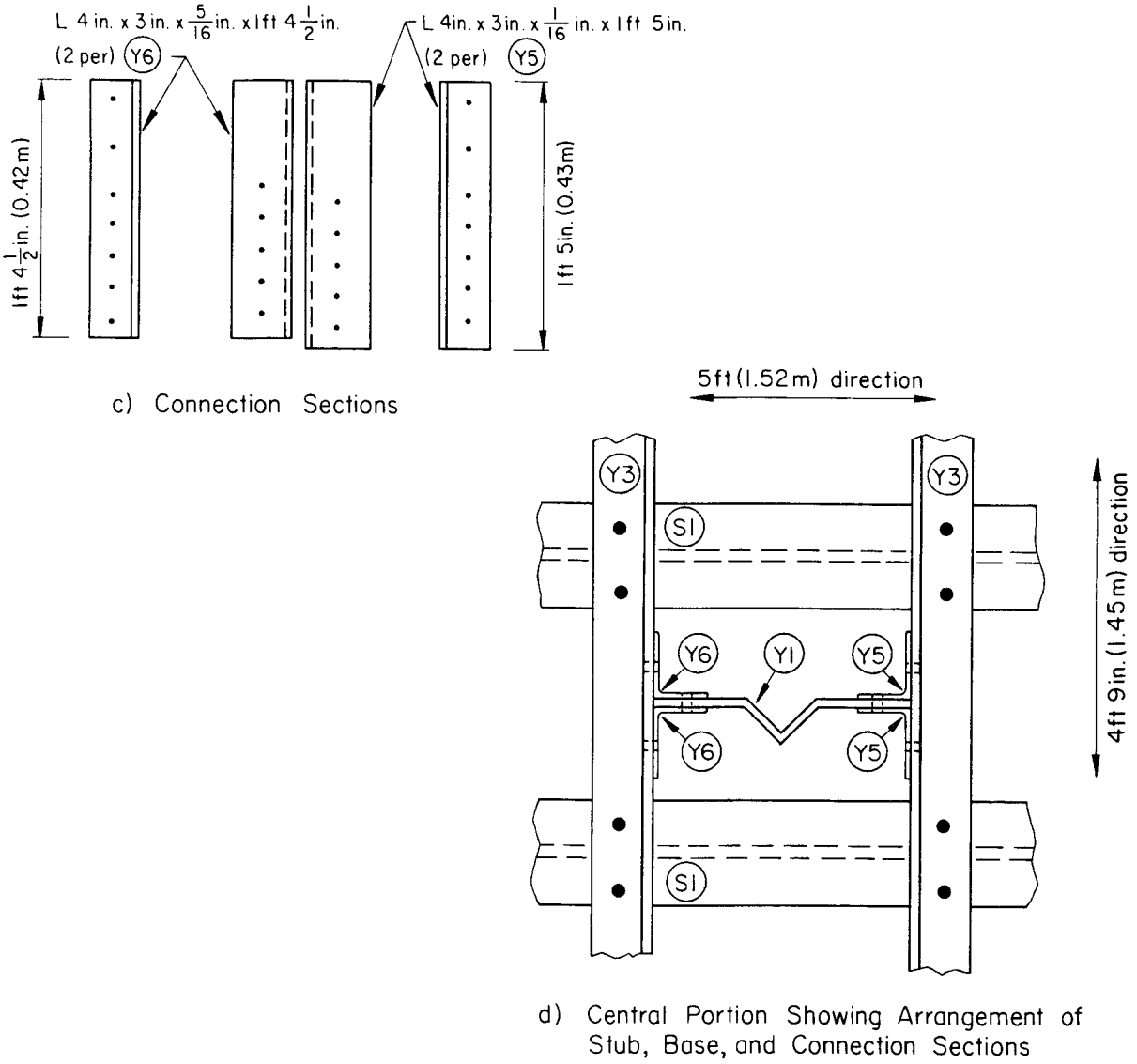

Figure 2-3. Structural Details of Hickling Station No. 4 (BA) Grillages (Continued)

line. Field measurements at the site verified the dimensions shown in Figure 2-3.

Figure 2-4 shows a plan view of the No. 4 (BA) grillages at Hickling Station and the coding assigned to each grillage. As shown, the centers of the foundation bases were offset 2.3 ft (0.70 m) from the ground line stub positions because of the stub angles. The separation distances at the adjacent foundation bases were approximately 25.3 ft (7.71 m), with 22 ft (6.71 m) between adjacent stub angles

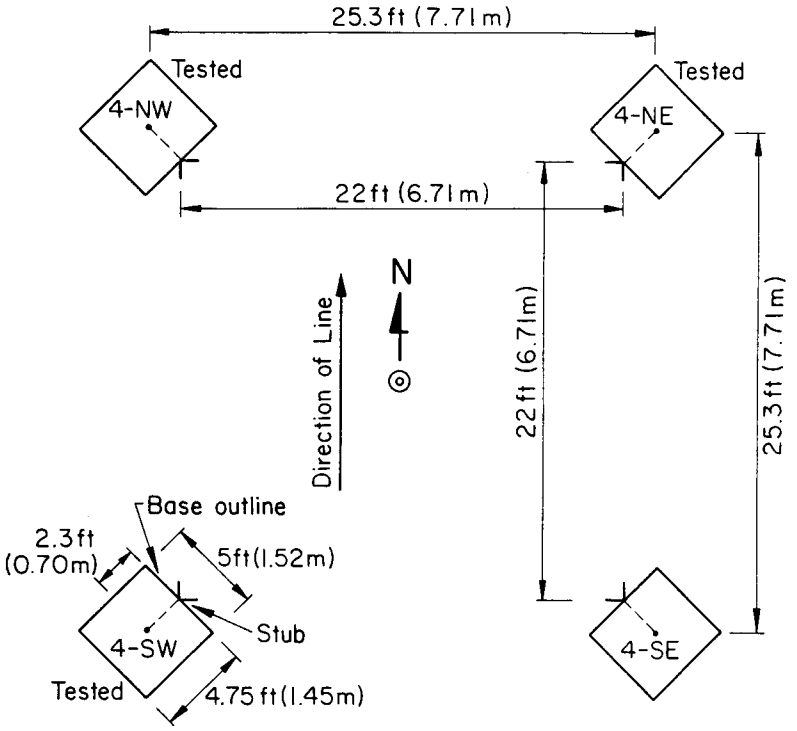

Figure 2-4. Plan View of Hickling Station No. 4 (BA) Grillages

at the ground line. Three of these grillages were tested, as noted on the figure.

Grillage Set No. 84

The locations of the No. 84 grillages at Hickling Station also are shown on Figure 2-2. The No. 84 structures were designed and fabricated in 1947 by the Lehigh Structural Steel Company.

Figure 2-5 shows details of the galvanized steel members used for the No. 84 grillages. Figure 2-5a shows the stub and stabilizing sections. The stubs were 6 in. x 6 in. x 5/8 in. (152 x 152 x 15.9 mm) angle sections having a total length of 10.2 ft (3.11 m). Prior to field testing, approximately 1.2 ft (0.4 m) of the stub was exposed above the ground line. Near the top of the stub, two 5 in. x 3-1/2 in. x 5/16 in. x 4 ft (127 mm x 89 mm x 7.9 mm x 1.22 m) stabilizing angles were attached. The grillage base sections, shown in Figure 2-5b, had plan dimensions of 7 ft x 7 ft (2.1 x 2.1 m), with a nominal embedment of 9.5 ft (2.9 m). The connection arrangement is shown in Figure 2-5c. Depending on the

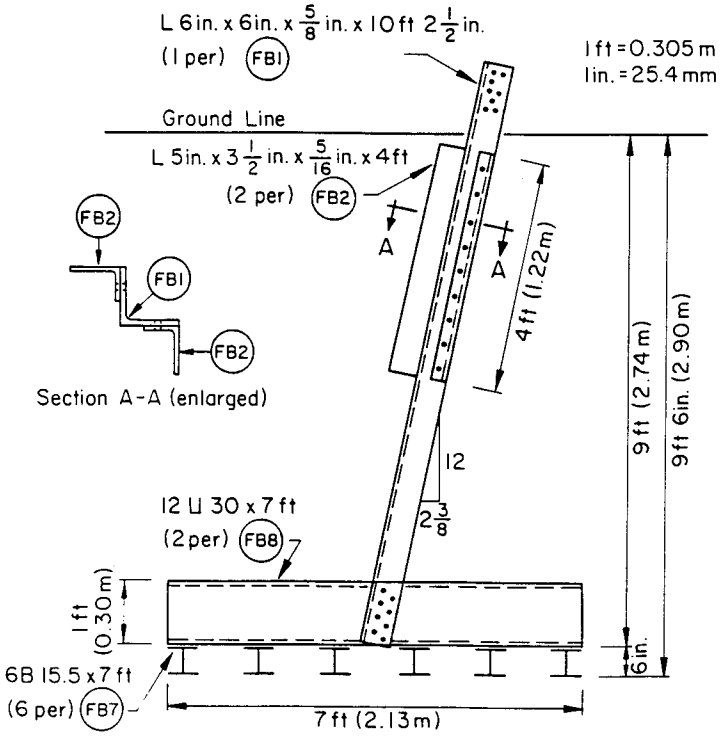

a) General Section

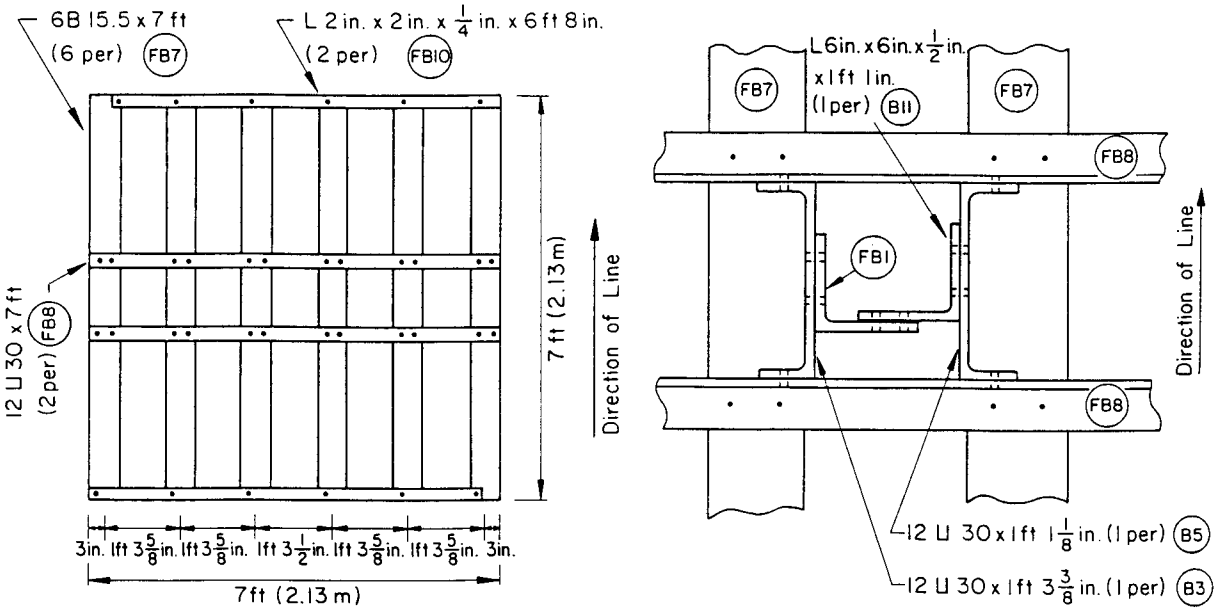

b) Base

c) Central Portion Showing Arrangement of Stub, Base, and Connection

Figure 2-5. Structural Details of Hickling Station No. 84 (Lehigh) Grillages

particular grillage, the stub was connected to opposite sides of the base, on the side farther away from the transmission line. The inclination from vertical of the stub toward center of the tower was approximately 15 degrees. This angle accounts for the orientation of the grillage footprint relative to the center of the tower and the stub inclination relative to both sides of the grillage.

Figure 2-6 shows a plan view of the No. 84 (Lehigh) grillages at Hickling Station and the coding assigned to each grillage. As shown, the position of the stub at the ground line was offset 2.5 ft (0.76 m) from the base, 9.5 ft (2.9 m) below the ground because of the stub inclination. The center-to-center spacing of the square grillages was 30.2 ft (9.2 m) at the base elevation. The stub spacing at the ground line was 26.7 ft (8.13 m). Three of these grillages were tested, as noted on the figure.

WYNCOOP CREEK SITE

The Wyncoop Creek site is located in Chemung County approximately 10 mi (16 km) southeast of Elmira, NY, as shown on Figure 2-1. Figure 2-7 shows that the test

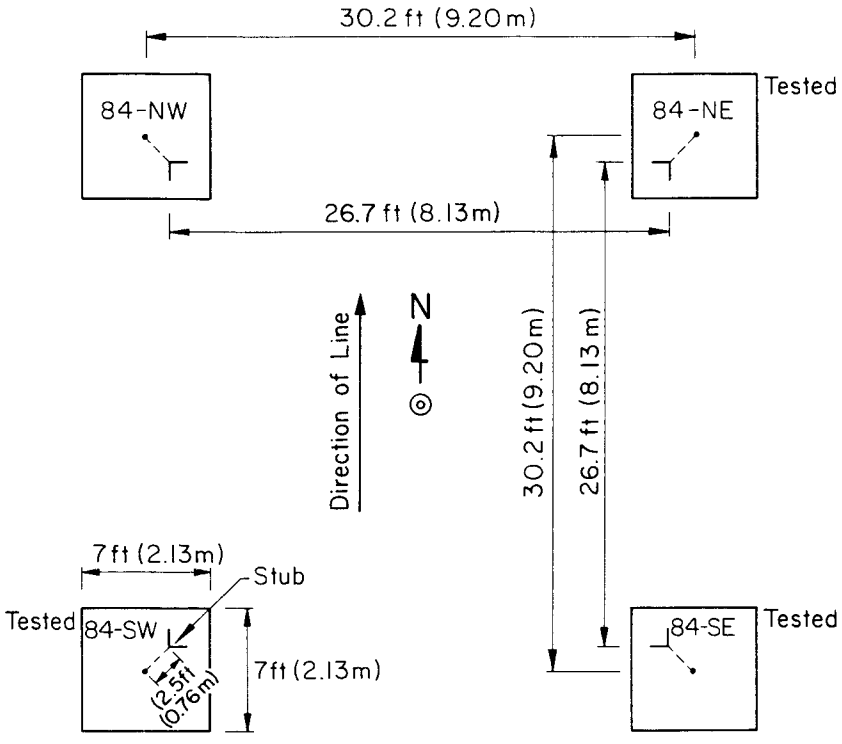

Figure 2-6. Plan View of Hickling Station No. 84 (Lehigh) Grillages

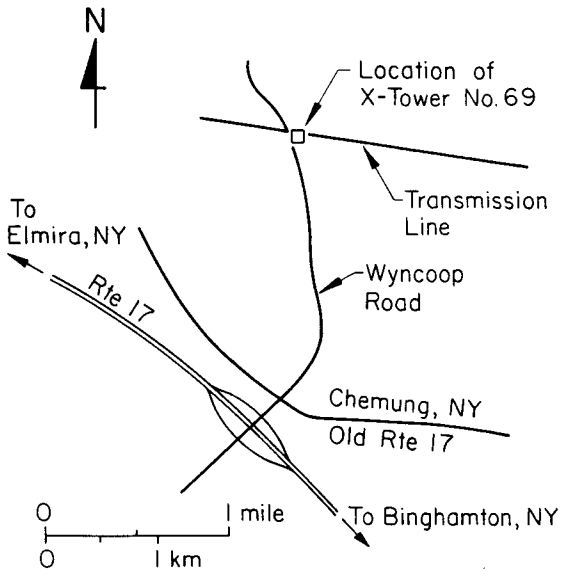

Figure 2-7. Wyncoop Creek Site

site is approximately 2 mi (3.2 km) north of the village of Chemung, NY, on Wyncoop Creek Road. The tower was located just off the top of slope of a small creek bed.

The X-type steel lattice tower was designed by the Lehigh Structural Steel Company in 1927 and installed in 1929. In 1983, a windstorm knocked down the upper portion of Tower 69, leaving the lower 10 ft (3.05 m) of the steel tower and the foundations intact. Prior to field testing, the remaining steel sections were removed, leaving the stub angles exposed above the ground line.

Figure 2-8 shows details of the structural members used to fabricate the X-tower grillage stub and base sections. The stub sections, shown in Figure 2-8a, consisted of 5 in. x 5 in. x 5/16 in. x 8 ft 2-1/2 in. (127 mm x 127 mm x 7.9 mm x 2.5 m) galvanized steel. Near the top of the stubs, two 4 in. x 3 in. x 1/4 in. x 4 ft 6 in. (102 mm x 76 mm x 6.4 mm x 1.37 m) angles were attached for additional lateral soil reaction. The grillage base sections, shown in Figure 2-8b, consisted of four light Z sections. As shown in Figure 2-8b, the grillage bases were H-shaped, with two 3 Z 6.7 x 3 ft (0.91 m) sections along the edges parallel to the line direction. The center portion of the bases was made from two 5 Z 11.6 x 2 ft 6 in. (0.76 m) sections with a center-to-center spacing of 8 in. (203 mm). The stub connections to the bases were made by bolting the stubs to a

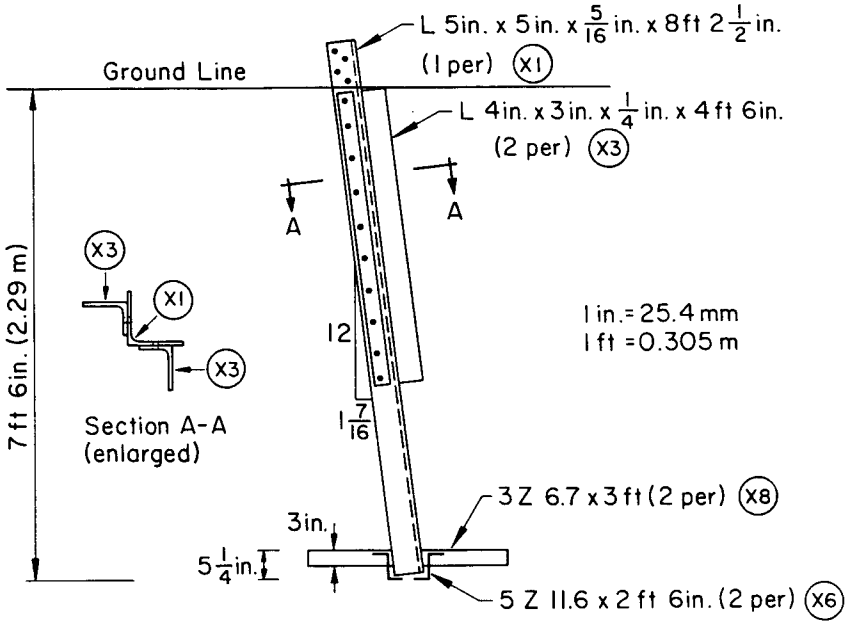

a) General Section

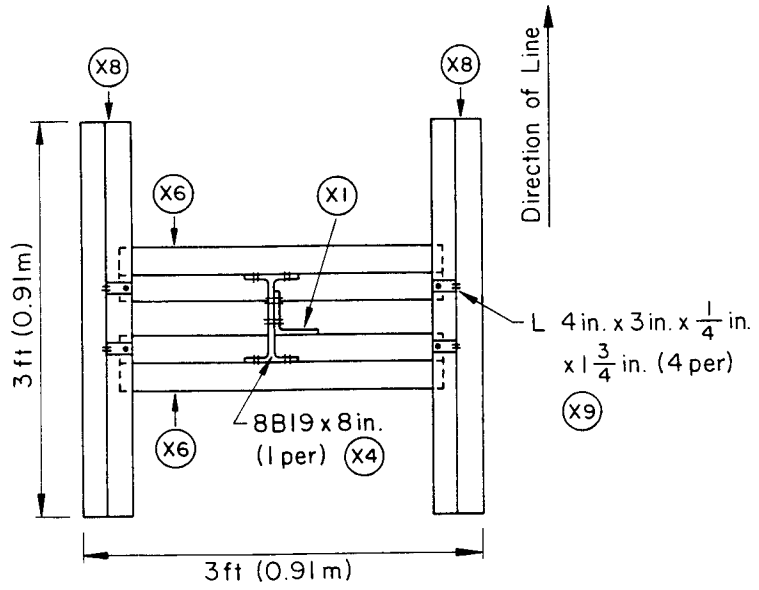

b) Base and Connection

Figure 2-8. Structural Details of Wyncoop Creek X-Tower (Lehigh) Grillages

small 8 B 19 x 8 in. (203 mm) steel member. The stubs were connected to the bases on the cross-member farther away from the tower center. The two-way inclination from vertical of the stub toward center of the tower was approximately 10 degrees. This angle accounts for the orientation of the grillage

footprint relative to the center of the tower and the stub inclination relative to both sides of the grillage.

The X-tower grillages at Wyncoop Creek had nominal embedments of 7.5 ft (2.29 m) from the ground line. For analysis purposes, the bases were taken as having a 3 ft (0.91 m) square footprint.

Figure 2-9 shows a plan view of the X-tower foundations at Wyncoop Creek. As shown, the stub at the ground line was offset 1.3 ft (0.40 m) from the base, 7.5 ft (2.29 m) below the ground, because of the stub inclination. Figure 2-9 also shows the coding of each grillage. The separation distances for foundation bases parallel to the transmission lines were 19.6 ft (5.97 m), with 17.8 ft (5.41 m) between the stub angles at the ground line. The grillage bases perpendicular to the transmission line were spaced more widely than the bases parallel to the line. The spacings between the bases perpendicular to the line were 20.1 ft (6.13 m), with 18.3 ft (5.57 m) separating the stub angles at the ground line. Two of these grillages were tested, as noted on the figure.

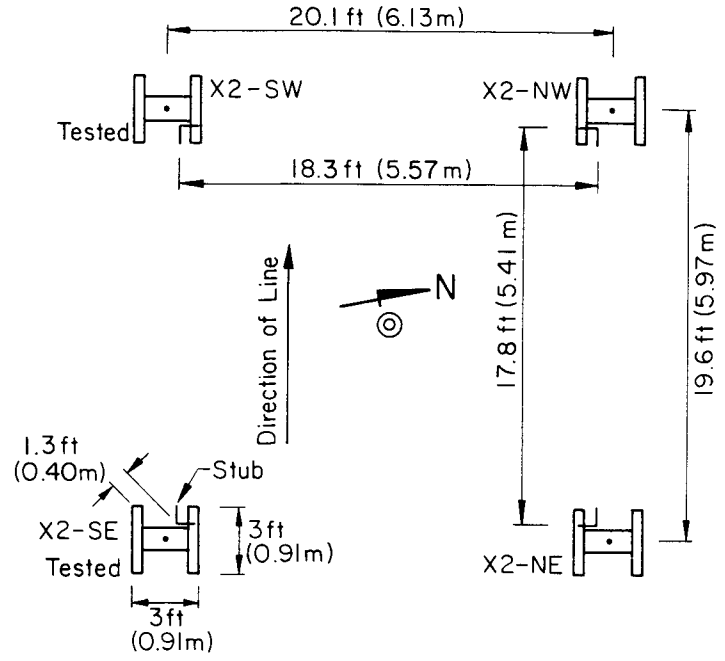

Figure 2-9. Plan View of Wyncoop Creek X-Tower (Lehigh) Grillages

CONDITION OF TEST GRILLAGES

Following the uplift tests, one of each grillage type was excavated to verify the structural details and to investigate the physical conditions of the grillages. All three grillage types were in excellent condition, with no noticeable structural distress. Minor surface corrosion was present, but there was no deep pitting or severely corroded areas. The bolts in the grillage bases could be loosened readily using sockets and adjustable wrenches. The galvanization between the separately bolted elements and on the bolts beneath the ground line was as clean as the galvanization above the ground line. Examples are shown in Appendix D.

SUMMARY

Two geographical locations within New York State were included in the full-scale field testing. These sites contained grillage foundations from towers that were no longer in service, resulting from line relocations and storm damage. The two test sites, Hickling Station and Wyncoop Creek, had three types of grillage foundations. Table 2-1 summarizes the main geometric data from the test grillages. Structural details of the steel sections were described in this section.

Table 2-1

SUMMARY OF GRILLAGE NUMBER AND GEOMETRIC DATA FOR ALL TEST SITES

Test Site and Structure	Grillage Number	Nominal Dimensions, ft (m)		D/B[a]
		Base, B	Depth, D	
Hickling Station, BA No. 4	4-NE 4-NW 4-SW	4.75 x 5 (1.45 x 1.52)	11.0 (3.35)	2.26
Hickling Station, Lehigh No. 84	84-NE 84-SE 84-SW	7 x 7 (2.13 x 2.13)	9.5 (2.90)	1.36
Wyncoop Creek, Lehigh X-Tower	X2-SE X2-SW	3 x 3 (0.91 x 0.91)	7.5 (2.29)	2.50

a - average D/B

Section 3

SUBSURFACE INVESTIGATION

This section contains the results of field investigations at the grillage test sites. Buffalo Drilling Company conducted the standard penetration tests (SPT) and provided the general drilling support, and A. J. Lutenegger of Clarkson University (now at the University of Massachusetts) performed a variety of specialized in-situ tests. All testing was performed under the supervision of the authors.

Prior to the in-situ testing, it was anticipated that difficulties might be encountered, because preliminary test borings indicated that granular soils were present with maximum particle sizes approaching 6 in. (150 mm) in diameter. This material size can present problems for in-situ tests. Therefore, a number of test techniques were attempted, including the standard penetration test (SPT), quasi-static cone penetration test (CPT), Menard pressuremeter test (PMT), borehole shear test (BST), flat-plate dilatometer test (DMT), and drive cone (dynamic cone penetration) test (DCT). A summary of the tests conducted at both sites is given in Table 3-1. Only the SPT and DCT could be conducted at the Wyncoop Creek site, because materials encountered at the site had particle dimensions greater than 12 in. (300 mm). Therefore, sophisticated testing could not be performed at this site.

TESTING PROCEDURES

Descriptions of the equipment, test procedures, advantages, and disadvantages of most of the tests done at the field sites are given elswhere (e.g., 1). Summaries are given below.

Standard Penetration Test (SPT)

The standard penetration tests were conducted in accordance with ASTM D1586 (2). Test borings were advanced using 3.75 in. (95 mm) I.D. augers, without the use of drilling mud or water. A standard 2 in. (51 mm) O.D. split spoon sampler, without liner, was driven for a distance of 24 in. (610 mm), with a safety

Table 3-1

SUMMARY OF IN-SITU TESTING

Site	Test Type	Number of Profiles
Hickling Station	SPT	12
	CPT	14
	PMT	8
	BST	4
	DCT	8
	DMT	3
Wyncoop Creek	SPT	4
	DCT	3

hammer and AW rods. The penetration resistances from driving the spoon with a 140 lb (63.6 kg) hammer were recorded at 6 in. (152 mm) intervals. The blow count was taken as the combined resistance over the 6 to 18 in. (152 to 457 mm) penetration range.

Cone Penetration Test (CPT)

An electric cone penetrometer was used to obtain the cone tip resistances, q_c, at 6 in. (152 mm) intervals. Testing procedures were in accordance with ASTM D3441 (3), using a 60° apex cone with a projected tip area of 1.56 in.^{2} (10 cm^2). A threaded connector adapted the cone thread to standard AW drilling rods, and a push rate of 0.8 in./sec (20 mm/sec) was employed.

Pressuremeter Test (PMT)

Menard pressuremeter tests were conducted in general conformance with ASTM Subcommittee D18.02.07 recommendations (4). A 3 in. (76 mm) diameter, NX-type GA three-cell probe was used, with an outer metallic sheath to protect the inner membrane from rupture. The test holes were made by driving a 3 in. (76 mm) O.D.

diameter split spoon sampler to the desired depth using a 140 lb (63.6 kg) hammer, as recommended by Briaud and Gambin (5).

Borehole Shear Test (BST)

Borehole shear tests were conducted using the procedures recommended by ASTM Subcommittee D18.02.12 (6). The BSTs were done in cavities made by advancing a 3 in. (76 mm) thin-walled sampler through a hollow-stem auger. Multiple stage testing (Method A) procedures were used, along with standard 5 $in.^2$ (32.3 cm^2) shear plates.

Drive Cone Test (DCT)

Drive cone tests were conducted at a number of locations at each site. A 2.25 in. (57 mm) diameter, 60° apex steel cone was attached to the bottom of AW rods and driven continuously into the ground using a 140 lb (63.6 kg) safety hammer. The number of hammer blows required to drive the cone 6 in. (152 mm) was recorded. These values then were added to give the blow counts over a 1 ft (0.3 m) distance.

Dilatometer Test (DMT)

Flat-plate dilatometer tests (7) were conducted according to the recommendations of ASTM Subcommittee D18.02.10 (8). Very few DMTs were conducted because of the gravelly nature of the soils. When testing was done, measurements were made at 1 ft (0.3 m) intervals.

HICKLING STATION TESTS

The in-situ tests at Hickling Station are divided into several subsets. The major division is between tests done inside and outside the backfilled soil zone. Where appropriate, summary figures and tables are given in the text, while more complete support data or original boring logs are given in Appendix A.

Test Locations

Table 3-2 lists the tests done at the Hickling Station site. The locations for the in-situ tests at grillage set No. 4 are shown in Figure 3-1. In this figure, the position of the stub angle is shown at ground surface elevation. The grillage dimensions at the base of the foundation are shown offset from the stub positions. The limits of the excavations at the ground surface made when

Table 3-2

IN-SITU TESTS AT HICKLING STATION

Test Type	Grillage	Test No.	Location
SPT	4-NE	SPT-1	Inside
	4-NW	SPT-1	Outside
	4-NW	SPT-2	Inside
	4-SE	SPT-1	Outside
	4-SE	SPT-2	Inside
	4-SW	SPT-1	Inside
	84-NE	SPT-1	Outside
	84-NE	SPT-2	Inside
	84-NW	SPT-1	Inside
	84-SE	SPT-1	Inside
	84-SW	SPT-1	Outside
	84-SW	SPT-2	Inside
CPT	4-NW	CPT-1	Inside
	4-NW	CPT-2	Outside
	4-SE	CPT-1,2	Inside
	4-SE	CPT-3,4	Inside
	84-NE	CPT-1,2	Inside
	84-NE	CPT-3,4	Outside
	84-SW	CPT-1,2,3	Inside
	84-SW	CPT-4	Outside
PMT	4-NW	PMT-1	Inside
	4-NW	PMT-2	Outside
	4-SE	PMT-1	Inside
	4-SE	PMT-2	Outside
	84-NE	PMT-1	Inside
	84-NE	PMT-2	Outside
	84-SW	PMT-1	Inside
	84-SW	PMT-2	Outside
BST	4-NW	BST-1,2,3,4	Outside
	4-SE	BST-1,2,3	Inside
	84-NE	BST-1,2,3	Inside
	84-SW	BST-1,2,3	Inside
DCT	4-NW	DCT-1	Inside
	4-NW	DCT-2	Outside
	4-SE	DCT-1	Inside
	4-SE	DCT-2	Outside
	84-NE	DCT-1	Outside
DCT	84-NE	DCT-2	Inside
	84-SW	DCT-1	Inside
	84-SW	DCT-2	Outside
DMT	84-NE	DMT-1,2,3	Inside

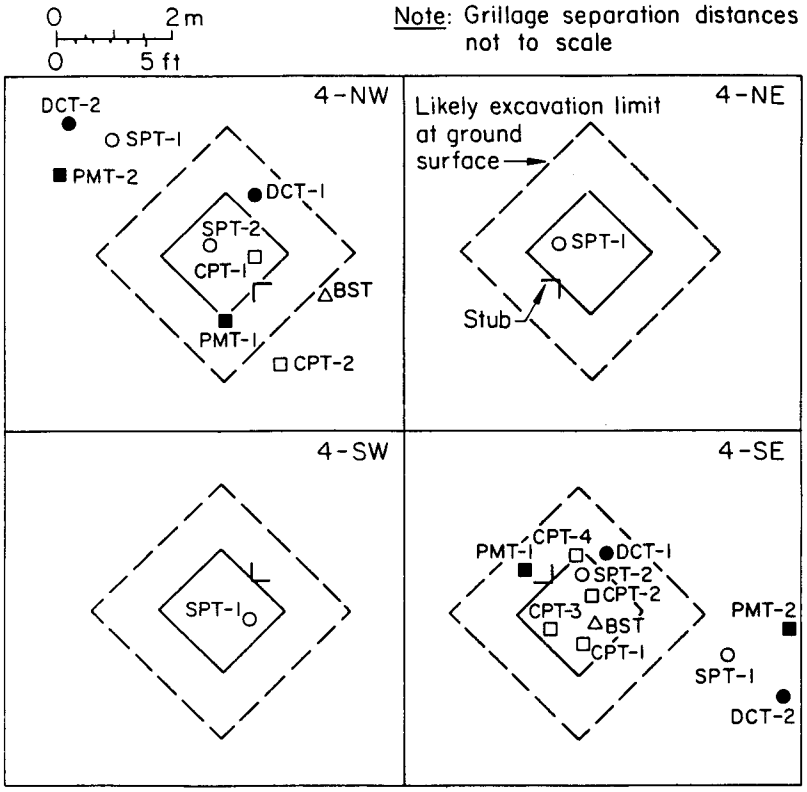

Figure 3-1. In-Situ Test Locations for Hickling Station Grillage Set No. 4

installing the steel grillages are shown as dashed lines. As noted in Section 2, discussions with the construction superintendent indicated a 10 ft x 10 ft (3.05 m by 3.05 m) surface excavation tapering down to the appropriate footing plan dimension of 4.75 ft x 5 ft (1.45 m x 1.52 m). In all likelihood, the base of the excavation was larger than the neat footing dimension to accommodate construction adjustments. All tests within or very near the surface excavation outline therefore were considered as being done on the backfill material.

Figure 3-2 shows the test locations at the No. 84 grillages. In this case, there was no information on the construction methods, and the excavation outline was determined by construction judgment. Again, all in-situ tests within the dashed lines on Figure 3-2 were considered as tests inside the backfilled soil.

Standard Penetration Tests (SPT)

In all, twelve SPT borings were made at the Hickling Station site; eight were in

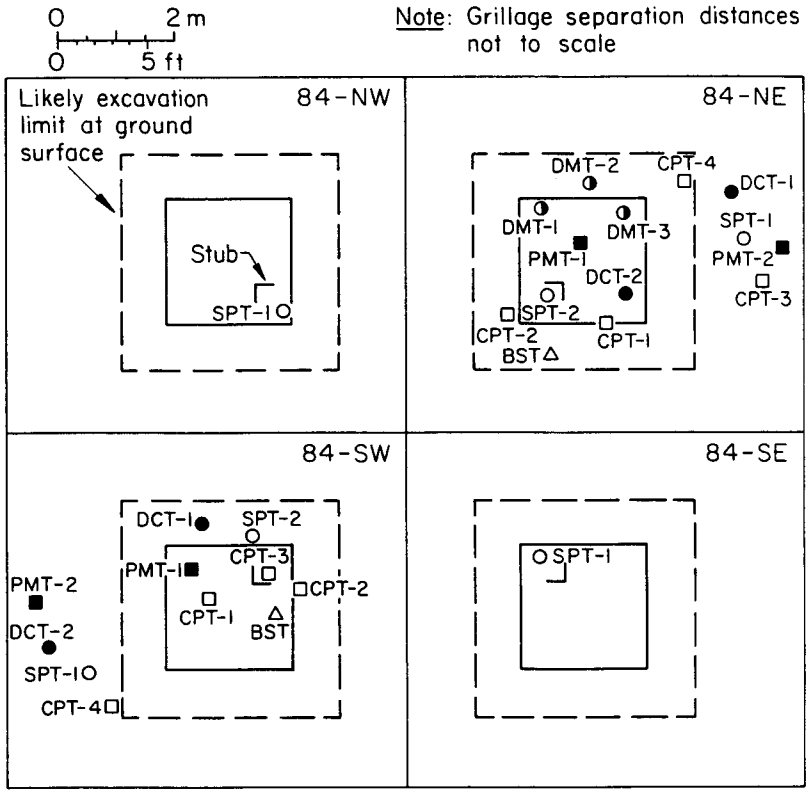

Figure 3-2. In-Situ Test Locations for Hickling Station Grillage Set No. 84

the backfill, and four were in the native soil. Appendix A contains the SPT boring logs.

The SPT data from the Hickling Station sites are broken into three sets. Since the construction dates for the grillage foundations were not the same, and different methods may have been used to backfill the excavations, the data were grouped by grillage type for the tests done inside the backfill. All tests done in the native soil, outside the likely excavation limits, were considered as a separate grouping.

Figure 3-3 shows a generalized soil profile as inferred from the SPT logs and split barrel samples. The soil consists primarily of brown sand and gravel. Test pits also showed cobbles in the 3 to 6 in. (76 to 152 mm) range. The boring logs indicated that the density ranged from loose to medium dense at the surface and increased with depth. Several logs indicated that the material

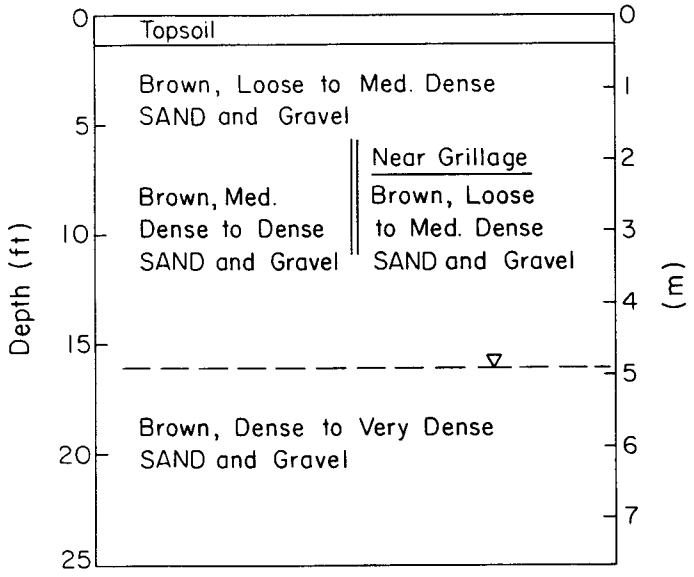

Figure 3-3. Generalized Soil Profile at Hickling Station Based on Field SPT Logs

directly above the grillages was loose, which may indicate minor soil compaction during construction. Ground water was observed in four of the twelve borings at an average depth of 15.9 ft (4.85 m).

An indication that the soils were granular with gravel- and cobble-sized particles also can be inferred from the SPT split-barrel recoveries. Table 3-3 lists the average percent recoveries and coefficients of variation (COV) for the Hickling Station SPTs, along with the boring depths and observed ground water depths. The average recovery was only 29 percent from the twelve borings, indicating that gravel-sized particles may have blocked the open end of the split-barrel, which would reduce the recovery and increase N.

Figure 3-4 shows the uncorrected SPT N values for borings made in the backfill over the No. 4 grillages. The average N values, along with $\pm$ one standard deviation (σ), also are shown in the figure. The average N value over the 9 ft (2.74 m) boring depth is roughly 15 blows/ft or 0.3 m. Table 3-4 gives ranges of relative densities as estimated from N values (9, 10). Based on the descriptions given in Table 3-4, the inside borings at the Hickling Station No. 4 grillages indicate soil in the medium relative density range.

The SPT N values for the borings made inside the backfill at the Hickling

Table 3-3

SPT BORING LOG DATA, HICKLING STATION

Grillage	Test No.	Boring Depth (ft)	Percent Recovery Average	Percent Recovery COV (%)	Ground Water Depth (ft)
4-NE	SPT-1	9.0	26	57	-
4-NW	SPT-1	20.0	45	44	16.0
4-NW	SPT-2	10.0	25	0	-
4-SE	SPT-1	20.0	38	51	17.0
4-SE	SPT-2	10.0	30	70	-
4-SW	SPT-1	10.0	31	73	-
84-NE	SPT-1	22.0	19	66	15.0
84-NE	SPT-2	9.0	30	39	-
84-NW	SPT-1	10.0	18	64	-
84-SE	SPT-1	10.0	26	69	-
84-SW	SPT-1	20.0	34	41	15.5
84-SW	SPT-2	8.7	24	91	-
Averages:			29	27	15.9

1 ft = 0.305 m

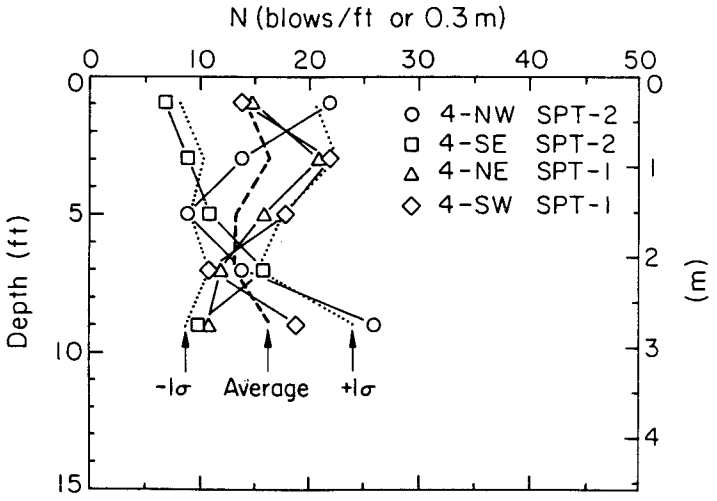

Figure 3-4. SPT N Values, Hickling Station Grillage Set No. 4, Inside

Station No. 84 grillages are shown in Figure 3-5, along with the average values. The N values average roughly 10 for the inside No. 84 tests, indicating a loose to medium relative density. This result may be indicative of lesser compaction

Table 3-4

RELATIVE DENSITY OF SAND VERSUS N

N Value (blows/ft or 0.3 m)	Relative Density	D_r (%)
0 to 4	very loose	0 to 15
4 to 10	loose	15 to 35
10 to 30	medium	35 to 65
30 to 50	dense	65 to 85
> 50	very dense	85 to 100

Source: Terzaghi and Peck (9), p. 341 and Lambe and Whitman (10), p. 31.

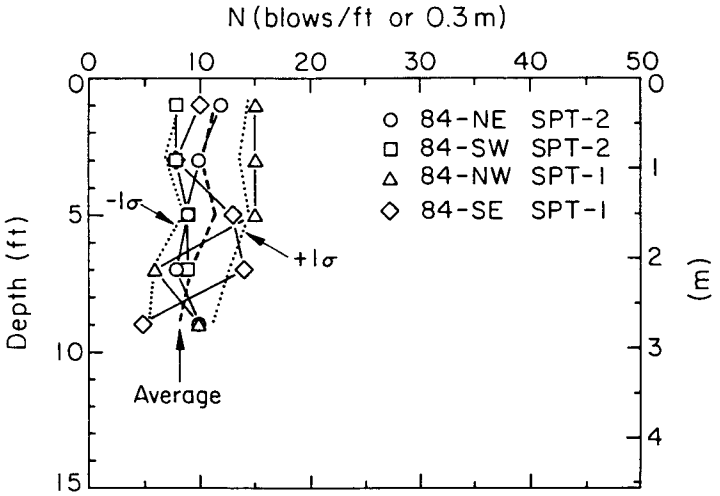

Figure 3-5. SPT N Values, Hickling Station Grillage Set No. 84, Inside

during construction than at the adjacent No. 4 grillages, which were installed approximately 10 years later. However, standard statistical methods indicate that there is no significant difference between the two profiles.

The SPT tests done outside the backfill zone were taken as being in the same material, since the borings were made within an approximate 50 ft (15.2 m)

radius. The SPT resistances for the borings made outside the backfill are shown in Figure 3-6. The average N values and ± one standard deviation ranges also are shown in the figure. The N values over the top 10 ft (3.05 m) are in the range of 10 to 15 blows/ft or 0.3 m. Below 10 ft (3.05 m), the N values increase steadily from about 15 at 10 ft (3.05 m) to nearly 50 at a depth of 20 ft (6.1 m). Therefore, below a 10 ft (3.05 m) depth, the SPT N values indicate a physical state increasing from dense to very dense.

For comparison purposes, the average SPT N values from the three data groupings are shown in Figure 3-7. The average N values over the upper 10 ft (3.05 m) are lower at the No. 84 grillages than at the No. 4 grillages. In the upper 10 ft (3.05 m), the differences between the average N values in the backfill and native soil at the No. 4 grillages are small.

The SPT data were used to estimate the relative densities, D_r, and effective stress friction angles, $\bar{\phi}$, for the backfill and native soil at the Hickling Station site. Kulhawy and Mayne (1) summarize methods for correcting measured SPT N values to consistent reference standards. The corrections to the measured blow counts are based on the dynamic efficiency of the field procedures and on the overburden stress. The corrected SPT N value is given by:

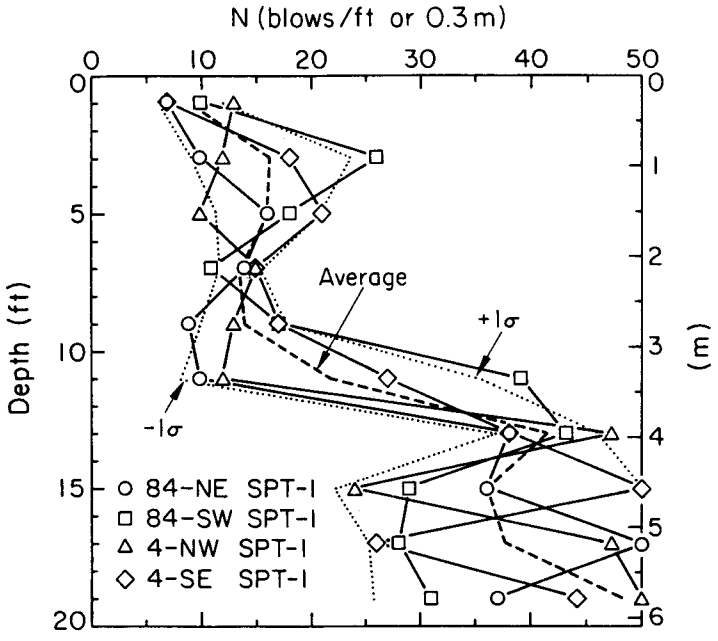

Figure 3-6. SPT N Values, Hickling Station Grillage Set Nos. 4 and 84, Outside

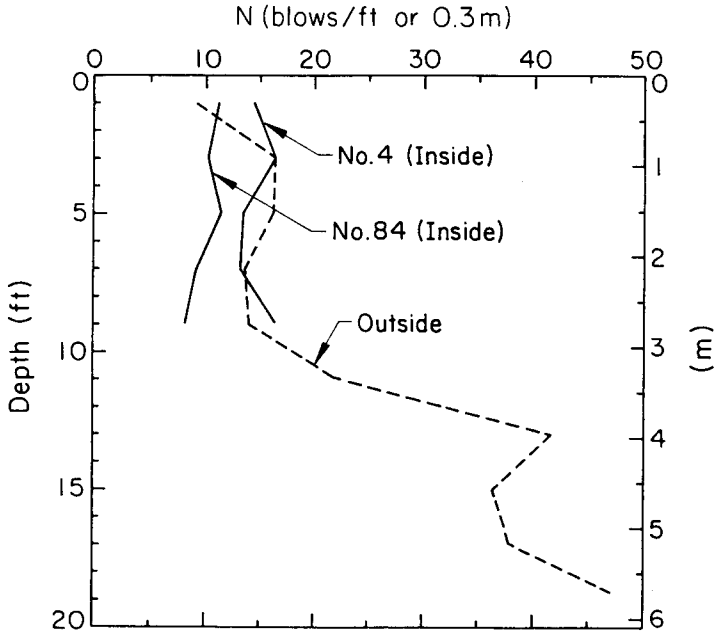

Figure 3-7. Average SPT N Values, Hickling Station

$$N_{60} = C_{ER}\ C_B\ C_S\ C_R\ N \qquad (3\text{-}1)$$

in which N_{60} = corrected N value for an average energy ratio of 60 percent, N = measured N value, and C_{ER}, C_B, C_S, and C_R are factors to account for energy ratio, borehole diameter, sampling method, and rod length, respectively. Suggested correction factors are given in Table 3-5. The numerical values of the correction factors applicable for the SPT data at Hickling Station are marked with an asterisk in Table 3-5. An average rod length factor of $C_R = 0.8$ was used for the data reduction.

The correction for overburden stress is given by:

$$(N_1)_{60} = C_N\ N_{60} \qquad (3\text{-}2)$$

in which $(N_1)_{60}$ = N value corrected to an overburden stress of one atmosphere, N_{60} = N value corrected for field procedures, as noted above, and C_N = overburden stress correction factor.

Several methods are available for computing C_N. Skempton (11) suggested the following for fine sands, which was used to correct the SPT N values from the

Table 3-5

SPT CORRECTION FACTORS FOR FIELD PROCEDURES

Factor	Equipment Variables	Correction Term	Correction Value
Energy ratio	Safety hammer	C_{ER}	0.9*
	Donut hammer		0.75
Borehole diameter	2.5 to 4.5 in. (65 to 115 mm)	C_B	1.0*
	6 in. (150 mm)		1.05
	8 in. (200 mm)		1.15
Sampling method	Standard sampler	C_S	1.0
	Sampler without liner		1.2*
Rod length	> 30 ft (> 10 m)	C_R	1.0
	20 to 30 ft (6 to 10 m)		0.95
	13 to 20 ft (4 to 6 m)		0.85
	10 to 13 ft (3 to 4 m)		0.75

Source: Kulhawy and Mayne (1), Skempton (11).
* - Used for grillage field tests

grillage field sites:

$$C_N = \frac{2}{(1 + \bar{\sigma}_{vo}/p_a)} \tag{3-3}$$

In Equation 3-3, $\bar{\sigma}_{vo}$ is the effective vertical stress and p_a is atmospheric pressure.

Relative density, D_r, also is dependent on such factors as aging, particle size, and stress history. The resulting equation for D_r is given by:

$$D_r^2 = \frac{(N_1)_{60}}{C_P \; C_A \; C_{OCR}} \tag{3-4}$$

in which C_P, C_A, and C_{OCR} are the correction factors given in Table 3-6. The numerical values used to reduce the grillage SPT data were $C_P C_A = 85$ and $C_{OCR} = 1$. The $C_P C_A$ product of 85 was selected to reflect the upper bound suggested by Kulhawy and Mayne (1) for coarse, aged, granular materials. Since the values of

Table 3-6

SPT CORRECTION FACTORS FOR SAND VARIABLES

Effect	Parameter	Correction Term	Correction Value
Particle size	D_{50} (in mm) of sand	C_P	$60 + 25 \log D_{50}$
Aging	Time (t in yrs.)	C_A	$1.2 + 0.05 \log (t/100)$
Overconsolidation	$OCR = \bar{\sigma}_p/\bar{\sigma}_{vo}$	C_{OCR}	$OCR^{0.18}$

Source: Kulhawy and Mayne (1), p. 2-26.

OCR could not be determined reliably, an OCR of one was used for reducing the SPT data.

The final equation for D_r in terms of field N values and all correction terms is given by:

$$D_r^2 = \frac{C_{ER}\ C_B\ C_S\ C_R\ C_N\ N}{C_P\ C_A\ C_{OCR}} \tag{3-5}$$

Upon substitution of the numerical values of correction factors used in reducing the grillage SPT data, Equation 3-5 becomes:

$$D_r^2 = \frac{N}{49.2\ (1 + \bar{\sigma}_{vo}/P_a)} \tag{3-6}$$

The SPT N values also were used to determine the effective stress friction angle, $\bar{\phi}$, at the Hickling Station sites. Several methods are available for estimating $\bar{\phi}$ from SPT N values, as summarized in (1). One approach is to use the N values to determine probable ranges of $\bar{\phi}$, similar to the approach given in Table 3-4 for estimating relative density, D_r. Table 3-7 lists two of the earlier correlations between N and $\bar{\phi}$ that can be used as a first approximation.

The approach taken for reducing the Hickling Station SPT also considers the effects of overburden stress. Figure 3-8 shows the relationship used to obtain

Table 3-7

N VERSUS $\bar{\phi}$ RELATIONSHIPS

N Value (blows/ft or 0.3 m)	Relative Density	Approximate $\bar{\phi}$ (degrees) (a)	(b)
0 to 4	very loose	< 28	< 30
4 to 10	loose	28 to 30	30 to 35
10 to 30	medium	30 to 36	35 to 40
30 to 50	dense	36 to 41	40 to 45
> 50	very dense	> 41	> 45

a - Source: Peck, Hanson, and Thornburn (12), p. 310.
b - Source: Meyerhof (13), p. 17.

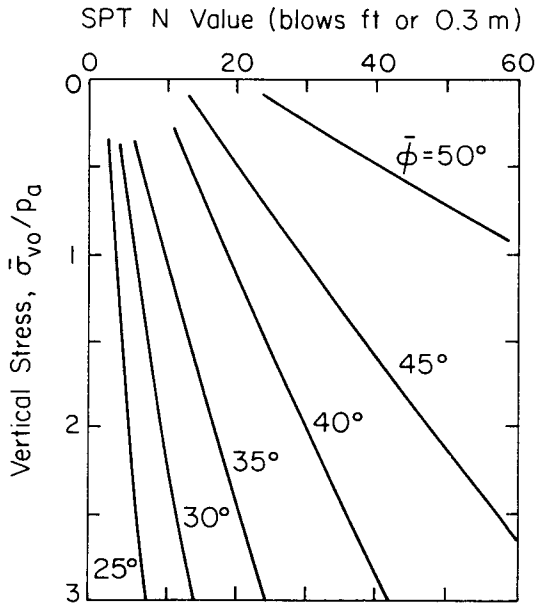

Figure 3-8. N versus $\bar{\phi}$ and Overburden Stress

Source: Schmertmann (14), p. 63.

$\bar{\phi}$ from SPT N values (14). To simplify the data reduction, the curves in Figure 3-8 can be represented by the following:

$$\bar{\phi} \approx \tan^{-1} [N/(12.2 + 20.3\ \bar{\sigma}_{vo}/p_a)]^{0.34} \quad (3\text{-}7)$$

Table 3-8 summarizes the N values measured for tests in the backfill at the No. 4 grillages at Hickling Station. The SPT data and correlated properties from the tests in the backfill at the No. 84 grillages are given in Table 3-9. Table 3-10 contains the data from the SPTs outside the backfill at the Hickling Station site.

In Tables 3-8, 3-9, and 3-10, each individual N value was used to calculate a relative density, D_r, and friction angle, $\bar{\phi}$. These D_r and $\bar{\phi}$ values then were averaged to determine the average values listed in the tables. This method of averaging was used for all in-situ data. An alternative approach would have been to first average the in-situ measurements at a given depth and then convert the average measurement to a correlated property. However, given that the correlations are nonlinear, the former approach is correct. Coefficients of variation (COV) in percent also are given, where the COV = standard deviation divided by the mean or average value. The effective unit weight of the soil at the Hickling Station site was estimated at $\bar{\gamma}$ = 120 pcf (18.85 kN/m^3). Given the variations in the SPT N values and the uncertainties in the correction factors and empirical correlations, a more precise value of the estimated soil unit weight at this point is not warranted.

Table 3-8

SPT DATA, HICKLING STATION GRILLAGE SET NO. 4, INSIDE

		N (blows/ft or 0.3 m) per Grillage and Boring				N		D_r		$\bar{\phi}$	
Depth (ft)	$\bar{\sigma}_v$ (tsf)	4-NE SPT-1	4-NW SPT-2	4-SE SPT-2	4-SW SPT-1	Avg.	COV (%)	Avg. (%)	COV (%)	Avg. (deg)	COV (%)
1	0.06	15	22	7	14	14.5	42.3	51.9	22.5	45.1	10.2
3	0.18	21	14	9	22	16.5	37.2	52.8	19.8	44.9	9.1
5	0.30	16	9	11	18	13.5	31.1	49.0	16.0	41.9	7.5
7	0.42	12	14	16	11	13.3	16.7	43.8	8.4	40.8	3.9
9	0.54	11	26	10	19	16.5	45.5	46.3	22.9	41.3	10.6
Averages:		15.0	17.0	10.6	16.8	14.9	34.6	48.8	17.9	42.8	8.3

1 ft = 0.305 m; 1 tsf = 0.98 ksc

Table 3-9

SPT DATA, HICKLING STATION GRILLAGE SET NO. 84, INSIDE

Depth (ft)	$\bar{\sigma}_v$ (tsf)	N (blows/ft or 0.3 m) per Grillage and Boring				N		D_r		$\bar{\phi}$	
		84-NE SPT-2	84-NW SPT-1	84-SE SPT-1	84-SW SPT-2	Avg.	COV (%)	Avg. (%)	COV (%)	Avg. (deg)	COV (%)
1	0.06	12	15	10	8	11.3	26.5	46.2	13.3	43.1	6.0
3	0.18	10	15	8	8	10.3	32.2	41.8	15.4	40.6	7.1
5	0.30	9	15	13	9	11.5	26.1	42.4	13.0	40.4	6.2
7	0.42	8	6	14	9	9.3	36.8	36.2	18.1	37.1	8.9
9	0.54	10	10	5		8.3	34.6	33.1	18.8	35.1	10.4
Averages:		9.8	12.2	10.0	8.5	10.1	31.3	39.9	15.7	39.3	7.7

1 ft = 0.305 m; 1 tsf = 0.98 ksc

Table 3-10

SPT DATA, HICKLING STATION GRILLAGE SET NOS. 4 AND 84, OUTSIDE

Depth (ft)	$\bar{\sigma}_v$ (tsf)	N (blows/ft or 0.3 m) per Grillage and Boring				N		D_r		$\bar{\phi}$	
		4-NW SPT-1	4-SE SPT-1	84-NE SPT-1	84-SW SPT-1	Avg.	COV (%)	Avg. (%)	COV (%)	Avg. (deg)	COV (%)
1	0.06	13	7	7	10	9.3	31.1	41.8	15.4	41.1	7.0
3	0.18	12	18	10	26	16.5	43.6	52.6	21.7	44.9	9.2
5	0.30	10	21	16	18	16.3	28.6	50.3	15.2	43.7	7.1
7	0.42	15	15	14	11	13.8	13.8	44.6	7.1	42.4	6.1
9	0.54	13	17	9	17	14.0	27.4	43.1	14.4	40.1	7.1
Averages:		12.6	15.6	11.2	16.4	14.0	28.9	46.5	14.8	42.4	7.3
11	0.66	12	27	10	39	22.0	62.0	50.6	32.3	42.4	14.7
13	0.78	47	38	38	43	41.5	10.5	69.6	5.2	49.1	2.0
15	0.90	24	56	36	29	36.3	38.8	62.3	18.9	46.5	7.6
17	1.02	47	26	50	28	37.8	33.1	61.8	16.9	46.3	7.2
19	1.14	81	44	37	31	48.3	46.6	67.5	22.2	47.7	8.4
21	1.26			18		18.0		40.9		38.2	
Averages:		42.2	38.2	31.5	34.0	34.0	38.2	58.8	19.1	45.0	8.0

1 ft = 0.305 m; 1 tsf = 0.98 ksc

Figure 3-9 gives the average D_r densities at grillage set No. 4 based on the SPT N value correlations given previously. The average D_r indicates a medium dense physical state for the backfill material, with the upper 3 ft (0.91 m) slightly denser than the lower material. The average D_r values for the backfill material at the No. 84 grillages are shown in Figure 3-10. Here, D_r shows a consistently decreasing trend as depth increases, with D_r about 50 percent at the surface and decreasing to roughly 40 percent at a depth of 9 ft (2.74 m). This trend suggests that the backfill near the grillage base was not well compacted.

Figure 3-11 shows the average D_r determined from the SPTs at Hickling Station

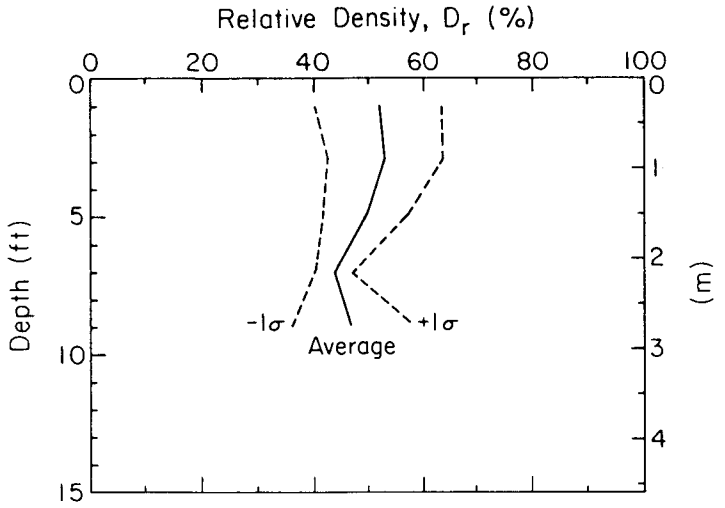

Figure 3-9. Average D_r from SPT, Hickling Station Grillage Set No. 4, Inside

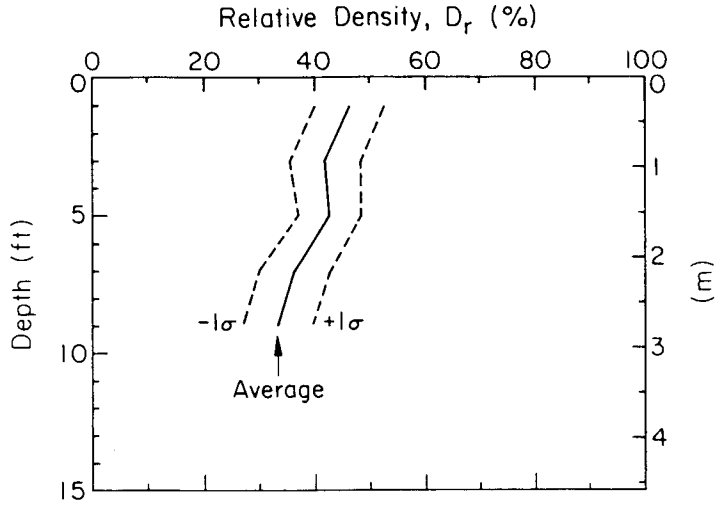

Figure 3-10. Average D_r from SPT, Hickling Station Grillage Set No. 84, Inside

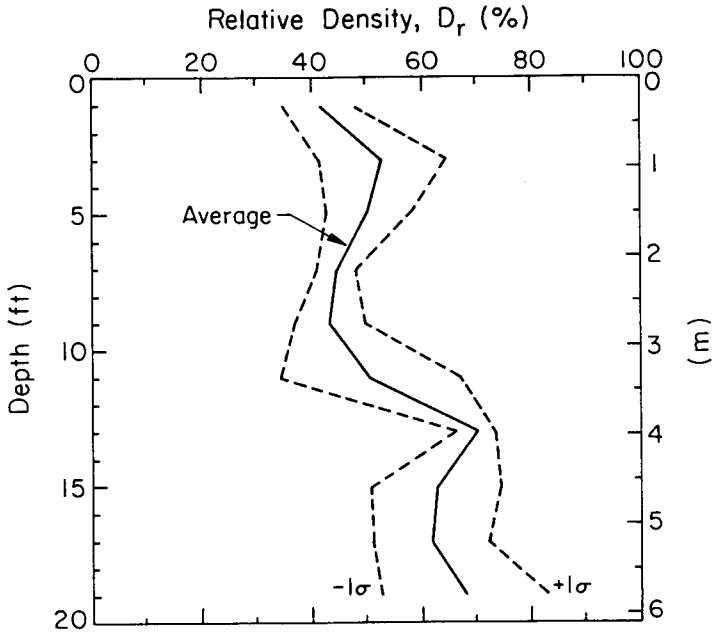

Figure 3-11. Average D_r from SPT, Hickling Station Grillage Set Nos. 4 and 84, Outside

outside the likely excavation limits. The upper 10 ft (3.05 m) was medium dense. Below 10 ft (3.05 m), the relative densities increase from roughly 50 to 70 percent at a depth of 20 ft (6.1 m), corresponding to a transition from medium dense to dense.

A comparison of the average D_r values in the backfill at grillage Nos. 4 and 84 with the average D_r outside the backfill is shown in Figure 3-12. Based on the SPT data, the relative density is greater at the No. 4 grillages than at the No. 84 grillages. Both sets of backfill data show lower D_r values near the grillage base than near the surface. There is no significant difference between backfill and native material D_r values at the No. 4 grillages, based on the SPT data.

The SPT N values also were used to estimate the effective stress friction angle, $\bar{\phi}$, at the Hickling Station site using Equation 3-7. Figure 3-13 shows the average $\bar{\phi}$ values $\pm$ one standard deviation for the backfill material at the No. 4 grillages. The friction angle decreases with depth, from $\bar{\phi} = 45°$ near the surface to about 41° near the grillage base.

Figure 3-14 shows the $\bar{\phi}$ values determined from the SPTs inside the backfill at

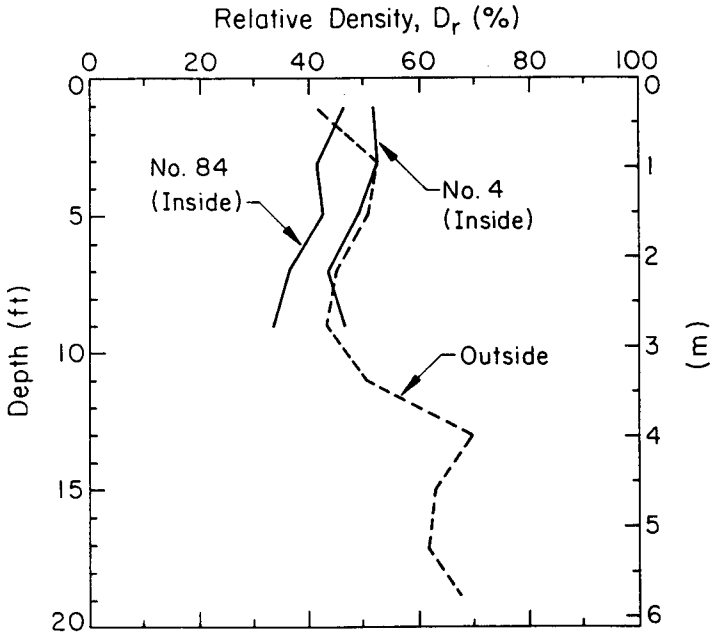

Figure 3-12. Average D_r from SPT, Hickling Station

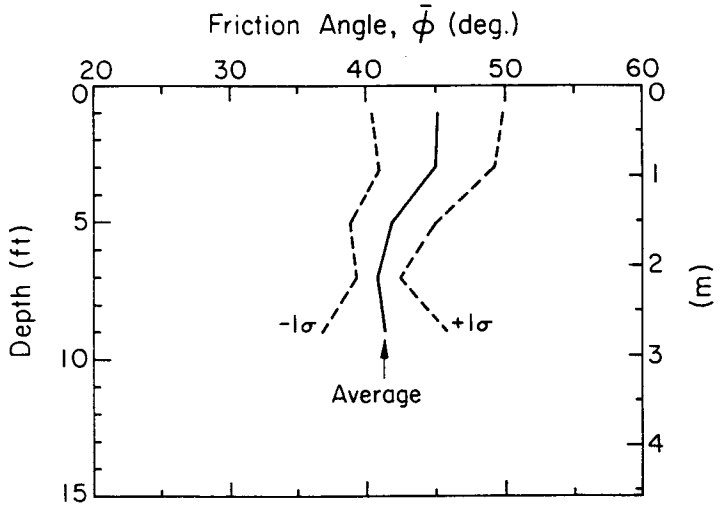

Figure 3-13. Average $\bar{\phi}$ from SPT, Hickling Station Grillage Set No. 4, Inside

the No. 84 grillages. As with D_r at those locations, $\bar{\phi}$ decreases steadily with depth, ranging from 46° near the surface to about 33° at a depth of 9 ft (2.74 m). Again, this trend indicates lesser compaction in the lower soil zone above the grillage than near the surface. The average $\bar{\phi}$ values from the SPTs outside the backfill are shown in Figure 3-15. Over the top 10 ft (3.05 m), the $\bar{\phi}$

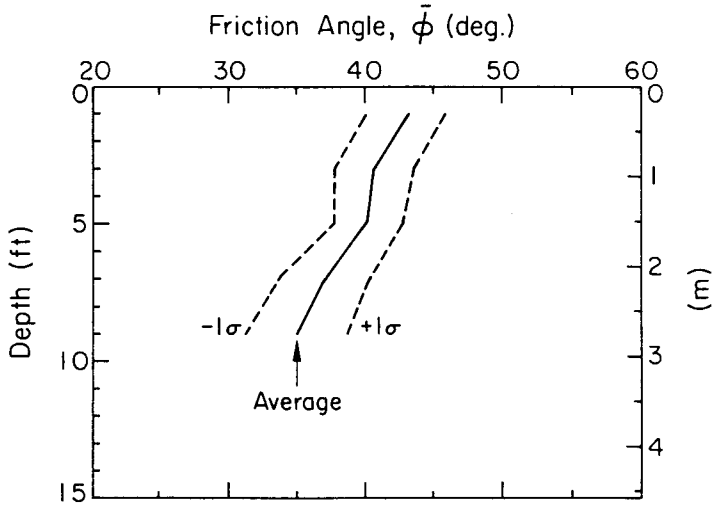

Figure 3-14. Average $\bar{\phi}$ from SPT, Hickling Station Grillage Set No. 84, Inside

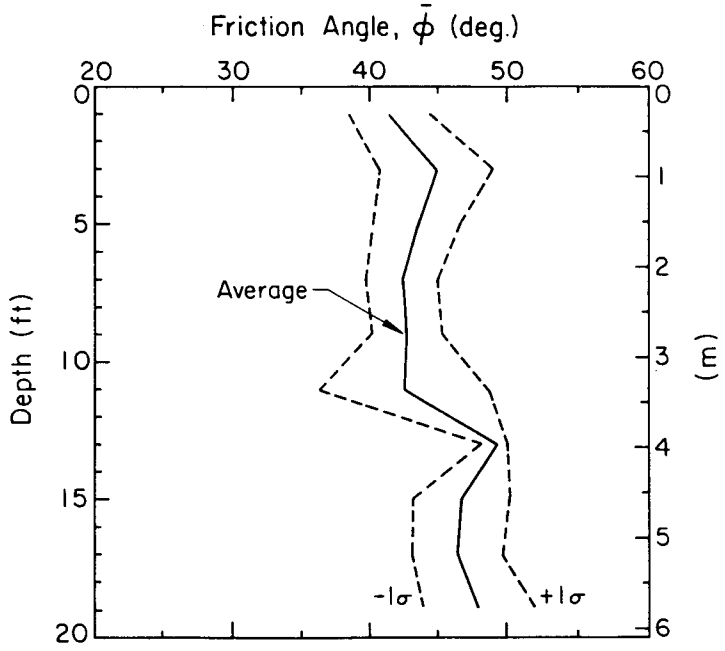

Figure 3-15. Average $\bar{\phi}$ from SPT, Hickling Station Grillage Set Nos. 4 and 84, Outside

values range from 40° to 45°, corresponding to a dense state. The friction angle in the lower 10 ft (3.05 m) is higher, with an average value of about 45° that corresponds to a very dense state.

A comparison of the average $\bar{\phi}$ values determined from the SPTs at the No. 4 and No. 84 backfill zones and native zones is shown in Figure 3-16. The SPT-based $\bar{\phi}$ values in the backfill at the No. 84 grillages are lower overall than at the No. 4 grillages and in the native soil. These comparisons indicate that the 3 to 8 ft (0.91 to 2.44 m) deep zone of soil in the backfill excavation is looser than the native soil, with the No. 84 backfill looser than that at the No. 4 grillages.

Cone Penetration Tests (CPT)

Electric cone penetration tests (CPTs) were conducted in the backfill zone above the grillages and in the native soil. In all, fourteen soundings were made at the Hickling Station site, with ten inside and four outside the backfill zone.

Figures 3-17 and 3-18 show the measured q_c and average q_c values, respectively, in the backfill at the No. 4 grillages. Despite the variability, a looser soil zone is evident between 3 to 5 ft (0.91 to 1.52 m). The measured and average q_c values for the tests in the backfill at the No. 84 grillages are shown in Figures 3-19 and 3-20, respectively. Sounding CPT-2 at grillage No. 84-SE showed large variability in q_c values, perhaps indicative of contact with gravel and cobbles. Despite these erratic readings, they were included in the averaging and account for the wider standard deviation ranges at about 1.6 ft (0.5 m)

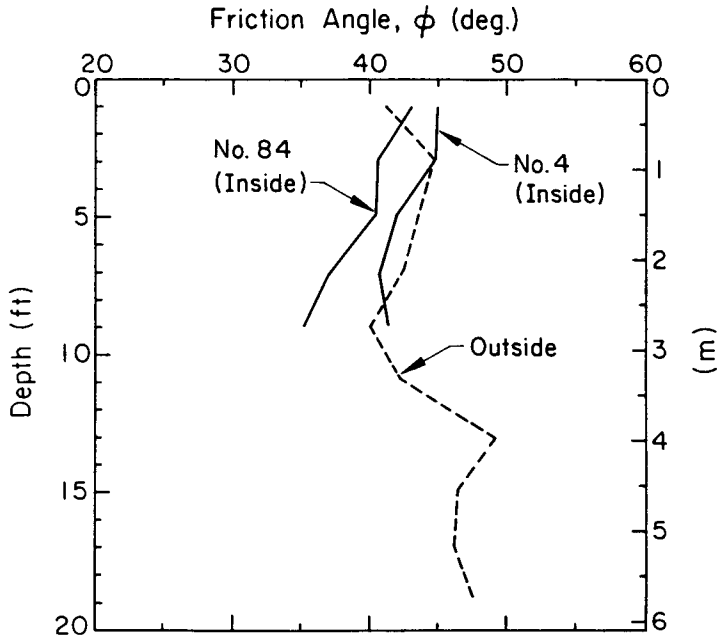

Figure 3-16. Average $\bar{\phi}$ from SPT, Hickling Station

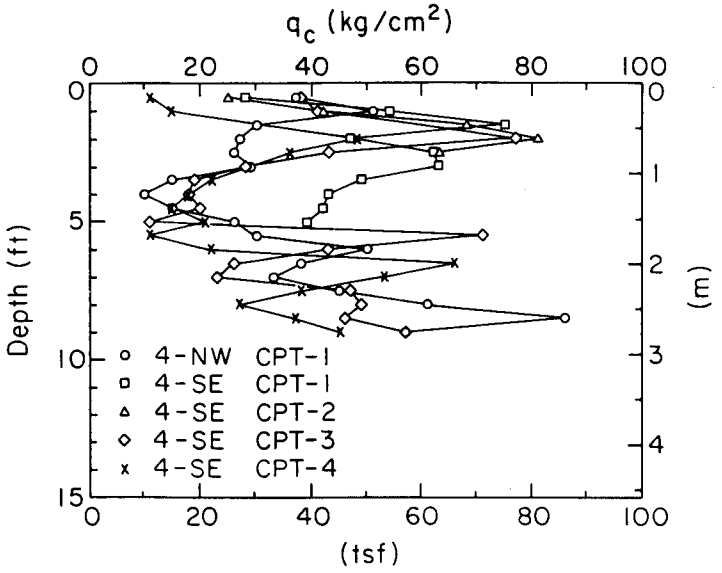

Figure 3-17. CPT q_c, Hickling Station Grillage Set No. 4, Inside

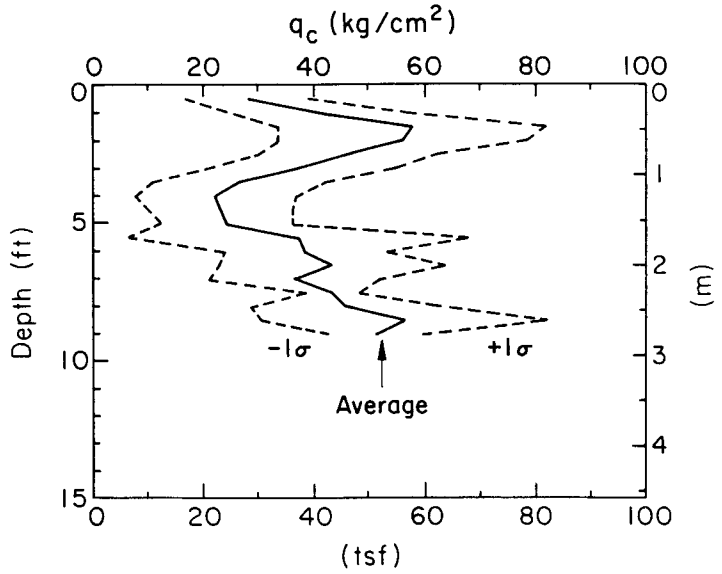

Figure 3-18. Average CPT q_c, Hickling Station Grillage Set No. 4, Inside

intervals shown in Figure 3-20. The q_c values at the No. 84 grillages show generally increasing resistance with depth.

The measured q_c values from the soundings done outside the backfill at Hickling Station are shown in Figure 3-21. The average q_c and $\pm$ one standard deviation range from these four soundings are shown in Figure 3-22. Note that there is a

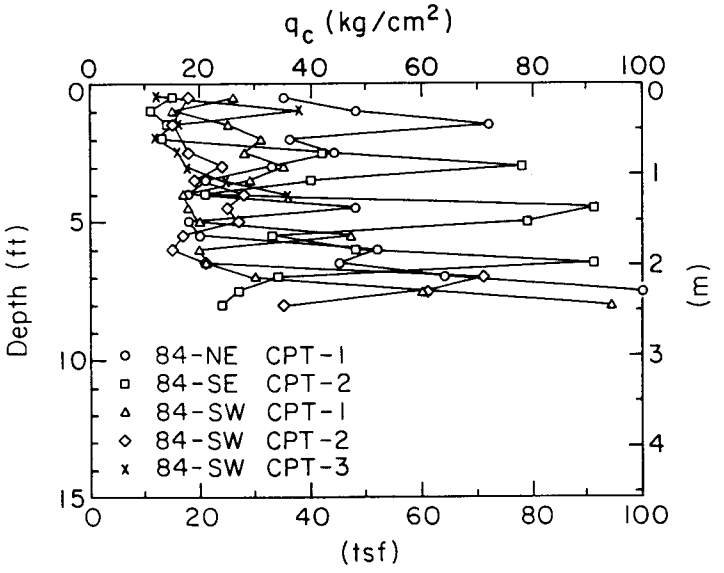

Figure 3-19. CPT q_c, Hickling Station Grillage Set No. 84, Inside

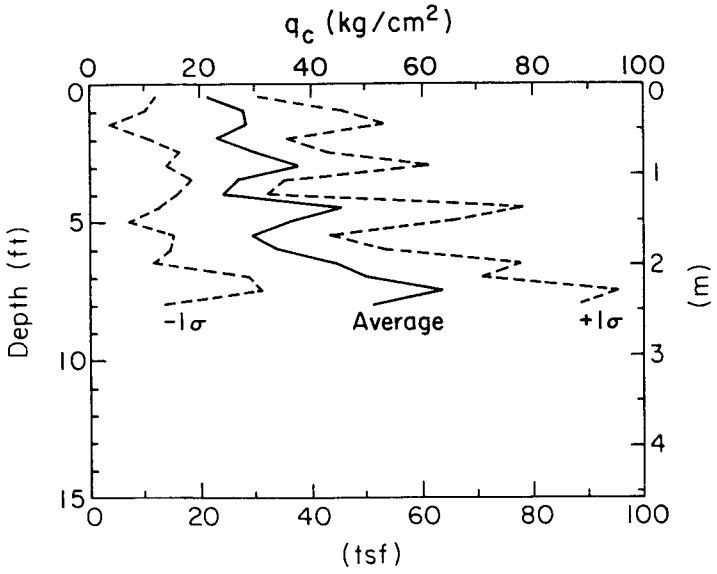

Figure 3-20. Average CPT q_c, Hickling Station Grillage Set No. 84, Inside

scale change between the figures showing inside and outside soundings.

The average CPT q_c values from the three data groupings are shown in Figure 3-23. At the No. 4 backfill sites, the average q_c ranged from roughly 20 to 50 ksc (20 to 51 tsf). At the No. 84 backfill sites, q_c ranged from 20 to 60 ksc (20 to 61 tsf). The q_c values in the native soil at the Nos. 4 and 84 grillages

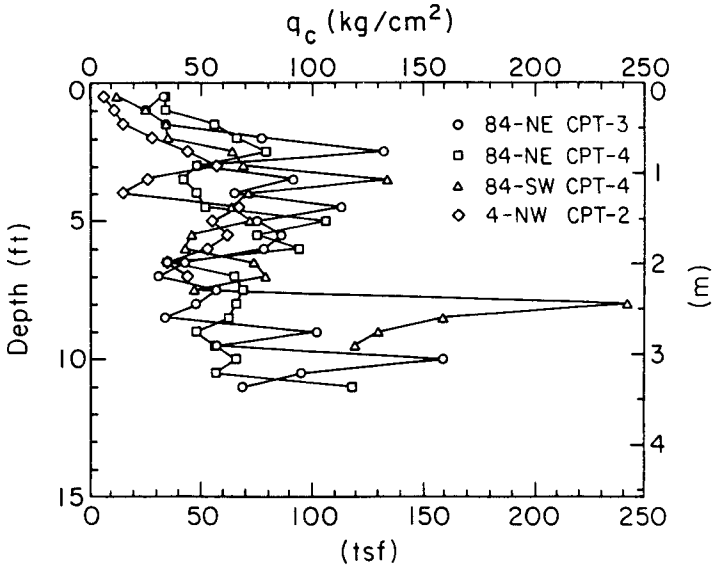

Figure 3-21. CPT q_c, Hickling Station Grillage Set Nos. 4 and 84, Outside

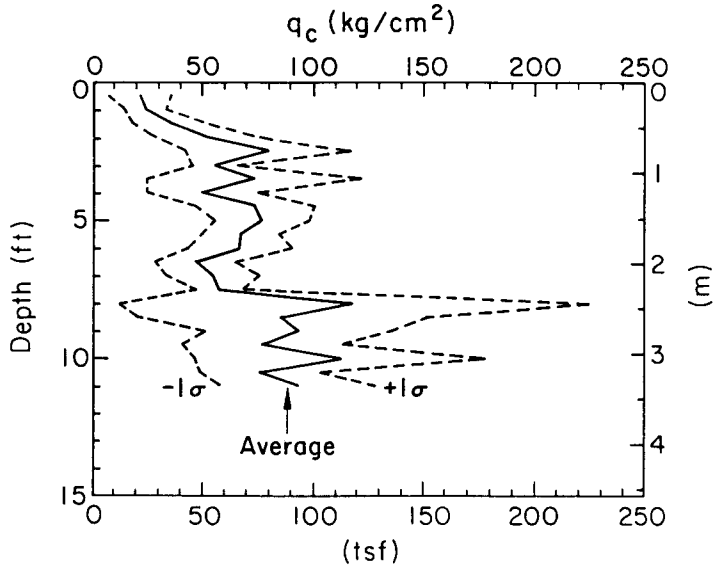

Figure 3-22. Average CPT q_c, Hickling Station Grillage Set Nos. 4 and 84, Outside

ranged from 20 to 80 ksc (20 to 82 tsf) in the upper 8 ft (2.44 m), with values of q_c over 110 ksc (112 tsf) from 8 to 11 ft (2.44 to 3.35 m). This trend indicates generally stiffer soil in the native zone than in the backfilled zones.

The CPT q_c values were used to estimate the relative density, D_r, effective

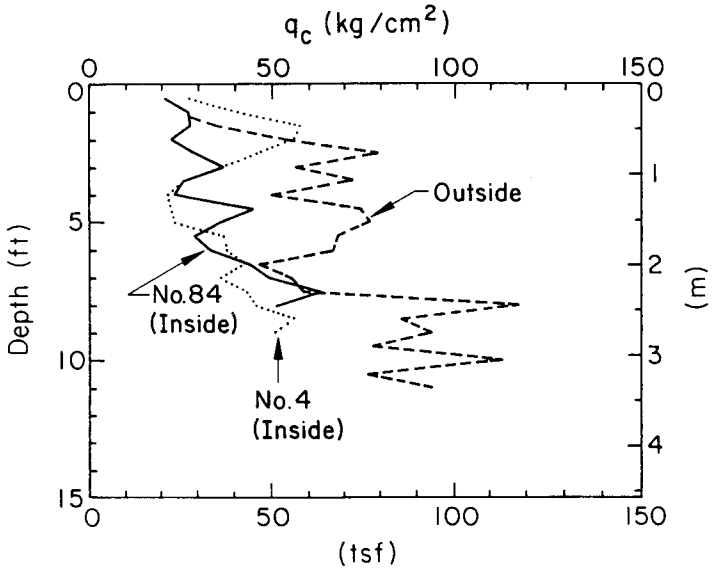

Figure 3-23. Average CPT q_c, Hickling Station

stress friction angle, $\bar{\phi}$, coefficient of horizontal soil stress, K_o, and Young's modulus, E. As with the SPT data reduction, the individual CPT q_c values at any depth were converted first to the specific property, after which the properties at that depth were averaged to determine the mean values. This procedure was followed because of the nonlinearity of the correlations used.

Traditional correlations between normalized cone tip resistance, q_c/p_a, and relative density, D_r, are given in Table 3-11. Qualitative descriptions of D_r also are given, along with estimated ranges of both D_r and $\bar{\phi}$.

A more comprehensive approach has been given by Kulhawy and Mayne (1). For normally consolidated (NC) sands, the relationship between D_r and q_c/p_a is given by:

$$D_r^2 = \frac{q_c/p_a}{305\ Q_c\ OCR^{0.18}\ (\bar{\sigma}_{vo}/p_a)^{0.5}} \qquad (3\text{-}8)$$

in which Q_c = compressibility factor (0.91 for high, 1.0 for medium, and 1.09 for low) and OCR = overconsolidation ratio. This relationship accounts for the effect of vertical stress on q_c by the inclusion of the $\bar{\sigma}_{vo}/p_a$ term, and it addresses soil compressibility and stress history. The compressibility factor

Table 3-11

q_c VERSUS $\bar{\phi}$

Normalized Cone Tip Resistance, q_c/p_a	Relative Density	D_r (%)	Approximate $\bar{\phi}$ (degrees)
< 20	very loose	< 20	< 30
20 to 40	loose	20 to 40	30 to 35
40 to 120	medium	40 to 60	35 to 40
120 to 200	dense	60 to 80	40 to 45
> 200	very dense	> 80	> 45

Source: Meyerhof (13), p. 17.

used was $Q_c = 1.0$, with an OCR = 1, as used with the SPT data.

The effective stress friction angle, $\bar{\phi}$, also can be correlated with q_c and $\bar{\sigma}_{vo}$. Figure 3-24 shows a suggested correlation between both q_c and $\bar{\sigma}_{vo}$ for various $\bar{\phi}$ values. The curves in Figure 3-24 can be approximated as follows (1):

$$\bar{\phi} \approx \tan^{-1} [0.1 + 0.38 \log (q_c/\bar{\sigma}_{vo})] \tag{3-9}$$

The coefficient of horizontal soil stress, K_o, is defined as $K_o = \bar{\sigma}_{ho}/\bar{\sigma}_{vo}$, in which $\bar{\sigma}_{ho}$ = horizontal effective stress. As will be shown later, K_o is extremely important in evaluating grillage uplift capacity. The horizontal effective stress in granular soils is related to the normalized cone tip resistance, q_c/p_a, and relative density, D_r, by (16):

$$\bar{\sigma}_{ho}/p_a = \frac{(q_c/p_a)^{1.25}}{35 \exp (D_r/20)} \tag{3-10}$$

in which D_r is expressed in percent. Once $\bar{\sigma}_{ho}/p_a$ is calculated, K_o can be evaluated readily.

In addition to D_r and $\bar{\phi}$, which relate to the physical state and strength of the

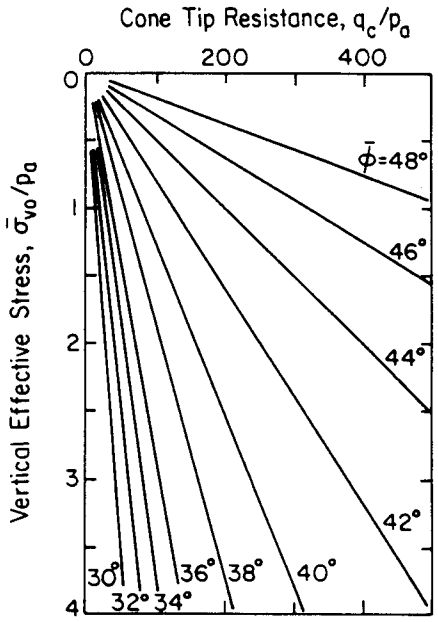

Figure 3-24. q_c versus $\bar{\phi}$ and Vertical Stress for NC, Uncemented Quartz Sands

Source: Robertson and Campanella (15), p. 726.

soil, deformational properties are necessary to evaluate foundation movements. The CPT q_c data were used to evaluate the constrained modulus, M. For normally consolidated sands, using the results of 24 sets of calibration chamber data, the relationship is given by (1):

$$M/q_c = 10^{(1.09 - 0.0075\ D_r)} \tag{3-11}$$

in which D_r is in percent.

From elastic theory, M is related to Young's modulus, E, through Poisson's ratio, ν, as follows:

$$E = \frac{M\ (1 + \nu)(1 - 2\nu)}{(1 - \nu)} \tag{3-12}$$

Table 3-12 lists typical drained values of Poisson's ratio for soils. Trautmann and Kulhawy (17) approximated ν for drained conditions by:

$$\nu \approx 0.1 + 0.3\ \phi_{rel} \tag{3-13}$$

Table 3-12

TYPICAL VALUES OF DRAINED POISSON'S RATIO

Soil	Drained Poisson's Ratio
Clay	0.2 to 0.4
Dense sand	0.3 to 0.4
Loose sand	0.1 to 0.3

Source: Kulhawy and Mayne (1), p. 5-4.

in which

$$\phi_{rel} = \frac{\bar{\phi} - 25^\circ}{45^\circ - 25^\circ} \qquad (0 \leq \phi_{rel} \leq 1) \tag{3-14}$$

with ϕ_{rel} = relative friction angle approximating the soil density state. For $\bar{\phi}$ in the range of 35° to 45°, Poisson's ratio from Equations 3-13 and 3-14 falls in the range of 0.25 to 0.40. The value of Poisson's ratio used to convert constrained modulus, M, to Young's modulus for the grillage sites was $\nu = 0.33$, midway between the estimated bounds.

Tables 3-13, 3-14, and 3-15 give the CPT q_c values and the correlated soil properties D_r, $\bar{\phi}$, K_o, and E for the soundings made at Hickling Station. In these tables, the values given in parentheses were considered unreasonable and were not used in the data reduction. Table 3-13 contains the data from the sounding at grillage set No. 4 in the backfill. The backfill sounding data for grillage set No. 84 are given in Table 3-14. Table 3-15 gives the CPT data from the soundings in the soil outside the backfilled zones.

Figure 3-25 shows the average D_r and $\pm$ one standard deviation ranges from the CPTs in the backfill at grillage set No. 4. The average CPT D_r decreases from about 75 percent near the surface to roughly 38 percent at a depth of 4 ft (1.22 m), and then it increases to about 45 percent at a depth of 9 ft (2.74 m). The average D_r values from the No. 84 backfill soundings are shown in Figure 3-26. The D_r values from the CPT are roughly constant over the 9 ft (2.74 m) depth,

Table 3-13

CPT DATA, HICKLING STATION GRILLAGE SET NO. 4, INSIDE

Depth (ft)	$\bar{\sigma}_v$ (ksc)	q_c (ksc) per Grillage and Sounding					q_c		D_r		$\bar{\phi}$		K_o		E^a	
		4-NW CPT-1	4-SE CPT-1	4-SE CPT-2	4-SE CPT-3	4-SE CPT-4	Avg. (ksc)	COV (%)	Avg. (%)	COV (%)	Avg. (deg)	COV (%)	Avg.	COV (%)	Avg. (ksc)	COV (%)
0.5	0.029	37	28	25	38	11	27.8	39.4	71.0	22.3	50.5	4.0	1.61	17.2	63	20.3
1.0	0.059	51	54	42	41	15	40.6	37.9	72.2	22.2	49.3	4.5	1.22	16.4	90	20.9
1.5	0.088	30	75	68	(114)	(4)	57.7	42.0	77.9	23.2	49.1	4.2	0.98	29.0	116	18.0
2.0	0.117	27	47	81	77	48	56.0	40.4	71.4	21.3	47.8	4.0	0.97	20.3	126	17.4
2.5	0.146	26	62	63	43	36	46.0	35.3	61.5	18.3	46.1	3.7	1.01	9.6	126	17.5
3.0	0.176	29	63	(134)	28	29	37.3	46.1	52.6	21.5	44.2	4.2	0.99	7.2	117	21.7
3.5	0.205	15	49		19	22	26.3	58.8	42.1	27.9	41.4	6.4	0.88	6.9	97	34.0
4.0	0.234	10	43		18	18	22.3	64.4	37.2	31.4	39.5	8.4	0.77	17.4	89	41.4
4.5	0.263	15	42		20	15	23.0	56.0	37.1	26.5	39.3	6.8	0.76	12.4	94	35.0
5.0	0.293	26	39		11	21	24.3	48.0	37.2	25.2	39.0	7.8	0.73	18.4	100	33.8
5.5	0.322	30			71	11	37.3	82.1	43.3	44.7	39.8	13.1	0.68	22.5	125	54.6
6.0	0.351	50			43	22	38.3	38.0	45.1	20.5	40.8	5.9	0.75	8.3	140	25.5
6.5	0.380	38			26	66	43.3	47.4	46.7	23.7	40.9	6.1	0.73	4.6	151	27.9
7.0	0.410	33			23	53	36.3	42.0	42.2	21.1	39.7	5.9	0.70	8.2	139	26.6
7.5	0.439	45			47	38	43.3	10.9	45.9	5.5	40.6	1.5	0.72	1.3	161	6.7
8.0	0.468	61			49	27	45.7	37.8	45.8	20.1	40.2	5.9	0.68	7.0	165	24.6
8.5	0.497	86			46	37	56.3	46.3	49.9	22.7	41.0	5.7	0.67	3.0	187	25.1
9.0	0.527				57	45	51.0	16.6	47.5	8.3	40.5	2.3	0.68	1.1	184	9.8
Averages:		35.8	50.2	55.8	38.6	30.2	39.6	43.9	51.5	22.6	42.8	5.6	0.86	11.7	126	25.6

a - for $\nu = 0.33$

1 ft = 0.305 m; 1 ksc = 1.02 tsf

Table 3-14

CPT DATA, HICKLING STATION GRILLAGE SET NO. 84, INSIDE

Depth (ft)	$\bar{\sigma}_v$ (ksc)	q_c (ksc) per Grillage and Sounding					q_c		D_r		$\bar{\phi}$		K_o		E^a	
		84-NE CPT-1	84-SE CPT-2	84-SW CPT-1	84-SW CPT-2	84-SW CPT-3	Avg. (ksc)	COV (%)	Avg. (%)	COV (%)	Avg. (deg)	COV (%)	Avg.	COV (%)	Avg. (ksc)	COV (%)
0.5	0.029	35	15	26	12	18	21.2	43.9	62.1	21.8	49.5	3.4	1.82	13.9	56	19.6
1.0	0.059	48	11	15	38	-	28.0	63.8	58.6	34.5	47.3	6.5	1.34	13.1	74	34.8
1.5	0.088	72	14	25	16	15	28.4	87.2	52.4	39.8	45.3	6.6	1.18	17.9	79	36.8
2.0	0.117	36	13	31	12	-	23.0	53.5	45.2	28.2	43.5	6.5	1.10	8.1	80	34.3
2.5	0.146	44	42	28	16	18	29.6	44.2	48.9	22.9	43.8	5.3	1.04	3.9	99	26.5
3.0	0.176	33	78	35	18	24	37.6	62.8	52.0	29.7	43.9	6.0	0.95	11.1	114	29.9
3.5	0.205	21	40	29	25	19	26.8	31.0	43.3	15.1	41.9	3.6	0.93	4.3	102	18.6
4.0	0.234	18	21	17	36	28	24.0	33.2	39.6	16.3	40.6	4.2	0.85	7.5	97	21.1
4.5	0.263	48	91	18	(171)	25	45.5	54.9	51.0	36.8	42.4	8.6	0.78	10.6	135	39.5
5.0	0.293	18	79	20		27	36.0	54.6	44.0	38.0	40.6	8.7	0.74	5.9	121	43.7
5.5	0.322	20	33	47		17	29.3	75.7	40.0	23.6	39.6	6.5	0.74	11.5	115	30.5
6.0	0.351	52	48	20		15	33.8	70.2	41.5	30.1	39.6	8.9	0.70	15.3	126	38.6
6.5	0.380	45	91	21		21	44.5	62.0	45.9	37.0	40.3	9.4	0.68	9.1	146	42.6
7.0	0.410	64	34	30		71	49.8	55.5	49.2	21.6	41.3	5.6	0.72	2.1	167	24.9
7.5	0.439	105	27	60		61	63.3	60.3	54.1	26.6	42.0	7.1	0.68	8.4	190	28.6
8.0	0.468		24	94		35	51.0	73.8	46.9	37.0	40.1	9.5	0.64	6.1	166	42.3
Averages:		43.9	41.3	32.3	21.6	28.1	35.7	57.9	48.4	28.7	42.6	6.7	0.93	9.3	117	32.0

a - for $\nu = 0.33$

1 ft = 0.305 m; 1 ksc = 1.02 tsf

Table 3-15

CPT DATA, HICKLING STATION GRILLAGE SET NOS. 4 AND 84, OUTSIDE

Depth (ft)	$\bar{\sigma}_v$ (ksc)	q_c (ksc) per Grillage and Sounding				q_c		D_r		$\bar{\phi}$		K_o		E^a	
		4-NW CPT-2	84-NE CPT-3	84-NE CPT-4	84-SW CPT-4	Avg. (ksc)	COV (%)	Avg. (%)	COV (%)	Avg. (deg)	COV (%)	Avg.	COV (%)	Avg. (ksc)	COV (%)
0.5	0.029	6	33	34	12	21.3	67.6	60.0	38.6	48.8	7.2	1.66	15.4	53	39.6
1.0	0.059	11	25	34	25	23.8	40.0	55.3	22.1	47.1	4.6	1.45	4.6	71	24.3
1.5	0.088	15	34	56	34	34.8	48.2	60.0	25.7	46.9	5.2	1.20	11.2	94	25.6
2.0	0.117	28	77	66	35	51.5	46.0	68.2	24.0	47.4	4.5	1.01	20.5	121	20.2
2.5	0.146	44	132	79	64	79.8	47.2	80.4	23.4	48.4	3.9	0.79	32.4	152	13.5
3.0	0.176	57	48	48	69	55.5	17.9	65.2	8.8	46.3	1.7	0.93	7.0	147	7.5
3.5	0.205	26	91	42	134	73.3	66.9	69.0	35.8	45.9	7.4	0.77	29.9	156	30.0
4.0	0.234	15	65	48	71	49.8	50.5	55.7	30.3	43.6	8.5	0.82	8.6	142	34.4
4.5	0.263	67	113	52	64	74.0	36.2	67.4	17.4	45.6	3.3	0.77	16.1	183	13.2
5.0	0.293	55	75	106	72	77.0	27.6	67.3	13.6	45.4	2.8	0.74	11.9	194	11.1
5.5	0.322	62	86	75	46	67.3	25.6	61.4	13.2	44.3	3.0	0.76	6.8	188	12.7
6.0	0.351	53	78	94	43	67.0	34.7	59.7	17.7	43.8	4.0	0.74	8.4	190	17.2
6.5	0.380	35	43	35	74	46.8	39.7	48.8	18.9	41.5	4.4	0.75	2.5	160	20.8
7.0	0.410	44	31	65	79	54.8	39.1	51.7	20.3	41.9	5.2	0.72	3.3	177	22.6
7.5	0.439		57	69	47	57.7	19.1	52.8	9.6	42.1	2.4	0.72	1.5	189	10.4
8.0	0.468		48	66	241	118.3	90.1	70.0	45.7	44.0	9.2	0.56	43.7	232	31.8
8.5	0.497		34	63	159	85.3	76.7	59.5	39.5	42.3	9.3	0.60	21.3	215	37.0
9.0	0.527		102	48	130	93.3	44.7	63.2	24.3	43.2	6.2	0.60	12.2	242	23.7
9.5	0.556		57	56	119	77.3	46.7	56.9	22.7	42.1	5.2	0.63	10.3	226	21.8
10.0	0.585		159	66		112.5	58.5	67.3	30.6	43.5	7.1	0.55	25.0	268	26.3
10.5	0.614		95	57		76.0	35.4	55.5	18.0	41.6	4.6	0.62	4.7	234	18.8
11.0	0.644		69	118		93.5	37.1	60.8	18.9	42.5	4.6	0.59	9.9	262	18.0
Averages:		37.0	70.5	62.6	79.9	67.2	45.2	61.6	23.6	44.5	5.2	0.82	14.0	177	21.9

a - for $\nu = 0.33$

1 ft = 0.305 m; 1 ksc = 1.02 tsf

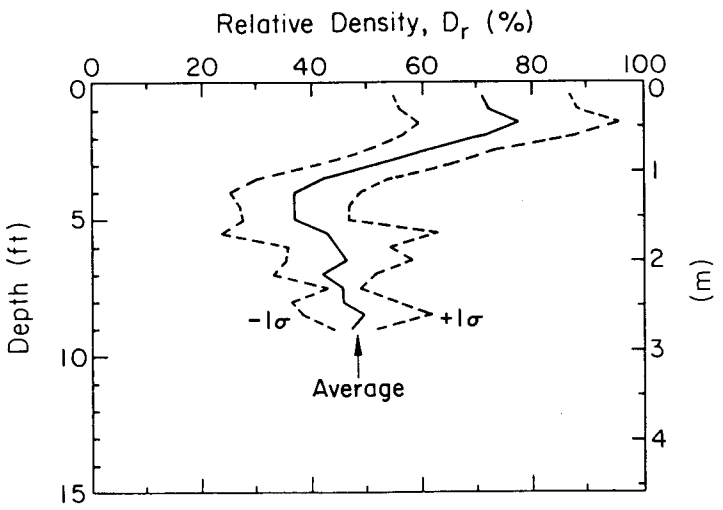

Figure 3-25. Average D_r from CPT, Hickling Station Grillage Set No. 4, Inside

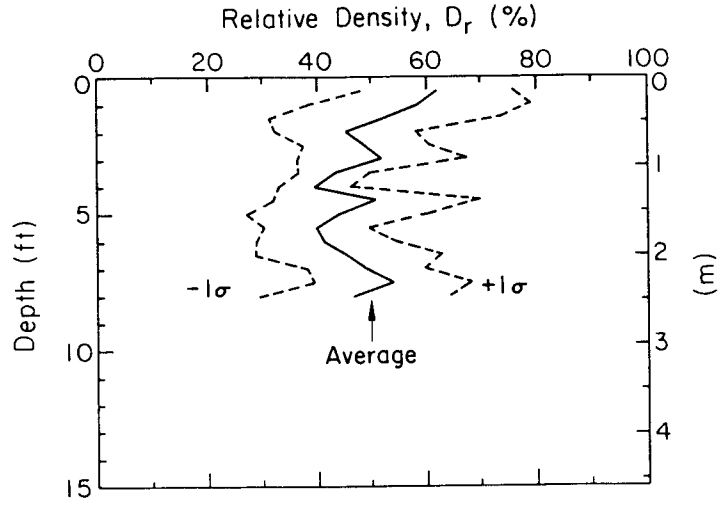

Figure 3-26. Average D_r from CPT, Hickling Station Grillage Set No. 84, Inside

approximately between 40 and 50 percent.

The average D_r values obtained from CPTs outside the backfill zone are shown in Figure 3-27. The erratic q_c values shown in Figure 3-21 again are reflected in the D_r profile. However, the trend line has a higher average value in the native soil than in the backfill.

The average D_r values computed from the CPT data for the backfill in both grillage sets and native soil are shown in Figure 3-28. In the upper 3 ft (0.91 m),

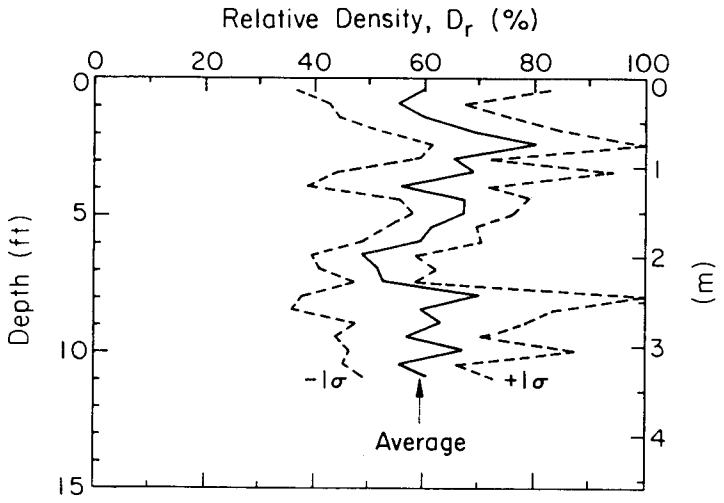

Figure 3-27. Average D_r from CPT, Hickling Station Grillage Set Nos. 4 and 84, Outside

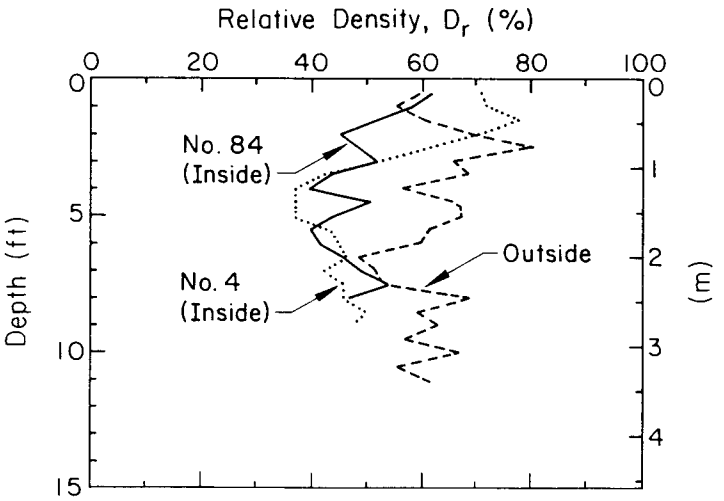

Figure 3-28. Average D_r from CPT, Hickling Station

the densities in the backfill at grillage set No. 4 are higher than those at grillage set No. 84. Below 3 ft (0.91 m), the D_r values in the backfill are nearly the same. The D_r values based on the CPT tests in the native soil generally are higher than those in the backfill, except near the ground surface.

Figure 3-29 shows the average friction angle of the backfill at grillage set No. 4. The friction angle from the CPT correlations decreases from 50° at the surface to about 40° at a depth of 4 ft (1.22 m), below which it remains nearly constant at 40°. The average $\bar{\phi}$ for the backfill at the No. 84 grillages, shown

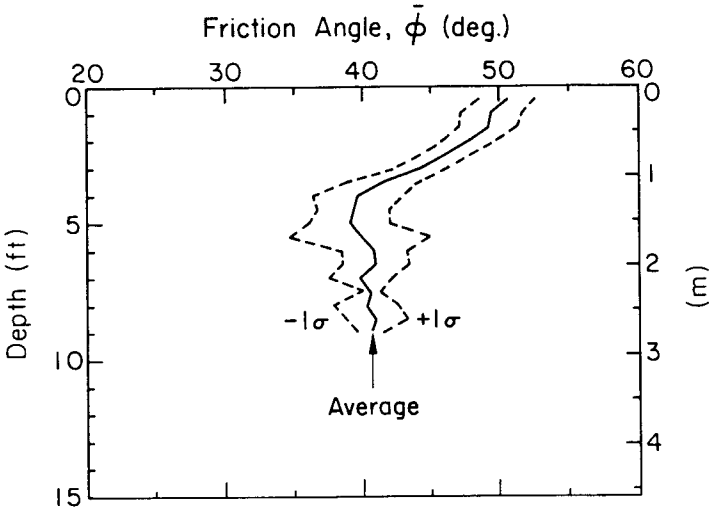

Figure 3-29. Average $\bar{\phi}$ from CPT, Hickling Station Grillage Set No. 4, Inside

in Figure 3-30, is very close to that for the No. 4 backfill.

Figure 3-31 gives the average $\bar{\phi}$ from the CPTs in the native soil outside the backfill zone. The friction angle in the native soil also begins at about 50° near the surface, but it shows a more gradual decrease with depth. At 6 ft (1.83 m), the native soil $\bar{\phi}$ is about 43°, which remains constant to the maximum sounding depth of 11 ft (3.35 m).

A comparison between the average $\bar{\phi}$ from the CPT soundings on both sets of

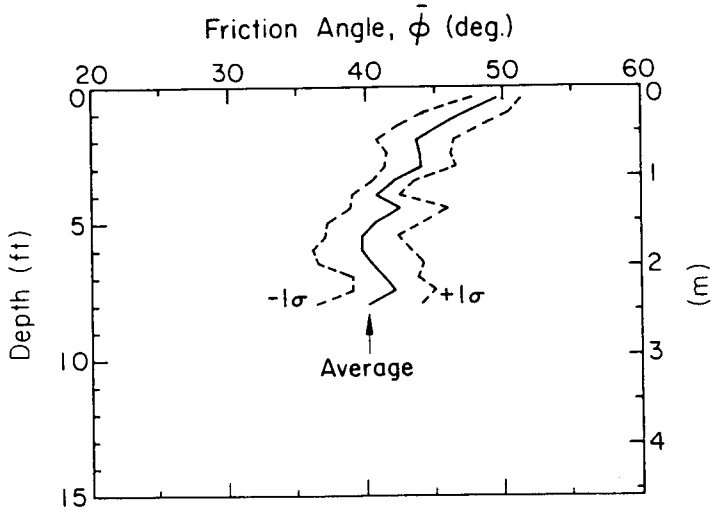

Figure 3-30. Average $\bar{\phi}$ from CPT, Hickling Station Grillage Set No. 84, Inside

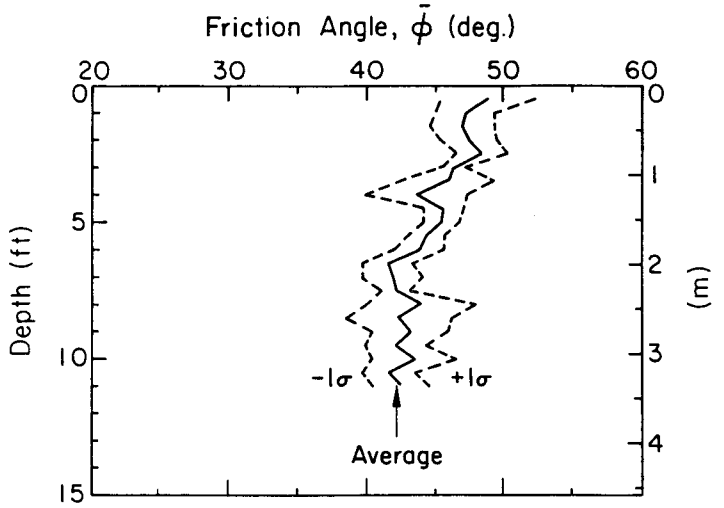

Figure 3-31. Average $\bar{\phi}$ from CPT, Hickling Station Grillage Set Nos. 4 and 84, Outside

backfill and the native soil is given in Figure 3-32. The outside $\bar{\phi}$ values are higher than those in the backfill, except for the first 2 ft (0.61 m). Again, this trend indicates that the native soil is in a more compact state than the backfill at either grillage set.

As described previously, the CPT q_c values also can be converted to a soil Young's modulus, E. Figure 3-33 shows the average CPT E from the tests in the backfill at grillage set No. 4. The data indicate a softer zone at a depth of 4

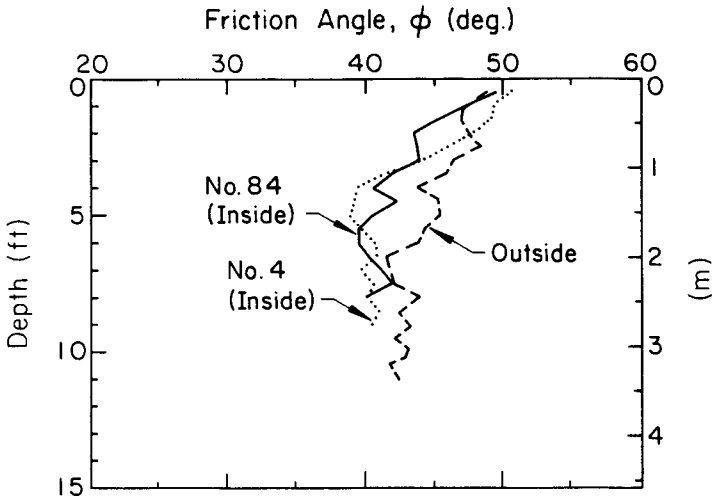

Figure 3-32. Average $\bar{\phi}$ from CPT, Hickling Station

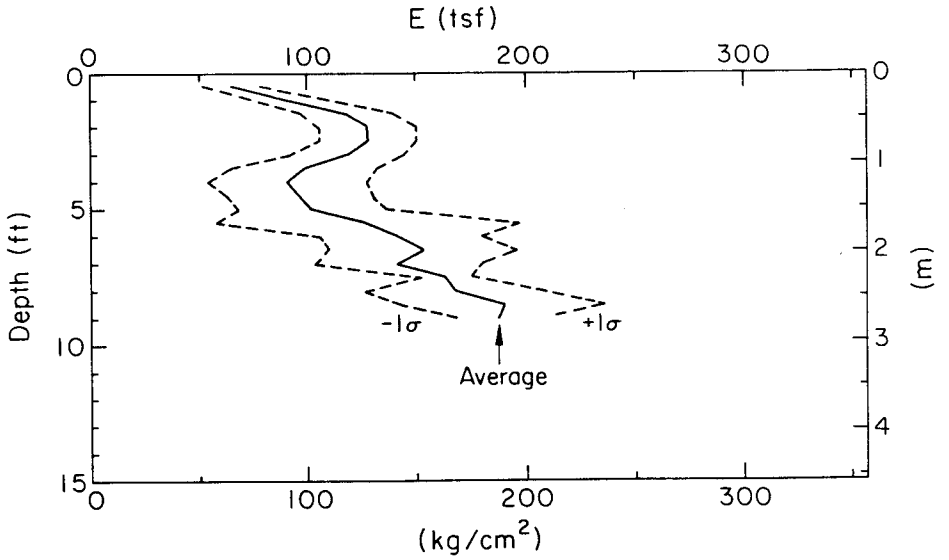

Figure 3-33. Average E from CPT, Hickling Station Grillage Set No. 4, Inside

to 6 ft (1.22 to 1.83 m), after which E increases. Figure 3-34 shows the CPT E values in the backfill at the No. 84 grillages. The general trend shows an increase in E with depth in the No. 84 backfill.

Figure 3-35 gives the average CPT E values from tests in the native soil. As shown, the modulus increases with depth from about 50 ksc (51 tsf) near the surface to 270 ksc (275 tsf) at a depth of 11 ft (3.35 m).

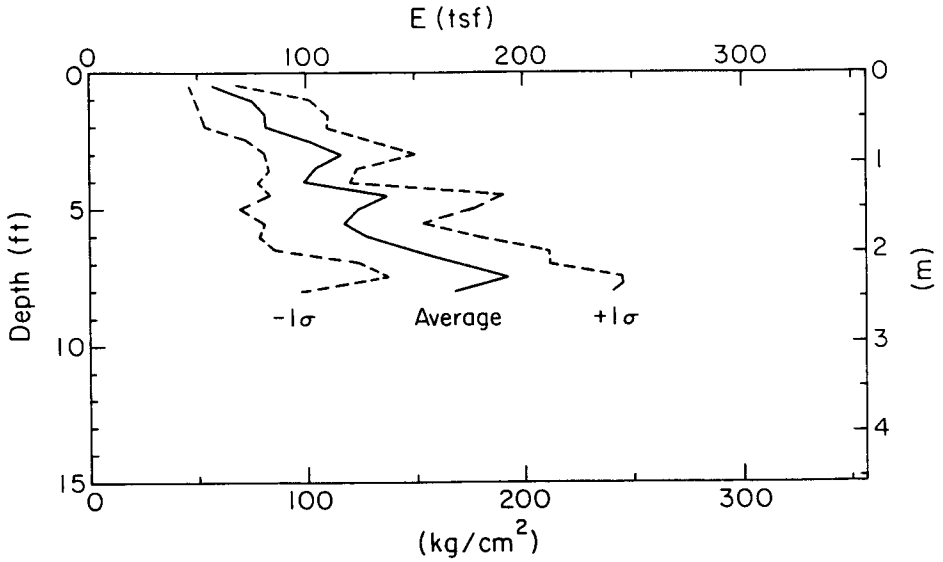

Figure 3-34. Average E from CPT, Hickling Station Grillage Set No. 84, Inside

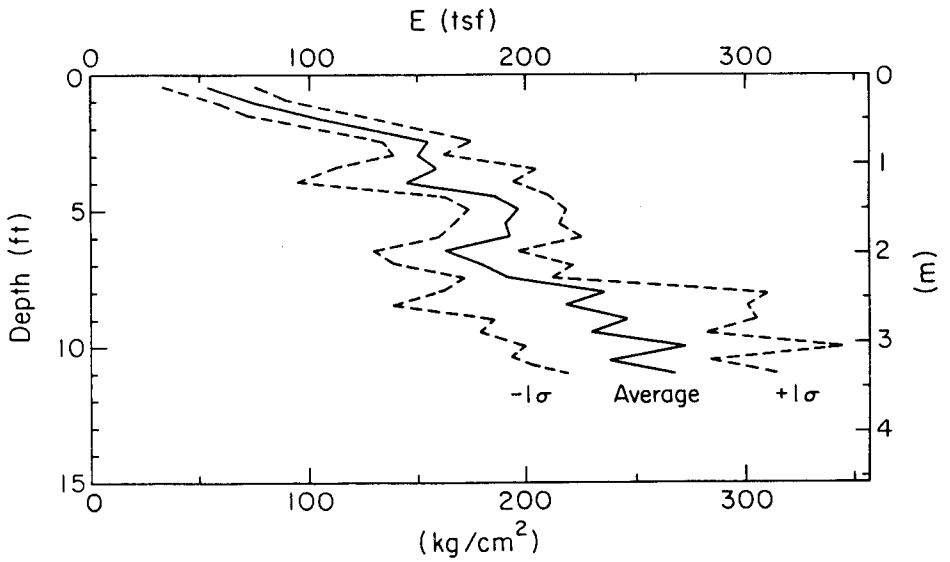

Figure 3-35. Average E from CPT, Hickling Station Grillage Set Nos. 4 and 84, Outside

The average CPT E values from the tests in the backfill at both grillage sets and the native soil are shown in Figure 3-36. The backfill at both grillages and the native soil have nearly the same CPT E values in the upper 2 ft (0.61 m). Between 2 and 7.5 feet (0.61 and 2.29 m), the backfill is softer than the native soil. The trend below 7.5 ft (2.29 m) indicates that the backfill to the depth of the grillage bases is softer than the native soil.

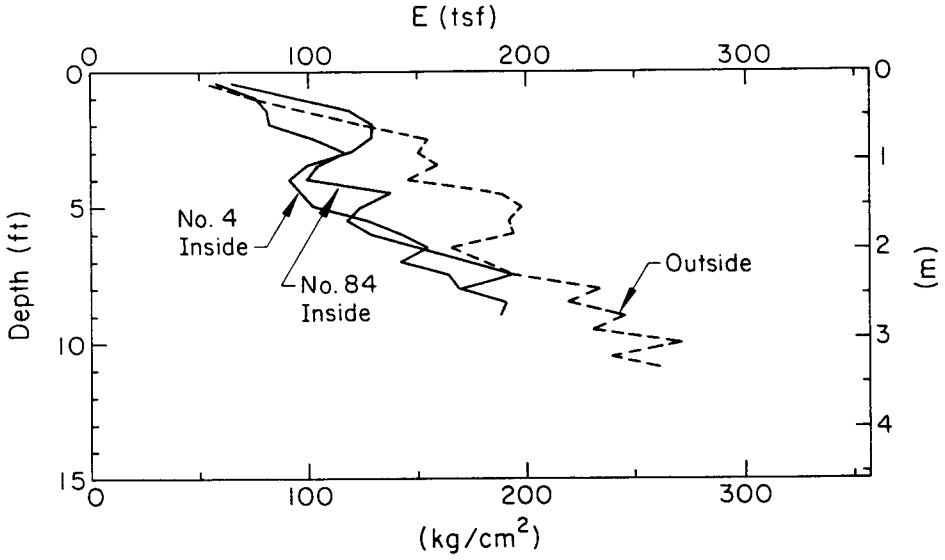

Figure 3-36. Average E from CPT, Hickling Station

The coefficient of horizontal soil stress, K_o, can be determined from the q_c values, as described earlier. Figure 3-37 shows the average K_o values determined from CPTs in the backfill at grillage set No. 4, while Figure 3-38 shows the values for the backfill at grillage set No. 84. The backfill CPT K_o values at both grillage sites are quite similar. There appears to be a break in the curves at about 4 ft (1.22 m), with K_o from 1.5 to 1.7 at the surface and decreasing to about 0.8 at a depth of 4 ft (1.22 m). From 4 to 8 ft (1.22 to 2.44 m), K_o in the backfill stays nearly constant at about 0.8.

Figure 3-39 gives the CPT K_o values from the tests in the native soil. The

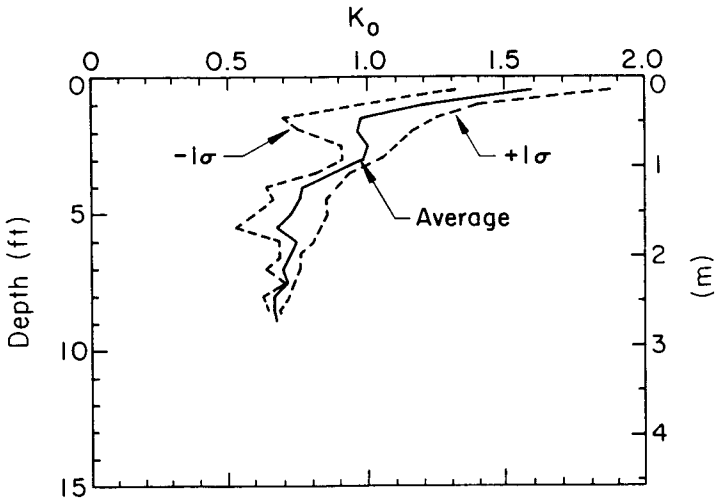

Figure 3-37. Average K_o from CPT, Hickling Station Grillage Set No. 4, Inside

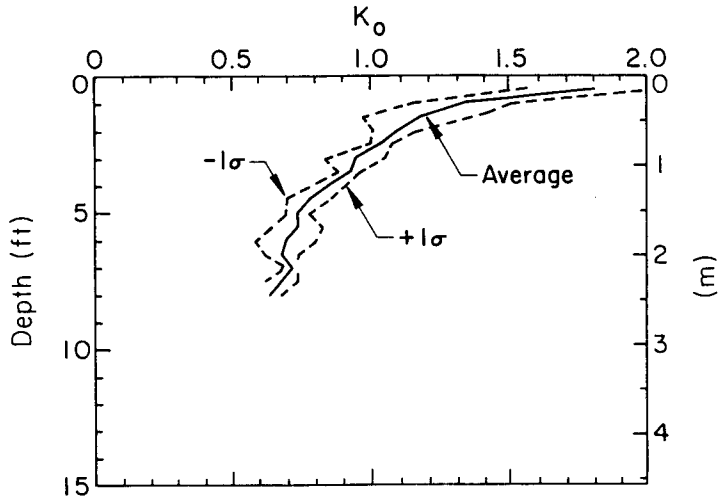

Figure 3-38. Average K_o from CPT, Hickling Station Grillage Set No. 84, Inside

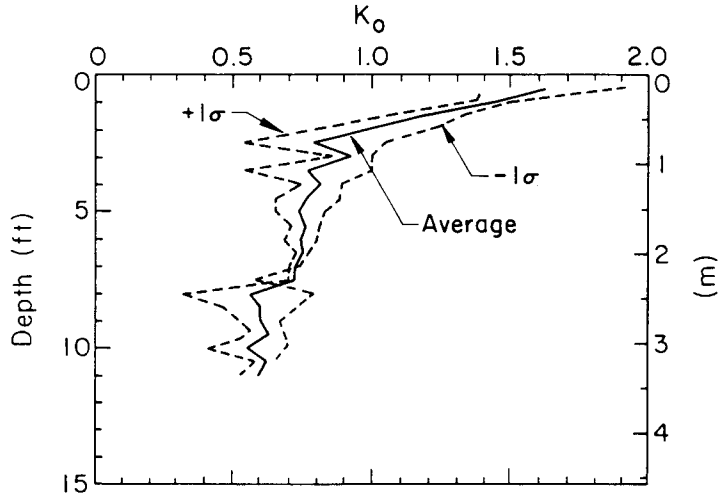

Figure 3-39. Average K_o from CPT, Hickling Station Grillage Set Nos. 4 and 84, Outside

trend in K_o is similar to that in the backfill, with higher K_o values in the upper 4 ft (1.22 m), followed by a decrease in K_o with increasing depth. At a depth of 11 ft (3.35 m), the native soil K_o is about 0.6.

The average backfill and native soil K_o values are compared in Figure 3-40. There is no significant difference between the two backfill zones and the native soil. Since the CPT K_o values were so similar, all of the individual K_o values again were averaged. The global average K_o from all the CPT soundings is shown

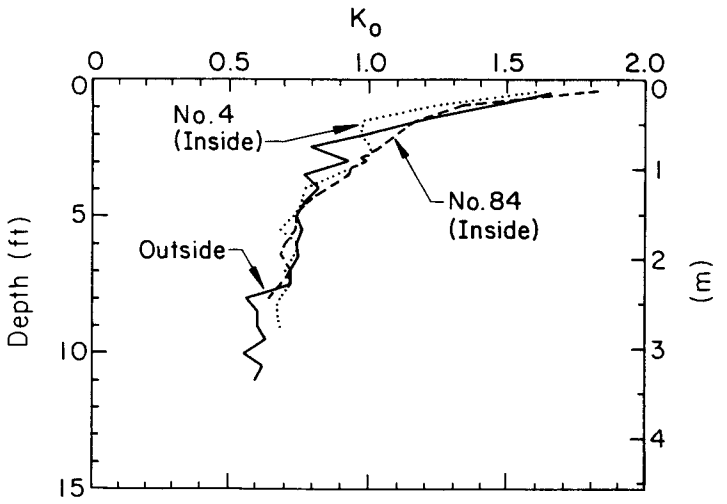

Figure 3-40. Average K_o from CPT, Hickling Station Grillage Set Nos. 4 and 84, Inside and Outside

in Figure 3-41. In the top 2 ft (0.61 m), K_o decreases from about 1.75 to 1.0. At a depth of 4 ft (1.22 m), K_o is about 0.8. From 4 to 11 ft (0.61 to 3.35 m), the combined average K_o derived from the CPT data decreases smoothly from 0.8 to 0.6.

Pressuremeter Tests (PMT)

Menard pressuremeter tests (PMT) were conducted in the backfill and native soil at the Hickling Station site. For most tests, an unload-reload cycle was performed in the pseudo-elastic range to estimate the reload modulus. No empirical correlations are required to determine several soil properties from the PMTs. However, the corrected pressure-volume data must be evaluated graphically to determine the initial PMT modulus, E_m, and the reload PMT modulus, E_r. These graphical evaluations may cause some variations in the interpreted properties.

The pressure-volume curves also must be evaluated graphically to estimate: (1) p_o, the expansion pressure or pressure at which recompression of the disturbed soil is complete, (2) p_c, the pressure at which the soil undergoes a transition from pseudo-elastic to plastic behavior, and (3) p_ℓ, the limit pressure.

The main parameters of interest from the PMTs are p_o and the moduli E_m and E_r. Often, p_o is taken as σ_{ho}, the total horizontal stress in the soil at the test depth. From this assumption, K_o, the coefficient of horizontal soil stress, can be determined by:

$$K_o = (p_o - u_o)/\bar{\sigma}_{vo} \qquad (3\text{-}15)$$

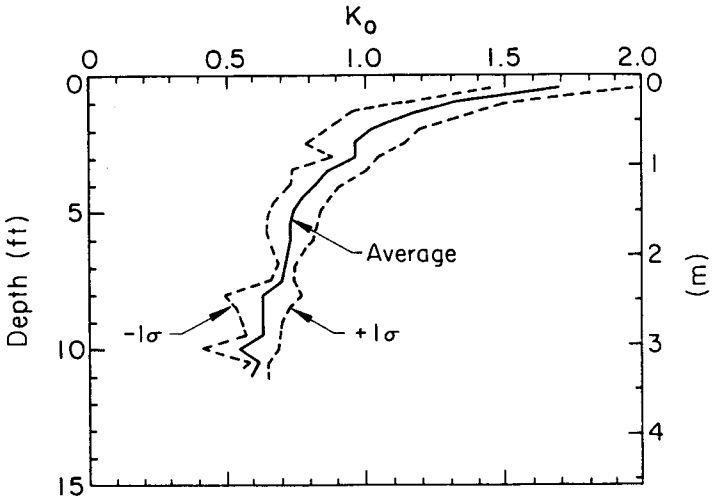

Figure 3-41. Average K_o from CPT, Hickling Station

in which u_o = initial pore water pressure. Since the ground water table was below the test depths at the time the PMTs were made, K_o can be estimated directly as:

$$K_o = p_o/\bar{\sigma}_{vo} \tag{3-16}$$

The PMT moduli values E_m and E_r often are taken as Young's modulus, E. These moduli are determined from the slope of the pseudo-elastic and unload-reload portions of the corrected pressure-volume curves. Poisson's ratio of 0.33 was used in the calculations.

Appendix A contains the corrected pressure-volume and creep curves from the PMTs done at Hickling Station. Tables 3-16 and 3-17 give the pressure data (p_o, p_c, and p_ℓ) from the PMT tests done in the backfill and native soil, respectively. The PMT moduli, E_m and E_r, are given in Table 3-18 for the backfill and in Table 3-19 for the native soil.

The K_o values found in both the backfill and native soil are of primary interest. Average pressure values and resulting K_o values from the backfill tests are given in Table 3-20, along with the average backfill moduli values. The average K_o and moduli values from the native soil PMTs are given in Table 3-21.

Figure 3-42 shows the average K_o values determined from the PMT tests inside the backfill at the Nos. 4 and 84 grillages. In this case, the data were not separated by grillage set, since there were too few data and the variabilities were high. The PMTs indicated much higher K_o values than did the CPTs. At a depth of 2 ft (0.61 m), the PMT K_o value is nearly 2.5. Between 4 and 6 ft (1.22 to 1.83 m), the backfill K_o decreases from about 1.2 to 0.8.

The PMT K_o values from the native soil tests are shown in Figure 3-43. These tests indicated much higher K_o values, almost double the PMT K_o values of the backfill. These high K_o values are questionable, particularly those in the upper few feet. Although the native K_o values are high below 4 ft (1.22 m), the range in K_o from 1.3 to 2 is reasonable.

As mentioned earlier, unload-reload cycles were conducted during the PMT testing. The initial PMT moduli calculated in the pseudo-elastic range, E_m, and the PMT unload-reload moduli, E_r, are shown in Figure 3-44. The initial moduli from the backfill tests are about one-third those of the native soil over the upper 5

Table 3-16

PMT PRESSURE DATA, HICKLING STATION GRILLAGE SET NOS. 4 AND 84, INSIDE

Depth (ft)	$\bar{\sigma}_v$ (kN/m^2)	PMT Pressures (kN/m^2) per Grillage and Test											
		4-NW PMT-1			4-SE PMT-1			84-NE PMT-1			84-SW PMT-1		
		P_o	P_c	P_ℓ	P_o	P_c	P_ℓ	P_o	P_c	P_ℓ	P_o	P_c	P_ℓ
2	11.5	34	350	635	17	95	310	32	180	595	-	140	380
4	23.0	64	300	715	18	110	345	16	-	525	19	170	505
6	34.5	41	210	-	-	275	790	30	150	435	43	180	710
8	46.0	47	300	770	29	250	495						

1 ft = 0.305 m; 1 kN/m^2 = 0.145 psi

Table 3-17

PMT PRESSURE DATA, HICKLING STATION GRILLAGE SET NOS. 4 AND 84, OUTSIDE

Depth (ft)	$\bar{\sigma}_v$ (kN/m^2)	PMT Pressures (kN/m^2) per Grillage and Test											
		4-NW PMT-2			4-SE PMT-2			84-NE PMT-2			84-SW PMT-2		
		P_o	P_c	P_ℓ	P_o	P_c	P_ℓ	P_o	P_c	P_ℓ	P_o	P_c	P_ℓ
2	11.5	93	300	735	61	375	940	61	540	1235	53	490	980
4	23.0	40	225	-	42	370	830	46	335	1390	48	420	1370
6	34.5	51	385	1190	52	380	-	57	-	-	41	430	1100
8	46.0	71	385	1010	73	385	-	77	255	850	94	450	-
10	57.5	53	-	-	173	330	1070	29	-	-	75	430	1300
12	69.0	69	290	810							115	720	-

1 ft = 0.305 m; 1 kN/m^2 = 0.145 psi

Table 3-18

PMT MODULI DATA, HICKLING STATION GRILLAGE SET NOS. 4 AND 84, INSIDE

Depth (ft)	$\bar{\sigma}_v$ (kN/m^2)	PMT Moduli (MN/m^2) per Grillage and Test							
		4-NW PMT-1		4-SE PMT-1		84-NE PMT-1		84-SW PMT-1	
		E_m	E_r	E_m	E_r	E_m	E_r	E_m	E_r
2	11.5	6.2	26.2	1.1	3.9	1.6	-	2.3	6.8
4	23.0	5.2	18.9	1.8	4.7	2.1	-	2.7	-
6	34.5	2.0	7.0	4.5	21.3	2.1	-	4.6	11.5
8	46.0	3.0	14.1	3.0	(70.7)				

1 ft = 0.305 m; 1 kN/m^2 = 0.145 psi; 1 MN/m^2 = 10.4 tsf

Table 3-19

PMT MODULI DATA, HICKLING STATION GRILLAGE SET NOS. 4 AND 84, OUTSIDE

Depth (ft)	$\bar{\sigma}_v$ (kN/m^2)	PMT Moduli (MN/m^2) per Grillage and Test							
		4-NW PMT-2		4-SE PMT-2		84-NE PMT-2		84-SW PMT-2	
		E_m	E_r	E_m	E_r	E_m	E_r	E_m	E_r
2	11.5	5.9	15.2	4.3	18.7	11.1	23.6	9.0	19.2
4	23.0	4.9	12.0	5.0	27.6	8.4	17.4	9.7	30.2
6	34.5	6.6	28.5	3.8	17.1	2.6	-	4.6	11.3
8	46.0	3.5	17.5	3.7	16.5	4.1	12.3	4.3	-
10	57.5	1.7	-	5.1	19.7	2.9	9.6	5.5	22.1
12	69.0	3.0	11.4			2.8	7.6	6.2	19.5

1 ft = 0.305 m; 1 kN/m^2 = 0.145 psi; 1 MN/m^2 = 10.4 tsf

ft (1.52 m). Below 5 ft (1.52 m), the inside and outside E_m values tend to converge. The unload-reload moduli are much higher than the initial moduli, as expected, because typical repeated loading moduli often are two to three times higher than initial moduli. Again, E_r in the outside native soil is about 60 percent higher than that in the backfill for the upper 5 ft (1.52 m). As with

Table 3-20

PMT REDUCED DATA, HICKLING STATION GRILLAGE SET NOS. 4 AND 84, INSIDE

Depth	$\bar{\sigma}_v$ (kN/m^2)	p_o (kN/m^2)		p_c (kN/m^2)		p_ℓ (kN/m^2)		K_o		E_m (MN/m^2)		E_r (MN/m^2)	
		Avg.	COV(%)	Avg.	COV(%)	Avg.	COV(%)	Avg.	COV(%)	Avg.	COV(%)	Avg.	COV(%)
2	11.5	27.4	34.6	191	58.2	480	33.2	2.38	34.6	2.8	84.1	12.1	101.9
4	23.0	29.3	79.4	193	50.2	522	29.0	1.27	79.4	2.9	52.6	11.8	85.0
6	34.5	38.0	18.4	204	26.2	645	28.9	1.10	18.4	3.3	44.4	13.3	55.2
8	46.0	37.9	33.1	275	12.9	632	30.7	0.82	33.1	3.0	1.2	14.1	-
Averages:		33.1	41.4	216	36.9	570	30.5	1.40	41.4	3.0	45.6	12.8	80.7

1 ft = 0.305 m; 1 kN/m^2 = 0.145 psi; 1 MN/m^2 = 10.4 tsf

Table 3-21

PMT REDUCED DATA, HICKLING STATION GRILLAGE SET NOS. 4 AND 84, OUTSIDE

Depth	$\bar{\sigma}_v$ (kN/m^2)	p_o (kN/m^2)		p_c (kN/m^2)		p_ℓ (kN/m^2)		K_o		E_m (MN/m^2)		E_r (MN/m^2)	
		Avg.	COV(%)	Avg.	COV(%)	Avg.	COV(%)	Avg.	COV(%)	Avg.	COV(%)	Avg.	COV(%)
2	11.5	67.0	26.1	426	25.5	972	21.1	5.83	26.1	7.6	40.0	19.2	17.8
4	23.0	43.8	8.6	338	24.5	1197	26.5	1.90	8.6	7.0	34.7	21.8	39.2
6	34.5	50.4	13.4	398	6.9	1145	5.6	1.46	13.4	4.4	37.9	19.0	46.1
8	46.0	78.7	13.5	518	43.2	930	12.2	1.71	13.5	3.9	9.5	15.4	17.9
10	57.5	82.6	76.5	380	18.6	1185	13.7	1.44	76.5	3.8	47.8	17.1	38.6
12	69.0	91.9	35.2	505	60.2	810	-	1.33	35.2	4.0	47.3	12.8	47.4
Averages:		69.0	28.6	428	29.8	1040	15.8	2.28	28.6	5.1	36.2	17.6	34.5

1 ft = 0.305 m; 1 kN/m^2 = 0.145 psi; 1 MN/m^2 = 10.4 tsf

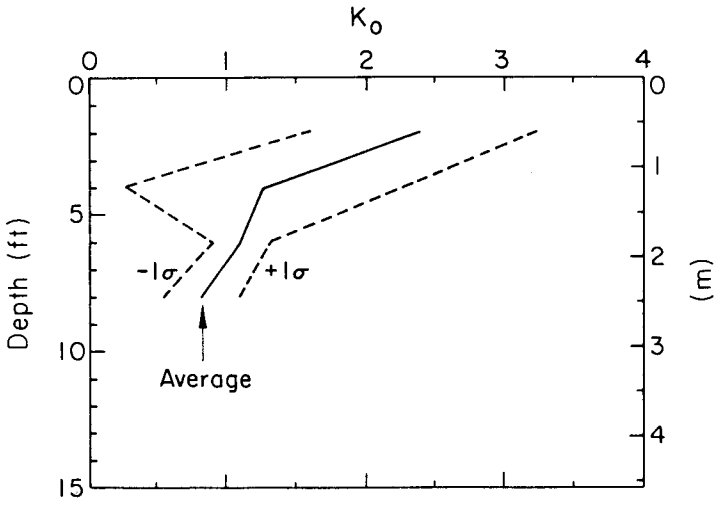

Figure 3-42. Average K_o from PMT, Hickling Station Grillage Set Nos. 4 and 84, Inside

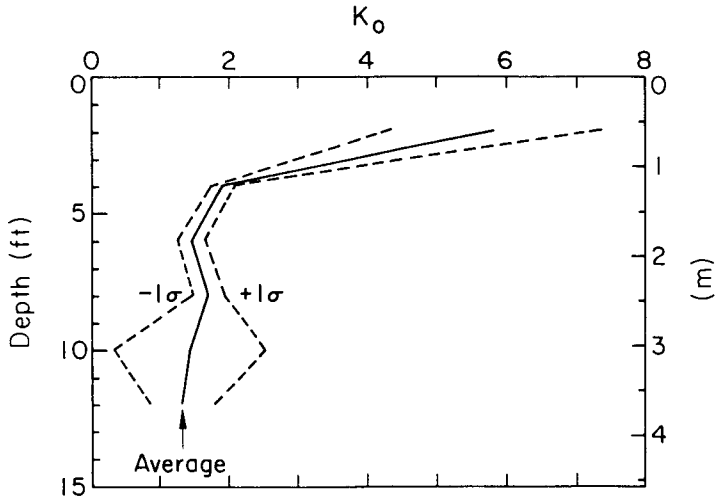

Figure 3-43. Average K_o from PMT, Hickling Station Grillage Set Nos. 4 and 84, Outside

the E_m values, the E_r values in the backfill and native soil tend to converge at a depth of 8 to 10 ft (2.44 to 3.05 m).

Borehole Shear Tests (BST)

Four BST profiles were done at the Hickling Station site, with three in the backfill and one in the native soil. Multiple stage testing methods were used for the BSTs, in which the normal stress exerted by the shear plates on the

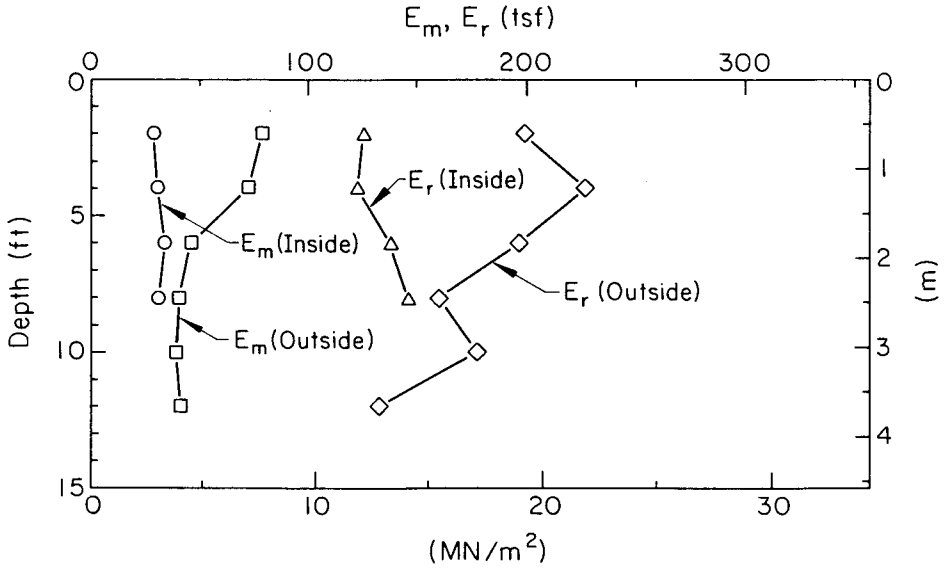

Figure 3-44. Average E_m and E_r from PMT, Hickling Station Grillage Set Nos. 4 and 84

borehole wall was increased without relocating the shear heads after each peak shear stress was recorded.

The BST can be used to provide an estimate of the plane strain friction angle that can be adjusted by a correction factor to determine an axisymmetric friction angle. However, given the gravelly nature of the site, such corrections are not justified. The authors are unaware of BST data reported in the literature for gravel.

Table 3-22 lists the individual BST results in terms of normal stress and peak shear stress on the borehole wall. Figure 3-45 shows the BST results for grillage 4-NW outside the backfill zone. Test data of normal versus shear stress for depths from 4 to 9 ft (1.22 to 2.74 m) are shown. There is no consistent trend in the data with depth, but the tests done at 4 ft (1.22 m) are higher than the others, and the deepest test at 9 ft (2.74 m) falls closest to the lower bound. The scatter in the data suggests that upper and lower bounds to the estimated friction angle are most appropriate. Since the soils at the test site primarily were coarse-grained, and there was no water observed in any of the borings, drained friction angles can be calculated from the BST data. The upper and lower bounds of friction angle, $\bar{\phi}$, estimated from the BST data for the test done outside the backfill are 38.3° and 32.7°, respectively. It should be

Table 3-22

BOREHOLE SHEAR TEST DATA

Test Location	Depth ft	Depth m	Normal Stress psi	Normal Stress kN/m^2	Shear Stress psi	Shear Stress kN/m^2
4-NW	4	1.22	7.7	53.3	7.1	48.8
BST-1			14.3	98.4	9.8	67.8
Outside			19.8	136.6	14.9	103.0
			25.8	177.6	21.4	147.3
4-NW	6	1.83	7.9	54.6	4.9	33.5
BST-2			14.1	97.0	8.7	59.7
Outside			20.0	138.0	11.7	80.9
			25.7	176.9	15.8	109.0
			31.7	218.6	21.4	147.3
4-NW	8	2.44	8.7	60.1	5.0	34.8
BST-3			14.3	98.4	8.1	55.6
Outside			20.6	142.1	12.0	82.7
			26.0	179.0	22.7	156.4
4-NW	9	2.74	8.1	56.0	5.8	40.2
BST-4			14.3	98.4	8.1	55.1
Outside			20.2	139.4	10.9	75.0
			26.0	179.0	14.8	101.7
			32.1	221.4	19.1	132.0
			38.0	262.3	24.0	165.4
4-SE	4	1.22	7.9	54.6	4.5	30.7
BST-1			14.3	98.4	8.1	56.0
Inside			20.1	138.7	8.3	56.9
			25.8	177.6	8.3	56.9
4-SE	6	1.83	7.9	54.6	6.1	42.0
BST-2			15.1	103.8	7.9	54.7
Inside			20.0	138.0	8.9	61.5
			26.2	180.4	8.3	56.9
4-SE	8	2.44	8.3	57.4	5.0	34.4
BST-3			14.2	97.7	9.5	65.6
Inside			20.2	139.4	11.9	81.8
			26.0	179.0	18.2	125.6
			31.9	220.0	21.0	144.6
84-NE	4	1.22	7.9	54.5	3.5	24.4
BST-1			15.8	109.0	5.6	38.9
Inside			23.7	163.5	10.5	72.3
			31.7	218.7	14.4	99.4
			39.6	273.2	14.2	97.6
			47.6	328.4	12.2	84.0

Table 3-22

BOREHOLE SHEAR TEST DATA (Continued)

Test Location	Depth ft	Depth m	Normal Stress psi	Normal Stress kN/m^2	Shear Stress psi	Shear Stress kN/m^2
84-NE	8	2.44	7.9	54.6	5.6	38.9
BST-2			13.9	95.6	9.3	63.8
Inside			19.8	136.6	13.0	89.5
			25.8	177.6	16.7	114.8
			31.7	218.6	24.5	169.0
84-NE	8.5	2.59	7.9	54.6	4.5	30.7
BST-3			11.9	82.1	5.8	39.7
Inside			15.9	109.3	7.3	50.6
			19.8	136.6	6.9	47:9
			23.8	163.9	5.9	40.7
			31.7	218.6	4.6	31.7
84-SW	4	1.22	8.1	56.0	5.5	38.0
BST-1			14.3	98.4	8.7	59.7
Inside			19.8	136.6	12.7	87.7
			25.7	176.9	19.3	132.9
			31.6	217.9	23.1	159.1
84-SW	6	1.83	7.9	54.7	5.4	37.1
BST-2			13.9	95.6	8.8	61.0
Inside			20.1	138.7	12.9	88.6
			26.0	179.0	17.4	119.8
			31.7	218.6	21.7	149.6
84-SW	8	2.44	7.9	54.6	6.3	43.4
BST-3			13.9	95.6	9.4	65.1
Inside			20.0	138.0	11.0	75.9
			25.9	178.3	14.3	98.5
			31.7	218.6	22.3	153.7

noted that unusually high shear stress values can occur because of "plowing" of the shear plates into gravel particles and may represent anomalous values.

Figures 3-46, 3-47, and 3-48 show BST data from tests done on the backfill material at grillage Nos. 4-SE, 84-NE, and 84-SW, respectively. Again, upper and lower bounds were established based on inspection of the data. For the tests done inside the backfill, the upper bound friction angle ranged from 33.7° to 36.5°. The lower bound friction angle ranged from 24.5° to 29.8°. Again, there

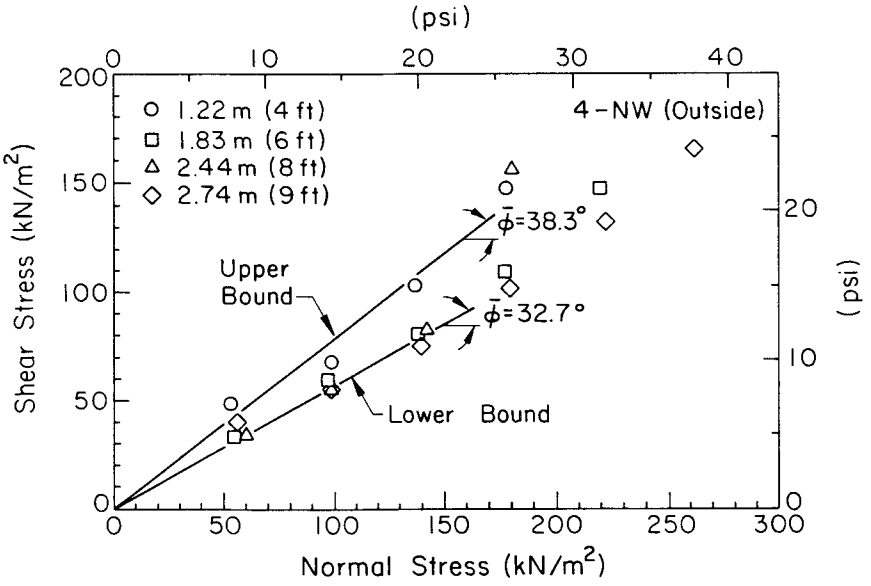

Figure 3-45. BST Normal versus Shear Stress, Hickling Station Grillage No. 4-NW, Outside

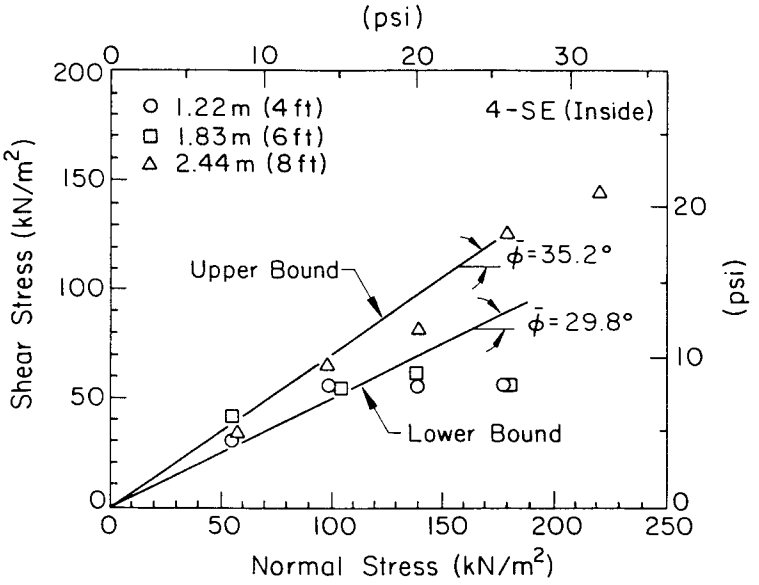

Figure 3-46. BST Normal versus Shear Stress, Hickling Station Grillage No. 4-SE, Inside

was no consistent trend of $\bar{\phi}$ with depth in the backfill, and there is a fair degree of scatter in the test results from a given depth at an individual grillage. However, the deep tests tended to have results closer to the lower bound envelopes.

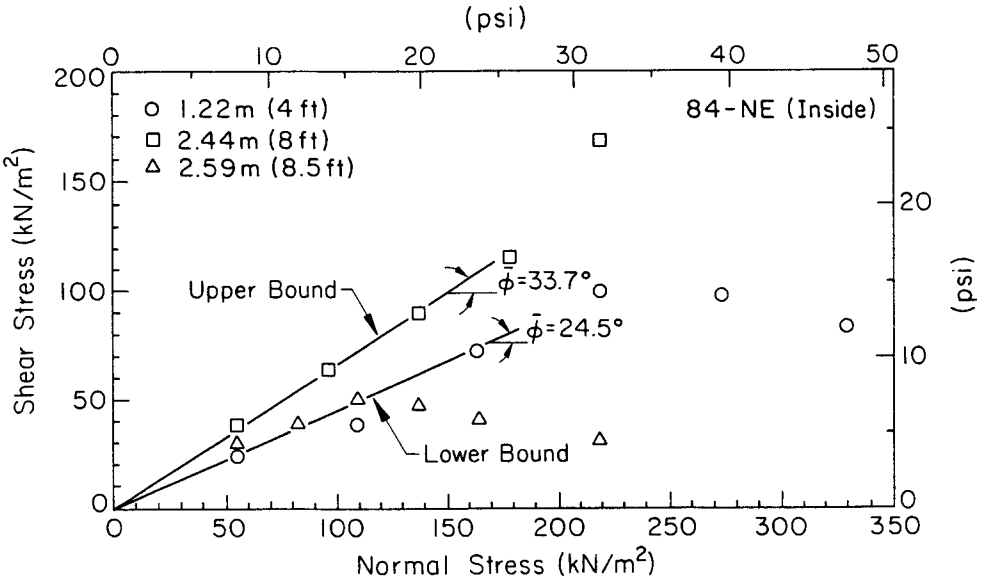

Figure 3-47. BST Normal versus Shear Stress, Hickling Station Grillage No. 84-NE, Inside

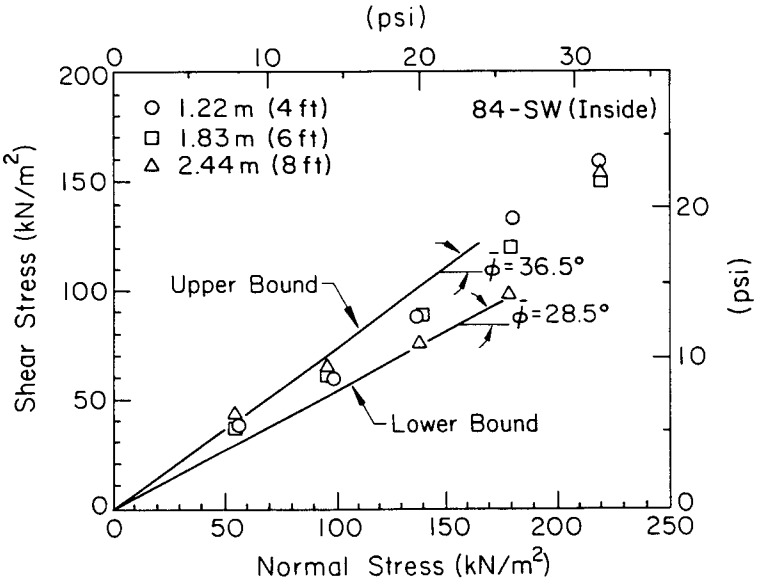

Figure 3-48. BST Normal versus Shear Stress, Hickling Station Grillage No. 84-SW, Inside

Table 3-23 summarizes the BST friction angles from tests done in the backfill and native soil. The average backfill lower bound friction angle was 27.6°, as compared with 32.7° for the lower bound on the native material. Correspondingly, the average $\bar{\phi}$ upper bound of the backfill was 35.1° versus 38.3° as the upper bound on the native soil. Although there are few test data, the average

Table 3-23

FRICTION ANGLES FROM BOREHOLE SHEAR DATA

Test Location	Friction Angle, $\bar{\phi}$ (deg) Lower Bound	Upper Bound
4-NW (Outside)	32.7	38.3
4-SE (Inside)	29.8	35.2
84-NE (Inside)	24.5	33.7
84-SW (Inside)	28.5	36.5
Average (Inside)	27.6	35.1
COV (%) (Inside)	10.1	4.0

backfill friction angles are nearly two standard deviations lower than the corresponding bounds for the native soil. These values indicate a looser backfill than the native soil.

These BST data can be used to provide estimates of the matrix [grain size < 0.08 in. (2 mm)] shear strength of the soil, because of the limited size of the shear plates relative to the particle sizes. The actual shear strength and friction angles probably are larger than those determined by the BST. The tendency from the BSTs was that the test data from the deep tests at 8 to 9 ft (2.44 to 2.74 m) often fell near the lower bound envelopes, indicating a generally decreasing $\bar{\phi}$ with increasing depth.

Drive Cone Tests (DCT)

Drive cone penetration tests (DCT) have been used in sands by a number of authors (18 - 21). More recently, DCT data have been presented for gravelly soils (22, 23). The difficulty with many of the investigations and correlations using DCTs occurs because the tests were not conducted using a standardized cone or standardized drop energy. Therefore, no well-defined correlations have been presented for estimating friction angles directly from DCT tests. Indirect correlations between DCT resistance and D_r have been suggested (22), along with

correlations between SPT N values and CPT q_c values (20). Since DCT correlations are speculative at the present time, the tests were used solely to provide a comparison of the relative strengths between the grillage backfill and native soil. Since the DCT cone is driven without stopping, other than to add more drill rod, these tests also provide a nearly continuous record of the stratigraphy. The typical presentation method is to plot cumulative blow counts over the sounding depth rather than blows per unit distance.

Tables 3-24 and 3-25 give the DCT data in terms of blows/ft or 0.3 m and cumulative blows/ft or 0.3 m for tests done in the Nos. 4 and 84 backfill, respectively. The native soil DCT data are given in Table 3-26.

Figure 3-49 shows the cumulative DCT N values for tests in the backfill at the Nos. 4 and 84 grillages. In the upper 7 ft (2.13 m), the test in the backfill at grillage No. 4-NW shows somewhat higher resistance, while the other tests almost are identical. Below 7 ft (2.13 m), the backfill DCTs at the No. 84 grillages show lower cumulative N values than the No. 4 grillage backfill, which again indicates a softer backfill near the grillage bases at the No. 84 sites.

Table 3-24

DCT DATA, HICKLING STATION GRILLAGE SET NO. 4, INSIDE

Depth (ft)	Drive Cone N_{DCT} (blows/ft or 0.3 m) per Grillage and Sounding				Cum.	
	4-NW, DCT-1		4-SE, DCT-1			
	per ft	Cum.	per ft	Cum.	Avg.	COV (%)
1	16	16	4	4	10.0	84.9
2	17	33	7	11	22.0	70.7
3	14	47	8	19	33.0	60.0
4	12	59	7	26	42.5	54.9
5	9	68	12	39	53.5	38.3
6	12	80	21	60	70.0	20.2
7	11	91	22	82	86.5	7.4
8	15	106	18	100	103.0	4.1
9	16	122	27	127	124.5	2.8
10	15	137	21	148	142.5	5.5
Average:						34.9

1 ft = 0.305 m

Table 3-25

DCT DATA, HICKLING STATION GRILLAGE SET NO. 84, INSIDE

Depth (ft)	Drive Cone N_{DCT} (blows/ft or 0.3 m) per Grillage and Sounding				Cum.	
	84-NE, DCT-2		84-SW, DCT-1			
	per ft	Cum.	per ft	Cum.	Avg.	COV (%)
1	6	6	6	6	6.0	0.0
2	10	16	6	12	14.0	20.2
3	8	24	11	23	23.5	3.0
4	7	31	9	32	31.5	2.2
5	8	39	9	41	40.0	3.5
6	9	48	13	54	51.0	8.3
7	8	56	12	66	61.0	11.6
8	10	66	10	76	71.0	10.0
9	5	71	7	83	77.0	11.0
10	3	74			74.0	
Average:						7.8

1 ft = 0.305 m

Figure 3-50 shows the cumulative DCT N values from all tests made in the native soil. In the upper 11 to 13 ft (3.35 to 3.96 m), the rate of increase in the cumulative N values is the same for all tests, indicating similar material. Below 11 to 13 ft (3.35 to 3.96 m), there is a stiffness transition, as indicated by the change of slopes in the data.

The average cumulative DCT N values for all test locations are shown in Figure 3-51. Based on the average values, the No. 84 backfill is less dense than the No. 4 backfill. The native soil had greater average driving resistance than either of the backfilled zones, although the difference may not be statistically significant.

Dilatometer Tests (DMT)

Flat-plate dilatometer tests were done at one grillage in the backfill. DMT testing was stopped because of damage to the blade and steel membrane. The DMT data consist of two field test readings, A and B, and two calibration readings, ΔA and ΔB. The A reading is the stress at which the steel membrane separates

Table 3-26

DCT DATA, HICKLING STATION GRILLAGE SET NOS. 4 AND 84, OUTSIDE

Depth (ft)	Drive Cone N_{DCT} (blows/ft or 0.3 m) per Grillage and Sounding: 4-NW, DCT-2 per ft	4-NW, DCT-2 Cum.	4-SE, DCT-2 per ft	4-SE, DCT-2 Cum.	84-NE, DCT-1 per ft	84-NE, DCT-1 Cum.	84-SW, DCT-2 per ft	84-SW, DCT-2 Cum.	Cum. Avg.	Cum. COV (%)
1	9	9	11	11	16	16	4	4	10.0	49.3
2	17	26	22	33	16	32	8	12	25.8	40.2
3	16	42	16	49	22	54	20	32	44.3	21.8
4	12	54	15	64	23	77	19	51	61.5	17.3
5	10	64	19	83	14	91	16	67	76.3	13.2
6	13	77	21	104	16	107	18	85	93.3	10.8
7	15	92	17	121	18	125	18	103	110.3	8.9
8	12	104	16	137	17	142	17	120	125.8	7.7
9	13	117	12	149	18	160	12	132	139.5	8.3
10	14	131	13	162	14	174	16	148	153.8	6.9
11	13	144	18	180	14	188	25	173	171.3	3.6
12	17	161	41	221	15	203	18	191	194.0	7.6
13	23	184			26	229	15	206	206.3	10.9
14	21	205			57	286	37	243	244.7	16.6
15	18	223			66	352	43	286	287.0	22.5
16	39	262					20	306	284.0	11.0
17	59	321					23	329	325.0	1.7
18	59	380					32	361	370.5	3.6
19							9	370	370.0	
20							23	393	393.0	
Average:										14.5

1 ft = 0.305 m

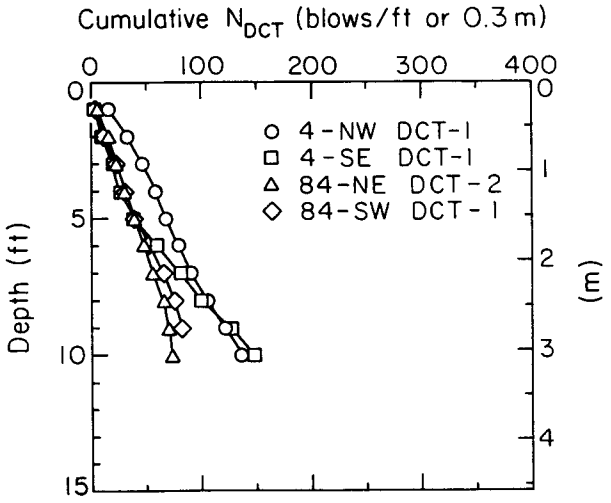

Figure 3-49. DCT Cumulative N, Hickling Station Grillage Set Nos. 4 and 84, Inside

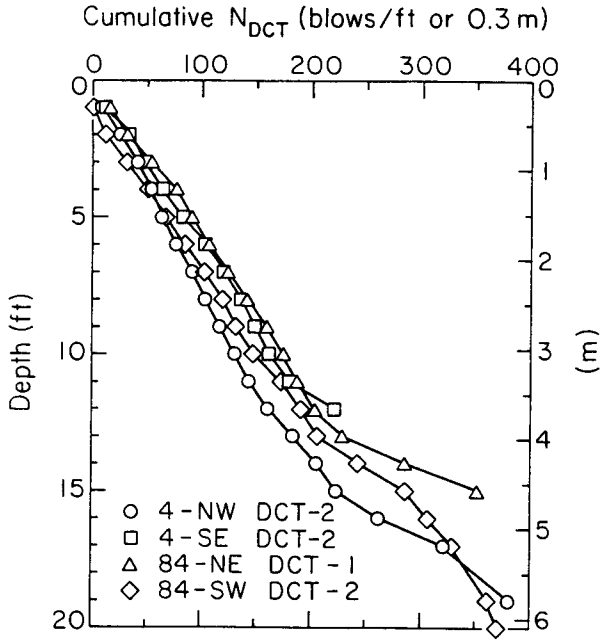

Figure 3-50. DCT Cumulative N, Hickling Station Grillage Set Nos. 4 and 84, Outside

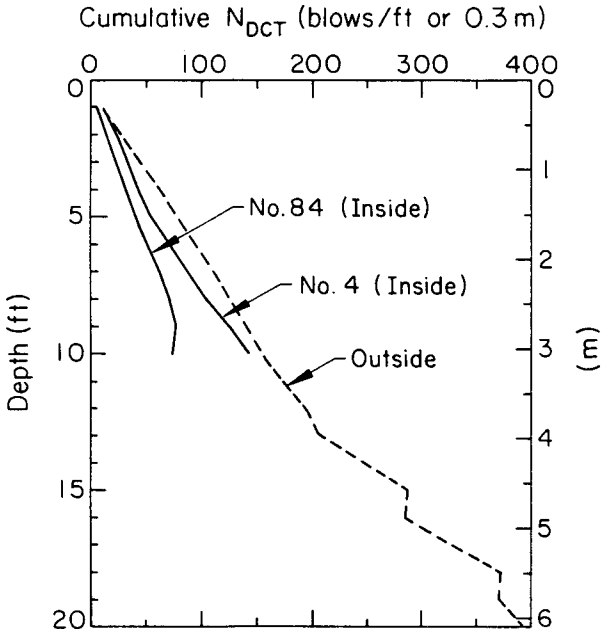

Figure 3-51. Average DCT Cumulative N, Hickling Station

from a sensing disk, which ideally represents initial soil contact. The B reading is made at an outward membrane deflection of 0.043 in. (1.1 mm). The ΔA

calibration reading represents the vacuum necessary for the steel membrane to remain seated on the sensing disk, and the ΔB reading corresponds to the stress required to move the membrane out 0.043 in. (1.1 mm) in air. These measurements are converted into the following (8):

$$p_o = 1.05(A + \Delta A - Z_m) - 0.05\ p_1 \tag{3-17}$$

$$p_1 = B - \Delta B - Z_m \tag{3-18}$$

in which Z_m = gage pressure deviation from zero when vented to the atmosphere.

These measurements then can be converted into the following index parameters (8):

$$I_D = (p_1 - p_o)/(p_o - u_o) \tag{3-19}$$

$$K_D = (p_o - u_o)/\bar{\sigma}_{vo} \tag{3-20}$$

$$E_D = 34.7\ (p_1 - p_o) \tag{3-21}$$

in which I_D = material index, K_D = horizontal stress index, E_D = dilatometer modulus, u_o = assumed hydrostatic pore water pressure, and $\bar{\sigma}_{vo}$ = effective vertical stress. Note that the coefficient used in computing E_D in Equation 3-21 originally was 38.2 (7).

These index parameters were used to determine a soil description, K_o values, and Young's modulus, E. Table 3-27 lists the DMT stresses p_o and p_1, along with the average index parameters and dilatometer moduli based on the equations given above.

The K_o values were determined using two methods. The original method proposed by Marchetti (7) was used, as given by:

$$K_o = (K_D/1.5)^{0.47} - 0.6 \tag{3-22}$$

A second method also was proposed by Marchetti (24), based on field data for sand from the Po River in Italy. This method further relies upon the normalized q_c/p_a values from the CPT. The expression for K_o using combined DMT/CPT data is:

Table 3-27

DMT DATA, HICKLING STATION GRILLAGE NO. 84-NE, INSIDE

Depth (ft)	$\bar{\sigma}_v$ (ksc)	84-NE Inside Avg. q_c (ksc)	DMT-1 P_o (bar)	DMT-1 P_1 (bar)	DMT-2 P_o (bar)	DMT-2 P_1 (bar)	DMT-3 P_o (bar)	DMT-3 P_1 (bar)	I_D Avg.	I_D COV (%)	K_D Avg.	K_D COV (%)	K_o[a] Avg.	K_o[a] COV (%)	K_o[b] Avg.	K_o[b] COV (%)	Dilatometer Modulus, E_D (bar) Avg.	Dilatometer Modulus, E_D (bar) COV (%)	Young's Modulus, E[c] (MN/m^2) Avg.
1	0.059	23.0			0.67	1.72	0.76	2.60	2.00	30.0	12.45	8.9	0.88	9.0	2.10	5.4	51	36.7	4.5
2	0.117	28.0	0.65	6.32	0.75	2.32	2.47	8.30	4.39	85.5	11.23	79.3	0.93	67.7	1.85	48.9	151	55.4	13.4
3	0.176	37.6	2.57	5.62	0.26	5.72	0.95	3.00	8.12	137.5	7.31	94.1	0.68	71.9	1.33	73.2	122	49.8	10.8
4	0.234	24.0	1.85	5.42	1.19	6.02	1.46	13.80	6.26	49.6	6.53	22.1	0.73	14.1	1.39	14.9	240	68.6	21.3
5	0.293	36.0			(5.57	10.72)													
7	0.410	49.8					1.07	4.80	3.49		2.66		0.43		0.71		129		11.5
8	0.469	51.0					0.83	3.30	2.98		1.81		0.39		0.49		86		7.6
Averages:									4.54	61.8	7.00	69.6	0.67	40.7	1.31	35.6	130	49.6	11.5

1 ft = 0.305 m; 1 ksc = 1.02 tsf = 0.098 MN/m^2; 1 bar = 1.04 tsf = 1.02 ksc = 0.10 MN/m^2

a - Marchetti (24)

b - Marchetti (7)

c - $E = E_D (1 - \nu^2)$; $\nu = 0.33$

$$K_o = 0.359 + 0.071\ K_D - 0.00093\ (q_c/\bar{\sigma}_{vo}) \qquad (3\text{-}23)$$

Young's modulus, E, also can be estimated from the dilatometer modulus, E_D, as given by:

$$E = E_D\ (1 - \nu^2) \qquad (3\text{-}24)$$

in which ν = Poisson's ratio. As described earlier, $\nu = 0.33$ was selected for the data reduction, corresponding to an approximate upper bound for loose sand and lower bound for dense sand.

Figure 3-52 shows soil descriptions and soil unit weights as related to the DMT parameters E_D and I_D. Table 3-28 gives soil descriptions and unit weights based on the DMT data at grillage No. 84-NE. Based on the correlations in Figure 3-52, the backfill at grillage No. 84-NE primarily is a loose sand with a normalized unit weight of $\gamma/\gamma_w \approx 1.75$. This normalized unit weight is equivalent

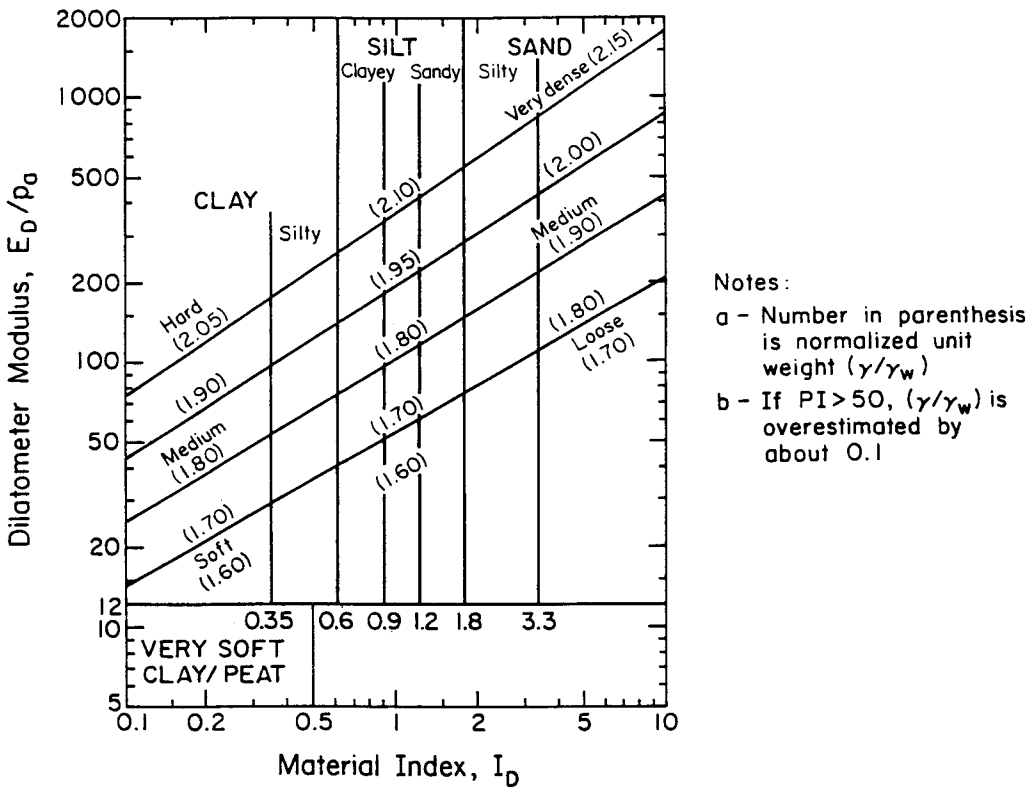

Figure 3-52. Determination of Soil Description and Unit Weight by DMT

Source: Schmertmann (8), p. 98.

Table 3-28

SOIL DESCRIPTIONS AND UNIT WEIGHTS FROM DMT, HICKLING STATION GRILLAGE NO. 84-NE, INSIDE

Depth (ft)	Avg. E_D/P_a	Avg. I_D	Soil Description	γ/γ_w
1	50	2.0	loose silty SAND	1.65
2	149	4.4	loose SAND	1.80
3	120	8.1	loose SAND	1.70
4	237	6.3	loose to medium SAND	1.85
7	127	3.5	loose SAND	1.80
8	85	3.0	loose silty SAND	1.65
Averages:	128	4.6	loose SAND	1.75

1 ft = 0.305 m

to γ = 109 pcf (17.2 kN/m^3), which may be lower than the actual value, considering the presence of gravel and cobbles at the site.

Figure 3-53 shows the backfill K_o values based on the DMTs at grillage No. 84-NE. The method based on DMT data alone (7) results in higher K_o values than obtained using the combined DMT/CPT method (24) by roughly a factor of two. The original Marchetti method (7) results in K_o values that are near 2 at the surface and decrease to 0.5 at a depth of 8 ft (2.44 m).

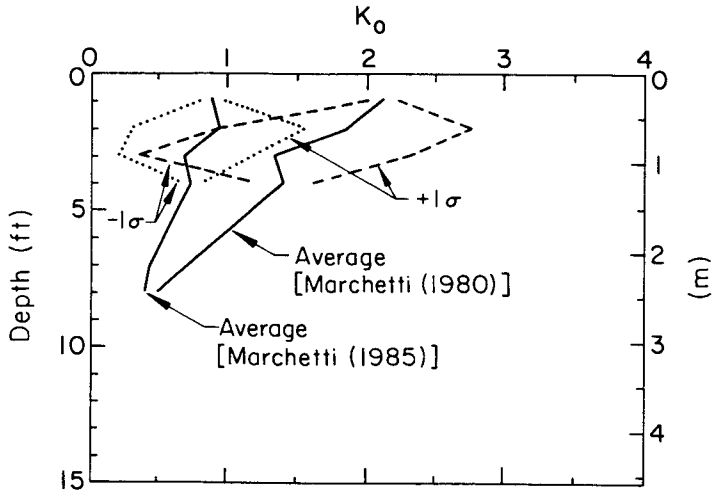

Figure 3-53. Average K_o from DMT, Hickling Station Grillage No. 84-NE, Inside

The moduli data from the few DMTs are shown in Figure 3-54. Despite the clear trend in increasing E with depth, the ± one standard deviation range is significant, indicating that the modulus could be between 80 and 350+ tsf (7.7 to 33.5+ MN/m^2). These DMT values are considered unreliable because of the presence of gravel.

Comparisons Between In-Situ Tests

Comparisons between the correlated soil properties are important, given the range of in-situ tests performed and the variability within each set of correlated data. In addition, the comparisons identify common trends in the data and test results that are unusually high or low. Final selection of the soil properties used in the uplift capacity predictions must be based on an evaluation of all test data. The following sections give the average results of D_r, $\bar{\phi}$, K_o, and E from the SPT, CPT, PMT, BST, and DMT results.

Figure 3-55 gives the average D_r values from SPT and CPT results in the backfill at grillage set No. 4. The CPT data show a loose zone between 3 and 5 ft (0.91 and 1.52 m). This looser zone was not identified with the SPT but, since the SPT data do not include direct values between 3 and 5 ft (0.91 and 1.52 m), the looser zone may have been missed because of the spacing of the SPT N values. The average D_r values from SPT and CPT results in the backfill at grillage set No. 84 are shown in Figure 3-56. The D_r values between the two in-situ tests are in close agreement, with the CPT values a bit higher than those determined from the SPT. The data intervals from the SPT, since they are spaced more

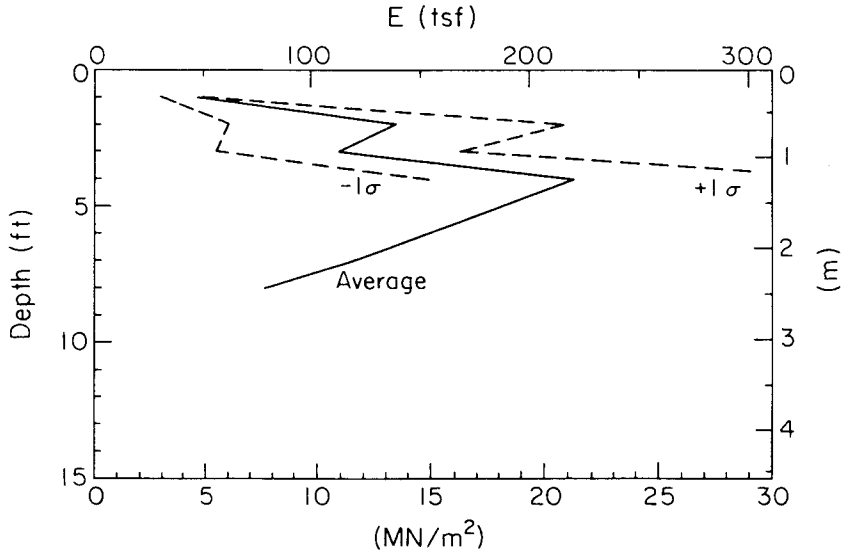

Figure 3-54. Average E from DMT, Hickling Station Grillage No. 84-NE, Inside

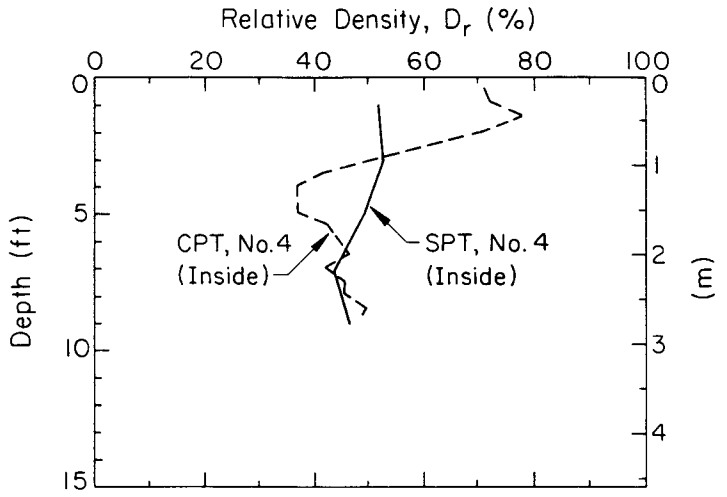

Figure 3-55. Average D_r from SPT and CPT, Hickling Station Grillage Set Nos. 4 and 84, Inside

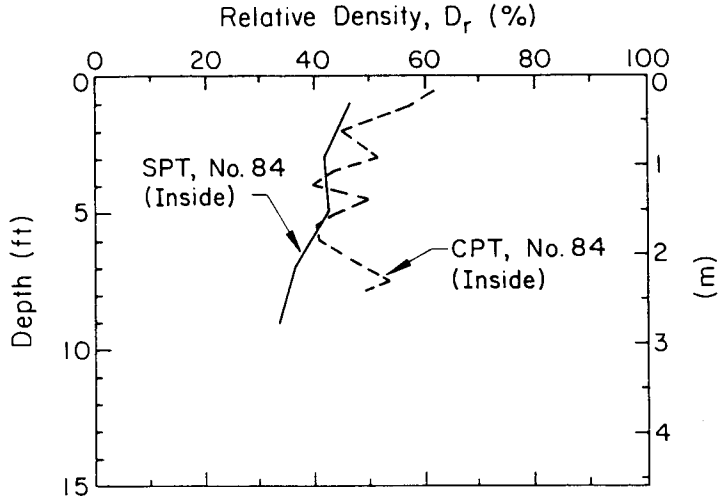

Figure 3-56. Average D_r from SPT and CPT, Hickling Station Grillage Set No. 84, Inside

widely than the CPT, do not show as high a variability as the D_r values from the CPT.

Figure 3-57 compares SPT and CPT D_r values in the native soil outside the backfill for both grillage sets. In the upper 11 ft (3.35 m), D_r from SPTs is about 10 percent less than the CPT D_r values.

Friction angle, $\bar{\phi}$, comparisons from the SPT and CPT measurements in the backfill

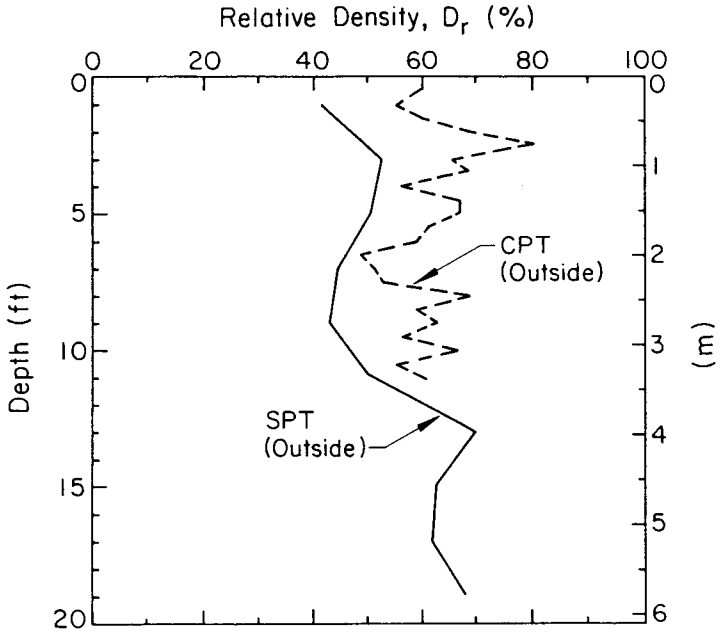

Figure 3-57. Average D_r from SPT and CPT, Hickling Station Grillage Set Nos. 4 and 84, Outside

at grillage set No. 4 are shown in Figure 3-58. Again, the SPT data do not evaluate the looser zone between 3 and 5 ft (0.91 and 1.52 m). However, the differences between the estimated $\bar{\phi}$ values are relatively small.

The $\bar{\phi}$ values from SPT and CPT data in the backfill at grillage set No. 84 are

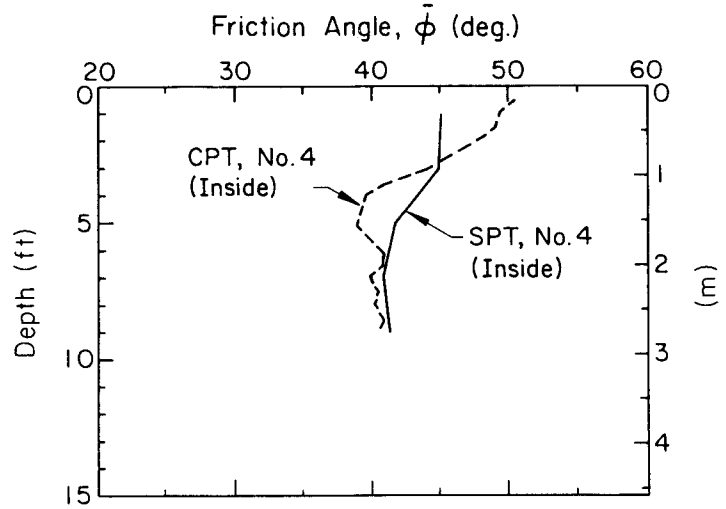

Figure 3-58. Average $\bar{\phi}$ from SPT and CPT, Hickling Station Grillage Set No. 4, Inside

shown in Figure 3-59. The trend lines between SPT and CPT $\bar{\phi}$ values are nearly parallel, with the CPT values a few degrees higher. The $\bar{\phi}$ values from CPTs in the backfill at grillage set Nos. 4 and 84 are nearly the same. The SPT data in the backfill at grillage set No. 4 agree well with both sets of CPT backfill $\bar{\phi}$ values, but they are higher than the SPT $\bar{\phi}$ values in the backfill at grillage set No. 84.

Figure 3-60 compares the friction angles determined from both SPT and CPT data in the native soil. Except for the upper few feet, the two test methods give similar $\bar{\phi}$ values from 3 to 11 ft (0.91 to 3.35 m), with the CPT data slightly higher.

Since there were similarities between the CPT and SPT friction angles in the backfill at both grillage sets and the native soil, the CPT and SPT data were averaged to determine an overall trend in $\bar{\phi}$. These trends are shown in Figure 3-61, along with the upper and lower bound ranges from BSTs done in the backfill and native soil. The average outside values from the SPT, CPT, and BST are higher than those from similar tests in the backfill. As described earlier, the BST results do not account for the presence of large gravel particles or cobbles in the soil, and therefore they are lower than values evaluated by other means. In addition, the BST gives values much lower than those normally observed with gravel and rockfill materials (25, 26). These studies and others consistently show $\bar{\phi}$ values for very coarse soils at low stress levels to be well above 40° when loose and above 50° when dense. The trend for the backfill $\bar{\phi}$ is about

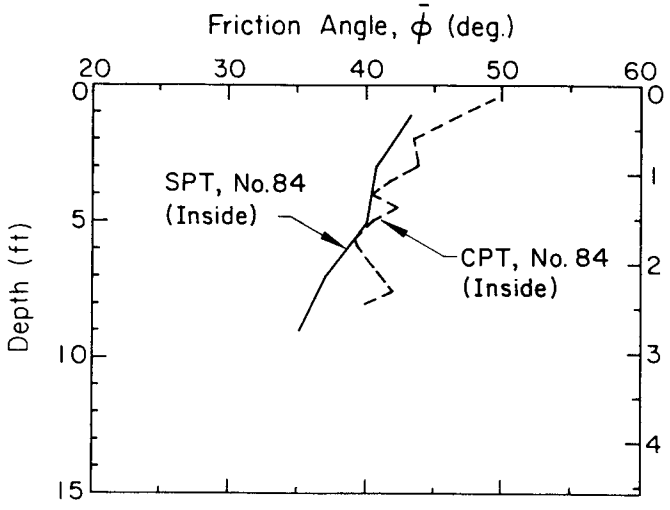

Figure 3-59. Average $\bar{\phi}$ from SPT and CPT, Hickling Station Grillage Set No. 84, Inside

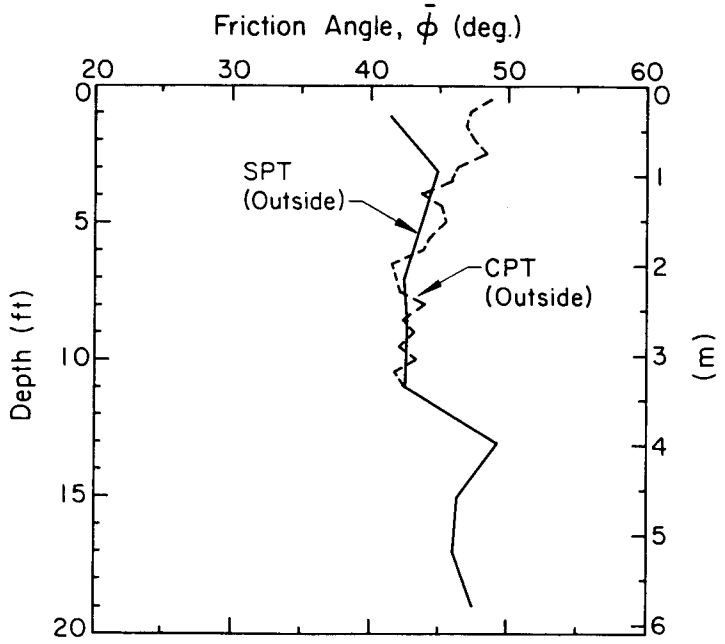

Figure 3-60. Average $\bar{\phi}$ from SPT and CPT, Hickling Station Grillage Set Nos. 4 and 84, Outside

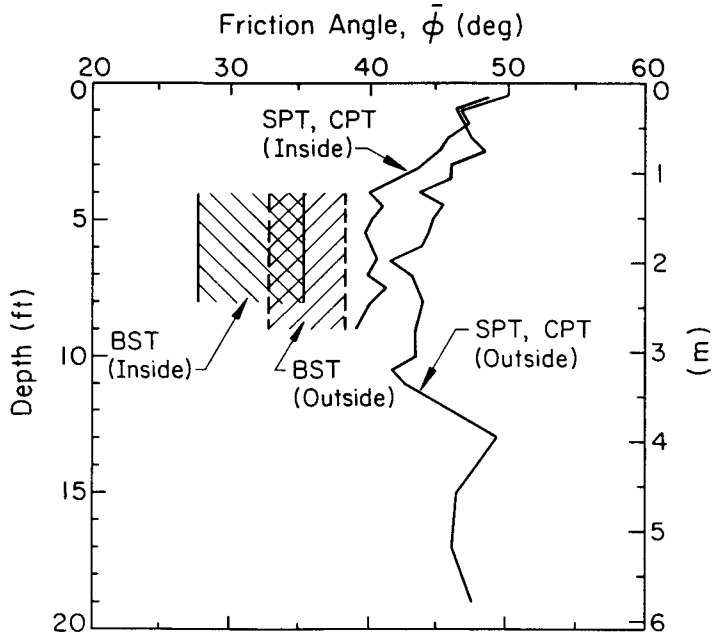

Figure 3-61. Average $\bar{\phi}$ from In-Situ Tests, Hickling Station

2 to 4 degrees lower than the native soil $\bar{\phi}$ over the upper 10 ft (3.05 m).

Simplified $\bar{\phi}$ profiles derived from the in-situ tests in the backfill and native

soil are shown in Figure 3-62. For the backfill, $\bar{\phi}$ decreases from 49° at the surface to 41° at a depth of 4 ft (1.22 m). From 4 to 8 ft (1.22 to 2.44 m), $\bar{\phi}$ in the backfill decreases from 41° to 40°. Below 8 ft (2.44 m), $\bar{\phi}$ in the backfill remains constant at 40°. For the native soil, $\bar{\phi}$ decreases from 49° at the surface to 43° at a depth of 6 ft (1.83 m). From 6 to 11 ft (1.83 m to 3.35 m), the native soil $\bar{\phi}$ decreases to 42°, followed by an increase in $\bar{\phi}$ as depth increases.

The CPT, PMT, and DMT data all were used to estimate K_o. The average K_o values determined in the backfill and native soil from these in-situ tests are shown in Figure 3-63. The PMT data in the native soil are noticeably higher than all the other values and probably are too high. The PMT backfill K_o values and those determined using methods given by Marchetti (7) are in reasonable agreement. The DMT (7) and combined DMT/CPT (24) methods bracket the K_o values determined from all the CPT tests. A simplified K_o profile from the in-situ tests is shown in Figure 3-64. The PMT data were considered abnormally high and were discounted heavily when evaluating the simplified profile. From Figure 3-64, K_o decreases from 2.0 at the surface to 1.0 at a depth of 4 ft (1.22 m). From 4 to 10 ft (1.22 to 3.05 m), K_o decreases to 0.75 and then remains constant.

The average moduli values determined from all the in-situ tests at Hickling Station are shown in Figure 3-65. There is a considerable range of moduli,

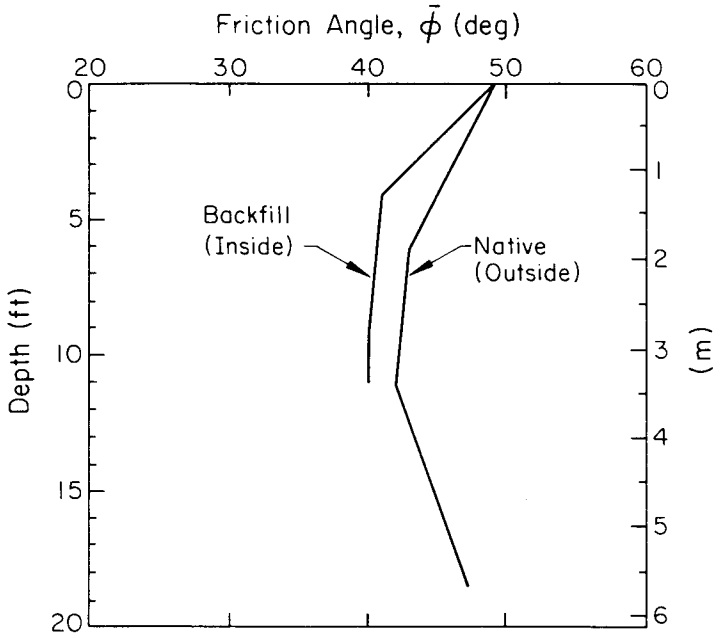

Figure 3-62. Simplified $\bar{\phi}$ Profile from In-Situ Tests, Hickling Station

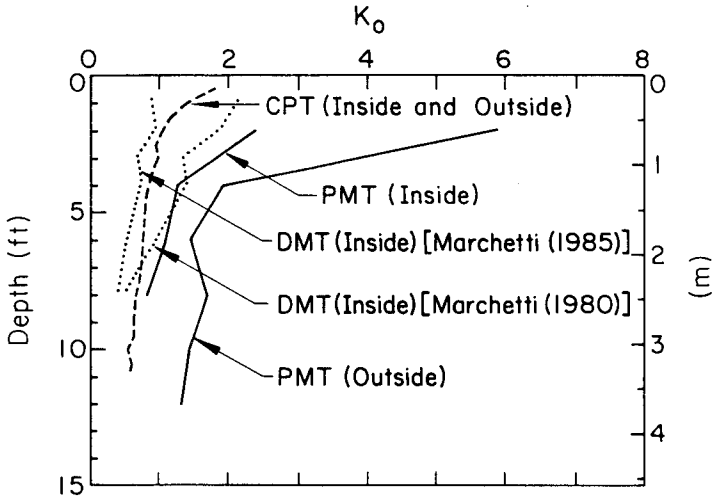

Figure 3-63. Average K_o from In-Situ Tests, Hickling Station

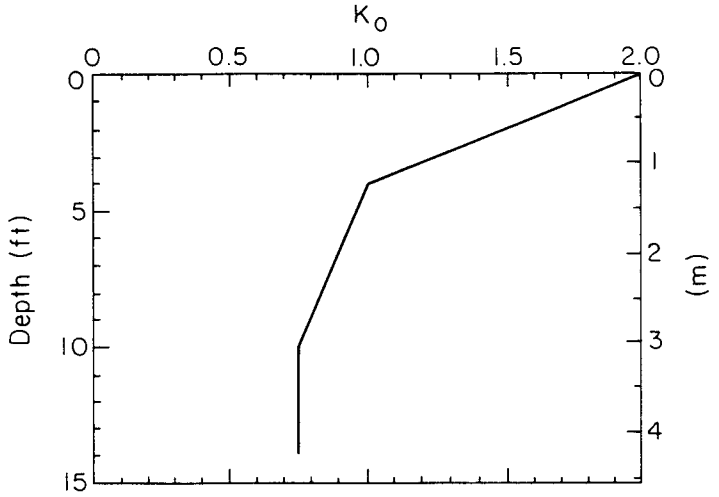

Figure 3-64. Simplified K_o Profile from In-Situ Tests, Hickling Station

depending on the test. The PMT initial moduli, E_m, are substantially lower than all other values. However, the unload-reload moduli, E_r, from the PMTs are within the range of moduli determined from CPT and DMT. A simplified modulus profile from the in-situ data is shown in Figure 3-66. A range of E is shown because there was no clear trend in the differences between the backfill and native soil profiles.

The moduli at the Hickling Station site range from 50 to 100 tsf (4.8 to 9.6 MN/

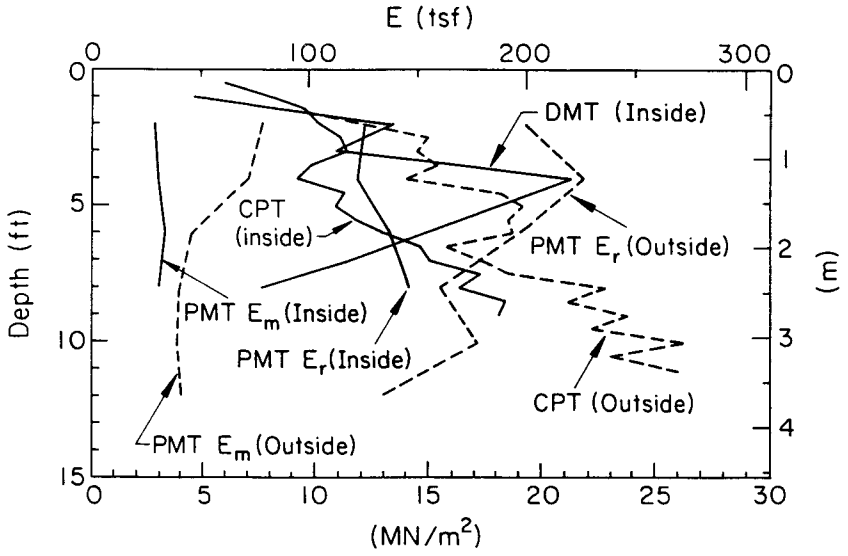

Figure 3-65. Average E from In-Situ Tests, Hickling Station

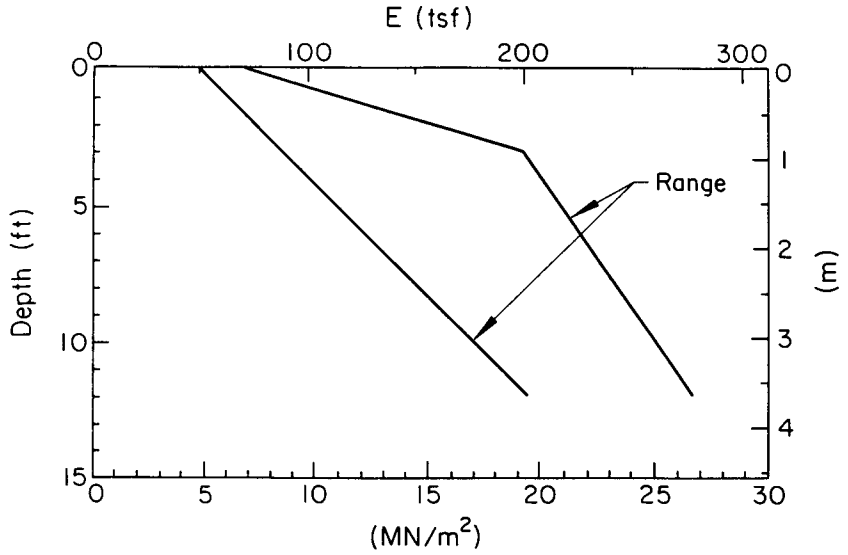

Figure 3-66. Simplified E Profile from In-Situ Tests, Hickling Station

m^2) at the surface to 200 to 275 tsf (19.1 to 26.3 MN/m^2) at a depth of 12 ft (3.66 m). In general, the native soil moduli tend to fall near the upper range shown in Figure 3-66.

WYNCOOP CREEK TESTS

The only in-situ tests conducted at the Wyncoop Creek site were the SPT and DCT. Summary tables of the in-situ data are given where appropriate in the text,

while support data and original boring logs are given in Appendix A.

Test Locations

Wyncoop Creek had one type of grillage foundation from a Lehigh X-tower. The grillages tested at Wyncoop Creek are referred to as Numbers X2-SE and X2-SW. The general site layout and structural details of these grillages are given in Section 2.

Table 3-29 lists the tests done at Wyncoop Creek. Because of the presence of large cobbles and other debris in the soil, additional in-situ testing was not possible. During excavation of the grillages, a high percentage of flat and platy boulders up to 1.5 ft (0.46 m) in diameter were found. These boulders were similar in size and shape to those in the adjacent creek bed approximately 20 ft (6.10 m) north of the old tower location. At grillage No. X2-SW, a piece of reinforced concrete approximately 3 ft x 0.3 ft x 0.3 ft (0.91 m x 0.09 m x 0.09 m) was found at a depth of roughly 5 ft (1.52 m).

The locations for the in-situ tests at Wyncoop Creek are shown in Figure 3-67. Note that while the uplift tests were done on grillage Nos. X2-SE and X2-SW, the in-situ testing was done at grillage Nos. X2-NE and X2-SW. The original plan had been to test opposite grillage Nos. X2-NE and X2-SW. However, grillage No. X2-NE was so close to the top of the adjacent creek bed that the reaction beam could not be set up without a great deal of difficulty and modification.

Table 3-29

IN-SITU TESTS AT WYNCOOP CREEK

Test Type	Grillage	Test No.	Location
SPT	X2-NE	SPT-1	Inside
	X2-NE	SPT-2	Outside
	X2-SW	SPT-1	Outside
	X2-SW	SPT-2	Inside
DCT	X2-NE	DCT-1	Inside
	X2-SW	DCT-1	Inside
	X2-SW	DCT-2	Outside

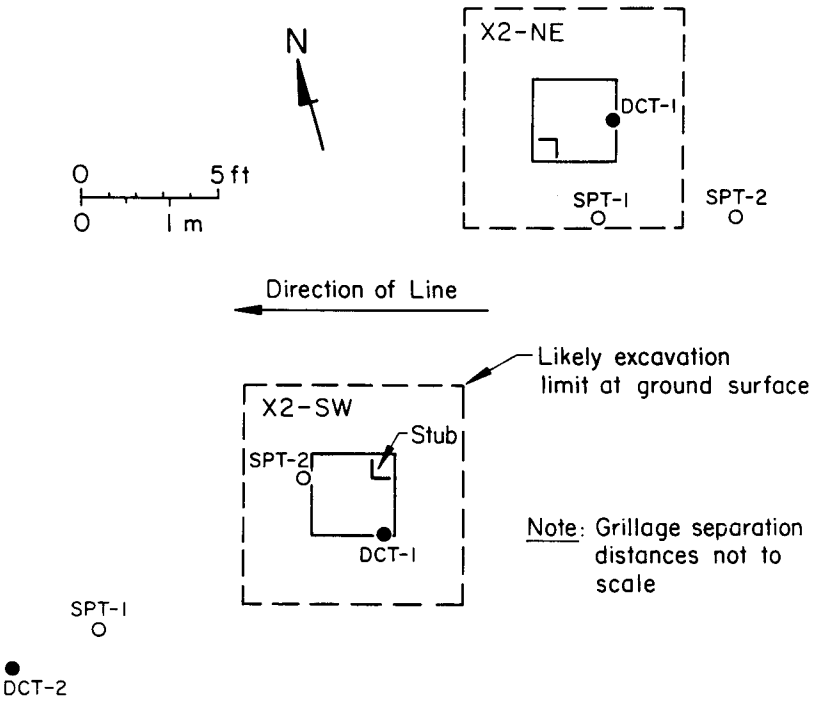

Figure 3-67. In-Situ Test Locations for Wyncoop Creek Grillages

The dashed lines in Figure 3-67 indicate likely limits for the excavations. No information was available on the construction methods or equipment used during installation of the grillages, so the excavation limits shown in Figure 3-67 have been estimated based on construction judgment and the depth and size of the grillage bases.

Standard Penetration Tests (SPT)

Four SPTs were done at the Wyncoop Creek site. Appendix A contains the boring logs for the two SPTs in the backfill and the two SPTs in the native soil.

Figure 3-68 shows a generalized soil profile as inferred from the SPT logs and excavation pits. The soil consists primarily of brown sand and gravel. Test pits also revealed large cobbles, boulders, and concrete, as described earlier. Ground water was observed at depths of 6 to 8 ft (1.83 to 2.44 m) in the excavation pits made when the grillages were removed.

An indication of the gravelly nature of the soil can be inferred from the SPT split-barrel recoveries given in Table 3-30. The average recovery was only 24

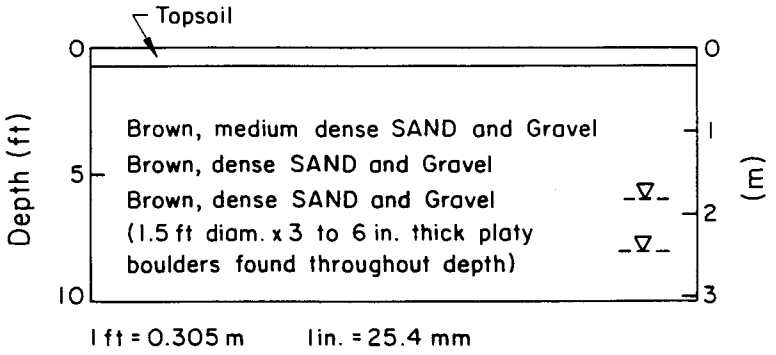

Figure 3-68. Generalized Soil Profile at Wyncoop Creek Based on Field SPT Logs

Table 3-30

SPT BORING LOG DATA, WYNCOOP CREEK

Grillage	Test No.	Boring Depth (ft)	Percent Recovery Average	Percent Recovery Cov (%)	Ground Water Depth (ft)
X2-NE	SPT-1	6.0	27	108	-
X2-NE	SPT-2	5.7	25	0	-
X2-SW	SPT-1	7.2	24	79	-
X2-SW	SPT-2	6.0	18	42	-
Averages:			24	57	6 - 8[a]

1 ft = 0.305 m

a - During grillage excavation, ground water observed at 6 to 8 ft (1.83 to 2.44 m) depth

percent, with very high coefficients of variation. As with the Hickling Station SPTs, gravel and cobbles significantly affected the sample recoveries and N values.

Figure 3-69 shows the SPT N values from both the inside and outside borings. No clear differentiation can be made between backfill and native soil resistances. The average N values from the four SPTs also are shown in the figure. The average N values increase from about 13 near the surface to near 29 at a depth of 5

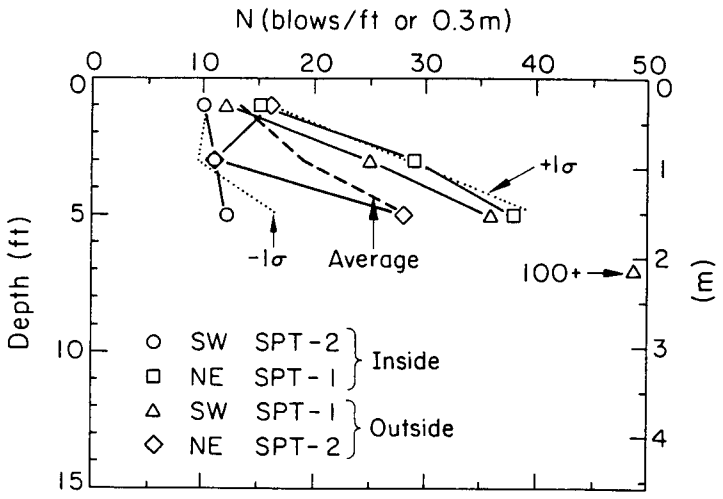

Figure 3-69. SPT N, Wyncoop Creek, Inside and Outside

ft (1.52 m). Based on the correlations given in Table 3-4, these N values would indicate a medium to dense relative density ranging from 45 to 65 percent.

Despite the known presence of cobbles and boulders, the N values were correlated with relative density, D_r, and effective stress friction angle, $\bar{\phi}$, using the averaging methods, blow count corrections, and correlation equations given previously. Tables 3-31 and 3-32 summarize the SPT data from tests in the backfill and native soil, respectively. Since the differences between backfill and native soil could not be distinguished, combined averages on the SPT data were used, as given in Table 3-33.

The combined average relative densities, D_r, from the SPT data are shown in Figure 3-70. The D_r values increase steadily from about 50 percent near the surface to about 65 percent at a depth of 5 ft (1.52 m). The high D_r values reflect the influence of the gravel, cobbles, and boulders.

The average friction angles, $\bar{\phi}$, from the SPT data are shown in Figure 3-71. The $\bar{\phi}$ values, also influenced by the boulders and cobbles, range from near 45° at the surface to 48° at a depth of 5 ft (1.52 m). These values represent somewhat upper bounds to $\bar{\phi}$ at the site.

Drive Cone Tests (DCT)

Three DCTs were done at the Wyncoop Creek site. The DCT data from all soundings

Table 3-31

SPT DATA, WYNCOOP CREEK GRILLAGE SET NO. X2, INSIDE

Depth (ft)	$\bar{\sigma}_v$ (tsf)	N (blows/ft or 0.3 m) per Grillage and Boring SW SPT-2	NE SPT-1	N Avg.	N COV (%)	D_r Avg. (%)	D_r COV (%)	$\bar{\phi}$ Avg. (deg)	$\bar{\phi}$ COV (%)
1	0.06	10	15	12.5	28.3	48.8	14.2	44.2	6.2
3	0.18	11	29	20.0	63.6	57.4	33.7	46.3	14.4
5	0.30	12	38	25.0	73.5	60.6	39.7	46.7	16.8
Averages:		11.0	27.3	19.2	55.2	55.6	29.2	45.7	12.5

1 ft = 0.305 m; 1 tsf = 0.98 ksc

Table 3-32

SPT DATA, WYNCOOP CREEK GRILLAGE SET NO. X2, OUTSIDE

Depth (ft)	$\bar{\sigma}_v$ (tsf)	N (blows/ft or 0.3 m) per Grillage and Boring SW SPT-2	NE SPT-1	N Avg.	N COV (%)	D_r Avg. (%)	D_r COV (%)	$\bar{\phi}$ Avg. (deg)	$\bar{\phi}$ COV (%)
1	0.06	12	16	14.0	20.2	51.8	10.2	45.4	4.4
3	0.18	25	11	18.0	55.0	54.8	28.6	45.6	12.3
5	0.30	36	28	32.0	17.7	71.1	8.9	50.5	3.4
7	0.42	(100+)							
Averages:		24.3	18.3	21.3	31.0	59.2	15.9	47.2	6.7

1 ft = 0.305 m; 1 tsf = 0.98 ksc

are given in Table 3-34. No significant differentiation between backfill and native soil could be made. Figure 3-72 shows the cumulative DCT N values. The data show a continuous, almost linear increase in cumulative N with depth. Since standardized correlations for DCT are not available, no soil properties have been estimated based on these in-situ tests. Even if reliable correlations

Table 3-33

SPT DATA, WYNCOOP CREEK GRILLAGE SET NO. X2, ALL BORINGS

Depth (ft)	$\bar{\sigma}_v$ (tsf)	N (blows/ft or 0.3 m) per Grillage and Boring				N		D_r		$\bar{\phi}$	
		SW SPT-2	NE SPT-1	SW SPT-1	NE SPT-2	Avg.	COV (%)	Avg. (%)	COV (%)	Avg. (deg)	COV (%)
1	0.06	10	15	12	16	13.3	20.8	50.3	10.6	44.8	4.7
3	0.18	11	29	25	11	19.0	49.4	56.1	25.8	45.9	11.0
5	0.30	12	38	36	28	28.5	41.5	65.8	23.6	48.6	10.6
7	0.42			(100+)							
Averages:		11.0	27.3	24.3	18.3	20.3	37.2	57.4	20.0	46.4	8.8

1 ft = 0.305 m; 1 tsf = 0.98 ksc

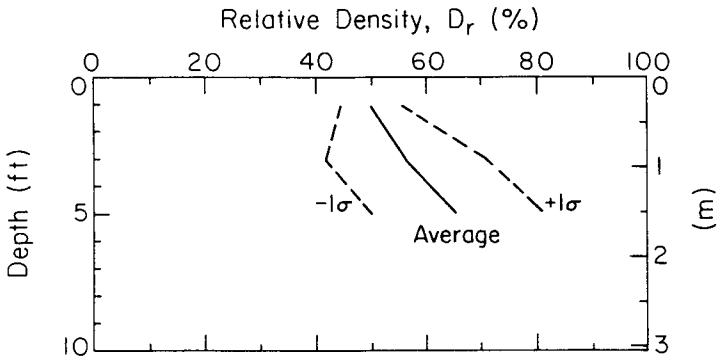

Figure 3-70. Average D_r from SPT, Wyncoop Creek, Inside and Outside

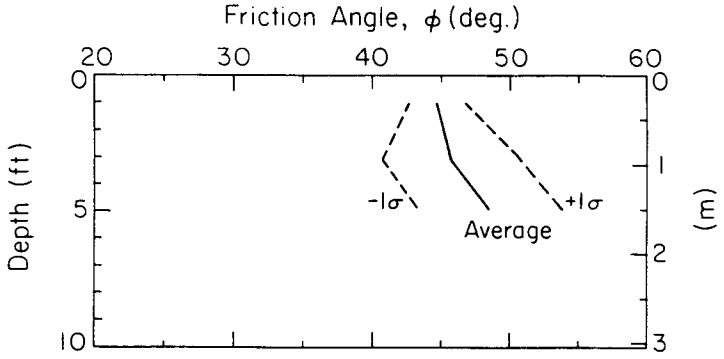

Figure 3-71. Average $\bar{\phi}$ from SPT, Wyncoop Creek, Inside and Outside

Table 3-34

DCT DATA, WYNCOOP CREEK GRILLAGE SET NO. X2, ALL BORINGS

Depth (ft)	Drive Cone N_{DCT} (blows/ft or 0.3 m) per Grillage and Sounding: X2-NE DCT-1 (Inside) per ft	X2-NE DCT-1 (Inside) Cum.	X2-SW DCT-1 (Inside) per ft	X2-SW DCT-1 (Inside) Cum.	X2-SW DCT-2 (Outside) per ft	X2-SW DCT-2 (Outside) Cum.	Cum. Avg.	Cum. COV (%)
1	8	8	7	7	8	8	7.7	7.5
2	12	20	12	19	18	26	21.7	17.5
3	31	51	7	26	21	47	41.3	32.5
4	21	72	8	34	42	89	65.0	43.3
5	17	89	14	48			68.5	42.3
6	19	108	17	65			86.5	35.2
Average:								29.7

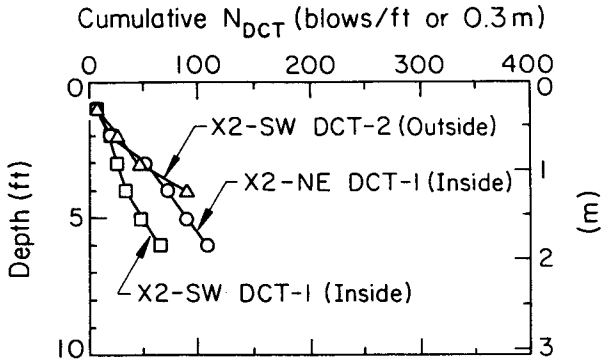

Figure 3-72. DCT Cumulative N, Wyncoop Creek, Inside and Outside

were available, the presence of large cobbles and boulders would make the interpretation questionable.

SUMMARY

Numerous types of in-situ tests were conducted at the grillage field sites to aid in evaluating the soil properties necessary to predict uplift capacity. Tests were conducted in the backfill and native soil to assess differences in

physical states. The main parameters determined from these in-situ tests were D_r, $\bar{\phi}$, K_o, and E.

At the Hickling Station site, the backfill over grillage set Numbers 4 and 84 was different from the native soil. The backfill was looser and softer than the native soil, as indicated by lower $\bar{\phi}$ and E. The K_o values in the backfill tended to be lower than those in the native soil. However, the PMT data in the native soil appeared to result in K_o values that were too high. Simplified soil profiles of $\bar{\phi}$, K_o, and E were determined for the Hickling Station site.

The Wyncoop Creek site consisted of soils that were poorly suited for sophisticated in-situ testing. However, estimates of the upper bound friction angle, $\bar{\phi}$, were made based on SPT data.

REFERENCES

1. Kulhawy, F. H. and Mayne, P. W., "Manual on Estimating Soil Properties for Foundation Design", Report EL-6800, Electric Power Research Institute, Palo Alto, July 1990, 306 p.

2. American Society for Testing and Materials, "Method of Penetration Test and Split-Barrel Sampling of Soils (D1586-84)", Annual Book of Standards, Vol. 4.08, ASTM, Philadelphia, 1989, pp. 221-225.

3. American Society for Testing and Materials, "Standard Test Method for Deep, Quasi-Static, Cone and Friction-Cone Penetration Tests of Soil (D3441-86)", Annual Book of Standards, Vol. 4.08, ASTM, Philadelphia, 1989, pp. 414-419.

4. Winter, E., "Suggested Practice for Pressuremeter Testing in Soils", Geotechnical Testing Journal, ASTM, Vol. 5, No. 3/4, Sept./Dec. 1982, pp. 85-88.

5. Briaud, J.-L. and Gambin, M., "Suggested Practice for Drilling Boreholes for Pressuremeter Testing", Geotechnical Testing Journal, ASTM, Vol. 7, No. 1, Mar. 1984, pp. 36-40.

6. Lutenegger, A. J., "Suggested Method for Performing the Borehole Shear Test", Geotechnical Testing Journal, ASTM, Vol. 10, No. 1, Mar. 1987, pp. 19-25.

7. Marchetti, S., "In-Situ Tests by Flat Dilatometer", Journal of the Geotechnical Engineering Division, ASCE, Vol. 106, No. GT3, Mar. 1980, pp. 299-321.

8. Schmertmann, J. H., "Suggested Method for Performing the Flat Dilatometer Test", Geotechnical Testing Journal, ASTM, Vol. 9, No. 2, June 1986, pp. 93-101.

9. Terzaghi, K. and Peck, R. B., Soil Mechanics in Engineering Practice, 2nd Ed., John Wiley and Sons, New York, 1967, 729 p.

10. Lambe, T. W. and Whitman, R. V., Soil Mechanics, John Wiley and Sons, New York, 1969, 553 p.

11. Skempton, A. W., "Standard Penetration Test Procedures and the Effects in Sand of Overburden Pressure, Relative Density, Particle Size, Aging, and Overconsolidation", Geotechnique, Vol. 36, No. 3, Sept. 1986, pp. 425-447.

12. Peck, R. B., Hansen, W. E., and Thornburn, T. H., Foundation Engineering, 2nd Ed., John Wiley and Sons, New York, 1974, 514 p.

13. Meyerhof, G. G., "Penetration Tests and Bearing Capacity of Cohesionless Soils", Journal of the Soil Mechanics and Foundations Division, ASCE, Vol. 82, No. SM1, Jan. 1956, pp. 1-19.

14. Schmertmann, J. H., "Measurement of In-Situ Shear Strength," Proceedings, ASCE Specialty Conference on In-Situ Measurement of Soil Properties, Vol. 2, Raleigh, 1975, pp. 57-138. (Closure: pp. 175-179.)

15. Robertson, P. K. and Campanella, R. G., "Interpretation of Cone Penetration Tests. Part I: Sand", Canadian Geotechnical Journal, Vol. 20, No. 4, Nov. 1983, pp. 718-733.

16. Kulhawy, F. H., Stas, C. S., and Mayne, P. W., "First Order Estimation of K_o in Sands and Clays", Foundation Engineering: Current Principles and Practices, Ed. F. H. Kulhawy, ASCE, New York, 1989, pp. 121-134.

17. Trautmann, C. H. and Kulhawy, F. H., "CUFAD - A Computer Program for Compression and Uplift Foundation Analysis and Design", Report EL-4540-CCM, Vol. 16, Electric Power Research Institute, Palo Alto, Oct. 1987, 148 p.

18. Coyle, H. M. and Bartoskewitz, R. E., "Prediction of Shear Strength of Sand by Use of Dynamic Penetration Tests", Research Record 749, Transportation Research Board, Washington, 1980, pp. 46-54.

19. Mohan, D., Aggarwal, V. S., and Tolia, D. S., "The Correlation of Cone Size in the Dynamic Cone Penetration Test with the Standard Penetration Test", Geotechnique, Vol. 20, No. 3, Sept. 1970, pp. 315-319.

20. Muromachi, T. and Kobyashi, S., "Comparative Study of Static and Dynamic Penetration Tests Currently in Use in Japan", Proceedings, 2nd European Symposium on Penetration Testing, Vol. 1, Amsterdam, 1982, pp. 297-302.

21. Palmer, D. J. and Stuart, J. G., "Some Observations on the Standard Penetration Test and a Correlation of the Test with a New Penetrometer", Proceedings, 4th International Conference on Soil Mechanics and Foundation Engineering, Vol. 1, London, 1957, pp. 231-236.

22. Hanna, A. W., Ambrosii, G., and McConnell, A. D., "Investigation of a Coarse Alluvial Foundation for an Embankment Dam", Canadian Geotechnical Journal, Vol. 23, No. 2, May 1986, pp. 203-215.

23. Rao, B. G., Narahari, D. R., and Balodhi, G. R., "Dynamic Cone Probing Tests in Gravelly Soils", Proceedings, 2nd European Symposium on Penetration Testing, Vol. 1, Amsterdam, 1982, pp. 337-344.

24. Marchetti, S., "On the Field Determination of K_o in Sand", Proceedings, 11th International Conference on Soil Mechanics and Foundation Engineering, Vol. 5, San Francisco, 1985, pp. 2667-2672.

25. Leps, T. M., "Review of Shearing Strength of Rockfill", Journal of the Soil Mechanics and Foundations Division, ASCE, Vol. 96, No. SM4, July 1970, pp. 1159-1170.

26. Marachi, N. D., Chan, C. K., and Seed, H. B., "Evaluation of Properties of Rockfill Materials", Journal of the Soil Mechanics and Foundations Division, ASCE, Vol. 98, No. SM1, Jan. 1972, pp. 95-114.

Section 4

LABORATORY CHARACTERIZATION OF SOILS FROM THE TEST SITES

This section describes the basic index and classification test results from the backfill and native soil at Hickling Station and the backfill at Wyncoop Creek. Laboratory testing also included drained triaxial compression tests on the Hickling Station soils for correlation of the in-situ test friction angle with that determined in the laboratory.

HICKLING STATION

Prior to the field tests, bag samples of material from the backfill and native soil were taken from an excavation pit near grillage No. 84-NW. This grillage was not tested in uplift because of disturbance resulting from soil sampling. The soils at the excavated grillages were not visually different. Color varied from light brown and tan to dark brown. Several large cobbles in the 3 to 12 in. (76 to 305 mm) range were found during sampling. In some instances, pockets of soil were found that were dominated by the larger-sized particles, and the surrounding finer matrix was insignificant.

Index and Classification Tests

Grain size analyses were performed on both the native and backfill samples. Mechanical analysis (1, 2) was used for the material greater than the No. 200 sieve (0.075 mm). Hydrometer analysis (2) was used for the fine fraction. Figure 4-1 shows the grain size distributions for the backfill and native soil. Both the native soil and backfill contain significant coarse fractions, with 5 to 10 percent by weight larger than 3 in. (76 mm). Roughly 35 percent of the backfill is larger than 0.75 in. (19 mm), as compared with 50 percent larger than 0.75 in. (19 mm) in the native soil. The backfill has about 34 percent finer than the No. 200 sieve (0.075 mm), compared with 9 percent fines in the native soil. Atterberg limits (3) were determined from several different samples of backfill and native soil. These limits and the grain size distribution curves were used to classify the soil, using the Unified Soil Classification System (USCS) (4). The grain size properties and Atterberg limits for the

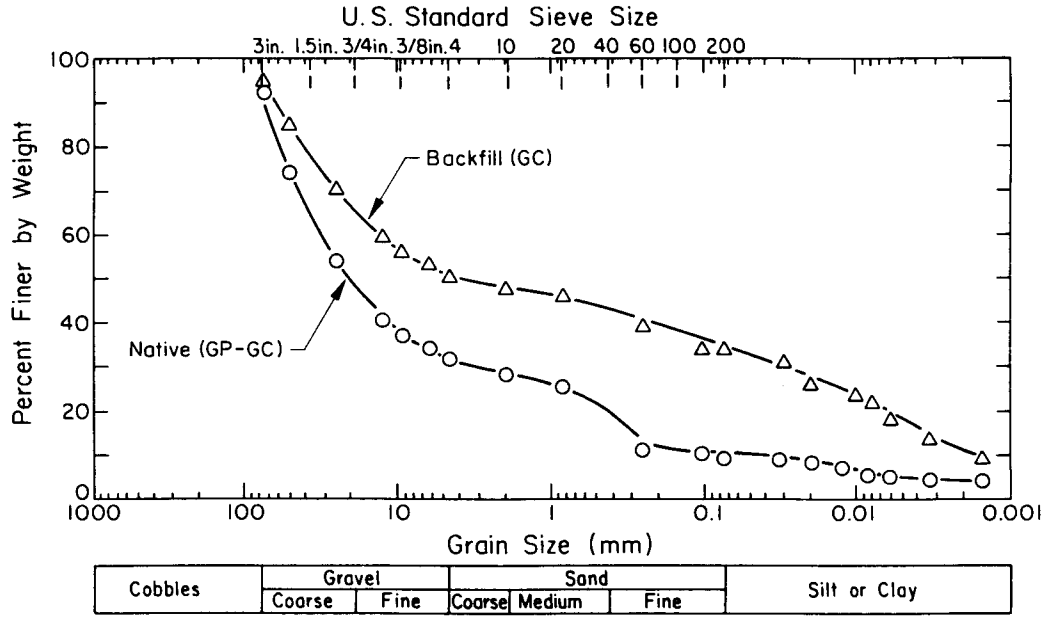

Figure 4-1. Grain Size Distributions for Backfill and Native Soil, Hickling Station

native soil and backfill are given in Table 4-1. In this table, D_{max}, D_{60}, D_{50}, D_{30}, and D_{10} refer to the maximum grain size and the grain sizes at 60, 50, 30, and 10 percent passing, respectively. Also given are the coefficient of uniformity, C_u, and the coefficient of curvature, C_c. The native soil was classified as a poorly graded gravel with clay, sand, cobbles, and boulders (GP-GC). The backfill was classified as a clayey gravel with sand and cobbles (GC). Note that these classifications are based on the gradations shown in Figure 4-1, which had a maximum particle size of 3 in. (76 mm). The boring logs do not indicate the significant cobble and boulder content, since the split barrel samplers had inside diameters of 1.5 in. (38 mm). Fractured rock could have been included in the split barrel samples and would have been identified as gravel-sized particles.

Moisture-Density Relations

Sand cone density tests (5) were performed at two depths over grillage No. 84-NW while collecting bag samples. As noted earlier, cobbles in the 3 to 12 in. (76 to 305 mm) range were present in the soil, which makes sand cone testing and interpretation difficult.

Tests were done at depths of 3 ft (0.91 m) and 5 ft (1.52 m) over the grillage

Table 4-1

SOIL INDEX PROPERTIES AND CLASSIFICATION, HICKLING STATION

	Native	Backfill
D_{max} (mm) [in-situ]	76 to 305+	76 to 203+
D_{60} (mm)	32	13
D_{50} (mm)	11	5
D_{30} (mm)	4	0.03
D_{10} (mm)	0.1	0.002
$C_u = D_{60}/D_{10}$	320	-
$C_c = D_{30}^2/(D_{60} \times D_{10})$	5	-
% cobbles [test sample]	7	5
% gravel	63	45
% sand	21	16
% fines	9	34
w_L (%)	29.8	33.9
w_P (%)	20.2	23.9
PI (%)	9.6	10.0
USCS group name	GP-GC	GC
USCS group description	Poorly graded gravel with clay, sand, cobbles, and boulders	Clayey gravel with sand and cobbles

1 in. = 25.4 mm

in the backfill. Test areas were selected that did not appear to have large cobbles so that suitable excavation sizes could be made for sand replacement. Table 4-2 gives the results of the sand cone tests. Dry unit weights, γ_d, were 86.2 pcf (13.55 kN/m^3) with a water content, w, = 25.7 percent at a depth of 3 ft (0.91 m), and γ_d = 95.2 pcf (14.95 kN/m^3) with a water content, w, = 11.8 percent at a depth of 5 ft (1.52 m). The unit weights from the sand cone measurements are lower than the bulk unit weight of the entire backfill, since the test locations were selected so that few cobbles were in the sample volume. The unit weights of the backfill probably were about 10 percent higher than those determined from the sand cone tests. A 10 percent increase in the unit weights

Table 4-2

SAND CONE TEST RESULTS, HICKLING STATION, BACKFILL

Depth ft (m)	Total Unit Weight pcf (kN/m^3)	Water Content (%)	Dry Unit Weight pcf (kN/m^3)
3 (0.91)	108.4 (17.03)	25.7	86.2 (13.55)
5 (1.52)	106.4 (16.72)	11.8	95.2 (14.95)

would result in total unit weights from γ_t = 117 to 119 pcf (18.4 to 18.7 kN/m^3). The unit weight used to determine the effective overburden stresses for the in-situ test data reduction was γ_t = 120 pcf (18.9 kN/m^3).

Compaction tests on both the native soil and backfill were conducted to determine the moisture-density relationships and to investigate the effects of grain size distribution on the resulting unit weights and optimum water contents. Materials with maximum sizes greater than 0.75 in. (19 mm) can not be tested using standard ASTM methods (6) without substantial modification of the grain size distributions, removing all material retained on the No. 4 sieve (4.76 mm) or retained on a 0.75 in. (19 mm) sieve.

The methods used for the Hickling Station soil involved the following modifications to the ASTM procedure (6). Two gradations each were made for the backfill and native soil. Gradations A were scalped of all material greater than 1 in. (25 mm). Gradations B were scalped of all material greater than 3/8 in. (9.5 mm) and reblended to make grain size distribution curves parallel to the original curves. The resulting grain size distributions for the modified backfill are shown in Figure 4-2. Figure 4-3 shows the modified grain size distributions for the native soil. A 5.5 lb (2.49 kg) rammer with a drop height of 12 in. (305 mm) was used to compact the soils. A 6 in. diameter (152 mm) mold was used for gradations A, and the soil was compacted in three layers with 25 blows per layer. A 4 in. diameter (102 mm) mold was used for gradations B, and the soil was compacted in three layers with 25 blows per layer. Table 4-3 lists the index characteristics for the original and modified gradations. Note that removal of the coarse fractions also changes the USCS classifications.

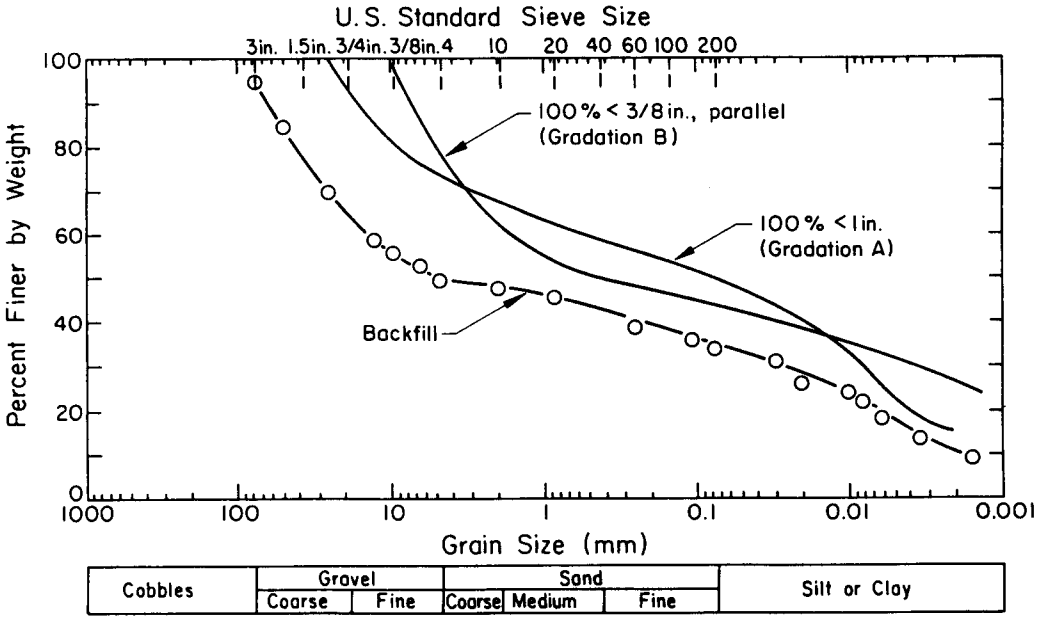

Figure 4-2. Grain Size Distributions for Moisture-Density Tests on Backfill Soil, Hickling Station

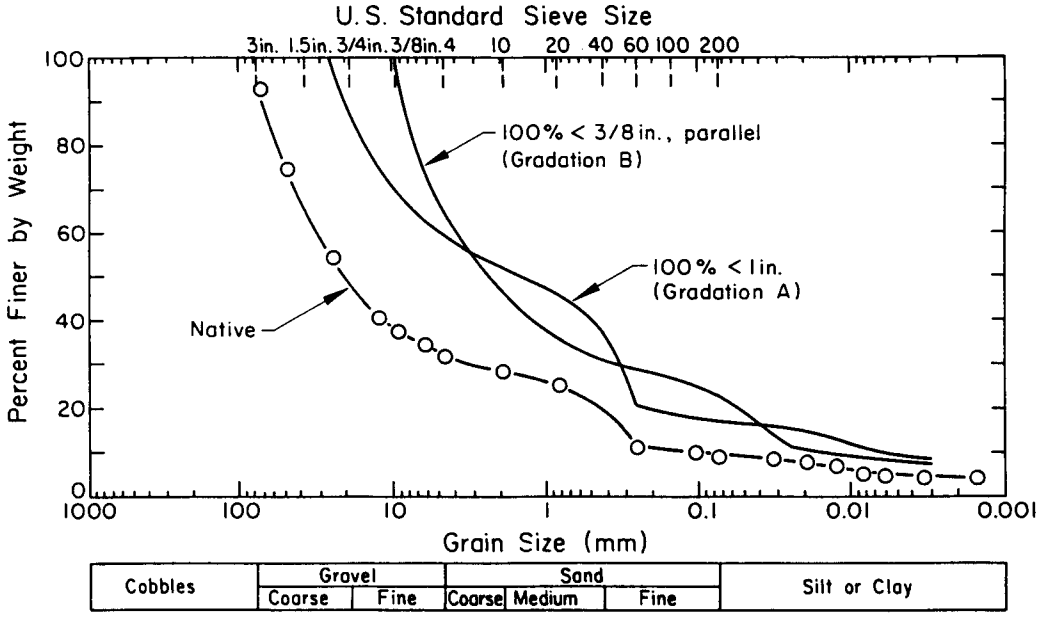

Figure 4-3. Grain Size Distributions for Moisture-Density Tests on Native Soil, Hickling Station

Figure 4-4 shows the compaction curves for the four soils. The native soil had a higher maximum dry unit weight than the backfill, and the tests done using the

Table 4-3

MODIFIED GRADATION CHARACTERISTICS, HICKLING STATION

	Native	Backfill
D_{max} (in.)		
Original	3 to 12	3 to 8
Gradation A	1	1
Gradation B	3/8	3/8
USCS group names:		
Original	GP-GC	GC
Gradation A	GC	SC
Gradation B	SC	CL

1 in. = 25.4 mm

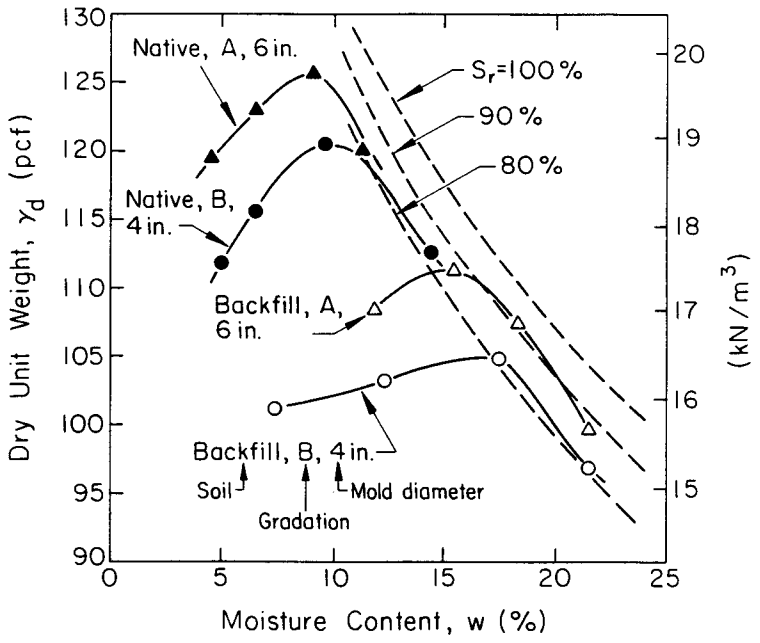

Figure 4-4. Compaction Test Results, Hickling Station

larger particle top size and larger mold resulted in higher maximum dry unit weights. On Figure 4-4, percent saturation, S_r, curves are shown for a specific gravity, G_s, of 2.66. Table 4-4 lists the results from the compaction tests. The decrease in optimum water content and increase in maximum dry unit weight

Table 4-4

MAXIMUM DRY UNIT WEIGHTS AND OPTIMUM MOISTURE CONTENTS, HICKLING STATION

	Native		Backfill	
	Gradation A	Gradation B	Gradation A	Gradation B
Maximum dry unit weight, pcf (kN/m^3)	125.8 (19.8)	120.8 (19.0)	111.8 (17.6)	105.4 (16.6)
Optimum moisture content (%)	9.1	9.8	15.1	16.7

with increasing maximum particle size is consistent with data obtained by Gordon, et al. (7), although different gradation blends were used. Since the compaction tests were not done using material all passing the No. 4 (4.76 mm) sieve, typical correction equations based on percentages of rock can not be applied. In this context, rock is used to describe material retained on the No. 4 (4.76 mm) sieve. However, Gordon, et al. (7) note that only small corrections to account for 3 in. (76 mm) maximum particle sizes are required if testing is done using material passing a 1.5 in. (38 mm) sieve. When 20 to 40 percent of the soil has particle sizes between 1.5 and 3 in. (38 and 76 mm), the correction factors applied to compaction tests scalped of larger than 1.5 in. (38 mm) sizes range from 1.02 to 1.04. These correction factors would be multiplied by the test maximum dry unit weights to estimate the maximums for 3 in. (76 mm) top size gradations. The factors to correct tests done using only minus No. 40 material would be 1.04 and 1.08 for 20 and 40 percent rock, respectively.

Given that the field soils contained particle sizes greater than 3 in. (76 mm), there are no straightforward methods that can be used to adjust lab compaction data. Since the original backfill was not as coarse as the original native material, but both grain size curves were modified for the same top size in the laboratory tests, an 8 percent correction was applied to the backfill and a 10 percent correction was applied to the native soil tests. These corrections result in a maximum dry unit weight of the backfill of 121 pcf (19.0 kN/m^3) and 138 pcf (21.7 kN/m^3) for the native soil. Optimum water contents also would be expected to decrease as maximum particle size increased beyond 3 in. (76 mm). By projecting a line of optimums through the peaks (maximum dry unit weights) of

the native soil compaction curves up to a dry unit weight of 138 pcf (21.7 kN/m^3), an optimum water content of about 7 percent can be estimated for the native soil. A similar projection through the peaks in the backfill compaction would result in an optimum water content of 12 percent at a maximum dry unit weight of 121 pcf (19.0 kN/m^3).

Strength Testing

Drained triaxial compression tests were done on both the backfill and native soils from the Hickling Station site. For maximum particle sizes on the order of 3 in. (76 mm) or greater, the specimen diameters required for triaxial testing using the full gradation would be at least 18 in. (457 mm), with lengths of 45 in. (1143 mm). Specimen sizes this large are not tested commonly. Therefore, the modified gradations were used to allow for equipment and time considerations.

Gradations B, with a maximum particle size of 3/8 in. (9.5 mm), were used for triaxial testing. The dry regraded soils were pulverized, moistened with distilled water, and allowed to equilibrate for 24 hours prior to specimen preparation. Specimens 2.8 in. (71 mm) in diameter by 5.8 in. (147 mm) long were compacted in six layers using the method of undercompaction (8). Six percent undercompaction was selected, based upon laboratory experience with the undercompaction method.

Physical states bracketing those in-situ were used for the strength testing. Specimens were compacted to various levels of relative compaction, RC, as defined by:

$$RC\ (\%) = 100\ (\gamma_d/\gamma_{dmax}) \tag{4-1}$$

in which γ_d = dry unit weight and γ_{dmax} = maximum dry unit weight from the compaction test. The estimated in-situ values of γ_{dmax} = 121 pcf (19.0 kN/m^3) for the backfill and 138 pcf (21.7 kN/m^3) for the native soil were used to calculate the relative compactions.

Specimens were consolidated isotropically, following back-pressure saturation, and were sheared drained by increasing the axial stress. Axial loads were applied hydraulically at a constant rate of strain. Strain rates were selected such that no excess pore water pressures developed during shear. The strain

rates were based on the times required for 100 percent consolidation during the consolidation phases, and they ranged roughly from 4 to 8 percent per hour, because of the relatively high fines content in the blended gradations. Chamber and pore water pressures were monitored continuously with electronic pressure transducers. Axial load and axial displacement were recorded by a 500 lb (2.2 kN) capacity load cell and a $\pm$ 2 in. ($\pm$ 51 mm) DCDT, respectively. Data were recorded using a Hewlett-Packard HP3852A data acquisition unit linked to an HP310 computer.

The initial physical states of the compacted specimens are given in Table 4-5, along with the effective consolidation stresses ($\bar{\sigma}_c$) for the triaxial tests. For the backfill tests, a RC of 75 percent was taken as representative of the field conditions. A RC of 80 percent was representative of the in-situ native soil. To investigate the effects of density changes on the stress-strain-strength characteristics, one test was run on each soil type at 10 percent lower RC and 15 percent higher RC than the nominal representative RC levels. The compaction water contents for each soil were 12 percent for the backfill and 7

Table 4-5

INITIAL PHYSICAL STATES AND CONFINING STRESSES FOR TRIAXIAL COMPRESSION TESTS, HICKLING STATION

Material	γ_d[a] (pcf)	γ_t[a] (pcf)	w[a] (%)	RC[b] (%)	$\bar{\sigma}_c$ (psi)
Native	96.6	103.4	7	70	12.0
	110.4	118.1	7	80	7.0
	110.4	118.1	7	80	12.0
	110.4	118.1	7	80	16.0
	131.1	140.3	7	95	12.0
Backfill	78.7	88.1	12	65	12.0
	90.8	101.7	12	75	9.5
	90.8	101.7	12	75	12.1
	90.8	101.7	12	75	19.1
	108.9	122.0	12	90	12.0

1 pcf = 0.157 kN/m^3
1 psi = 6.895 kN/m^2
a - As compacted
b - Based on γ_{dmax} = 138 pcf (21.7 kN/m^3) for native soil,
γ_{dmax} = 121 pcf (19.0 kN/m^3) for backfill.

percent for the native soil. These were the estimated optimum water contents of the field gradations, as inferred from the series of compaction tests.

Figure 4-5 shows the locations of the triaxial test specimens in comparison to the compaction curves expressed in terms of RC. Each compaction curve has been normalized by its respective maximum dry unit weight, as were the water contents. Figure 4-5 also shows that, although each soil gradation had different maximum dry unit weights and optimum water contents, the shape of each curve was the same. The similarity in shape of the normalized compaction curves also suggests that the gradational modifications necessary for the strength tests would not have a strong influence on the test results.

The deviator stress (σ_1 - σ_3) versus axial strain (ϵ_a) curves from the native soil tests with RC = 80 percent are shown in Figure 4-6. As confining stress increases, the maximum deviator stress and initial stiffness increases. No decrease in peak deviator stress occurred at the maximum test strains of 17 to 18 percent. Failure was defined as the maximum deviator stress at the completion of the test. The lack of a distinct peak in the stress-strain curves shown in Figure 4-6 indicates that, at RC = 80 percent, the soil was in a relatively loose state. No data points are shown because the electronic data acquisition gives nearly continuous data recording.

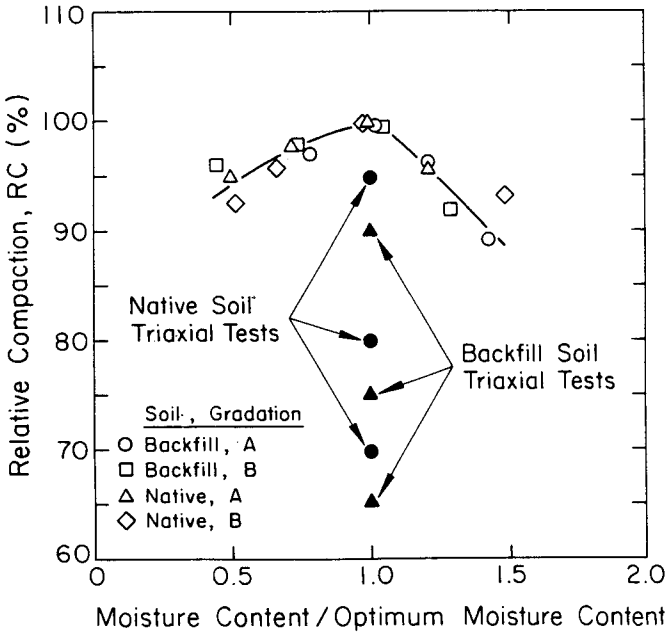

Figure 4-5. Triaxial Test Physical States Compared with Normalized Compaction Curves

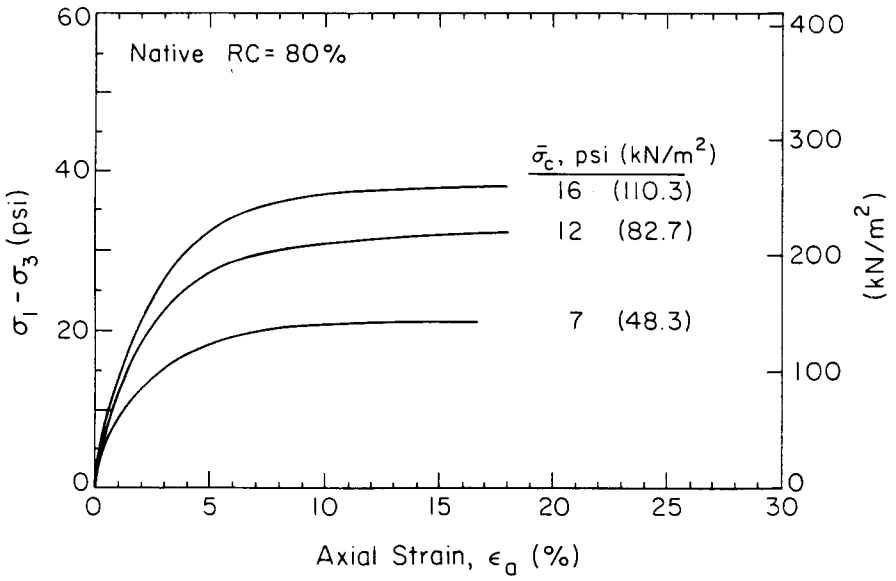

Figure 4-6. Stress-Strain Curves for Native Soil, RC = 80 percent, Hickling Station

Two additional tests were performed on the backfill at other compaction levels. Figure 4-7 shows a comparison between tests performed at $\bar{\sigma}_c$ = 12 psi (82.7 kN/m^2) with RC values of 70, 80, and 95 percent. At a RC of 70 percent, the soil was softer and had a lower deviator stress at failure than the baseline RC of 80 percent. The test at RC = 95 percent was terminated at 8.2 percent axial strain because the axial load at that strain approached the capacity of the testing device. However, the high RC test had a noticeably higher initial stiffness and would have had a substantially higher peak strength.

Stress paths in terms of $q = (\sigma_1 - \sigma_3)/2$ and $\bar{p} = (\bar{\sigma}_1 + \bar{\sigma}_3)/2$ are shown in Figure 4-8 for the native soil triaxial tests. The friction angle, $\bar{\phi}$, is related to $\bar{\alpha}$ in Figure 4-8 by $\sin \bar{\phi} = \tan \bar{\alpha}$. The friction angle decreases slightly as $\bar{p}$ at failure, $\bar{p}_f$, increases, as indicated by the slight curvature of the failure envelope. The secant friction angles, $\bar{\phi}_{sp}$, ranged from 33.2° to 37.1° for the test done at RC of 80 percent. The $\bar{\phi}_{sp}$ for the test done at RC = 70 percent was 32.6°.

The triaxial stress-strain curves for the native soil with RC of 75 percent are shown in Figure 4-9. For these tests, there was a distinct change in stiffness at axial strains of 1 percent that was common to all three effective confining stresses. The initial tangent moduli for the backfill tests at RC = 75 percent

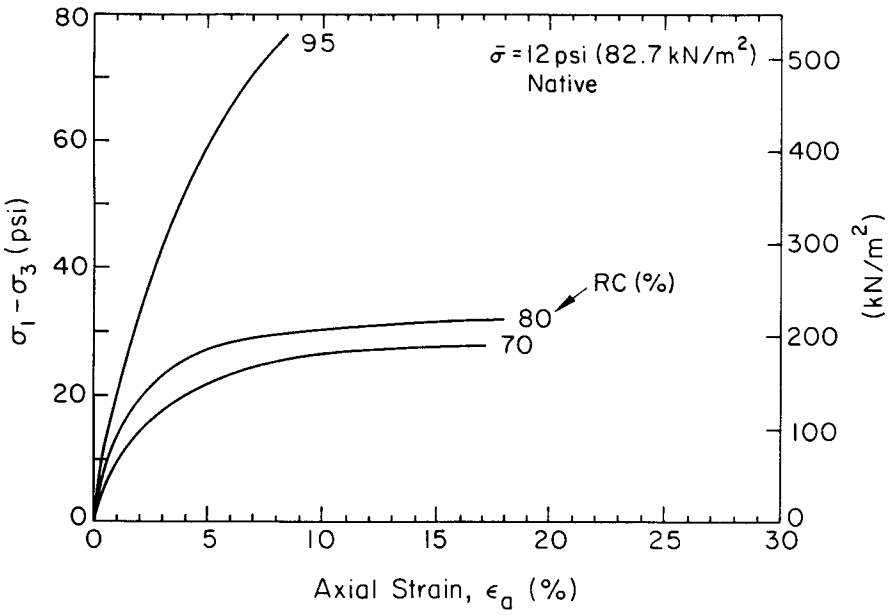

Figure 4-7. Effect of RC on Stress-Strain Curves for Native Soil, Hickling Station

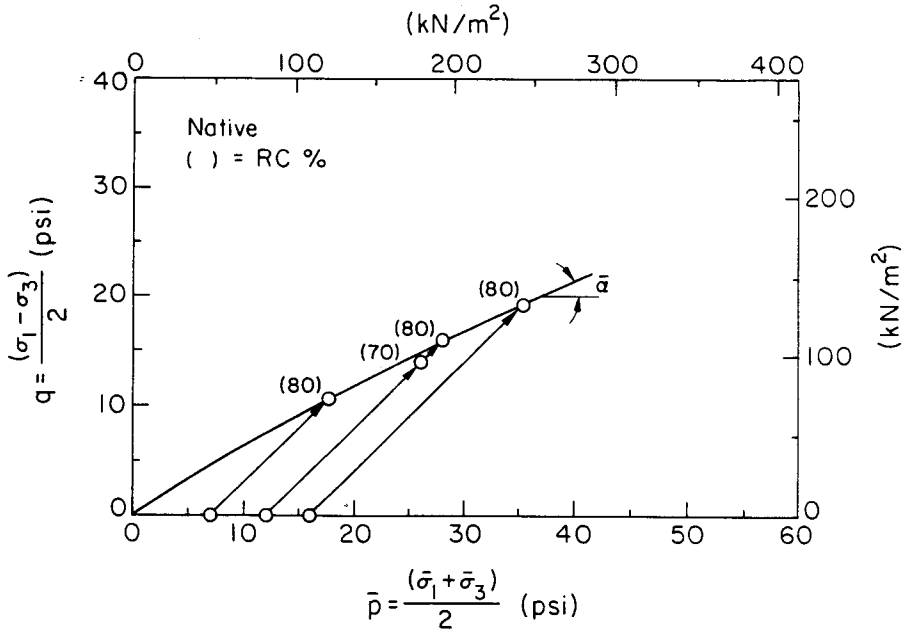

Figure 4-8. $\bar{p}$ versus q for Native Soil, Hickling Station

were lower than those of the native soil. Beyond 1 percent axial strain, the deviator stress continued to increase. Failure for these tests was defined at 25 percent strain.

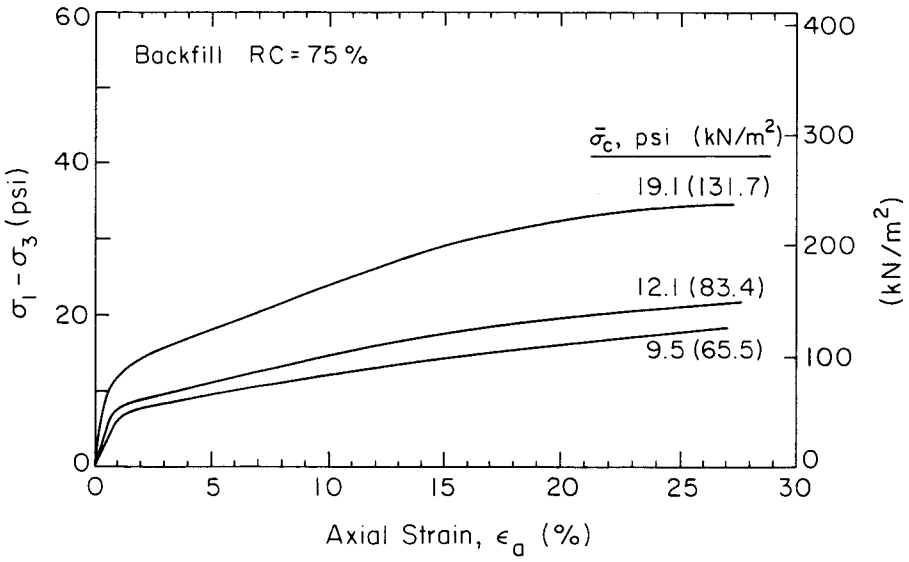

Figure 4-9. Stress-Strain Curves for Backfill, RC = 75 percent, Hickling Station

Figure 4-10 shows the effect of RC on the stress-strain curves and deviator stresses at failure for the backfill soil. Tests at RC = 65 and 75 percent had similar stress-strain trends, with the RC = 65 percent material having a lower initial stiffness and lower deviator stress at failure than the test done at RC = 75 percent. A distinctly different stress-strain curve resulted from the RC = 90 percent test. This test showed a slight decrease in strength following a peak, indicative of a moderately dense physical state. The strain at peak deviator stress also was well-defined and substantially smaller than that from the low RC tests. A similar shape would have been expected from the RC = 95 percent test on the native soil, had larger strains developed.

Stress paths for the backfill tests are shown in Figure 4-11. The failure envelope for the RC = 75 percent tests is nearly linear, with only slight curvature at low stresses. This lack of curvature is typical of tests on loose material. The average friction angle for the tests with RC = 75 percent is 29° [$\bar{\phi} = \sin^{-1}$ (tan 25.9°)]. The secant friction angles, $\bar{\phi}_{sp}$, for backfill tests at RC = 65 and 90 percent are 26.9° and 41.7°, respectively.

Table 4-6 lists the triaxial test conditions, axial strains at failure, ϵ_f, and secant friction angles, $\bar{\phi}_{sp}$, from all the triaxial tests. The secant friction angles decrease as confinement, $\bar{\sigma}_c$, increases for a given RC, and they increase

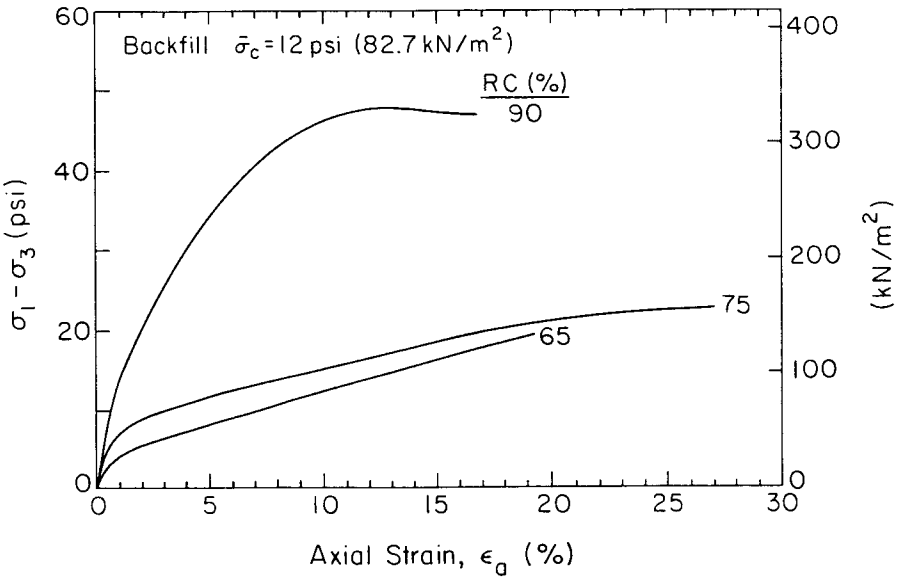

Figure 4-10. Effect of RC on Stress-Strain Curves for Backfill, Hickling Station

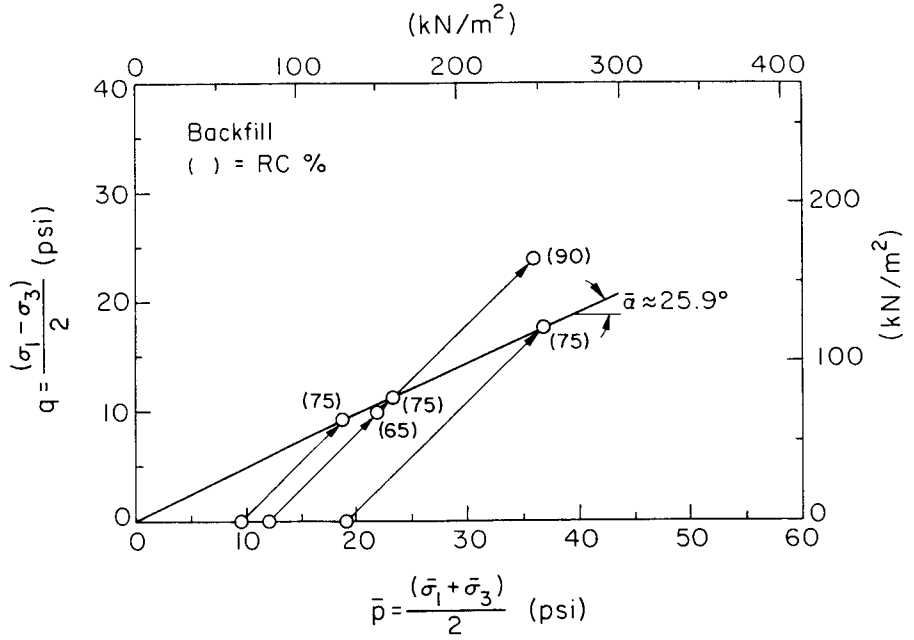

Figure 4-11. $\bar{p}$ versus q for Backfill Soil, Hickling Station

as RC increases for a given $\bar{\sigma}_c$. This trend is shown in Figure 4-12, where $\bar{\phi}_{sp}$ is plotted against mean stress at failure, $\bar{p}_f = (\bar{\sigma}_1 + \bar{\sigma}_3)_f/2$. At a RC of 80 percent, $\bar{\phi}_{sp}$ in the native soil decreases noticeably as $\bar{p}_f$ increases. The decrease in $\bar{\phi}_{sp}$ at RC = 75 percent for the backfill is only slight.

Table 4-6

TRIAXIAL STRENGTHS, HICKLING STATION

Material	RC (%)	$\bar{\sigma}_c$ (psi)	ϵ_f (%)	$(\sigma_1 - \sigma_3)_f$ (psi)	$\bar{\phi}_{sp}$ (deg)
Native	70	12.0	17.3	28.1	32.6
	80	7.0	16.9	21.3	37.1
	80	12.0	18.0	32.1	34.9
	80	16.0	18.0	38.7	33.2
	95	12.0	-	-	-
Backfill	65	12.0	18.9	19.8	26.9
	75	9.5	25.0	18.5	29.6
	75	12.1	25.0	22.5	28.8
	75	19.1	25.0	35.3	28.7
	90	12.0	12.8	47.8	41.7

1 psi = 6.895 kN/m^2

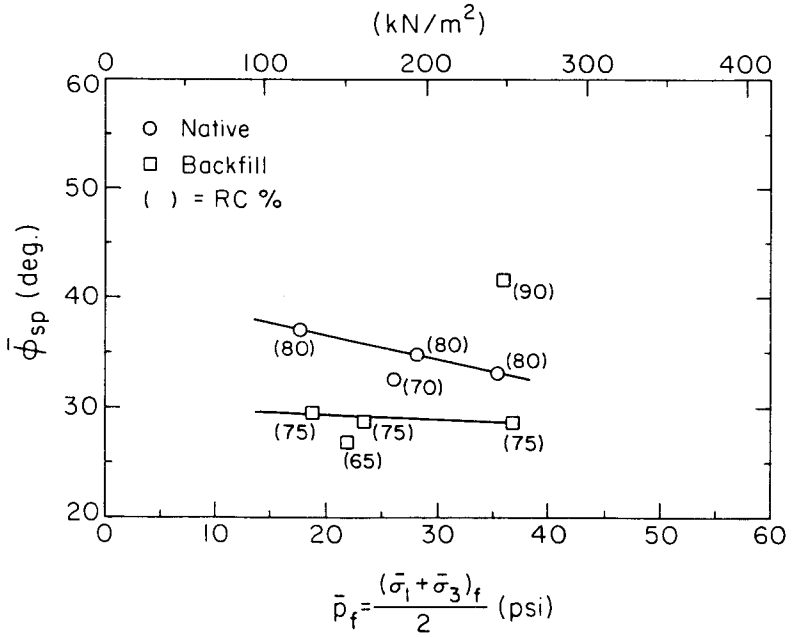

Figure 4-12. $\bar{\phi}_{sp}$ versus $\bar{p}_f$ from Triaxial Tests, Hickling Station

Although few data are available, there appears to be a relationship between the normalized failure stress, $\bar{p}_f/\bar{p}_o$ (with $\bar{p}_o$ = initial mean stress = $\bar{\sigma}_c$), the level

of relative compaction, RC, and the secant friction angle, $\bar{\phi}_{sp}$. Figure 4-13 shows $\bar{\phi}_{sp}$ versus RC for various levels of normalized failure stress. Although only two data points have the same $\bar{p}_f/\bar{p}_o$ value, a trend is apparent. Figure 4-13 indicates that, for triaxial compression tests, $\bar{\phi}_{sp}$ increases as both RC and $\bar{p}_f/\bar{p}_o$ increase. The dashed lines on Figure 4-13 are not conclusive, since additional test data would be required to substantiate the trends, which would hold only for triaxial compression stress paths.

The triaxial data are bracketed by the data obtained from the in-situ borehole shear tests. For the estimated relative compaction of the backfill (RC $\approx$ 75 percent), the triaxial compression test data yielded $\bar{\phi}_{sp}$ from 28.7° to 29.6°. The BST data from inside the backfill ranged from 27.6° to 35.1° for the average upper and lower bounds, respectively. The upper and lower bounds from BSTs done in the native soil were 32.7° and 38.3°, respectively, as compared with the triaxial data that gave $\bar{\phi}_{sp}$ of 33.2° to 37.1° at a RC of 80 percent. A comparison of these lab and in-situ $\bar{\phi}$ values is shown in Figure 4-14. Considering the differences in the two types of tests and gradational effects, the agreement is good. This agreement gives further evidence that the $\bar{\phi}$ values from the BST were representative of the matrix. It also indicates that the lab data are significantly lower than the values estimated from the SPT and CPT.

WYNCOOP CREEK

Since the soil at Wyncoop Creek contained a high percentage of cobbles and boulders, along with concrete debris, additional testing beyond simple index and classification tests was not justified. The result of the index testing can,

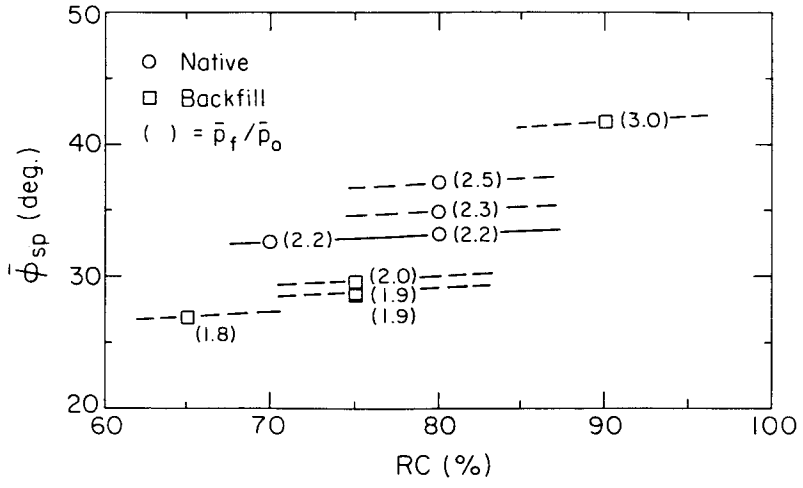

Figure 4-13. $\bar{\phi}_{sp}$ versus RC for Normalized Failure Stresses, Hickling Station

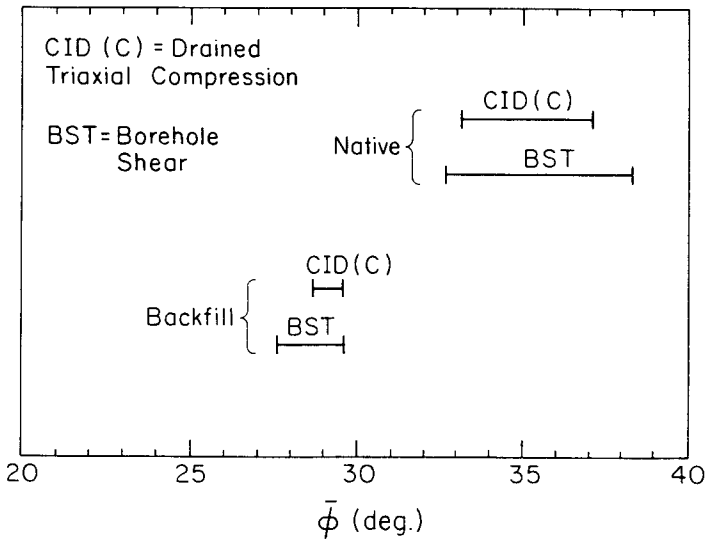

Figure 4-14. $\bar{\phi}$ from Triaxial Tests and In-Situ BST, Hickling Station

however, be used to estimate probable ranges of engineering properties.

The grain size distribution curve for the backfill at Wyncoop Creek is shown in Figure 4-15. Boulders and large cobbles were not included in the mechanical analyses. The index properties and USCS classification are given in Table 4-7. The backfill at Wyncoop Creek is finer than both the backfill and native soil at the Hickling Station site, neglecting the cobbles, boulders, and concrete debris. The fines in the Wyncoop Creek backfill were borderline ML and CL-ML. The resulting classification is a silty clayey sand with gravel, cobbles, and boulders (SC-SM).

SUMMARY

Triaxial compression tests were performed on scalped and reblended soil from the Hickling Station site. The physical states of the triaxial specimens were based on compaction data and corrections to account for large particle sizes. The native soil was compacted to a higher dry unit weight and relative compaction than was the backfill. The resulting friction angles were dependent on the effective confinement and physical state, with the backfill friction angles less than those from tests run on the native soil. The bulk backfill was a GC material, and the native soil was a GP-GC material. The scalped, reblended, Gradation B specimens were classified as CL for the backfill and SC for the native soil. Friction angles from triaxial tests were in general agreement with the

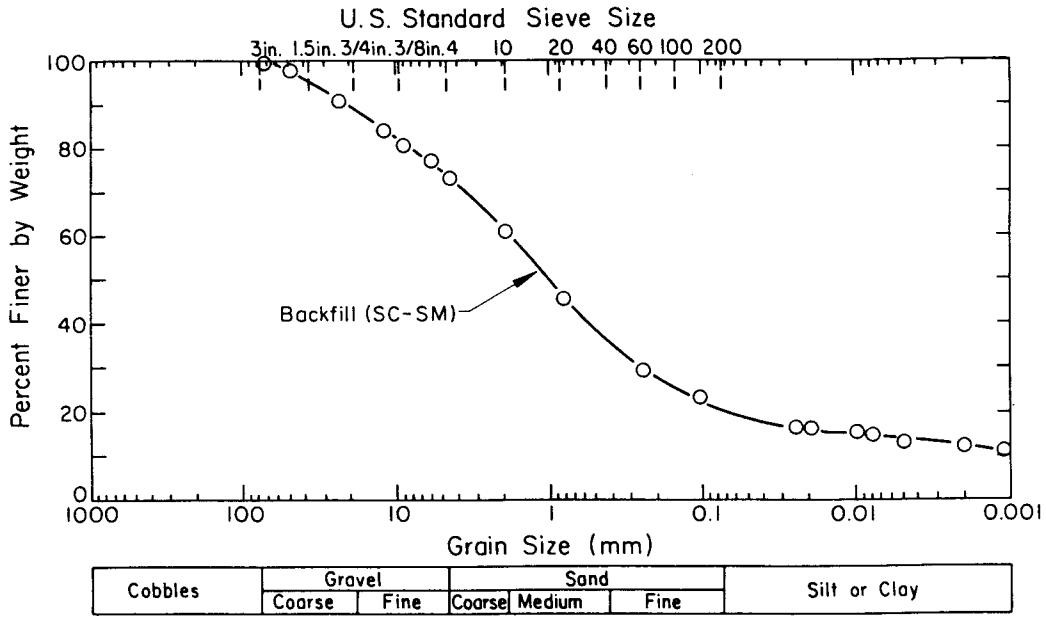

Figure 4-15. Grain Size Distribution for Backfill, Wyncoop Creek

Table 4-7

SOIL INDEX PROPERTIES AND CLASSIFICATION FOR BACKFILL, WYNCOOP CREEK

D_{max} (mm) [in-situ]	76 - 457
D_{60} (mm)	1.8
D_{50} (mm)	1.1
D_{10} (mm)	≈ 0.0005
% cobbles [test sample]	0
% gravel	27
% sand	54
% fines	19
w_L (%)	27.0
w_P (%)	20.9
PI (%)	6.1
USCS group name	SC-SM
USCS group designation	Silty clayey sand with gravel, cobbles, and boulders

1 in. = 25.4 mm

in-situ BST data, but they were lower than those estimated from the SPT and CPT.

The Wyncoop Creek backfill contained cobbles, boulders, and concrete debris. Laboratory testing other than index and classification tests would not have been representative of the bulk in-situ behavior and were not performed. The backfill was classified as a silty clayey sand with gravel, cobbles, and boulders. Strength properties of the Wyncoop Creek material are expected to be similar to, and somewhat lower than, those estimated for the Hickling Station backfill.

REFERENCES

1. American Society for Testing and Materials, "Standard Practice for Dry Preparation of Soil Samples for Particle-Size Analysis and Determination of Soil Constants (D421-85)", Annual Book of Standards, Vol. 4.08, ASTM, Philadelphia, 1990, pp. 89-90.

2. American Society for Testing and Materials, "Standard Method for Particle Size Analysis of Soils (D422-63)", Annual Book of Standards, Vol. 4.08, ASTM, Philadelphia, 1990, pp. 91-97.

3. American Society for Testing and Materials, "Standard Test Method for Liquid Limit, Plastic Limit, and Plasticity Index of Soils (D4318-84)," Annual Book of Standards, Vol. 4.08, ASTM, Philadelphia, 1990, pp. 591-601.

4. American Society for Testing and Materials, "Standard Test Method for Classification of Soils for Engineering Purposes (D2487-85)", Annual Book of Standards, Vol. 4.08, ASTM, Philadelphia, 1990, pp. 295-304.

5. American Society for Testing and Materials, "Standard Test Method for Density of Soil in Place by the Sand-Cone Method (D1556-82)", Annual Book of Standards, Vol. 4.08, ASTM, Philadelphia, 1990, pp. 212-216.

6. American Society for Testing and Materials, "Standard Test Methods for Moisture-Density Relations of Soil and Soil-Aggregate Using 5.5-lb (2.49-kg) Rammer and 12-in. (305-mm) Drop (D698-78)", Annual Book of Standards, Vol. 4.08, ASTM, Philadelphia, 1990, pp. 160-164.

7. Gordon, B. B., Hammond, W. D., and Miller, R. K., "Effect of Rock Content on Compaction Characteristics of Clayey Gravel", Compaction of Soils (STP 377), ASTM, Philadelphia, 1964, pp. 31-46.

8. Ladd, R. S., "Preparing Test Specimens Using Undercompaction," Geotechnical Testing Journal, ASTM, Vol. 1, No. 1, Mar. 1978, pp. 16-23.

Section 5

FIELD UPLIFT TEST EQUIPMENT AND PROCEDURES

This section describes the equipment and procedures used to perform the field uplift tests, including details of the load reaction and application systems. The methods used to obtain both grillage stub and ground surface movements are described, and the load increment and duration criteria are presented.

UPLIFT TEST EQUIPMENT

Reaction Beam

A 40 ft (12.2 m) long reaction beam was fabricated from two WF 30 x 132 beams, attached side by side using 1/2 in. (12.7 mm) thick plate bracing, with a spacing of 10 in. (254 mm) between the inside flange edges. Cover plates 1/2 in. (12.7 mm) thick were welded to the top and bottom of the flanges to increase the bending capacity of the reaction beam. Figure 5-1a shows a profile of the reaction system, with a plan view given in Figure 5-1b. The beam was supported on wood cribbing made of 10 in. x 10 in. (254 mm x 254 mm) and 8 in. x 8 in. (203 mm x 203 mm) hardwood timbers. The base dimensions of the timber cribbing were 5.8 ft x 10 ft (1.78 m x 3.05 m). A 4 in. (102 mm) thick steel bearing plate with a 6 in. (152 mm) central hole was used to bridge the top of the beam flanges and transfer the jack loads to the reaction system. An angle plate was used on the bearing plate to position a hydraulic jack so that the loads could be applied along the axis of the stub. Separate angle plates were made for each grillage set, based on the stub inclination angles given previously.

The timber cribbing was positioned so that the stub angle was approximately centered between the reaction bearing areas, with a slightly shorter distance separating the back of the stub from the nearest edge of the cribbing. Dimensions of the beam and cribbing, and positioning of the cribbing, were such that an imaginary line projected upward at 30° off vertical from the grillage base was well within the cribbing separation distance. This distance was used so that the reaction loads would have minimal, if any, influence on the uplift capacities. The position of the bases for the three grillage sets (Numbers X2,

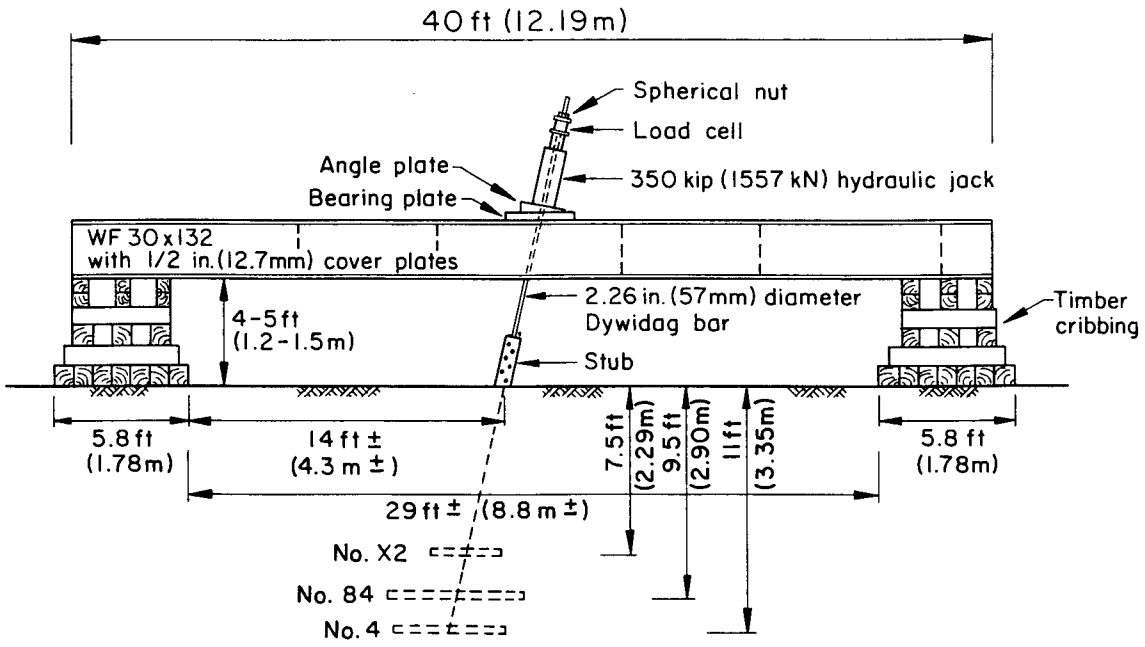

a) Profile

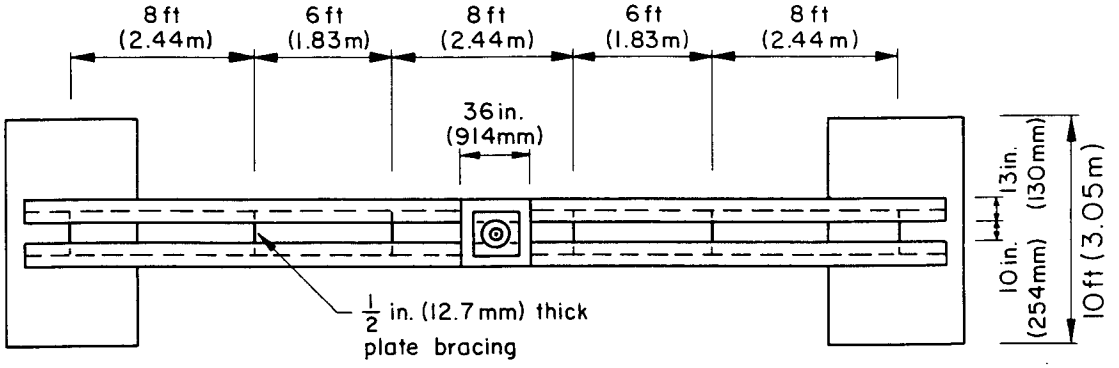

b) Plan

Figure 5-1. Load Reaction System

84, and 4) are shown in Figure 5-1a relative to the reaction pads.

Connections

Bolted angle connections were used at the grillage stubs. Figure 5-2 shows a typical field connection. Angle sections were fabricated to match the field stubs and existing bolt pattern. Analyses for shear and bearing indicated that

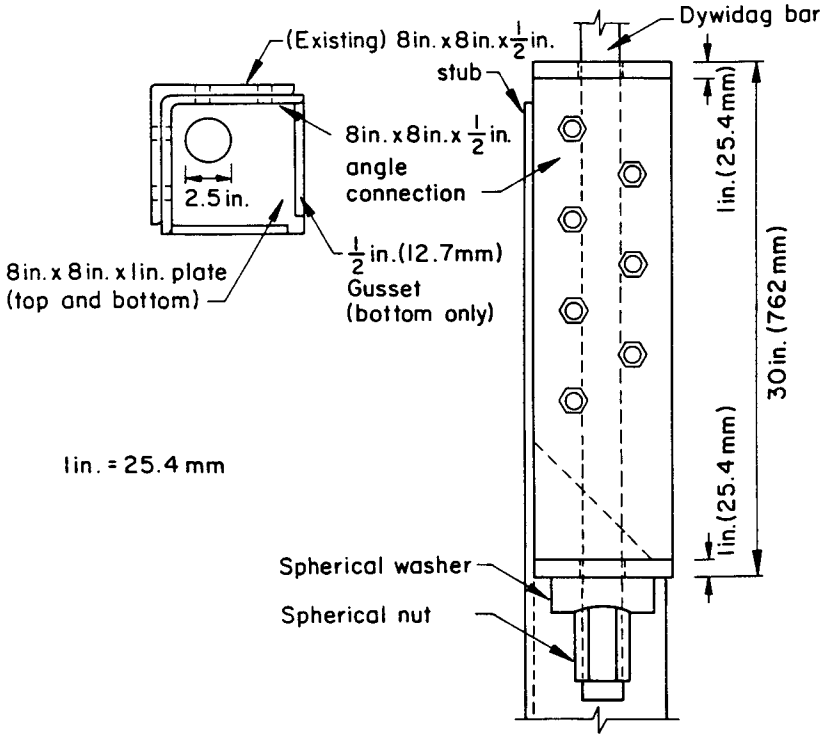

Figure 5-2. Typical Field Connection (Hickling Station, No. 4)

the existing bolt pattern of the field stubs could be used without additional welds or bolt holes. High strength ASTM A325 bolts were used to connect the angles to the field stubs. One inch (25 mm) thick plates were welded to the top and bottom of the angle connections, with a cutout for the 2.26 in. (57 mm) diameter Dywidag bar. On the bottom of the connection angle, 1/2 in. (12.7 mm) thick angle gussets were welded to increase the base strength. A spherical washer and spherical nut were used at the base of the angle connections to transfer the uplift loads. Table 5-1 gives the dimensions of the stub angles and connection angles used at each test site, along with the number of bolts used. At the Wyncoop Creek site, four bolts from the stabilizing wing sections were removed to allow for a longer connection section with additional bolts. The angle connection lengths ranged from 24 to 30 in. (610 to 762 mm) long, depending on the grillage being tested. Since the connections were similar in concept for each of the three grillage types, detailed drawings are not given for the Hickling Station No. 84 and Wyncoop Creek No. X2 grillages.

The upper connection and positioning for the hydraulic jack and load cell are

Table 5-1

CONNECTION DIMENSIONS

Site	Stub		Connection		
	Angle Size (in.)	Bolt Hole Diameter (in.)	Angle Size (in.)	Bolt Diameter (in.)	No. of Bolts
Hickling Station, No. 4	8 x 8 x 1/2	13/16	8 x 8 x 1/2	3/4	14
Hickling Station, No. 84	6 x 6 x 5/8	13/16	6 x 6 x 5/8	3/4	16
Wyncoop Creek, No. X2	5 x 5 x 5/16	11/16	5 x 5 x 1/2	5/8	12

1 in. = 25.4 mm

shown in Figure 5-3. The jack had a capacity of 350 kips (1557 kN), and the load cell capacity was 300 kips (1334 kN). The jack was located on the angle plate, in line with the axis of the grillage stub. The donut-type load cell was sandwiched between a steel plate and a spherical washer, on top of the hydraulic ram. A spherical nut on the Dywidag bar held the load cell and washers in position.

Load

A nitrogen-driven pump was used to apply pressure within a gas-hydraulic fluid reservoir. The pump was supplied by Dudgeon, Inc., as was the hydraulic jack. A pressure regulator was used to control the nitrogen pressure, and a 6 in. (152 mm) diameter pressure gage was used to monitor hydraulic pressure. Calibration data were supplied by the manufacturer. During calibration, the output force of the hydraulic cylinder at 2, 4, and 6 in. (51, 102, and 152 mm) displacement was measured, along with the hydraulic gage reading. The calibration data were not dependent on ram extension over this range. The calibration curve for the hydraulic jack and gage is shown in Figure 5-4 and is given by:

$$\text{Force (kips)} = 0.7 + 0.0464 \times \text{gage (psi)} \qquad (5\text{-}1)$$

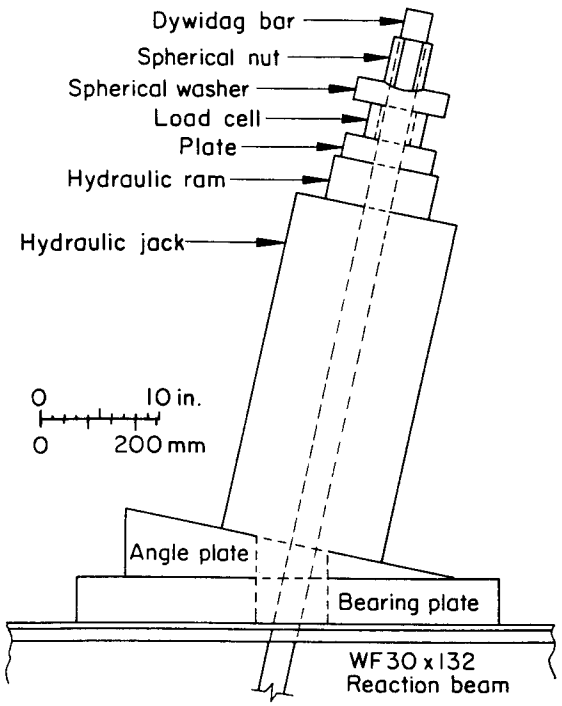

Figure 5-3. Upper Connections and Positioning of Hydraulic Jack and Load Cell

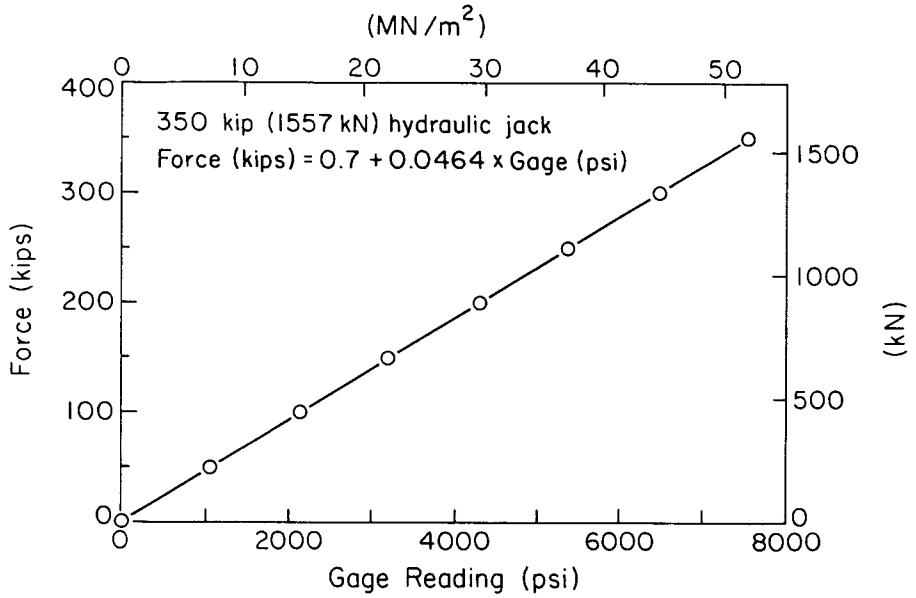

Figure 5-4. Hydraulic Jack and Gage Calibration

Loads also were monitored using an electronic load cell. The load cell was a donut-type with a 5 in. (127 mm) O.D., 3 in. (76 mm) I.D., and a height of 3 in. (76 mm). The load cell was manufactured by A. L. Design, Inc. Two calibrations were done at Cornell University on the load cell, one prior to field testing and the second after testing was completed. The load cell calibration curves are shown in Figure 5-5. Prior to field testing, the load cell had a measured sensitivity of 3.355 mV/V. The recalibration following testing resulted in a sensitivity of 3.428 mV/V, which was 2.2 percent higher than the initial calibration value. The multiple field load cycles were the most probable cause of the shift. Routine experience with electrical resistance strain gage circuits often shows an effect of cycling on long-term gage sensitivity and response. The higher sensitivity was used to reduce the final data, although the 2.2 percent difference is not significant for this application.

During testing, data were recorded from both systems. The load cell was the primary method used to obtain the uplift load. Excitation voltage for the load cell was provided by a Hewlett-Packard (HP) 6200B power supply, and a Fluke 8060A 3-1/2 digit, digital voltmeter (DVM) was used to monitor the excitation voltage. A HP 3456 6-1/2 digit DVM was used to monitor the output from the load cell. This DVM has math capabilities that allowed the load cell calibration

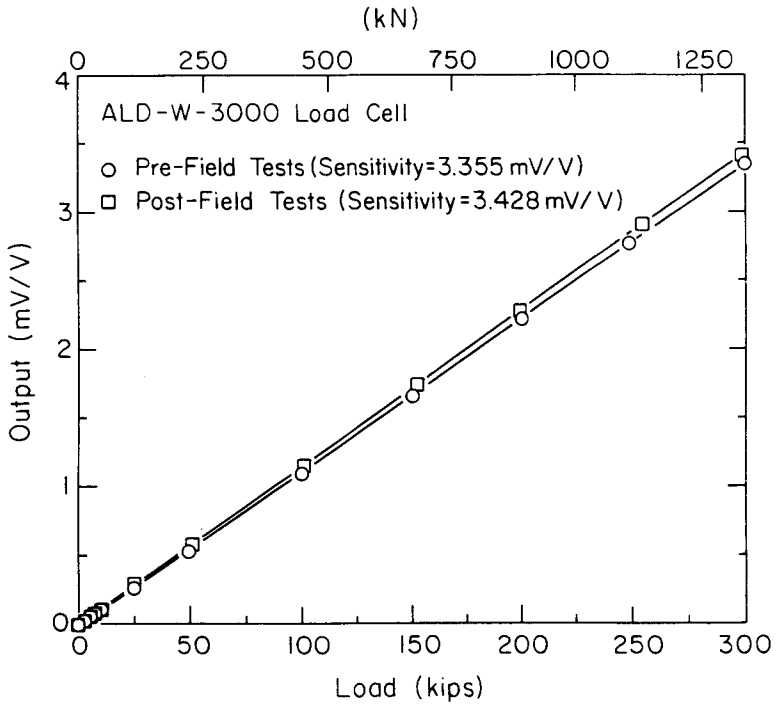

Figure 5-5. Load Cell Calibration

constant and any initial unbalanced bridge voltage to be programmed. Therefore, the HP 3456 DVM displayed the load cell reading directly in engineering units of kips. A Honda EX 3300 gas-powered generator was used to supply line voltage to the HP 6200B power supply and HP 3456 DVM, while the Fluke 8060A DVM was battery-powered. The generator turned out to be one of the more important pieces of field equipment. Since testing began in the morning and continued all day, the continuous operation of a noisy generator would have been troublesome. This generator was very quiet and provided extremely smooth power without surges and variations.

The hydraulic jack force was monitored with the 6 in. (152 mm) diameter pressure gage that had a full-scale of 10,000 psi (68.9 MN/m^2) with minor gradations that could be estimated to 10 psi (68.9 kN/m^2). Therefore, the precision of the pressure gage was on the order of $\pm$ 0.5 kip ($\pm$ 2.2 kN). Pertinent information on both the hydraulic jack and load cell are given in Table 5-2.

Displacement

Two displacement systems were used to measure stub movement. The primary system was optical leveling. A series of benchmarks was established at the test sites as vertical elevation references. A graduated scale was mounted vertically on the stub and a fixed-position level was used to record elevation changes. Elevations were read with a Lietz B1 level located roughly 25 ft (7.62 m) from the stub. The scale was read to the nearest 0.005 ft (1.5 mm).

The secondary displacement system consisted of a 0.001 in. (0.025 mm) sensitivity, 2 in. (51 mm) range dial gage mounted on a light reference beam. The reference beam was located just in front of the stub, with the dial gage stem contacting the base of the connection angle at a tilt so it was parallel to the stub. The reference beam was 20 ft (6.10 m) long, placed perpendicular to the reaction beam, with the ends of the reference beam equidistant from the stub. This layout represented the secondary system, because the 2 in. (51 mm) range often required that the gage be repositioned. Also, possible slippage between the bolted connection and stub would affect the dial gage readings. As will be shown in a later section, large stub movements coupled with the limited 2 in. (51 mm) dial gage range was the main reason the optical survey was used as the primary method for measuring stub displacement. Use of optical systems also is regarded as the simplest and most reliable method (1).

Table 5-2

HYDRAULIC JACK AND LOAD CELL DATA

a) Hydraulic jack

Manufacturer	Serial Number	Capacity (kips)	Stroke (in.)
Richard Dudgeon, Inc. Stamford, CT	RJ1225	350	11.75

b) Hydraulic pump and gage

Manufacturer	Serial Number	Pressure Rating (psi)	Dial Diameter (in.)	Sensitivity (kip/psi)
Richard Dudgeon, Inc. Stamford, CT	1202080	10000	6	0.0464

c) Load cell

Manufacturer	Model	Serial Number	Capacity (kips)	Excitation (volts)	Sensitivity (mV/V)
A. L. Design, Inc. Amherst, NY	ALD-W-3000	870504	300	10.0	3.428

1 in. = 25.4 mm
1 kip = 4.45 kN
1 psi = 6.895 kN/m^2

Ground surface displacements also were monitored using an arrangement of wooden hubs located near the stubs. Hub elevations were monitored by optical survey and a leveling rod. The array was laid out in a typical pattern, as shown in Figure 5-6. Exact hub locations for each test will be given in a later section.

TEST LOADING PROCEDURE

Load testing of grillage foundations requires different equipment than that necessary for drilled shafts, as given in EPRI EL-5915 (2). This observation is

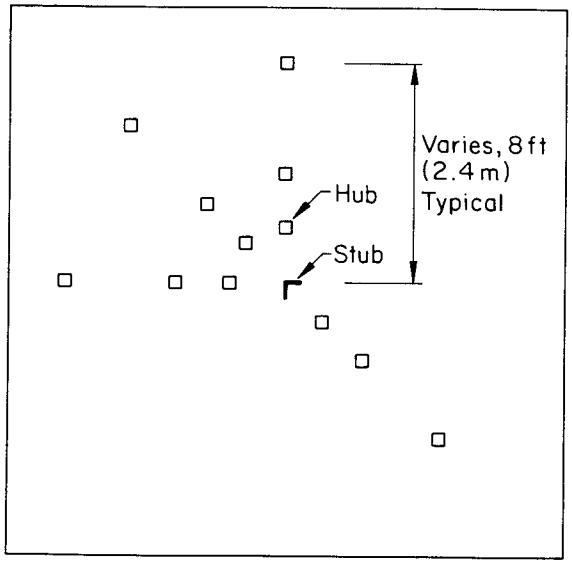

Figure 5-6. Typical Geometric Hub Arrangement

particularly true regarding tests generating large displacements, exceeding 10 in. (254 mm). However, many of the general recommendations given in EPRI EL-5915 (2) still can be used. A modified quick maintained load procedure was used for the field uplift tests. Test loads were applied as quickly as possible using the hydraulic pump, in increments of ten percent of the estimated failure load. For loads up to 50 percent of the estimated maximum, the load was maintained for 10 minutes, and readings were made every two and one-half minutes. For loads in excess of 50 percent of the estimated maximum, the load was maintained for 16 minutes, with readings made every four minutes.

At each time interval, a set of measurements was made, consisting of stub displacements by optical survey and dial gage, loads from jack and load cell, hub displacements, reference beam elevation, bearing pad elevation, and reaction beam deflection. If negligible creep occurred between each time interval (2.5 or 4 minutes), the next load was applied. If creep displacements developed of more than ten percent of the incremental deflection caused by the initial load application, then an equilibrium procedure was planned. Creep displacements, however, just did not occur. At high loads, say greater than 90 to 95 percent of the maximums, it was sometimes difficult to maintain the desired load. In those cases, the pump was run continuously, and stub displacements were recorded as quickly as the optical leveling permitted.

At least two, and often three or more, unload-reload cycles were performed during each test. At 30 percent of the estimated failure load, the loads were decreased to 20, 10, and 0 percent. The foundations then were reloaded to 60 percent of the estimated maximum, followed by unloading to 40, 20, and 0 percent. Finally, the grillages were loaded to their maximum and unloaded, in steps of 20 percent.

During the testing, it often was necessary to unload and reposition the hydraulic jack. Even though the stroke capacity was rated at 11.75 in. (298 mm), a maximum stroke of roughly 9 in. (229 mm) could be obtained. When the maximum stroke was reached, the grillage was unloaded, the ram was retracted, and the upper spherical nut was adjusted.

SUMMARY

Loads were applied along the axis of each stub through a bolted connection. The 40 ft (12.2 m) reaction beam was described, along with the equipment used to monitor load and displacement. An electronic load cell was the primary load measuring system, with redundancy given by a calibrated hydraulic jack. Calibrations were given for both systems, with pre- and post-calibrations on the load cell.

The primary system for measuring stub displacements was an optical survey. A reference beam with dial gage was used for redundancy. Ground movements were monitored using an array of wooden hubs.

The loading procedure principally was a modified quick maintained load method. The grillages were subjected to several unload-reload cycles prior to applying the maximum possible loads.

REFERENCES

1. Dunnicliff, J., Geotechnical Instrumentation for Monitoring Field Performance, John Wiley and Sons, New York, 1988, 577 p.

2. Hirany, A. and Kulhawy, F. H., "Conduct and Interpretation of Load Tests on Drilled Shaft Foundations: Detailed Guidelines", Report EL-5915, Vol. 1, Electric Power Research Institute, Palo Alto, 1988, 374 p.

Section 6

UPLIFT TEST RESULTS

This section presents the results from the eight field uplift tests on the grillages. Three tests each on grillage types No. 4 and No. 84 were conducted at the Hickling Station site, while two were tested at the Wyncoop Creek site. Table 6-1 lists the grillages tested and test dates. Axial load versus axial displacement results are shown, along with the ground displacement patterns. Typical deflections of the load reaction system are given. Comparisons are shown for the load determined from the load cell force and the hydraulic jack pressure gage. Interpretations of the failure loads are presented, and a recommendation is made for predicting displacements for grillages in granular soil. Uplift capacities are shown to be dependent both on the foundation depth, D, and width, B, as well as the D/B ratio.

HICKLING STATION

Load versus Displacement

The No. 4 grillages at Hickling Station had base dimensions of 4.75 ft x 5.0 ft (1.45 m x 1.52 m) and a nominal design embedment of 11 ft (3.35 m). At each site, several elevation benchmarks were established. The elevations at the top of the stub and ground line were measured by optical survey. Knowing the steel stub lengths and inclination angles, stub connection details, and grillage base thicknesses, as given in Section 2, the elevations at the bases of the foundations were calculated. The differences between the ground line elevations and the base elevations were the field embedments. These embedments are given in Table 6-2 for the No. 4 grillages at Hickling Station. As shown in this table, the average embedment was 10.5 ft (3.20 m), as compared with the nominal design depth of 11 ft (3.35 m). This 0.5 ft (0.15 m) difference occurred because of site grading and other activities over the 40 years since the grillages were installed. The average field D/B was 2.15, compared with the design D/B of 2.25.

Figure 6-1 shows the load-displacement curves for the Number 4 grillages. The

Table 6-1

TEST GRILLAGES

Site	Grillage Number	Test Number	Test Date
Hickling Station	4-NW	1	2 June 1987
	4-NE	2	4 June 1987
	4-SW	6	17, 18 June 1987
Hickling Station	84-SE	3	8, 9 June 1987
	84-NE	4	10, 11 June 1987
	84-SW	5	15, 16 June 1987
Wyncoop Creek	X2-SE	7	22, 23 June 1987
	X2-SW	8	24 June 1987

Table 6-2

FIELD EMBEDMENT DEPTHS, GRILLAGE SET NO. 4, HICKLING STATION

Stub	Elevation (ft)			Embedment Depth (ft)
	Top of Stub	Ground Line	Grillage Base[a]	
4-NE	103.9	100.6	90.3	10.3
4-NW	103.9	101.1	90.3	10.8
4-SE	104.0	100.7	90.4	10.3
4-SW	104.0	100.8	90.4	10.4
Average:				10.5

1 ft = 0.305 m

a - Stub elevation minus 13.9 cos 12°

shapes of the backbone or primary loading curves for all three grillages are remarkably similar. The main differences are the test displacement levels. The maximum loads and displacements measured in these tests are given in Table 6-3.

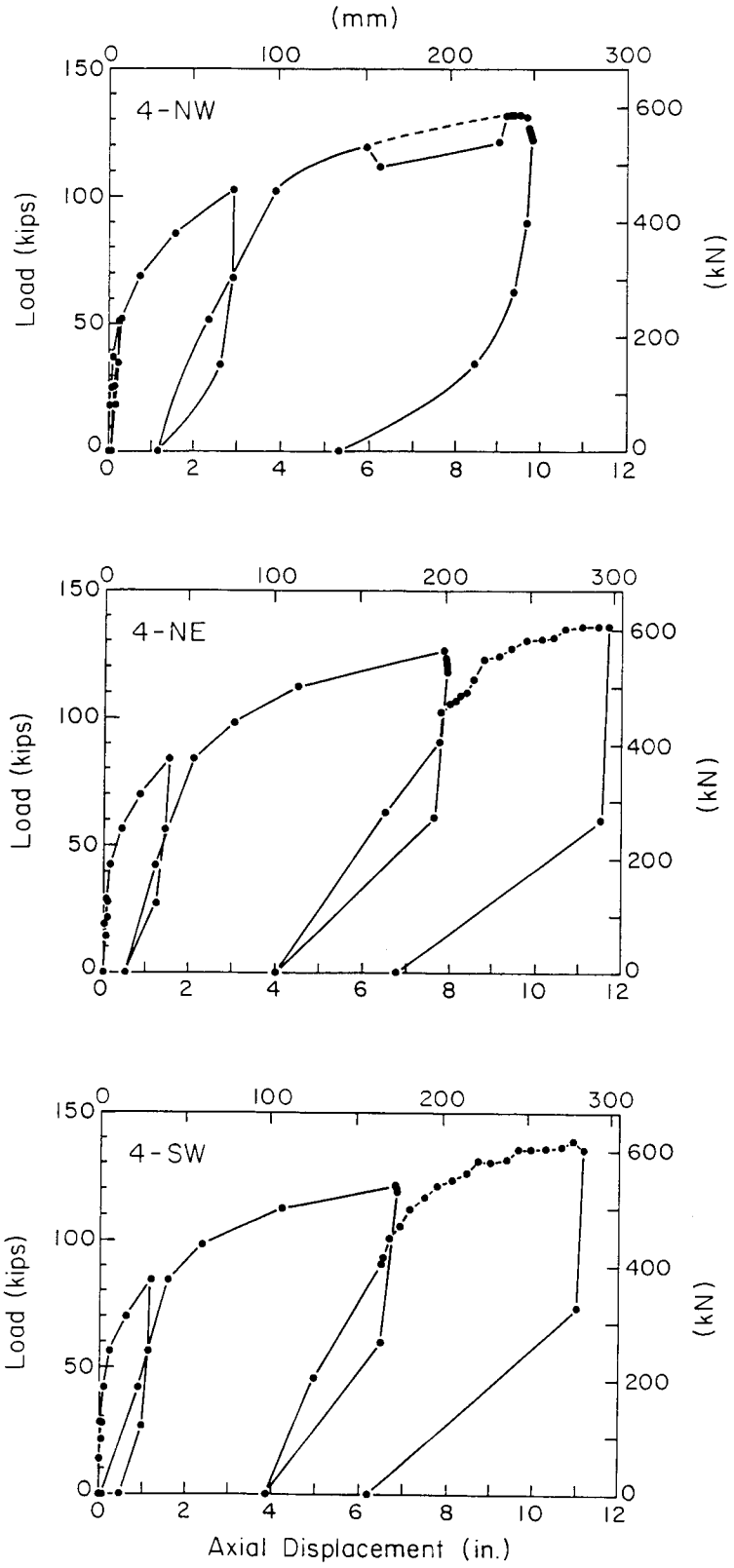

Figure 6-1. Grillage Load versus Displacement, Set No. 4, Hickling Station

Table 6-3

MAXIMUM LOADS AND DISPLACEMENTS, GRILLAGE SET NO. 4, HICKLING STATION

Grillage Number	Maximum Axial Load		Maximum Axial Displacement	
	kips	kN	in.	mm
4-NW	132	587	9.6	244
4-NE	136	605	11.8	300
4-SW	139	618	11.0	279
Averages:	136	603		
COV(%)	2.6	2.6		

The maximum loads ranged from 132 to 139 kips (587 to 618 kN). The maximum displacements of 9.6 to 11.8 in. (244 to 300 mm) are not necessarily related, since the tests could have been continued to larger displacements, subject to the jack limitations.

Axial displacements of 1 in. (25 mm) generally corresponded to loads of 75 to 85 kips (334 to 378 kN), which correspond to about 55 to 65 percent of the maximum applied load. At loads greater than 75 to 85 kips (334 to 378 kN), displacements increased rapidly.

Figure 6-2 shows comparisons between the load cell readings (the primary load system) and those determined from the hydraulic gage. The readings are in good agreement, with the gage readings tailing off slightly for test 4-SW. The hydraulic jack calibrations at 2, 4, and 6 in. (25, 51, and 102 mm) ram extensions were identical. However, at large displacements, the ram was near its full extension of about 9 in. (229 mm). Despite the rated extension of 11.75 in. (298 mm), only 9 in. (229 mm) could be obtained during the tests. Repeated adjustments of the spherical nut on the top of the Dywidag bar, as described earlier, were necessary to achieve the large field displacements.

The No. 84 grillages at Hickling Station had base dimensions of 7 ft x 7 ft (2.13 x 2.13 m) and a nominal design embedment of 9.5 ft (2.90 m). The field embedments are given in Table 6-4, which shows an average embedment of 9.3 ft

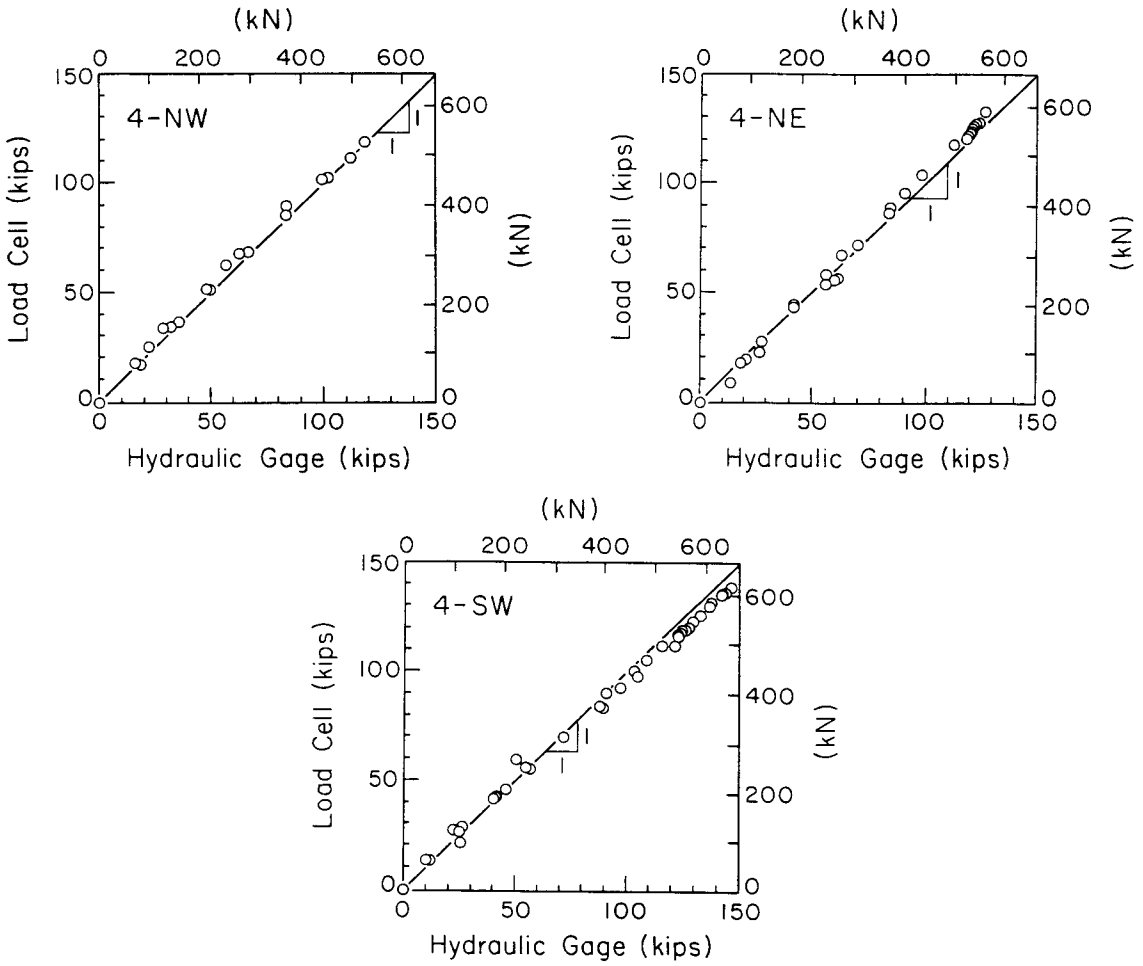

Figure 6-2. Load Cell versus Hydraulic Gage, Set No. 4, Hickling Station

(2.83 m). The average D/B was 1.33, while the design D/B was 1.36.

Table 6-5 and Figure 6-3 give the load-displacement data for the No. 84 grillages. The curves in Figure 6-3 are similar in general, but with slightly more variability than the No. 4 grillages. The maximum loads and axial displacements from these tests are given in Table 6-5. The maximum loads ranged from 151 to 165 kips (672 to 734 kN), at displacements of 9.6 to 11.9 in. (244 to 302 mm). At axial displacements of 1 in. (25 mm), the loads were 103 to 107 kips (458 to 476 kN), which correspond to 65 percent of the maximum load, a value similar to those obtained from the No. 4 grillages at 1 in. (25 mm) displacement. At loads greater than 65 percent of the maximums, the displacements increased rapidly with additional applied forces.

Table 6-4

FIELD EMBEDMENT DEPTHS, GRILLAGE SET NO. 84, HICKLING STATION

Stub	Elevation (ft)			Embedment Depth (ft)
	Top of Stub	Ground Line	Grillage Base[a]	
84-NE	100.7	99.5	90.3	9.2
84-NW	100.7	99.7	90.3	9.4
84-SE	100.7	99.4	90.3	9.1
84-SW	100.7	99.8	90.3	9.5
Average:				9.3

1 ft = 0.305 m
a - Stub elevation minus 10.2 cos 15° minus 0.5 ft

Table 6-5

MAXIMUM LOADS AND DISPLACEMENTS, GRILLAGE SET NO. 84, HICKLING STATION

Grillage Number	Maximum Axial Load		Maximum Axial Displacement	
	kips	kN	in.	mm
84-SE	165	734	11.9	302
84-NE	165	734	9.6	244
84-SW	151	672	10.7	272
Averages:	160	712		
COV(%)	5	5		

Figure 6-4 shows the load cell and hydraulic gage readings from the No. 84 tests. For applied loads greater than about 100 kips (445 kN), the divergence between the load cell and gage increases, with the gage readings higher than those recorded using the load cell. This divergence indicates that the ram on

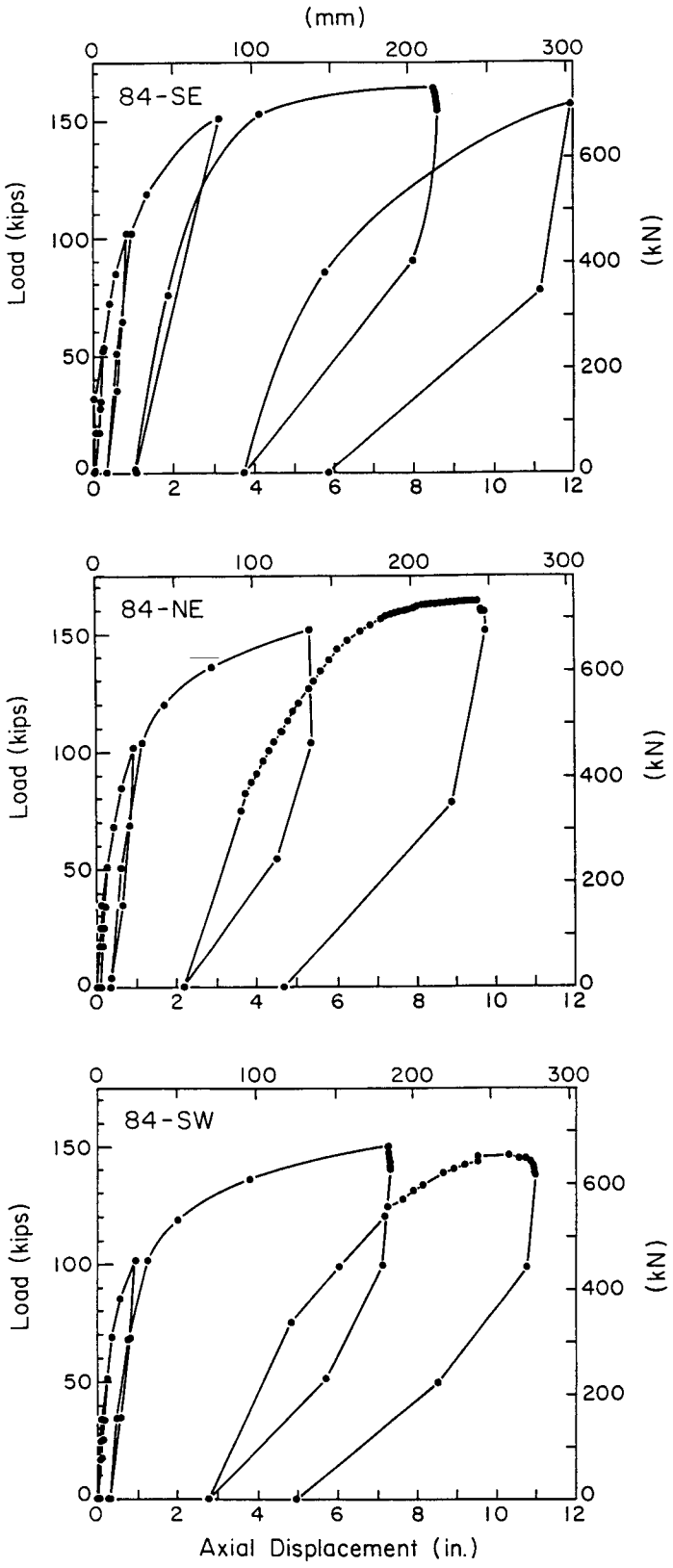

Figure 6-3. Grillage Load versus Displacement, Set No. 84, Hickling Station

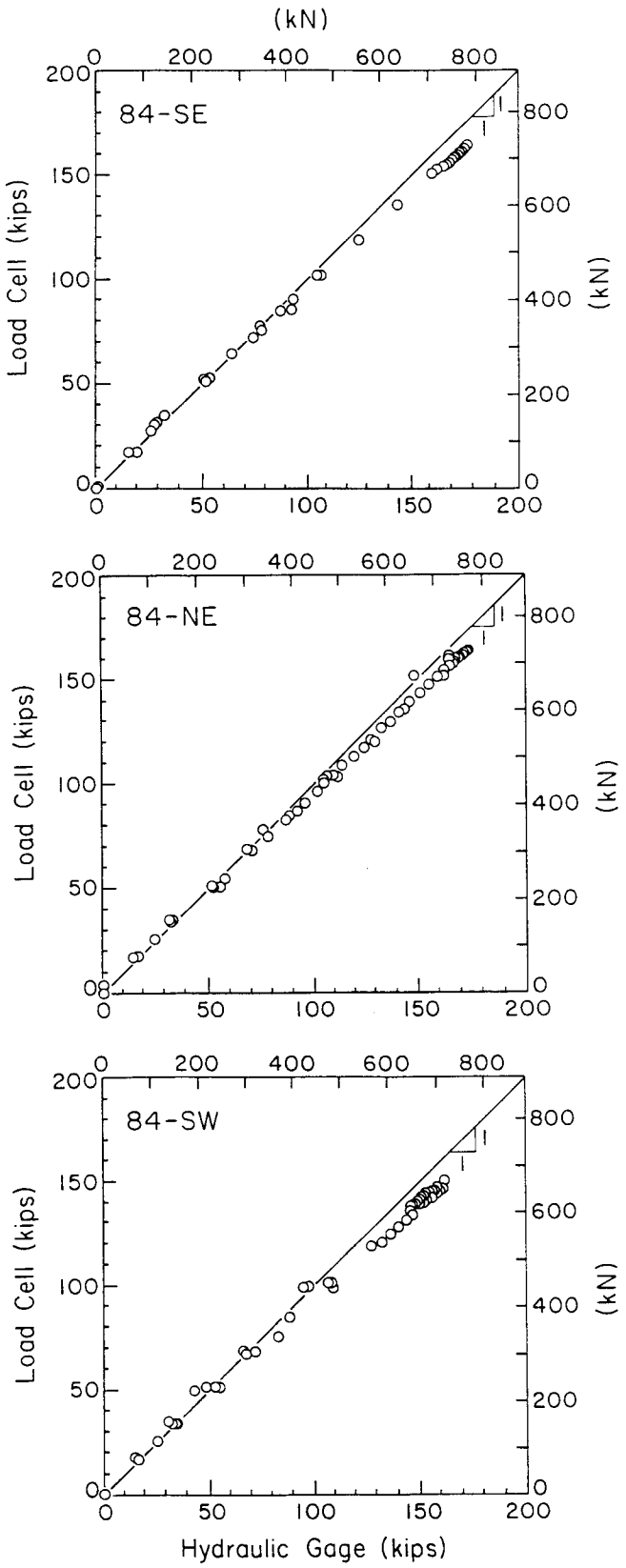

Figure 6-4. Load Cell versus Hydraulic Gage, Set No. 84, Hickling Station

the jack may have reached its extension capacity, even though additional hydraulic pressure was applied.

As noted previously, a full set of test measurements at a given load increment also consisted of an optical survey of the reaction beam deflection, reaction pad settlement, and reference beam elevations. Figure 6-5 shows the results of these measurements for test No. 84-SW, as a representative data set. The location of the displacements on the reference beam was directly below the hydraulic jack on the lower flange. The reaction pad settlements shown were measured on

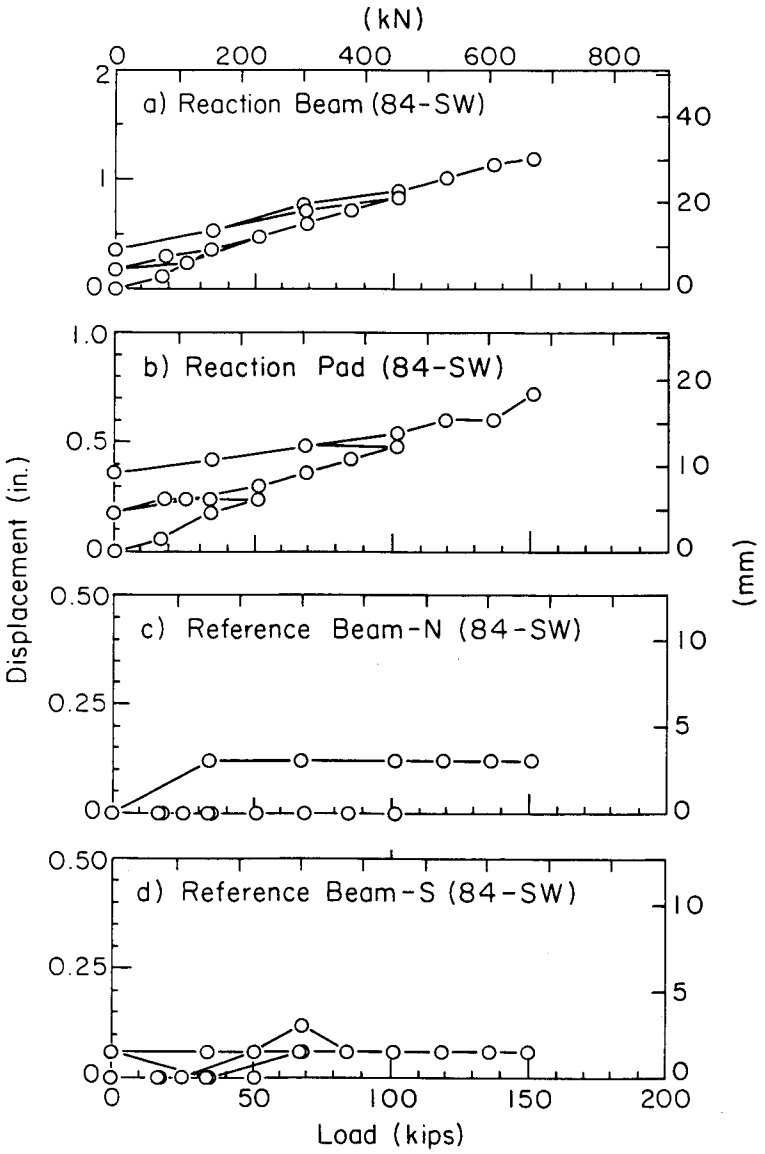

Figure 6-5. Typical System Movements, Grillage No. 84-SW, Hickling Station

the inside edge of the pad on the back side of the stub. The maximum reaction beam deflection, shown in Figure 6-5a, was approximately 1.2 in. (30 mm) at the peak load. The reaction pad settlement at peak load was on the order of 0.75 in. (19 mm). Figures 6-5c and 6-5d show the elevation changes at the fixed ends of the reference beam, which were located 10 ft (3.05 m) away from the stub. The displacements were small, about 0.1 in. (2.5 mm), and were about equal to the resolution of the optical leveling system.

Ground Movements

Ground surface movements were measured using an array of wooden hubs placed around the stub. Survey readings of hub movement were made at each load level, unless continuous jacking was being done.

Figure 6-6 shows the hub positions at grillage No. 4-NW, which was the first uplift test and where only nine hubs were used. The number of hubs was increased to 12 for all subsequent tests. This figure also shows the displacement of hub numbers 1, 4, and 7 versus applied uplift load. These hubs were the closest to the stub. The hub measurements indicate very little ground surface movement until the applied load was about 100 kips (445 kN). The maximum movement of the closest three hubs was 0.35 in. (8.9 mm) at a load of 100 kips (445 kN). At this same load, the stub movement was 3 in. (76 mm). At a load of 60 percent of the maximum, the stub displacement was about 1 in. (25 mm), while the ground surface movements were less than 0.1 in. (2.5 mm).

Figure 6-7 shows contours of ground surface displacement (in inches) for grillage No. 4-NW. At a load of 102 kips (454 kN), there was very little ground surface movement. However, as loads increased beyond 102 kips (454 kN), the surface displacements increased. At 122+ kips (543+ kN) (the + sign designates loads that were slightly above the indicated values), the maximum ground displacement in the vicinity of the stub was 1.5 to 2 in. (38 to 51 mm).

The hub locations at grillage No. 4-SW are shown in Figure 6-8, which also shows the displacements of the closest hubs (numbers 1, 4, 7, and 10). Up to about 100 kips (445 kN), the surface movements are small, but they increase substantially beyond that load. Contours of ground surface displacement at grillage No. 4-SW are shown in Figure 6-9. At a load of 98 kips (436 kN), the maximum displacement contour is 0.2 in. (5.1 mm). Beyond this load, the extent of ground movements increases both in magnitude and areal extent. At a stub load

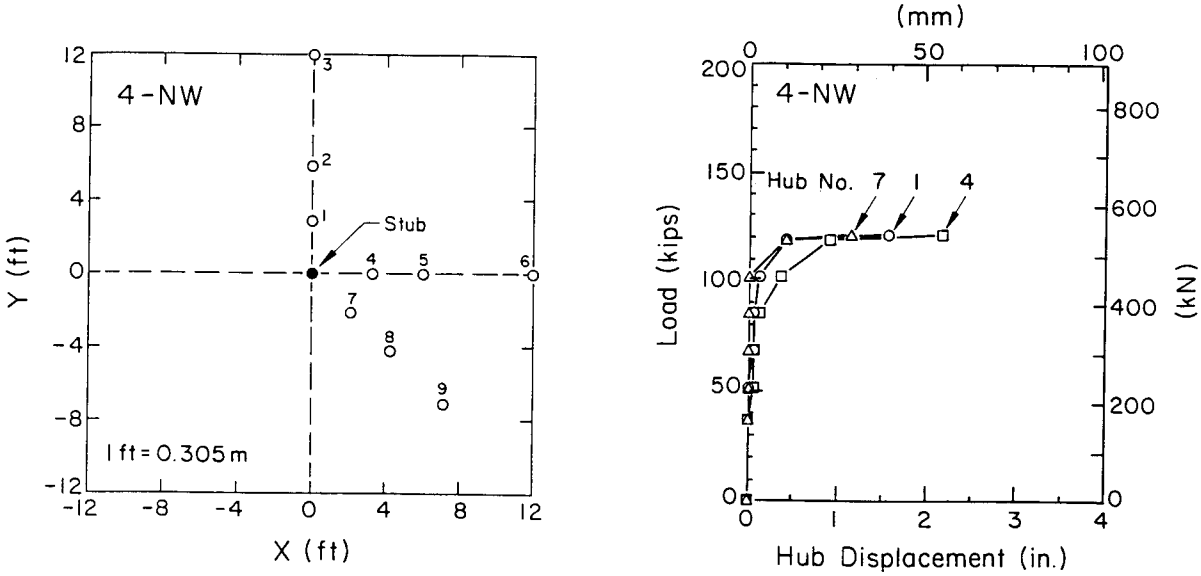

Figure 6-6. Hub Positions and Displacements, Grillage No. 4-NW, Hickling Station

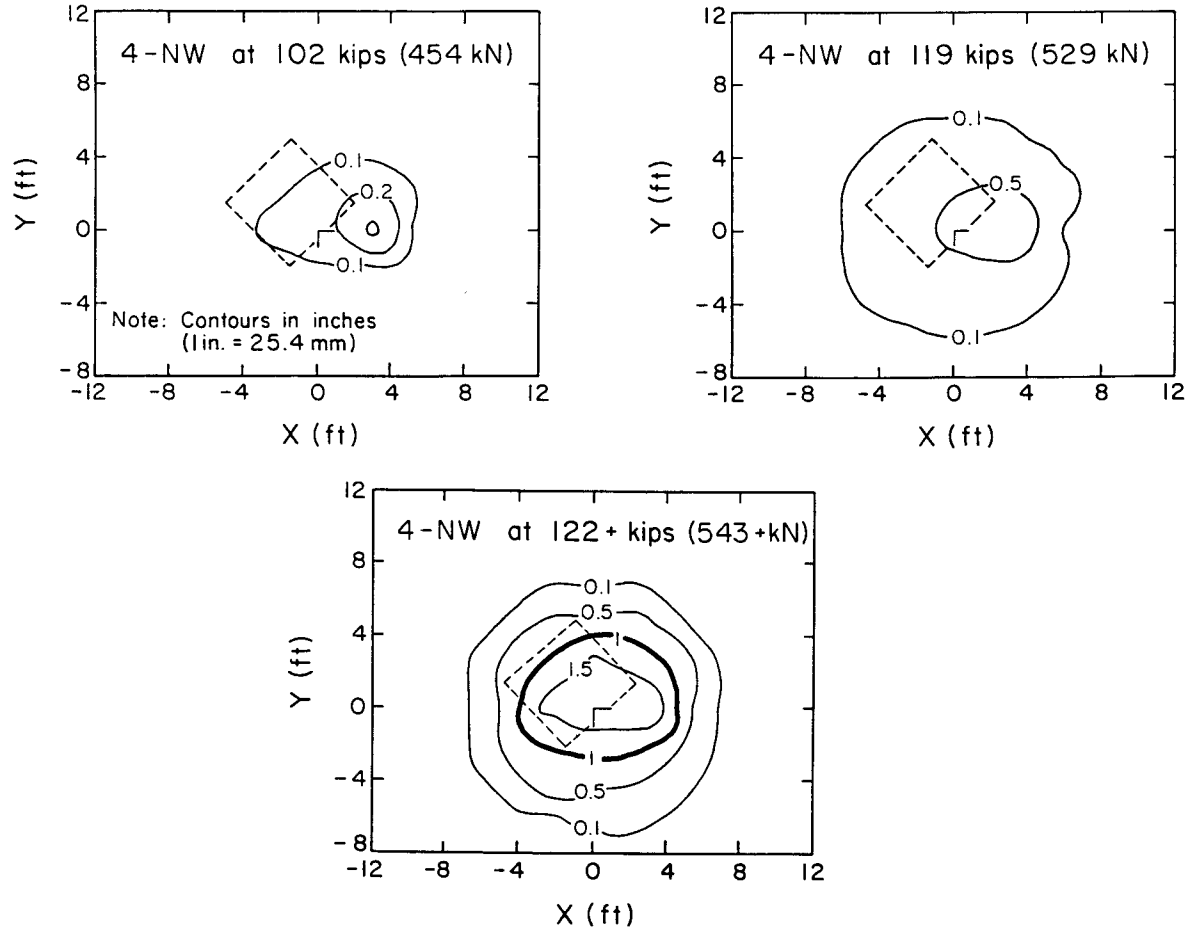

Figure 6-7. Ground Surface Displacements, Grillage No. 4-NW, Hickling Station

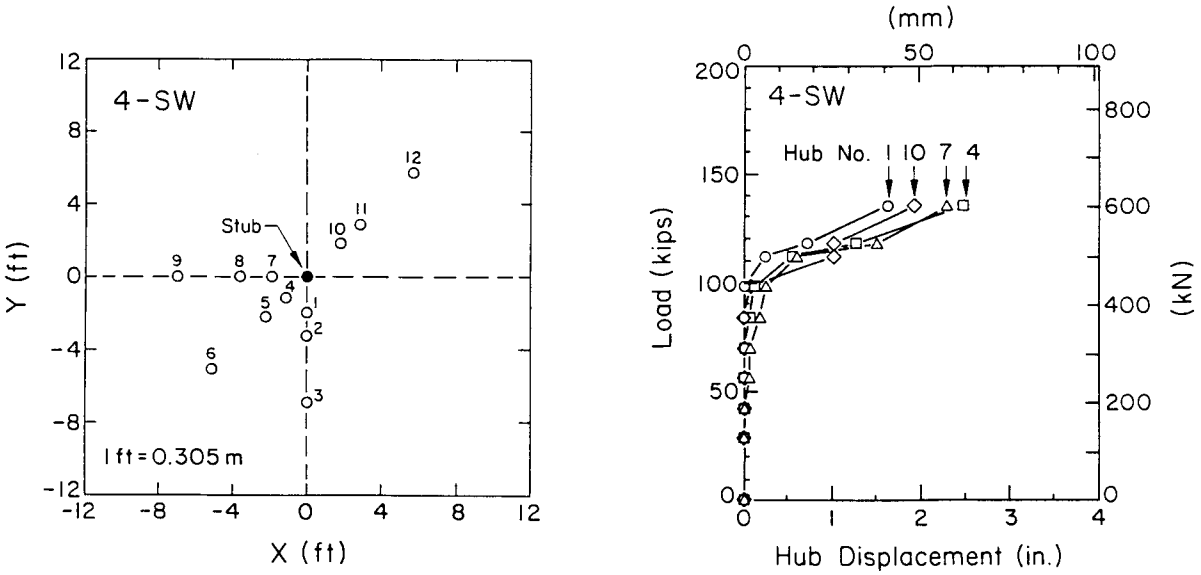

Figure 6-8. Hub Positions and Displacements, Grillage No. 4-SW, Hickling Station

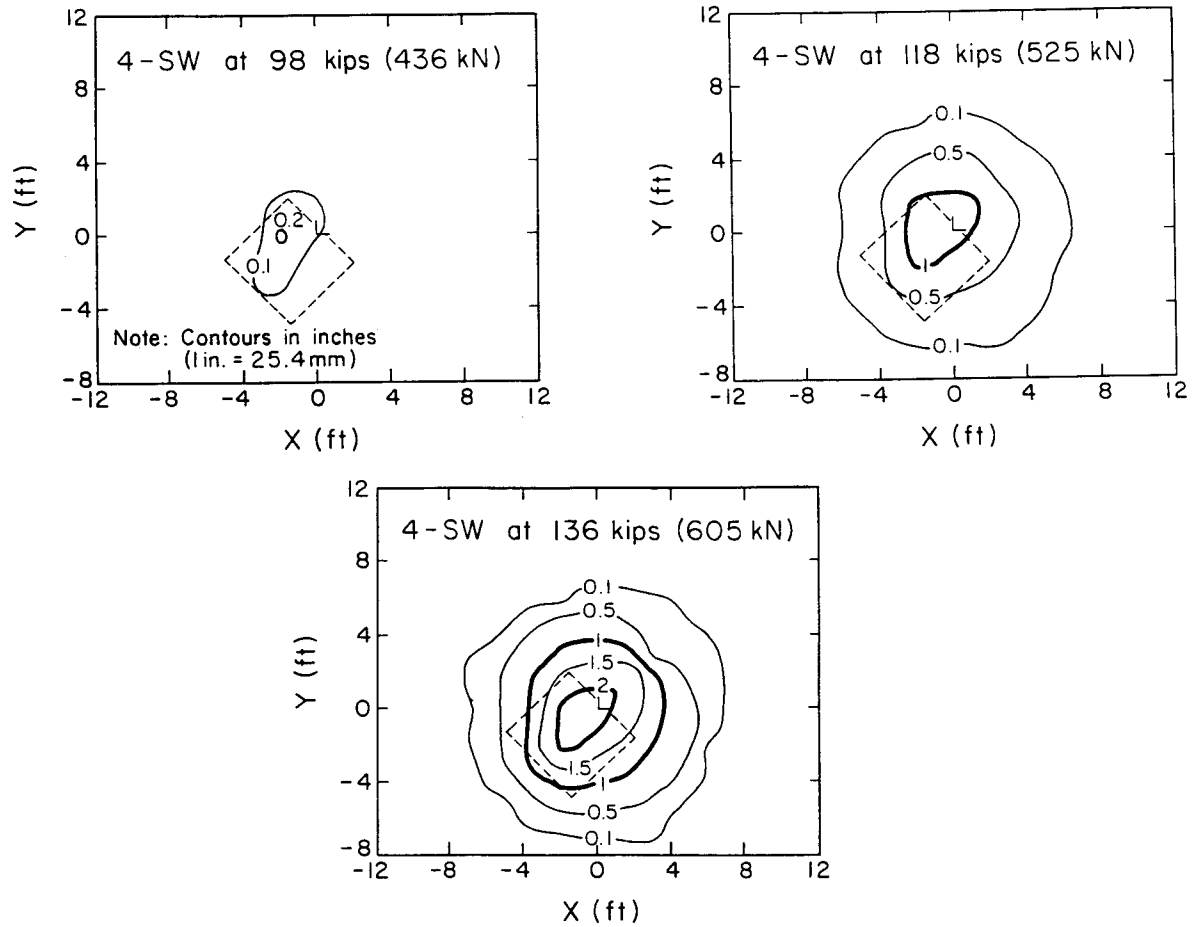

Figure 6-9. Ground Surface Displacements, Grillage No. 4-SW, Hickling Station

of 136 kips (605 kN), the ground displacement near the stub was 2 in. (51 mm), compared to the stub movement of nearly 10 in. (254 mm).

The hub locations and displacements of the closest hubs for grillage No. 4-NE are shown in Figure 6-10. At loads near 100 kips (445 kN), the surface movements again are small, on the order of 0.3 in. (7.6 mm). Displacements increase rapidly beyond 100 kips (445 kN). The contours of ground surface displacement at grillage No. 4-NE are shown in Figure 6-11. At a load of 130 kips (578 kN), the maximum displacement contour is 2.5 in. (64 mm). The stub displacement at 130 kips (578 kN) was nearly five times that amount.

The hub layout for grillage No. 84-SE is shown in Figure 6-12, along with the displacements for the four hubs closest to the stub. At 120 kips (534 kN), corresponding to 75 percent of the maximum load, the ground displacements are on the order of 0.25 in. (6.4 mm). The stub displacement at 120 kips (534 kN) was about 1.2 in. (30 mm). Although the maximum stub displacement for the test was 11.9 in. (302 mm) and the maximum hub displacement was 5.2 in. (132 mm), all but 1 in. (25 mm) of this displacement was recoverable upon reloading.

The contours of ground surface displacement for grillage No. 84-SE are shown for several load levels in Figure 6-13. Only about 0.4 in. (10 mm) displacement had developed at a load of 136 kips (605 kN), which was about 85 percent of the maximum applied loading. Ground displacements accumulated rapidly for loading beyond 153 kips (681 kN), with maximum ground displacements of 5 in. (127 mm). These ground displacements were nearly centered about the grillage base.

The hub layout for grillage No. 84-NE is shown in Figure 6-14, which also includes the hub displacements in the vicinity of the stub. At a load of 120 kips (534 kN), only slight ground displacements developed, equal to 0.2 in. (5.1 mm). At higher loads, the ground movements increased quickly. The contours of ground surface displacement for grillage No. 84-NE are shown in Figure 6-15. At a load of 152 kips (676 kN), the maximum surface movement is about 2 in. (51 mm), again centered about the grillage base.

Figure 6-16 shows the hub positions for grillage No. 84-SW and the displacements at hub numbers 1, 4, 7, and 10. At an applied axial load of 100 kips (445 kN), the ground movements were less than 0.3 in. (7.6 mm), while the stub displacement was 1 in. (25 mm). Displacements on the ground surface grew rapidly with loading beyond 100 kips (445 kN). The surface displacement patterns are shown

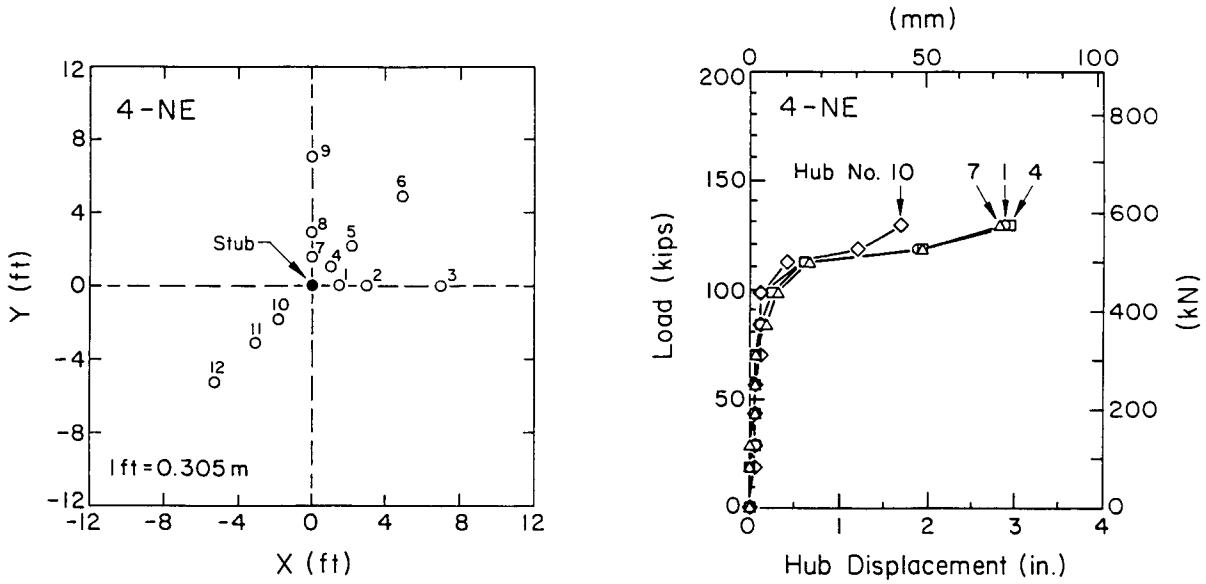

Figure 6-10. Hub Positions and Displacements, Grillage No. 4-NE, Hickling Station

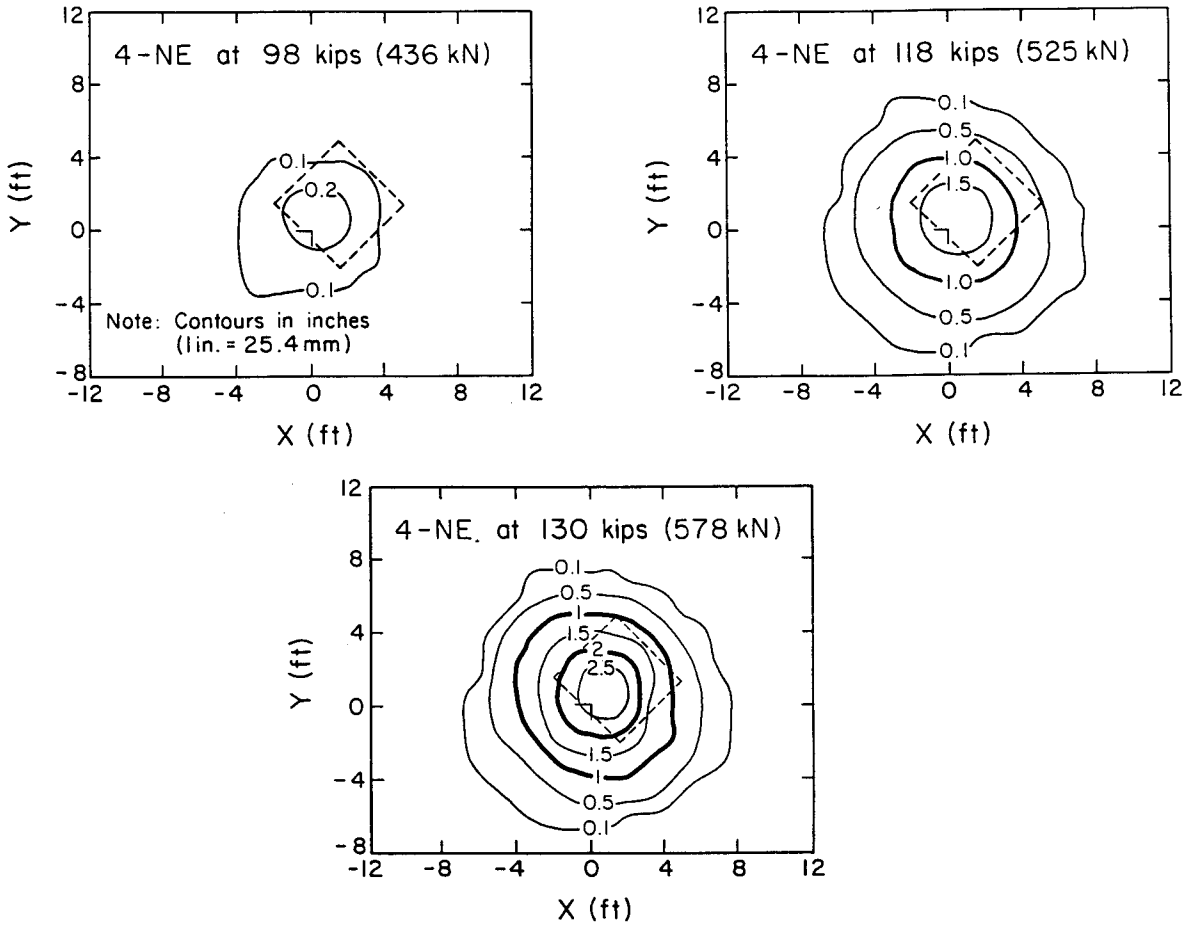

Figure 6-11. Ground Surface Displacements, Grillage No. 4-NE, Hickling Station

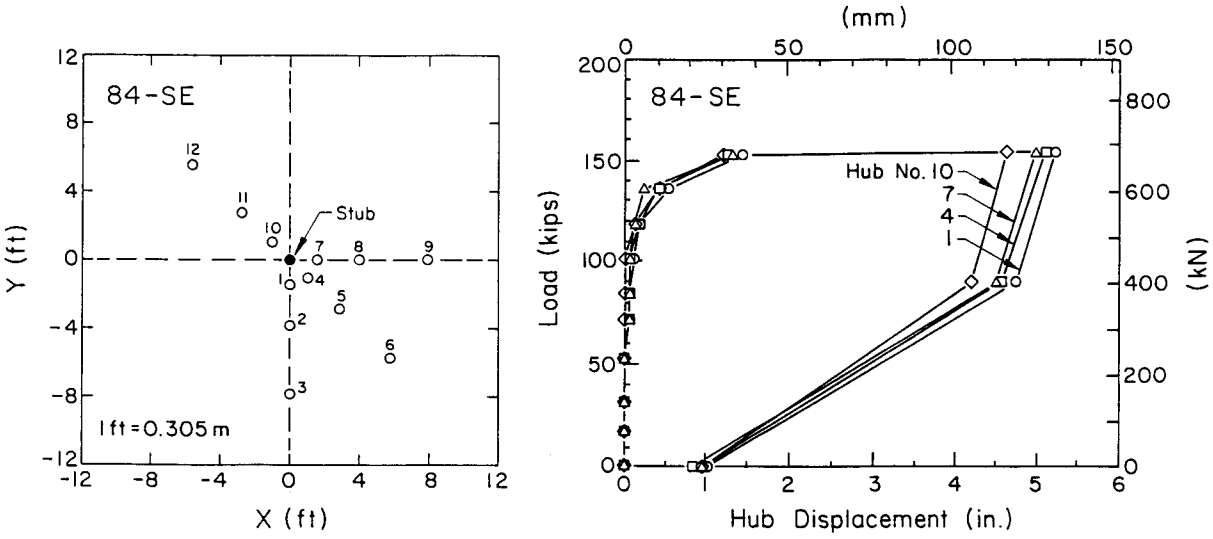

Figure 6-12. Hub Positions and Displacements, Grillage No. 84-SE, Hickling Station

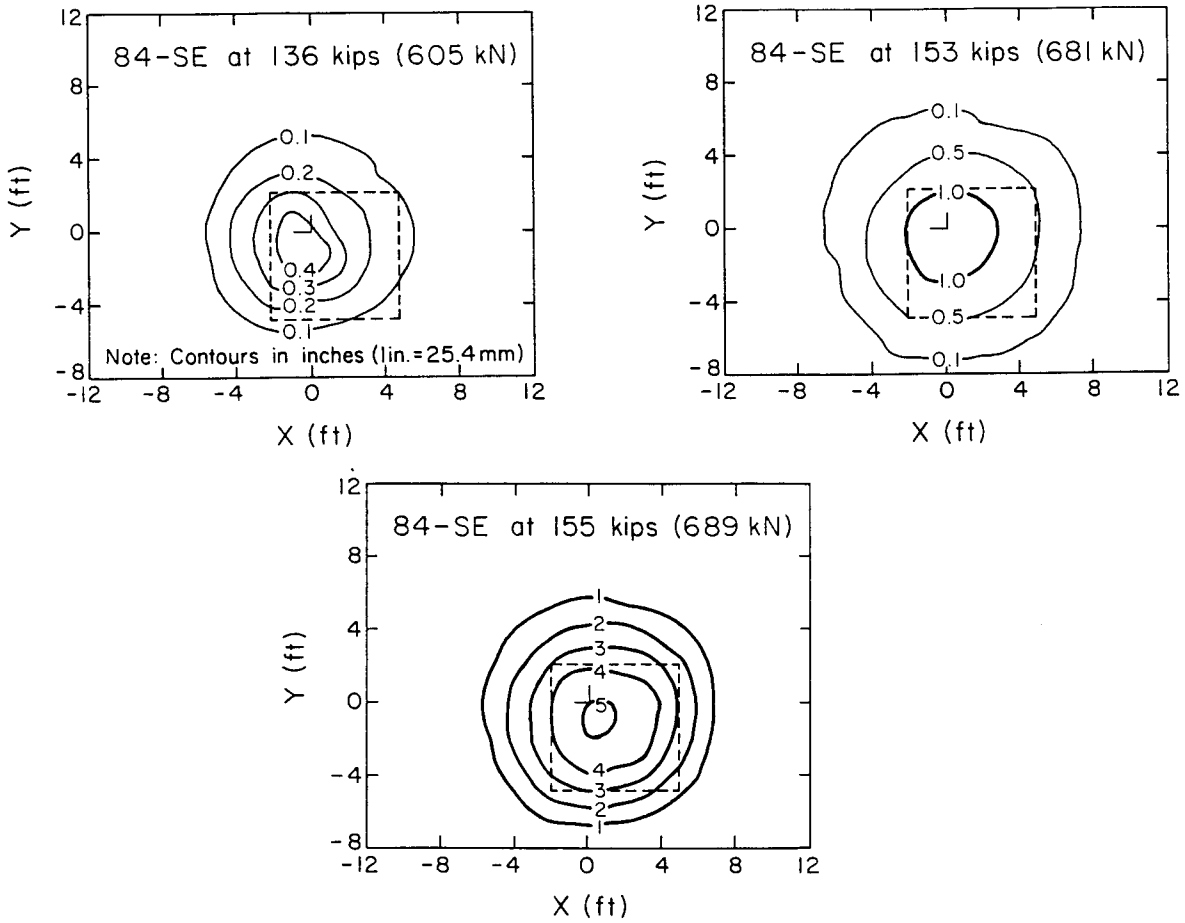

Figure 6-13. Ground Surface Displacements, Grillage No. 84-SE, Hickling Station

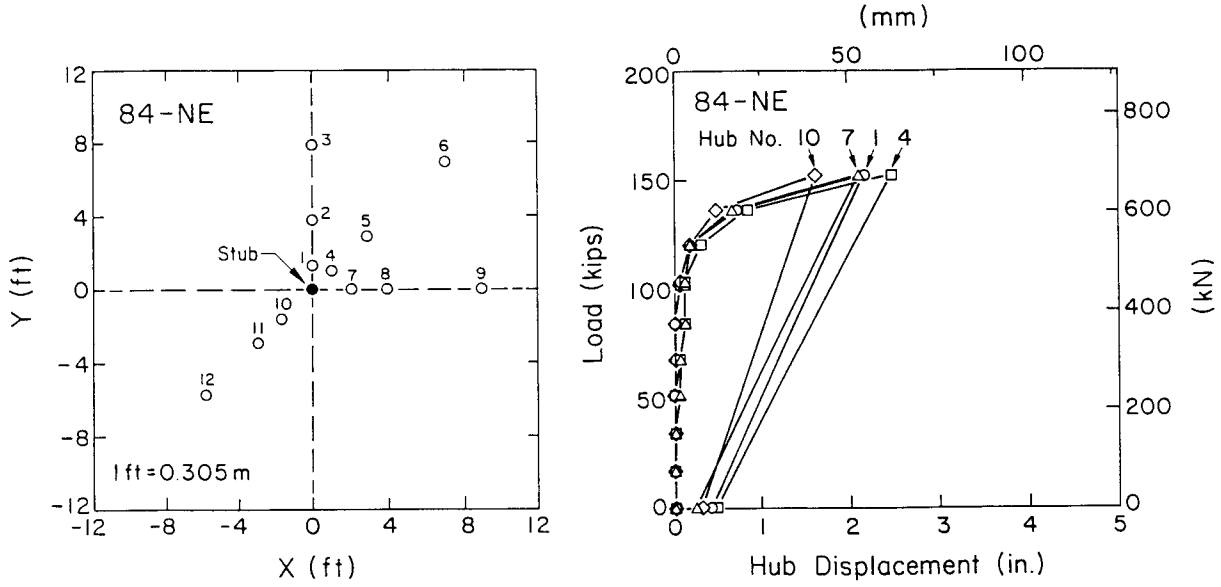

Figure 6-14. Hub Positions and Displacements, Grillage No. 84-NE, Hickling Station

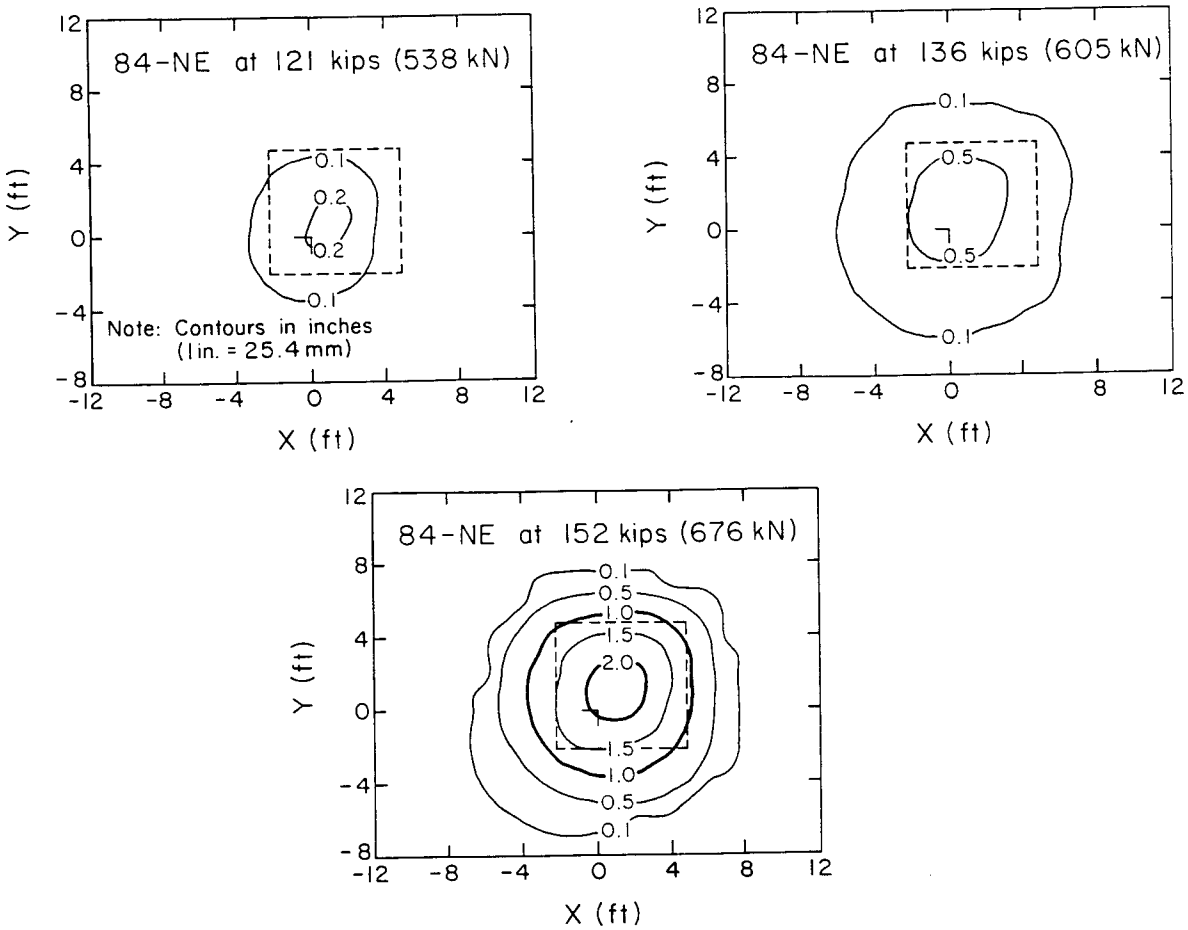

Figure 6-15. Ground Surface Displacements, Grillage No. 84-NE, Hickling Station

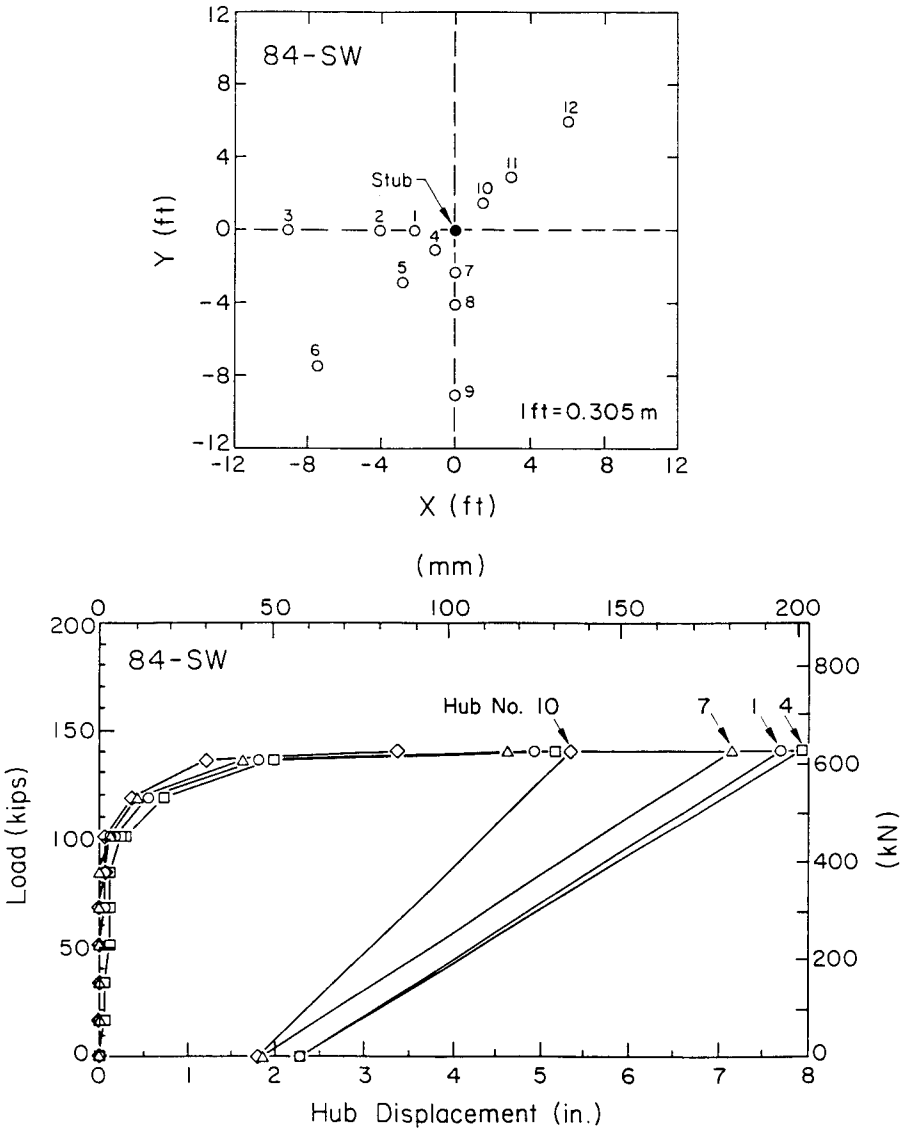

Figure 6-16. Hub Positions and Displacements, Grillage No. 84-SW, Hickling Station

in Figure 6-17 for loads of 119 to 141 kips (529 to 627 kN). At the maximum grillage load, the ground displacements were greater than 7 in. (178 mm) near the stub, while the stub displacement was 10.7 in. (272 mm) at the maximum load.

WYNCOOP CREEK

Load versus Displacement

The No. X2 grillages at Wyncoop Creek had H-shaped bases that were considered as 3 ft x 3 ft (0.91 m x 0.91 m) square. The design embedments were 7.5 ft (2.29

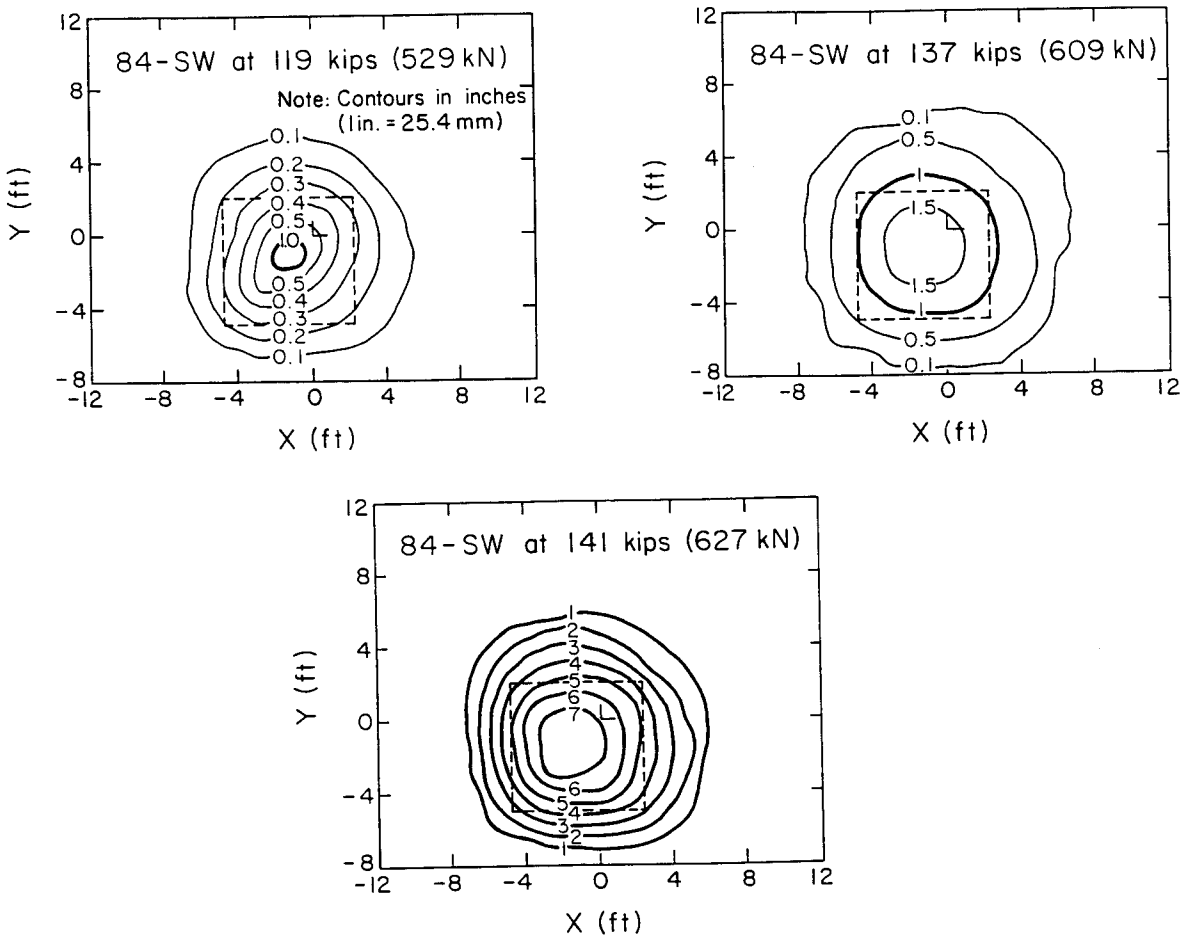

Figure 6-17. Ground Surface Displacements, Grillage No. 84-SW, Hickling Station

m), while the field test embedments are given in Table 6-6. The field site required some grading, resulting in an average embedment of 7.2 ft (2.19 m). The reduced embedments resulted in an average D/B of 2.43 versus 2.50 at a design embedment of 7.5 ft (2.29 m).

Figure 6-18 shows the load-displacement results for the No. 2 grillages. For No. X2-SW, the uplift resistance increased almost continuously with applied load. The maximum loads and axial displacements for these tests are given in Table 6-7. The maximum loads were 45 kips (200 kN) for grillage No. X2-SE and 58 kips (258 kN) for grillage No. X2-SW. Test displacements ranged from 12.3 to 14.3 in. (312 to 363 mm).

Comparisons of load cell and hydraulic gage readings from the two tests are

Table 6-6

FIELD EMBEDMENT DEPTHS, GRILLAGE SET NO. X2, WYNCOOP CREEK

Stub	Elevation (ft)			Embedment Depth (ft)
	Top of Stub	Ground Line	Grillage Base[a]	
X2-NE	101.7	100.9	93.6	7.3
X2-NW	101.8	101.1	93.7	7.4
X2-SE	101.9	100.8	93.8	7.0
X2-SW	101.8	100.9	93.7	7.2
Average:				7.2

1 ft = 0.305 m
a - Stub elevation minus 8.21 cos 10°

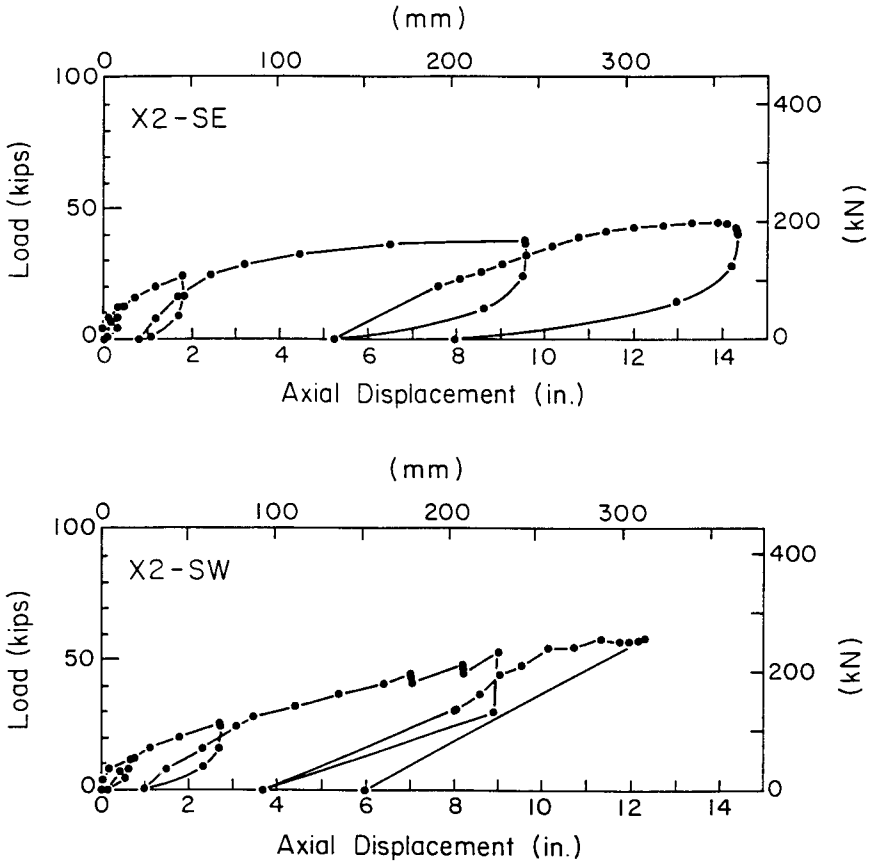

Figure 6-18. Grillage Load versus Displacement, Set No. X2, Wyncoop Creek

Table 6-7

MAXIMUM LOADS AND DISPLACEMENTS, GRILLAGE SET NO. X2, WYNCOOP CREEK

Grillage Number	Maximum Axial Load		Maximum Axial Displacement	
	kips	kN	in.	mm
X2-SE	45	200	14.3	363
X2-SW	58	258	12.3	312
Averages:	52	229		
COV(%)	18	18		

shown in Figure 6-19. Deviations between the two load measuring systems begin at 25 to 40 kips (111 to 178 kN). These differences are thought to result from the large ram extensions of greater than 6 in. (152 mm).

Ground Movements

The hub locations at grillage No. X2-SE are shown in Figure 6-20, together with the hub displacements for the four hubs closest to the stub. At an axial load of 25 kips (112 kN), the ground movements were less than 0.3 in. (7.6 mm), while the stub displacement was 2.5 in. (64 mm).

Ground surface displacement contours for grillage No. X2-SE are shown in Figure 6-21 for loads of 36 kips and 40 kips (160 kN and 178 kN). As shown in Figure 6-20, surface displacements spread rapidly as the load was increased. At a load of 40 kips (178 kN), the surface uplift was 7 in. (178 mm). At the same load, the stub displacement was 11 in. (279 mm).

The hub positions at grillage No. X2-SW are shown in Figure 6-22, together with the displacements at hub numbers 1, 4, 7, and 10. As with the stub axial displacement, ground movements continued throughout loading. At this grillage, there were larger differences between hub movements near the stub. For all other tests, the hub movements near the stubs were quite similar until displacements became large. However, at a load of 20 kips (89 kN), all the hub movements were in close agreement, with displacements equal to 0.3 in. (7.6 mm) or less.

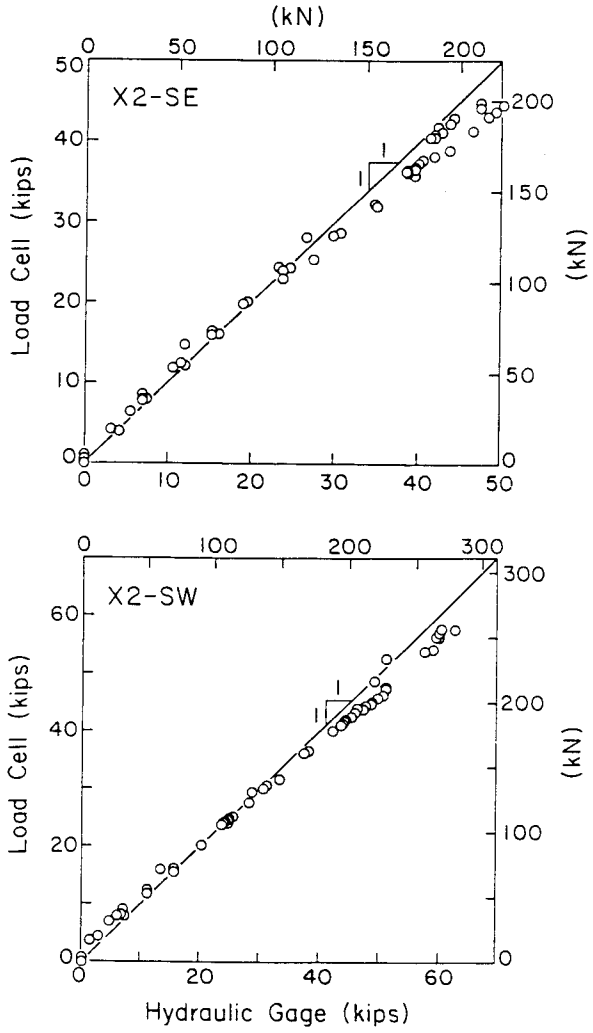

Figure 6-19. Load Cell versus Hydraulic Gage, Set No. X2, Wyncoop Creek

The stub displacement at 20 kips (89 kN) was 1.8 in. (46 mm). Beyond a 25 kip (111 kN) load, ground displacements accumulated rapidly. Figure 6-23 shows contours of ground surface movement at 36 kips and 58 kips (160 kN and 258 kN) axial uplift loads on grillage No. X2-SW. Surface movements exceeded 5 in. (127 mm) for this test, while stub movements were roughly 2.5 times larger. The contours for this test are not well-centered above the foundation, probably because of the large number of boulders present.

INTERPRETATION OF TEST RESULTS

The load and displacement conditions were evaluated using the procedures given

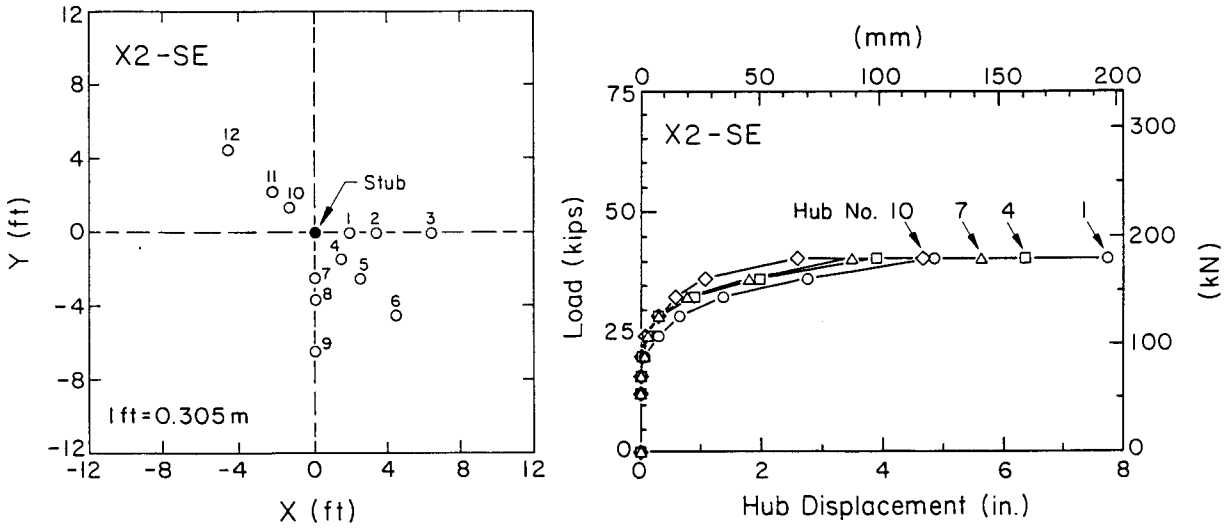

Figure 6-20. Hub Positions and Displacements, Grillage No. X2-SE, Wyncoop Creek

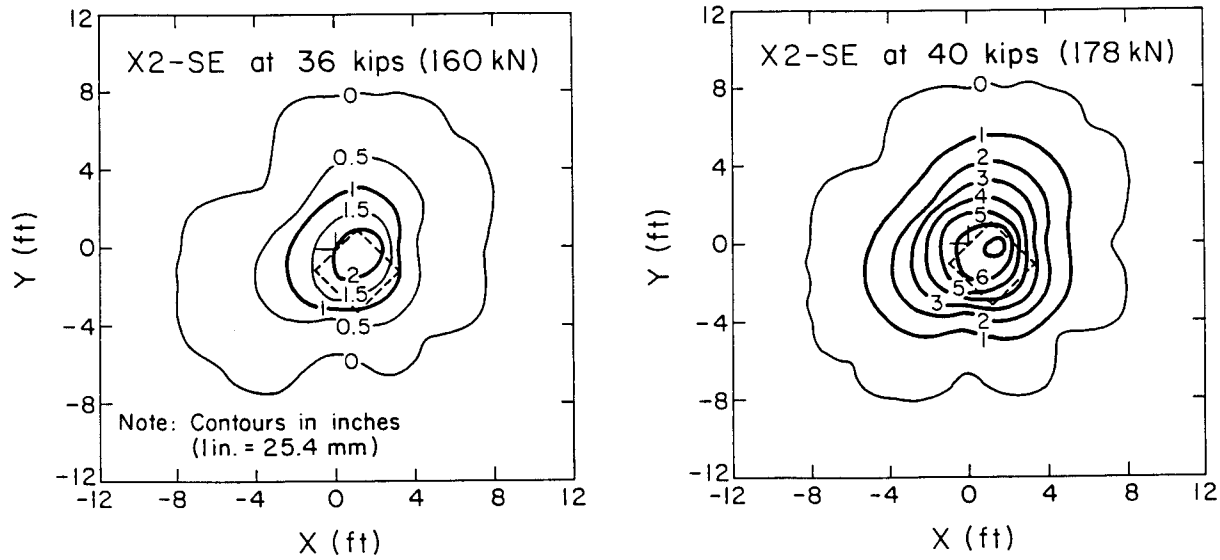

Figure 6-21. Ground Surface Displacements, Grillage No. X2-SE, Wyncoop Creek

by Trautmann and Kulhawy (1). This procedure is shown schematically in Figure 6-24, where a slope-tangent method is used. The interpreted failure load, Q_u, is defined by the intersection of tangents to the initial and final portions of the load-displacement curve. Two displacement parameters also are shown: (1) z_f, the displacement at Q_u, and (2) z_{50}, the displacement at one-half of Q_u.

Figure 6-25 shows the backbone load-displacement curve for the tests on grillage

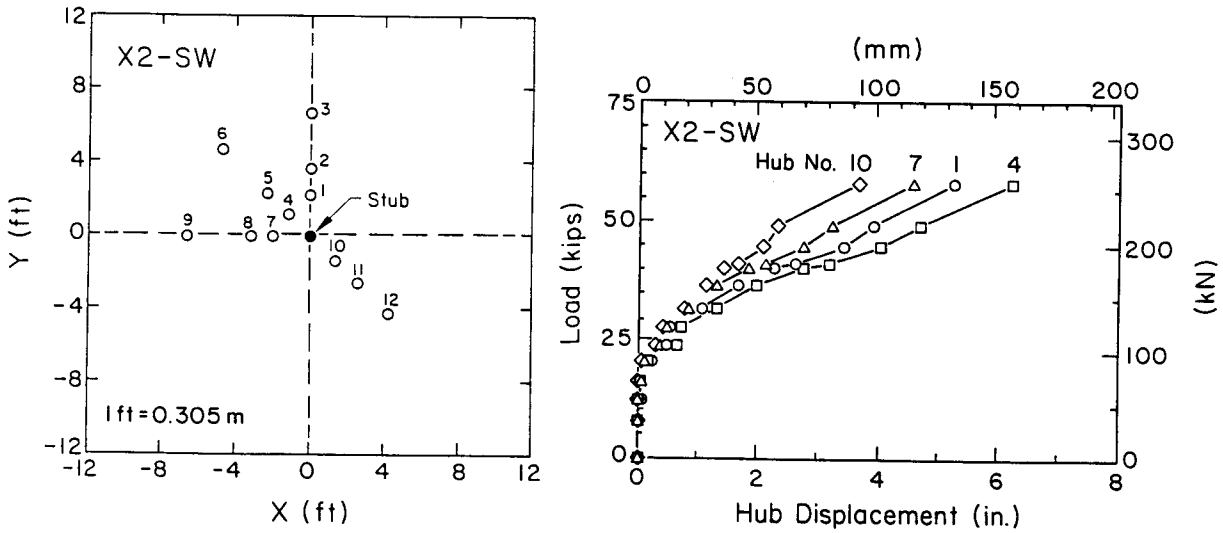

Figure 6-22. Hub Positions and Displacements, Grillage No. X2-SW, Wyncoop Creek

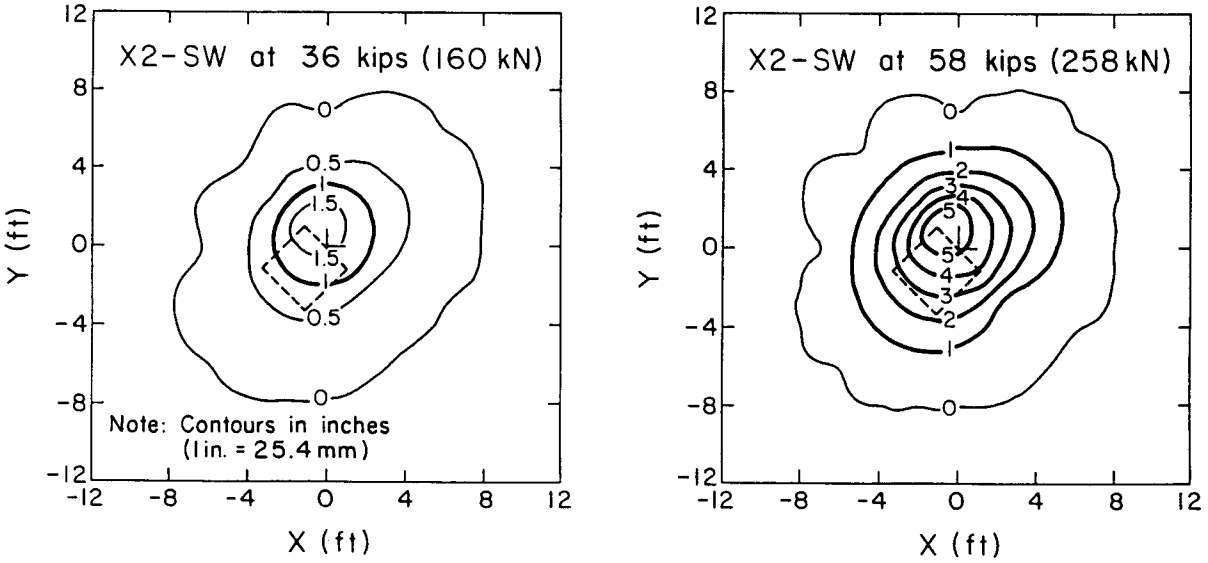

Figure 6-23. Ground Surface Displacements, Grillage No. X2-SW, Wyncoop Creek

set No. 4 at Hickling Station. For clarity, the unload-reload points are not shown. Since the backbone data are so similar, only one load-displacement curve requires interpretation. The interpreted failure load, Q_u, for the No. 4 grillages was 104 kips (463 kN), at a displacement, z_f, of 3.0 in. (76 mm).

The uplift tests on the No. 84 grillages at Hickling Station showed more variability, as shown in Figure 6-26. The initial slope of all three curves is the

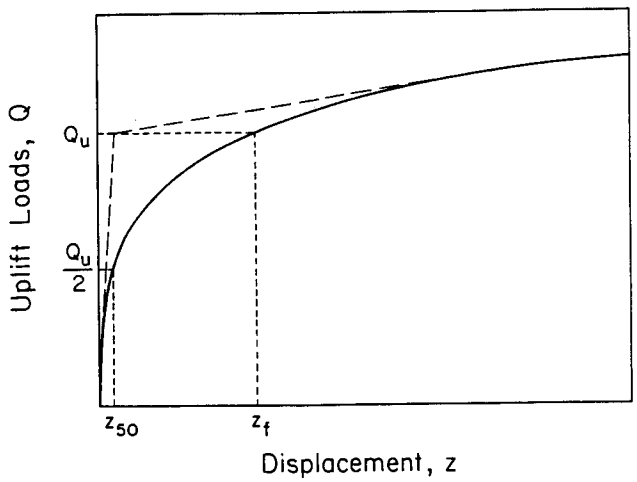

Figure 6-24. Interpretation of Load Test Data

Source: Trautmann and Kulhawy (1), p. 172.

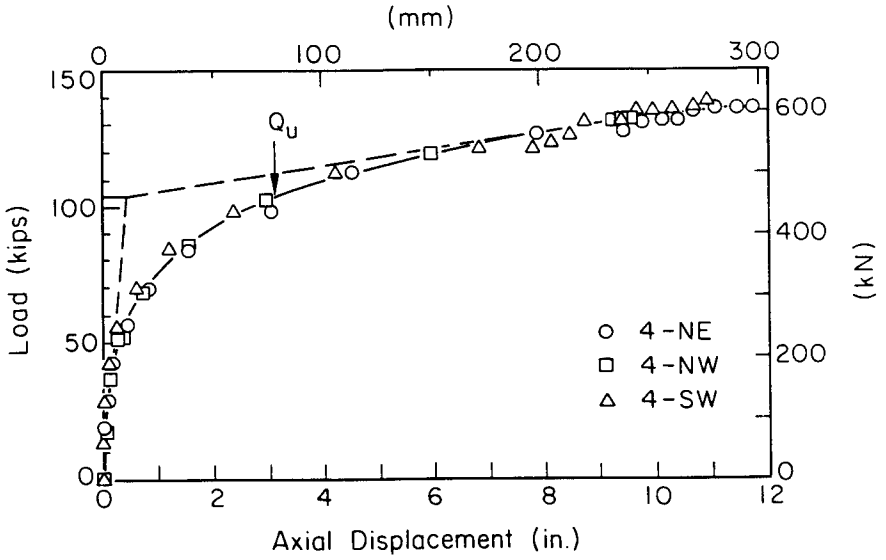

Figure 6-25. Interpreted Failure Loads, Grillage Set No. 4, Hickling Station

same, but the maximum loads and final tangents are different. Therefore, interpreted failure loads were defined for each of the three tests. These interpreted failure loads ranged from 126 to 146 kips (560 to 649 kN), with displacements ranging from 2.6 to 3.3 in. (66 to 84 mm).

The Wyncoop Creek results are shown in Figure 6-27. The backbone data from

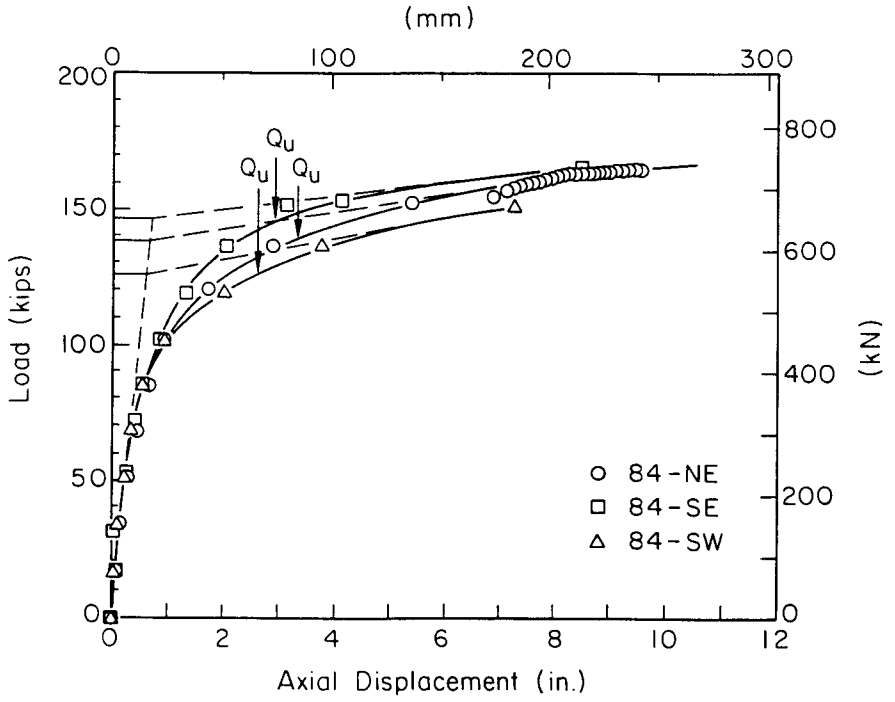

Figure 6-26. Interpreted Failure Loads, Grillage Set No. 84, Hickling Station

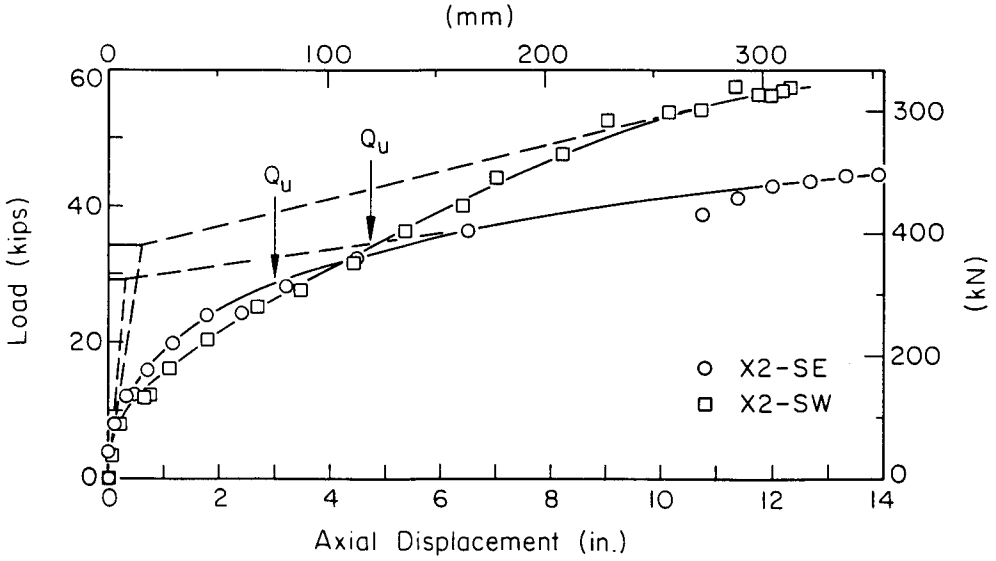

Figure 6-27. Interpreted Failure Loads, Grillage Set No. X2, Wyncoop Creek

grillage No. X2-SE shows the same general shape as the curves from all the Hickling Station tests, and the failure load can be interpreted readily. For grillage No. X2-SE, the interpreted failure load was 29 kips (129 kN) at a

displacement of 3.1 in. (76 mm). Grillage No. X2-SW data are not interpreted as clearly. There are four zones in the curve, including an initial tangent portion, a transitional zone, and two linear sections. The first linear section falls between 2.5 in. (64 mm) and 8 in. (203 mm) displacement. The second linear zone occurs at displacements greater than 8 in. (203 mm). The cause of the uncharacteristic shape from grillage No. X2-SW is not known, although the presence of the large, flat, platy boulders could have had a large effect. The interpreted failure load for grillage No. X2-SW is 34 kips (153 kN) at a displacement of 4.7 in. (119 mm).

Table 6-8 summarizes the interpreted failure conditions for all of the grillages. The failure loads, Q_u, and the corresponding displacements, z_f, are given, along with the displacements at one-half the failure load, z_{50}. The Hickling Station grillages had nearly the same displacement pattern, with z_{50} ranging from 0.3 to 0.4 in. (7.6 to 10.2 mm) and z_f ranging from 2.6 to 3.3 in. (66 to 84 mm).

Trautmann and Kulhawy (1) analyzed data from nineteen uplift tests conducted on grillages in granular soils. A statistical evaluation of those data revealed that the displacements z_f and z_{50}, normalized by the embedment depth, D, apparently were distributed log-normally.

The data from the eight tests in this study were analyzed in a similar manner. The geometric mean of the normalized displacements $(z/D)_{avg}$ was calculated by:

$$(z/D)_{avg} = \exp\left[\frac{\sum_{i=1}^{n} \ln(z/D)_i}{n}\right] \qquad (6\text{-}1)$$

in which n = number of observations and $(z/D)_i$ = normalized displacement of the i observation.

The geometric standard deviation, s, was evaluated by:

$$s^2 = \exp\left[\frac{\sum_{i=1}^{n} [\ln(z/D)_i - \ln(z/D)_{avg}]^2}{n-1}\right] \qquad (6\text{-}2)$$

Table 6-8

INTERPRETED FAILURE CONDITIONS

Site	Grillage	Interpreted Failure Load, Q_u		Displacements			
				z_{50}		z_f	
		kips	kN	in.	mm	in.	mm
Hickling Station	4 (all)	104	463	0.30	7.6	3.0	76
Hickling Station	84-SE	146	649	0.40	10.2	3.0	76
	84-NE	138	614	0.35	8.9	3.3	84
	84-SW	126	560	0.30	7.6	2.6	66
Averages:		137	609	0.35	8.9	3.0	76
Wyncoop Creek	X2-SE	29	129	0.55	14.0	3.1	79
	X2-SW	34	153	1.25	31.8	4.7	119
Averages:		32	141	0.90	22.9	3.9	99

Table 6-9 gives the normalized displacements for the field test grillages. In each case, the displacements were normalized by the individual test embedment depth, D.

One-sided confidence limits $(z/D)_{1-\alpha}$ were evaluated by:

$$(z/D)_{1-\alpha} = \exp\left[\ln(z/D)_{avg} + t_\alpha \ln s\right] \qquad (6\text{-}3)$$

in which $(z/D)_{1-\alpha}$ = displacement under load that is exceeded for only α percent of foundations, and t_α = one-sided Student's t for n - 1 degrees of freedom at the $1 - \alpha$ level.

The statistics from the nineteen grillage tests in granular soil (1) and the eight tests done in this study are given in Table 6-10 for $\alpha = 0.05$, representing a 95 percent confidence level. Table 6-10 presents statistics for all 27 test data as well, since the eight additional tests increase the data base by 42

Table 6-9

NORMALIZED DISPLACEMENTS FOR FIELD TEST GRILLAGES

Site	Grillage	D ft (m)	z_{50}/D (%)	z_f/D (%)
Hickling Station	4-NW	10.8 (3.29)	0.23	2.31
	4-NE	10.3 (3.14)	0.24	2.43
	4-SW	10.4 (3.17)	0.24	2.40
Hickling Station	84-SE	9.1 (2.77)	0.37	2.75
	84-NE	9.2 (2.80)	0.32	2.99
	84-SW	9.5 (2.90)	0.26	2.28
Wyncoop Creek	X2-SE	7.0 (2.13)	0.65	3.69
	X2-SW	7.2 (2.19)	1.45	5.44
Geometric Mean, $(z/D)_{avg}$ (%)			0.37	2.90
Geometric Standard Deviation, s (%)			1.91	1.35

percent. The key points shown in Table 6-10 are that the failure displacements from the Hickling Station and Wyncoop Creek data are substantially larger than those presented previously (1). The reason is that large displacements were imposed in these field tests; the prior field tests had imposed displacements that were not large enough to define the complete backbone curve. If large displacements are not imposed, then the interpreted failure load, Q_u, is likely to be too small, as are the displacements, z_{50} and z_f. The typical data presented in (1) indicated maximum test displacements from 1.2 to 3.9 in. (30 to 100 mm), as compared with the maximum displacements of 9.6 to 14.3 in. (244 to 363 mm) imposed during these field tests.

The load-displacement data can be fitted to a hyperbolic equation of the form:

$$\frac{Q}{Q_u} = \frac{(z/D)}{a + b(z/D)} \tag{6-4}$$

in which Q/Q_u = normalized load, z/D = normalized displacement, and a and b are curve-fitted constants. By using $(z/D)_{50}$ and $(z/D)_f$, the average normalized displacements at $Q/Q_u = 0.5$ and $Q/Q_u = 1.0$, respectively, Equation 6-4 can be

Table 6-10

RESULTS OF DATA ANALYSIS FOR GRILLAGES IN GRANULAR SOILS

Source	n[a]	Geometric Mean, $(z/D)_{avg}$ (%)	Geometric Std. Dev., s (%)	t-Value[b]	95% Confidence Limit (%)
a) Displacement at 50 % of Interpreted Failure Load, $(z/D)_{50}$					
Trautmann and Kulhawy (1)	19	0.21	2.01	1.74	0.72
This study	8	0.37	1.91	1.90	1.27
Combined	27	0.25	2.08	1.71	0.88
b) Displacement at Interpreted Failure Load, $(z/D)_f$					
Trautmann and Kulhawy (1)	19	1.08	2.06	1.74	3.79
This study	8	2.90	1.35	1.90	5.15
Combined	27	1.45	2.20	1.71	5.55

a - number of observations
b - at $(1 - \alpha) = 95\%$

solved for:

$$a = \frac{(z/D)_{50}\ (z/D)_f}{(z/D)_f - (z/D)_{50}} \qquad (6\text{-}5)$$

$$b = \frac{(z/D)_f - 2(z/D)_{50}}{(z/D)_f - (z/D)_{50}} \qquad (6\text{-}6)$$

Table 6-11 lists the average normalized displacements, $(z/D)_{50}$ and $(z/D)_f$, and hyperbolic curve constants a and b at the 95 percent confidence limit, based on the data given in Table 6-10. Also given in Table 6-11 are the design constants for uplift-resisting spread foundations in both granular and cohesive soils (1). This previous design recommendation used upper bounds of $(z/D)_{50} = 0.01$ and

Table 6-11

LOAD-DISPLACEMENT CONSTANTS FOR GRILLAGES IN GRANULAR SOIL AT 95 PERCENT CONFIDENCE LIMITS

Source	Average Normalized Displacement		Hyperbolic Curve Constant	
	$(z/D)_{50}$	$(z/D)_f$	a	b
Trautmann and Kulhawy (1) (n = 19)	0.0072	0.0379	0.009	0.766
This study (n = 8)	0.0127	0.0515	0.017	0.073
Combined (n = 27)	0.0088	0.0555	0.010	0.817
Previous design recommendation (1)	0.01	0.04	0.013	0.667
Revised design recommendation	0.01	0.06	0.012	0.800

$(z/D)_f = 0.04$ as practical limits. However, the displacements at the defined failure conditions may have been too low, since the tests upon which the data base was generated did not have large uplift displacements. The inclusion of data from this study, conducted at large uplift displacements, suggests a revised design upper bound of $(z/D)_f = 0.06$, while maintaining the same value of $(z/D)_{50} = 0.01$.

A comparison of the previous and revised load-displacement relationships is shown in Figure 6-28. Up to 50 percent of the interpreted failure load, the design curves are the same. However, at larger loads, the revised recommendation results in larger displacements. At loads of 80 percent of Q_u, the previous design recommendation results in displacements that are 15 percent lower than the revised recommendation.

Figure 6-29 shows comparisons between the revised load-displacement relationship and the field test data from the grillage sets at Hickling Station. For these data, the revised design recommendation is conservative. The field test data show substantially stiffer load-displacement curves than the design

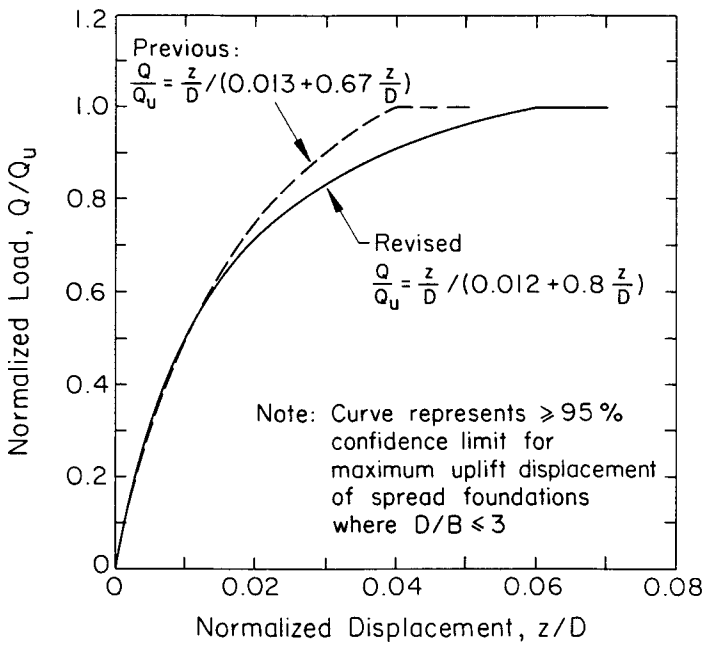

Figure 6-28. Revised Load-Displacement Relationship for Design of Uplift-Resisting Grillages in Granular Soils

recommendation, as intended by using the 95 percent confidence limits.

The Wyncoop Creek comparisons are shown in Figure 6-30. The data from grillage No. X2-SE fall to the left of the design recommendation. The data from grillage No. X2-SW are close to the design limit up to about 50 percent of the interpreted failure load. Between 50 and 100 percent of this failure load, the normalized field displacements are greater than those predicted based on the revised design recommendation. However, the data from grillage No. X2-SW did not display a typical load-displacement shape, probably because of the unusual soil conditions of large, flat, platy boulders.

For the three grillage types that were tested, there was no common foundation width, B, or embedment depth, D. However, there was replication for each of the three grillage types. Important geometric factors known to influence uplift capacity are B, D, and the depth-to-width ratio, D/B. The effective soil unit weight, $\bar{\gamma}$, contributes to the uplift capacity in an amount proportional to $\bar{\gamma}DB^2$, as a weight term. Frictional side resistance plus the weight of soil above the grillage make up the uplift capacity, Q_u. Model studies (2) have shown that an increase in D/B causes a substantial increase in uplift capacity, but these

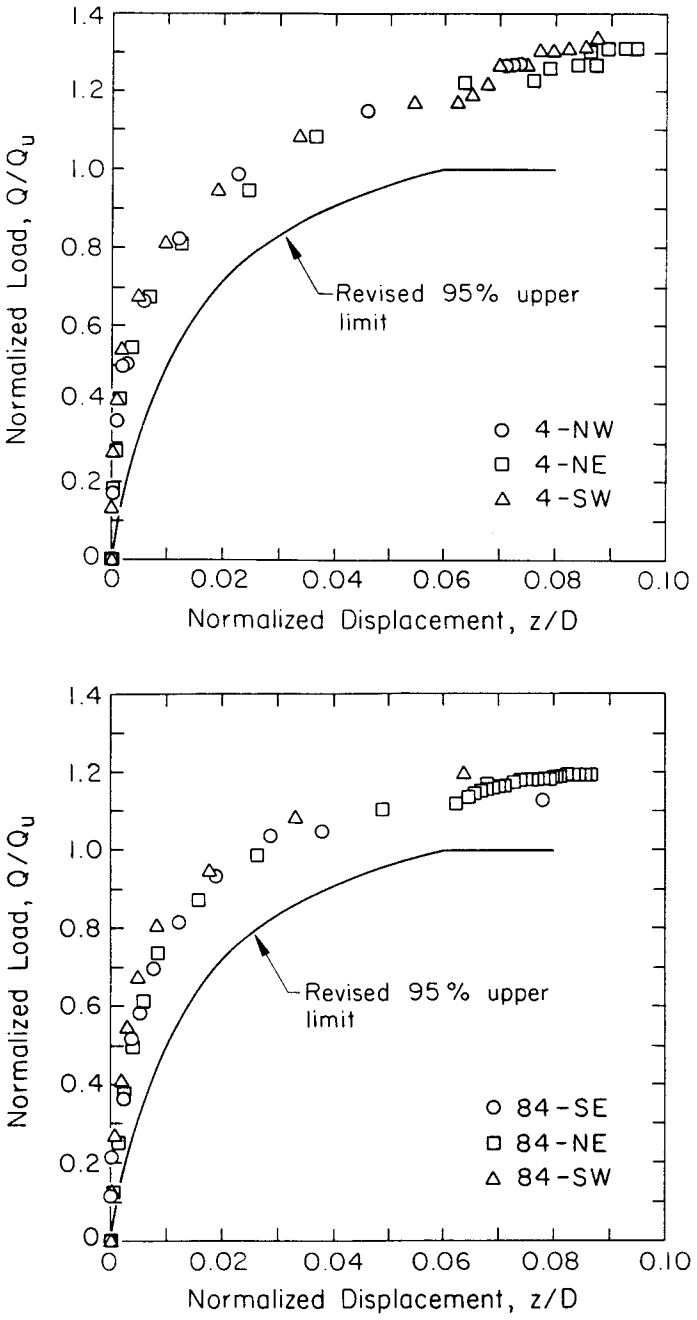

Figure 6-29. Comparison of Revised Load-Displacement Relationship with Field Test Data, Grillage Sets No. 4 and 84, Hickling Station

studies did not separate the effects of the increase in the weight term, $\bar{\gamma}DB^2$, from the side resistance capacity. Increasing D/B alone does not necessarily increase capacity.

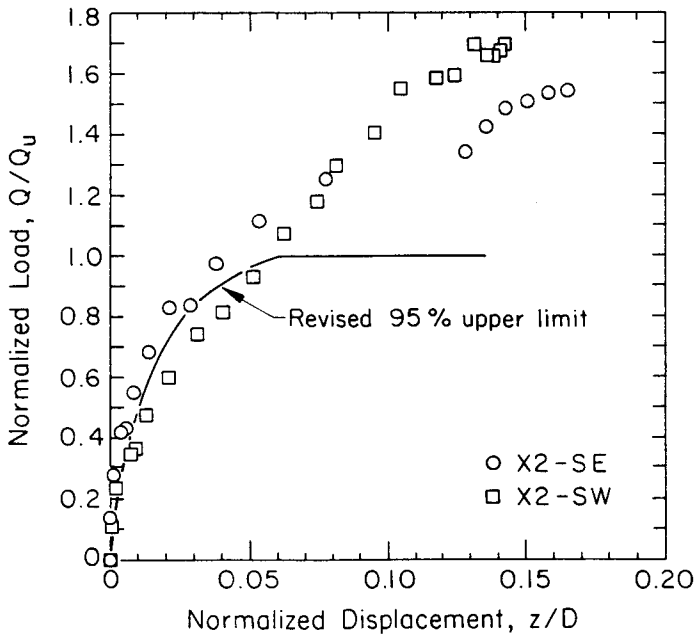

Figure 6-30. Comparison of Revised Load-Displacement Relationship with Field Test Data, Grillage Set No. X2, Wyncoop Creek

Table 6-12 summarizes the weight components of the uplift capacities from the field tests, based on a soil unit weight of $\bar{\gamma}$ = 120 pcf (18.9 kN/m^3) and a weight term, W, given by:

$$W = \bar{\gamma}BD^2 \tag{6-7}$$

The portion of the interpreted failure load, Q_u, from effects other than weight alone can be characterized by an uplift capacity factor, F_u, given by:

$$F_u = (Q_u - W)/Q_u \tag{6-8}$$

As indicated in Table 6-12, the grillages at Wyncoop Creek had the highest D/B ratios but the lowest capacities, primarily because they had the lowest D and B. The grillages with the greatest capacity were the No. 84 grillages at Hickling Station. These No. 84 grillages had the largest width, B, but depths, D, and D/B ratios between the No. 4 and No. X2 grillages. Table 6-12 lists the uplift capacity factors, F_u, from the field uplift tests. The weight factor, W_u, can be expressed simply as:

$$W_u = 1 - F_u \tag{6-9}$$

Table 6-12

UPLIFT CAPACITY FACTORS FROM FIELD UPLIFT TESTS

Site	Grillage	Q_u (kips)	D (ft)	B (ft)	D/B	$W^a = \bar{\gamma}DB^2$ (kips)	$F_u = (Q_u - W)/Q_u$
Hickling Station	4-NW	104	10.8	4.9[b]	2.21	30.9	0.70
	4-NE	104	10.3	4.9	2.11	29.4	0.72
	4-SW	104	10.4	4.9	2.13	29.7	0.71
Hickling Station	84-SE	146	9.1	7.0	1.30	53.5	0.63
	84-NE	138	9.2	7.0	1.31	54.1	0.61
	84-SW	126	9.5	7.0	1.34	55.9	0.56
Wyncoop Creek	X2-SE	29	7.0	3.0	2.33	7.6	0.74
	X2-SW	34	7.2	3.0	2.40	7.8	0.77

a - based on $\bar{\gamma}$ = 120 pcf (18.9 kN/m^3)
b - average
1 ft = 0.305 m
1 kip = 4.45 kN

The uplift capacity factor, F_u, which is primarily from side resistance, is shown in Figure 6-31, along with the uplift weight factor, W_u, as a function of D/B. As D/B increases, the fraction of Q_u from weight decreases, resulting in an increasing contribution from side resistance. Note that the trends shown in Figure 6-31 apply only to these test grillages in granular soil, although similar trends should be expected for cohesive soils.

The trends shown in Figure 6-31 can be expressed in several forms. A simple linear regression through the eight data points results in:

$$F_u = 0.42 + 0.14\ (D/B) \qquad (6\text{-}10)$$

This relationship indicates that, at D/B of 1, roughly 55 percent of the capacity of these test grillages in granular soil is caused by side resistance, and 45 percent results from the weight of the overlying soil. At D/B of 3, nearly 85 percent of the capacity is from side resistance, and only 15 percent is from the weight of soil.

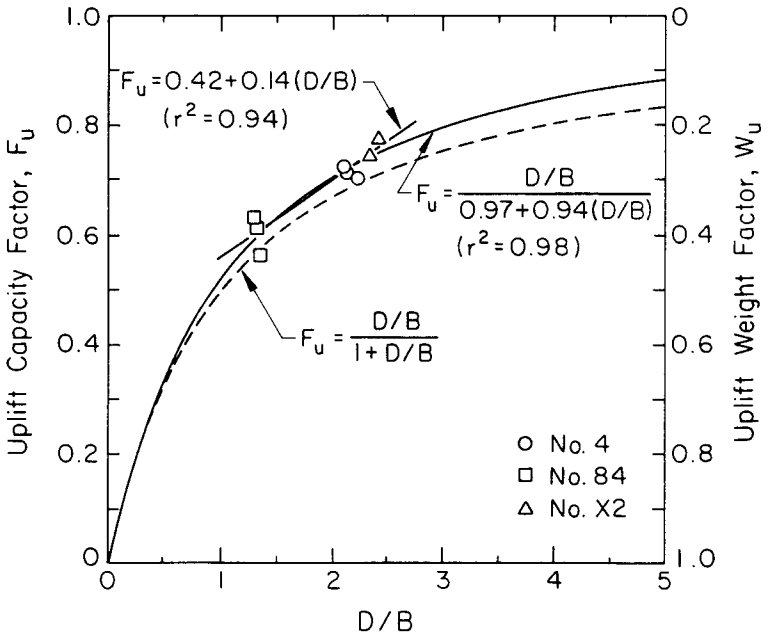

Figure 6-31. Uplift Capacity Factors F_u and W_u versus D/B

However, there are two physically important considerations to the uplift capacity factors. The first consideration is that, in the limit as D/B goes to zero, the uplift capacity resulting from side resistance will go to zero, and the weight of the soil and foundation will be the only contributor to total uplift. The second consideration is that, as D/B gets large, the side resistance contribution gets large and, at D/B of ∞, the uplift capacity should approach one.

The uplift capacity factors in Table 6-12 were fitted to a hyperbolic model to address the two physical considerations given above. The form of the hyperbolic equation used to represent the uplift capacity factor is:

$$F_u = \frac{D/B}{\alpha_1 + \beta_1 \, (D/B)} \tag{6-11}$$

in which α_1 and β_1 are regression parameters. Equation 6-11 can be transformed into a linear model, as given by:

$$\frac{D/B}{F_u} = \alpha_1 + \beta_1 \, (D/B) \tag{6-12}$$

In Equations 6-11 and 6-12, there are physical interpretations to the α_1 and β_1 parameters. The initial slope of the curve is equal to $1/\alpha_1$, and $1/\beta_1$ is equal to the asymptote of the curve at D/B = ∞. The regression through the data resulted in the following equation, which also is shown in Figure 6-31:

$$F_u = \frac{D/B}{0.97 + 0.94\ (D/B)} \tag{6-13}$$

For the field uplift tests that had D/B values of about 1.3 to 2.4, the hyperbolic model fits the data well. As explained previously, at D/B = ∞, the hyperbolic curve should be asymptotic to F_u = 1.0. Note that, in Equation 6-13, the value of $1/\beta_1$ = 1.06 is close to one. In addition, the α_1 parameter is close to one. For the data available from these field tests, the uplift capacity factor may be approximated by the following equation, which also is shown in Figure 6-31:

$$F_u = \frac{D/B}{1 + D/B} \tag{6-14}$$

Once F_u has been calculated, and the weight, W, of the soil in the prism above the grillage and grillage weight are known, then the uplift capacity can be estimated by:

$$Q_u = W/(1 - F_u) \tag{6-15}$$

Table 6-13 lists the interpreted (measured) uplift capacities and the uplift capacities based on F_u values calculated using Equations 6-10, 6-13, and 6-14. The W values are given in Table 6-12. The uplift capacities based on Equations 6-10 and 6-13 are in good agreement with the interpreted failure loads. The simplified form given by Equation 6-14 results in the lowest calculated capacities, about 10 percent lower, on average, than those interpreted from the field uplift tests.

The lines shown in Figure 6-31 strictly are applicable only to the grillages tested in this study, and they reflect particular combinations of in-situ stress, ground water conditions, and both native and backfill soil properties.

The ground displacement patterns, based on the surface hub movements, also displayed similar trends for most tests. Figure 6-32 shows the vertical hub

Table 6-13

COMPARISON OF MEASURED AND CALCULATED UPLIFT CAPACITIES

Site	Grillage	Q_u (kips) Measured[a]	Eq. 6-10	Eq. 6-13	Eq. 6-14
Hickling Station	4-NW	104	114	112	99
	4-NE	104	103	103	91
	4-SW	104	105	105	93
Hickling Station	84-SE	146	134	131	123
	84-NE	138	136	134	125
	84-SW	126	142	140	131
Wyncoop Creek	X2-SE	29	30	29	25
	X2-SW	34	32	30	27
Average Measured/Calculated:			0.99	1.01	1.10
COV(%)			7	8	9

a - Measured = interpreted failure load
1 kip = 4.45 kN

displacement versus the vertical stub displacement for No. 4 grillages. Also shown on this figure are the interpreted displacements at Q_u, z_f. In this figure, vertical stub movements and the vertical component of z_f are used.

For the No. 4 grillages, the ground surface movements are small until failure. Following failure, there is a noticeable slope change in the hub versus stub displacement curves. The hubs with the greatest movement were No. 4 and No. 7. Hub No. 4 was the one closest to the center of the grillage.

The hub versus stub displacements at the No. 84 grillages are shown in Figure 6-33. The movement patterns for the No. 84 grillages show a more continuous ground surface movement, as compared with the No. 4 grillages at the same site.

For the No. 84 grillages, the movement of hubs No. 1, 4, and 7 are nearly identical. These hubs were located close to the center of the grillage. Hub No. 10, located away from the grillage centers, consistently showed smaller vertical movements.

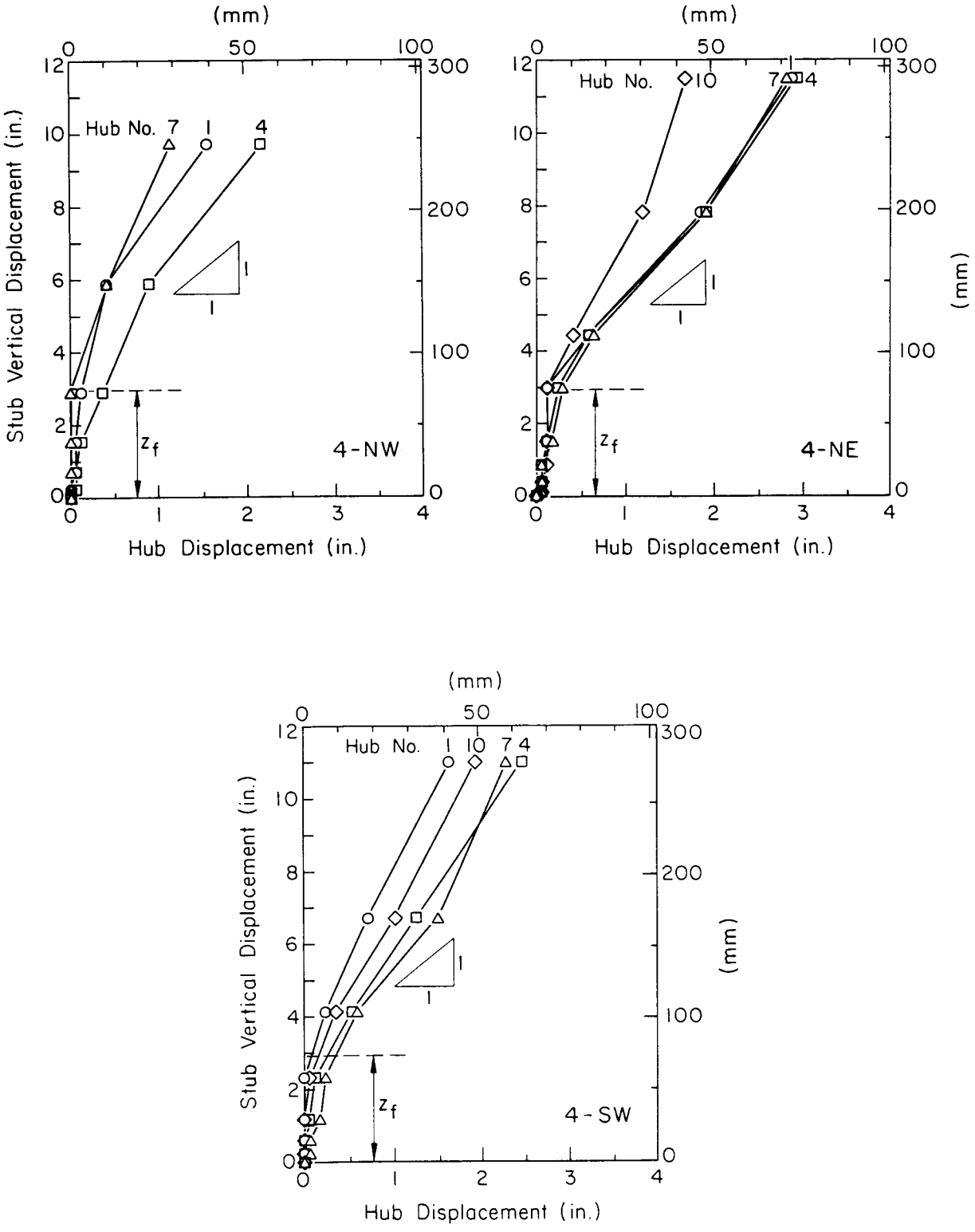

Figure 6-32. Hub versus Stub Displacements, Set No. 4, Hickling Station

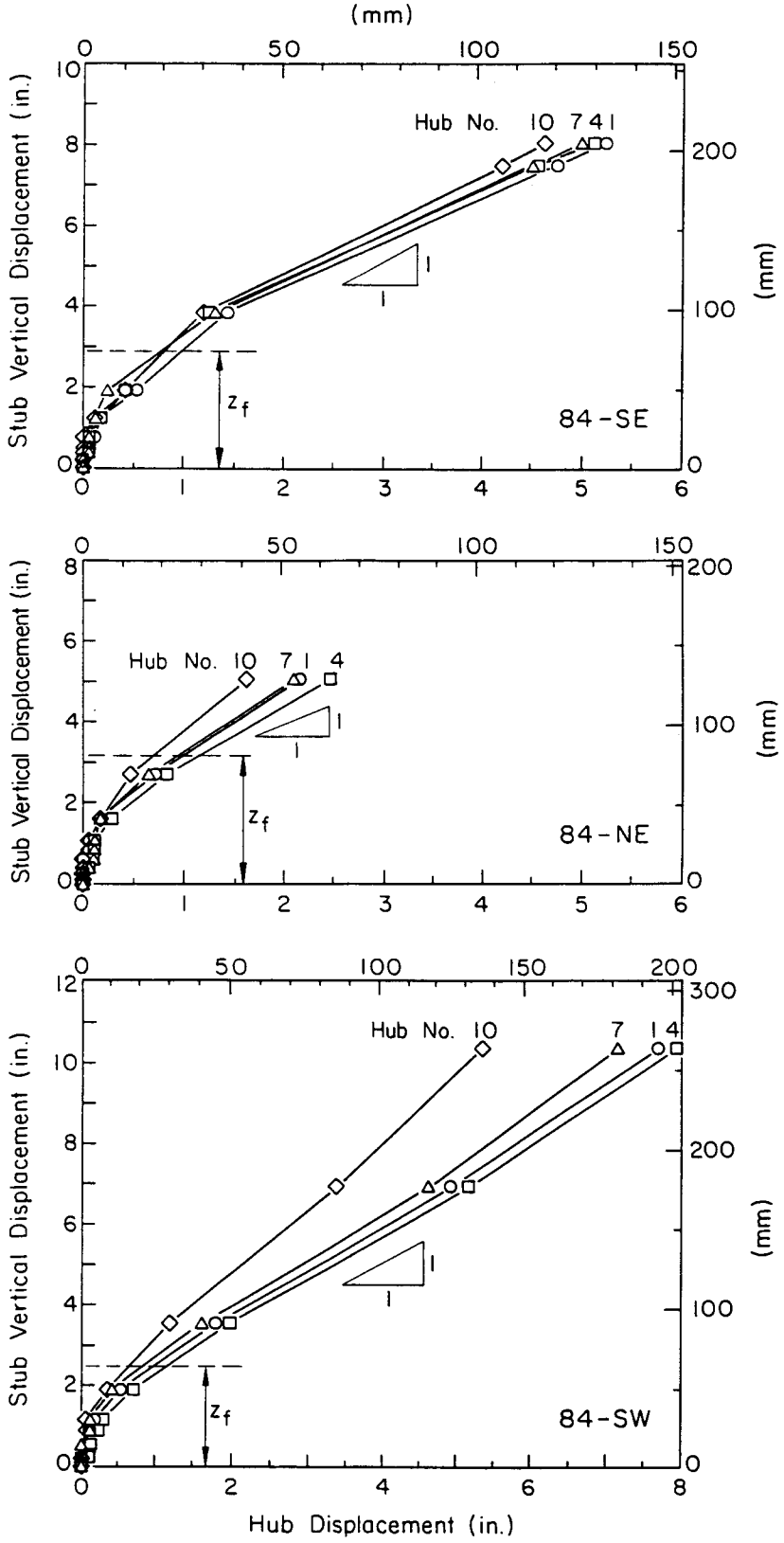

Figure 6-33. Hub versus Stub Displacements, Set No. 84, Hickling Station

The hub versus stub displacements for the No. X2 grillages at the Wyncoop Creek site are shown in Figure 6-34. The ground movements at No. X2-SE show a distinctive change in slope at z_f. This pattern is consistent with the characteristic shape of the load-displacement curve, which was readily interpreted using

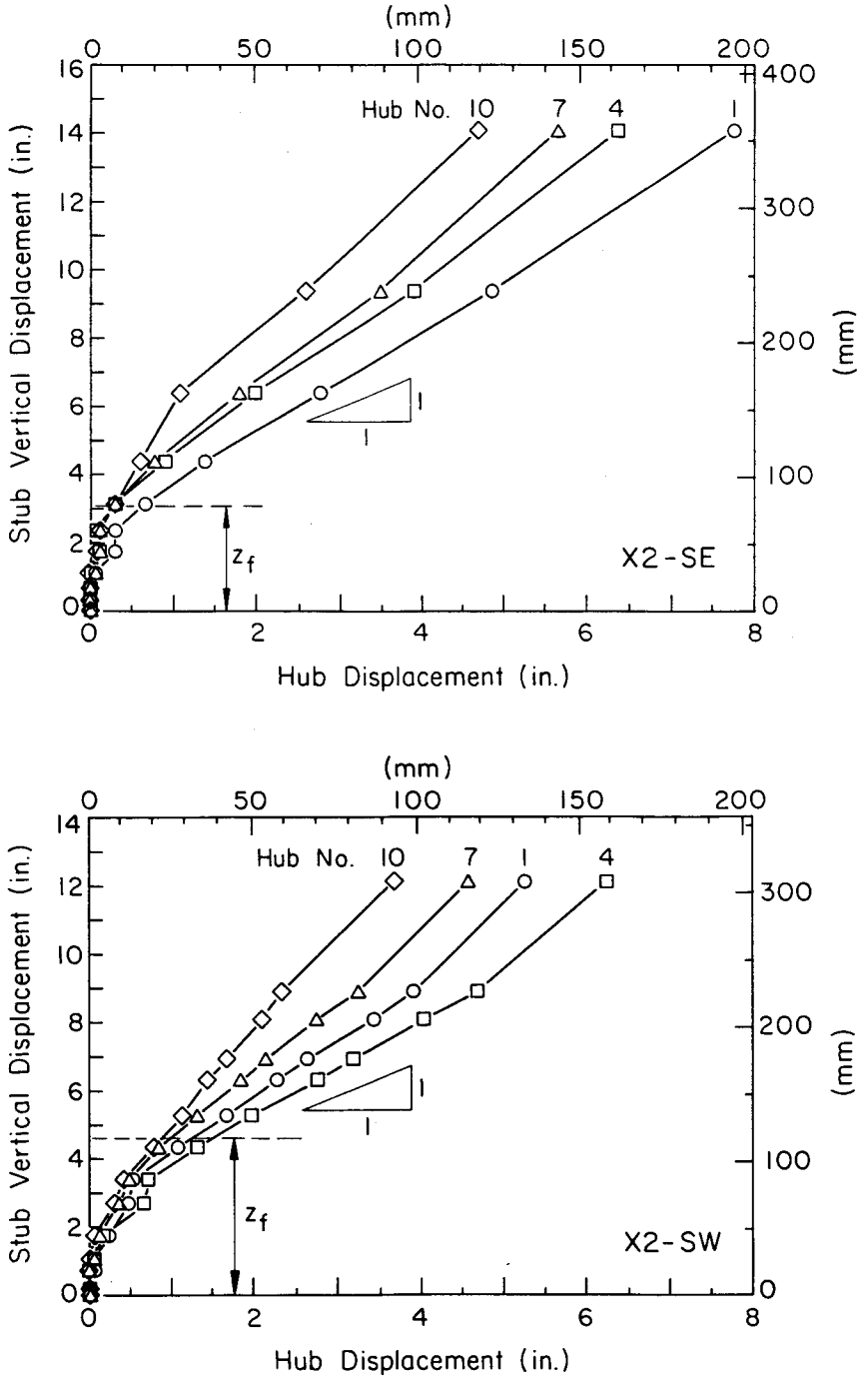

Figure 6-34. Hub versus Stub Displacements, Set No. X2, Wyncoop Creek

the slope-tangent method. However, there is a greater range of central hub movements at the Wyncoop Creek grillage than at the Hickling Station grillages. For No. X2-SW, there is a small zone where little ground motions occurred, followed by continuous increases in ground surface movement at nearly the same rate as the stub vertical movement.

The stub and hub vertical movements can be used to calculate a soil strain, ϵ_f, at the interpreted failure displacement, z_f, as given by:

$$\epsilon_f = (\delta_h - z_f \cos \theta)/D = (\delta_h - \delta_s)/D \qquad (6\text{-}16)$$

in which δ_h = maximum hub vertical movement, δ_s = vertical component of stub movement = $z_f \cos \theta$, θ = stub inclination angle, and D = embedment depth. The stub inclination angles were 12 and 15 degrees for the Hickling Station No. 4 and No. 84 grillages, respectively, and 10 degrees for the Wyncoop Creek grillages. Table 6-14 lists the maximum hub and stub movements at the failure displacements for all test grillages, along with the soil strains. The average soil strains at the interpreted failure conditions range from 1.6 to 3.6 percent, with the largest strains developing at the Wyncoop Creek grillages. The strains developed in the steel stub have been neglected, since they are much smaller than those developed in the soil. The steel stub strains, ϵ_s, would be calculated by:

$$\epsilon_s = Q_u/AE_f \qquad (6\text{-}17)$$

in which Q_u = interpreted failure load, A = stub cross-sectional area, and E_f = stub Young's modulus. For these steel grillage stubs and $E_f = 29 \times 10^6$ psi (200 GPa), the stub strains are on the order of 0.02 to 0.06 percent, and therefore they can be neglected.

The maximum soil strains at failure versus uplift capacity factors, F_u and W_u, are shown in Figure 6-35. The lines shown on the figure are speculative, but there is an apparent trend. For uplift capacity factors less than $F_u = 2/3$, the anticipated soil strain at failure, ϵ_f, should be less than two percent, with the soil strain at failure (in percent) about equal to three times the uplift capacity factor. As more of the uplift capacity results from side resistance, larger soil strains are required to reach failure. The magnitude of strain will be dependent on the backfill and native soil physical state and the in-situ stress conditions. At one end of the scale, however, the decrease in soil

Table 6-14

GROUND MOVEMENTS AT FAILURE

Site	Grillage	δ_h = Maximum Hub Disp. (in.) at z_f		δ_s = Stub Disp. (in.) at z_f[a]	ϵ_f (%)
		Max.	Hub No.		
Hickling Station	4-NW	0.4	4	2.9	1.9
	4-NE	0.3	7	2.9	2.1
	4-SW	0.4	7	2.9	2.0
Average:		0.4		2.9	2.0
Hickling Station	84-SE	1.0	1	2.9	1.7
	84-NE	1.2	4	3.2	1.8
	84-SW	0.9	4	2.5	1.4
Average:		1.0		2.9	1.6
Wyncoop Creek	X2-SE	0.5	1	3.1	3.1
	X2-SW	1.1	4	4.6	4.1
Average:		0.8		3.9	3.6

a - $\delta_s = z_f \cos \theta$;
1 in. = 25.4 mm

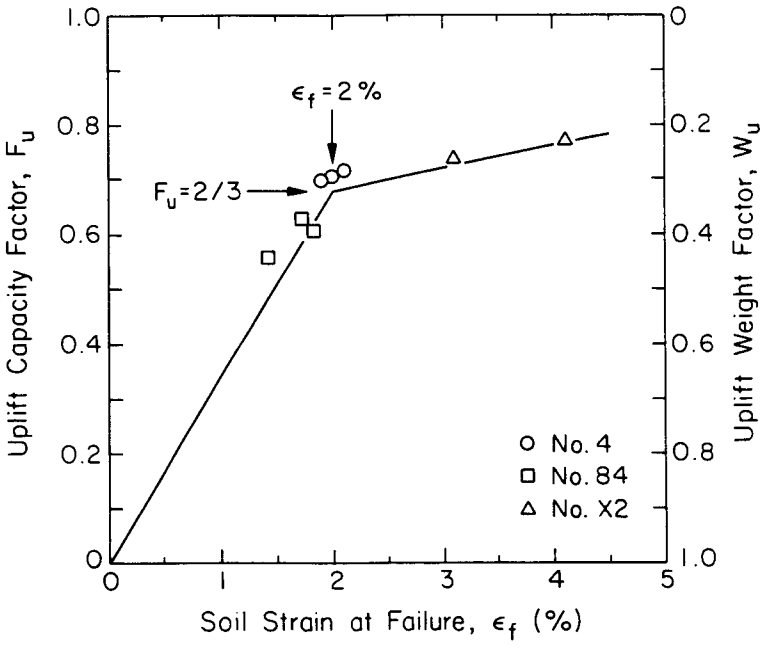

Figure 6-35. Uplift Capacity Factors F_u and W_u versus Soil Strain at Failure

strain with decreased side resistance frictional component is intuitive. If no side resistance was caused by friction and all of the capacity resulted from soil weight alone, the relative displacement of the ground surface with respect to the stub displacement would be zero.

SUMMARY

Eight uplift tests were performed on three types of steel grillages at two field sites. In seven of the eight tests, a well-defined load-displacement backbone curve was used with a slope-tangent method for defining the interpreted failure load and displacements. For one of the tests, there were two linear ranges in the load-displacement curve at large [greater than 2.5 in. (64 mm)] displacements, making the interpretation of failure conditions less well-defined. For most tests, the stub displacement at failure was on the order of 3 in. (76 mm).

The results of previous studies of load-displacement patterns for steel grillages in granular soils were compared with the results obtained in this study. A revised recommended design curve was presented based on all of the data. The main difference between the previous design recommendation and that given herein is in the displacements predicted at loads greater than 50 to 60 percent of the interpreted failure load.

For the test grillages in granular soils, uplift capacity factors were presented indicating the fractions of capacity attributable to side resistance and weight. The relative contributions of side resistance and weight are dependent on both D and B, as well as the D/B ratio.

Maximum soil strains at failure for the test grillages ranged from 1.4 to 4.1 percent, with larger strains associated with tests at higher D/B and higher side resistance contributions to the uplift capacity.

REFERENCES

1. Trautmann, C. H. and Kulhawy, F. H., "Uplift Load-Displacement Behavior of Spread Foundations", Journal of Geotechnical Engineering, ASCE, Vol. 114, No. 2, Feb. 1988, pp. 168-184.

2. Kulhawy, F. H., Nicolaides, C. N., and Trautmann, C. H., "Experimental Investigation of the Uplift Behavior of Spread Foundations in Cohesionless Soil", Report EL-xxxx, Electric Power Research Institute, Palo Alto, 1990, being finalized.

Section 7

GRILLAGE CAPACITY EVALUATION

This section presents a brief overview of the models that have been suggested traditionally for predicting the drained uplift capacity of grillages. Then, the results of the in-situ and laboratory geotechnical property tests are used in the recommended vertical shear model to predict the capacities of the test grillages. The measured and predicted capacities are compared, and general guidelines are suggested for using these results in practice.

MODELS FOR SPREAD FOUNDATION UPLIFT CAPACITY

The methods for predicting the uplift capacity of spread foundations can be grouped into four broad categories: (a) cone, (b) shear, (c) curved surface, and (d) bearing capacity or cavity expansion models, as shown in Figure 7-1. None of these methods have proven to be flexible and general enough to accommodate all of the ranges of conditions encountered in practice. Some have correlated well with specific data sets, but these correlations have been limited to a range of specific soil, site, and geometric conditions.

The cone methods (1 - 4) assume that the resistance is provided by the weight of the foundation and soil within a cone of failure, varying from 0 to $\bar{\phi}$, the effective stress friction angle of the soil. This approach does not explain the mechanics of failure, and it ignores any contribution of side resistance. Furthermore, it assumes that a conical or frustrum-shaped failure surface will form under all conditions. Other failure shapes occur under a variety of conditions (5, 6). These methods generally are conservative at shallow depth (depth, D, to width, B, less than 1 to 2) and unconservative for greater depths.

The shear methods (1, 2, 6, 7) assume failure along a vertical shear surface extending upward from the perimeter of the foundation, which is not correct for all soil and geometric conditions. For example, shallow foundations in stiff soils may fail occasionally in a cone mode.

The curved surface methods (5, 8, 9) assume that failure occurs along a curved

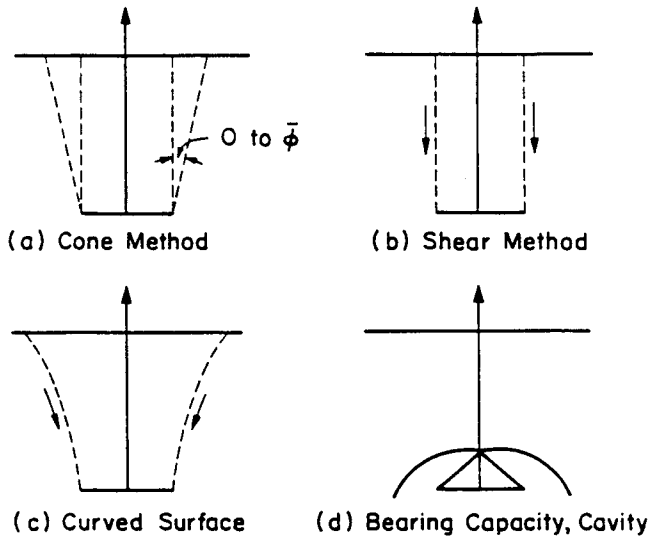

Figure 7-1. Uplift Capacity Models

surface. This pattern of failure limits the applicability of these methods, which have given reasonable correlations for shallow foundations, especially in denser soils. This pattern of failure may not apply for deeper foundations.

The bearing capacity or cavity expansion models (9, 10) assume that failure occurs by a punching shear. This is reasonable for deeper foundations in intermediate soil stress states, but it is not a general approach.

A more general approach was proposed by Kulhawy, et al. (11), in which the uplift capacity is given, as shown in Figure 7-2, by:

$$Q_u = Q_{su} + Q_{tu} + W \tag{7-1}$$

in which Q_u = uplift capacity, Q_{su} = side resistance along a general shear surface, Q_{tu} = tip resistance, and W = weight of foundation (W_f) and enclosed soil (W_s). Fundamentally, this is a shear model that reflects a cylindrical or rectangular mode of failure of the foundation. However, this general approach includes two modifications to the basic failure mode to allow for observed behavior. For foundations with a small depth to width (D/B) ratio, in soil deposits with high horizontal stress, a cone or wedge shear may develop. Also, a punching shear type of failure can develop where the backfill is too weak to mobilize any significant side resistance. This generalized model is shown in Figure 7-3.

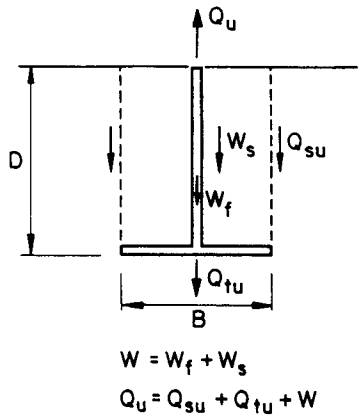

Figure 7-2. Basic Equilibrium Model

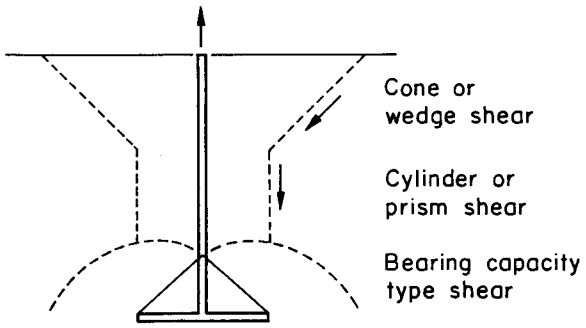

Figure 7-3. Generalized Uplift Behavior Pattern

The mechanism of side resistance development for spread foundations is similar to that for drilled shafts (11). This mechanism shows the development of Riedel shears, which become continuous displacement shears at large foundation movements and determine the location of the failure surface (12). For the basic cylindrical mode, the failure surface is located at the interface between the native soil and backfill. Within a cone or wedge shear, the failure surface is located in the native soil. For the punching shear mode, the shearing surface is more likely to be in the backfill. The exact location of the shear surface would depend upon the changes introduced in the soil stress field by backfilling and excavation. Consider the following two extremes. When a spread foundation is placed in loose native soil and backfilled with well-compacted material, the stiff backfill can be uplifted like a rigid mass with shearing resistance developed along the backfill-native soil interface. At the other extreme, with a loose backfill dumped in a stiff native soil, it is very likely that a punching type of failure develops. The backfill is weak and compressible, and therefore the foundation "punches" through it, locating the failure surface in the backfill (13).

The location of the shear surface determines which soil properties control capacity. For a spread foundation hypothetically constructed in an excavation the same size as the foundation, three choices exist. For interface failure, the weaker of the backfill or native soil controls. For the punching mode, backfill properties control. Finally, for the cone or wedge shear, a combination of native soil and backfill properties may govern.

GENERALIZED APPROACH FOR DRAINED CONDITIONS

The generalized shear model applies to all soil conditions. However, all subsequent discussion will be restricted to drained conditions, as appropriate for the field uplift tests conducted in this study. From Equation 7-1, the uplift capacity is given by the sum of the side resistance, tip resistance, and weight. The weight of the soil is calculated as the product of the effective unit weight of the backfill and the volume of the hole it occupies.

Tip resistance, in general, is derived by suction and tension. Suction can not develop under drained conditions because it is an undrained phenomenon. Since soils generally are weak in tension, the tip resistance will be negligible and will be assumed to be zero.

Side resistance is mobilized along the shear surface and is a function of the soil stress and strength, as well as the foundation geometry. For drained conditions, the side resistance is given by (11):

$$Q_{su} = \int_o^D \tau(z)\ dz = \frac{K}{K_o} \int_o^D P(z)\ K_o(z)\ \bar{\sigma}_v(z)\ \tan\left[\bar{\phi}(z) \cdot \frac{\delta}{\bar{\phi}}\right]\ dz \qquad (7\text{-}2)$$

in which P = foundation perimeter, K = operative horizontal stress, K/K_o = ratio of operative to in-situ horizontal stress, $\bar{\sigma}_v$ = vertical effective stress ($\bar{\gamma}z$), $\bar{\phi}$ = soil angle of friction, δ = interface angle of friction, and K_o = in-situ horizontal stress coefficient.

This equation applies strictly to the basic cylindrical or rectangular shear pattern where the failure surface is vertical. In this case, K, $\bar{\gamma}$, and $\bar{\phi}$ correspond to the properties of the weaker of the backfill or host soil, or the one with the lower horizontal stress (11).

Where a cone or wedge failure develops, a reduction in capacity occurs because of horizontal stress relaxation (14). In this case, the capacity can be computed as:

$$Q_{su}(\beta_r) = Q_{su}(\beta)\ \beta_r/\beta \qquad (7\text{-}3)$$

in which $\beta_r = (2 + \beta)/3$ and $\beta = K \tan \bar{\phi}$. For the "cone" cases, the failure surface is located typically in the native soil. Therefore, K, $\bar{\gamma}$, and $\bar{\phi}$ would

correspond to those of the native soil.

Equation 7-3 is an empirical formula derived from limited data on drilled shafts. Such a data base does not exist for spread foundations, and it is debatable whether it should apply strictly for spread foundations. Cone breakout requires further study and validation.

Where punching failure controls as an upper bound on the capacity, the maximum load, Q_{um}, is given by:

$$Q_{um} = A_f \, (\bar{q}_q \, N_q \, \zeta_{qr} \, \zeta_{qs} \, \zeta_{qd}) + \bar{W}_f + Q_{tu} \tag{7-4}$$

in which A_f = foundation area, $\bar{q}_q$ = effective surcharge ($\bar{\gamma}D$) on A_f, $\bar{W}_f$ = effective weight of the foundation alone, N_q = bearing capacity factor [$e^{\pi \tan \bar{\phi}} \tan^2(45 + \bar{\phi}/2)$], ζ_{qr} = modification factor for soil rigidity, ζ_{qs} = modification factor for anchor shape, ζ_{qd} = modification factor for anchor depth, and Q_{tu} = tip resistance. This punching limit is effectively a bearing capacity failure and represents an upper bound on the uplift capacity (10, 11). The ζ terms are given as:

$$\zeta_{qr} = \exp\{[(-4.4 + 0.6 \, B/L) \tan \bar{\phi}] + [(3.07 \sin \bar{\phi})(\log_{10} 2I_r)/(1 + \sin \bar{\phi})]\} \qquad (\leq 1.0) \tag{7-5}$$

$$\zeta_{qs} = 1 + (B/L) \tan \bar{\phi} \tag{7-6}$$

$$\zeta_{qd} = 1 + 2 \tan \bar{\phi} \, (1 - \sin \bar{\phi})^2 \, [(\pi/180) \tan^{-1}(D/B)] \tag{7-7}$$

in which D = foundation depth, B = foundation width, L = foundation length, $\bar{\phi}$ = soil angle of friction, and I_r = soil rigidity index, given by:

$$I_r = \frac{G}{\bar{q}_i \tan \bar{\phi}} = \frac{E}{2(1 + \nu)} \frac{1}{\bar{q}_i \tan \bar{\phi}} \tag{7-8}$$

in which G = shear modulus, E = elastic modulus, ν = Poisson's ratio, and $\bar{q}_i$ = effective surcharge ($\bar{\gamma}z$) at a height of B/2 above the foundation base (13).

VARIABLES AFFECTING UPLIFT BEHAVIOR

Fundamentally, the following variables affect the uplift behavior: (a) in-situ

soil stress state, (b) backfill stress state, (c) foundation geometry, (d) construction method, and (e) foundation rigidity. The potential influence of each variable is described in the following.

Soil Stress State

The in-situ horizontal soil stresses can control the mechanism of failure. These stresses are described by a horizontal stress coefficient, K, which is the ratio of horizontal to vertical effective stress. The value of K is a function of the initial in-situ stresses in the soil and any changes that occur during foundation excavation through loading. The initial stresses are given by the horizontal stress coefficient at rest, K_o, and changes in K occur from foundation excavation, backfilling, and loading. The final stress state is given by:

$$K_{final} = K_o + \Delta K_{excavation} + \Delta K_{backfilling} + \Delta K_{loading} \qquad (7\text{-}9)$$

If the variation of K_{final} with depth could be determined, the shearing resistance could be predicted by Equation 7-2, assuming a vertical shear surface.

At present, no analytical methods exist that predict directly the changes in K caused by construction and loading. Therefore, a precise evaluation of K_{final} is difficult. To overcome this problem, the changes in K can be either measured in well-instrumented large-scale load tests or inferred from uplift load test measurements. The latter approach is approximate because it depends on the accuracy of the analysis model.

The former option is more reliable. However, if direct measurements are not possible, a correlation with the in-situ K_o may prove helpful. In this instance, the following empirical equation can be used to predict K_o (15):

$$K_o = (1 - \sin \bar{\phi}) \left[\frac{OCR}{OCR_{max}(1 - \sin \bar{\phi})} + \frac{3}{4}\left(1 - \frac{OCR}{OCR_{max}}\right)\right] \qquad (7\text{-}10)$$

in which OCR = maximum $\bar{\sigma}_v$/current $\bar{\sigma}_v$ and OCR_{max} = maximum $\bar{\sigma}_v$/minimum $\bar{\sigma}_v$. The angle of friction, $\bar{\phi}$, can be correlated to the soil density, and the OCR can be estimated from the geologic history of the soil.

Consideration of the influence of soil stress state on the uplift capacity is relatively recent. Initial attempts focused on separating data according to

density alone (6, 8), but there was still significant scatter when measured and predicted values of uplift capacity were compared. These inconsistencies were attributed to the fact that the soil density alone can not describe the stress history of the soil (16). To address this issue, the influence of OCR on peak uplift load was investigated, and it was found that the latter increases with increasing OCR, as shown in Figure 7-4.

Therefore, to assess the influence of soil stress state on the uplift capacity of spread foundations, a profile of horizontal stress with depth is required, incorporating the soil density, $\bar{\phi}$, and OCR.

Backfill Stress State

Nearly all methods of analysis for the uplift capacity of spread foundations neglect the backfill stress level. However, the densification of the backfill modifies the stress field over the foundation, which can affect the failure mode and uplift behavior.

To illustrate the potential influence of the backfill stress state, consider the

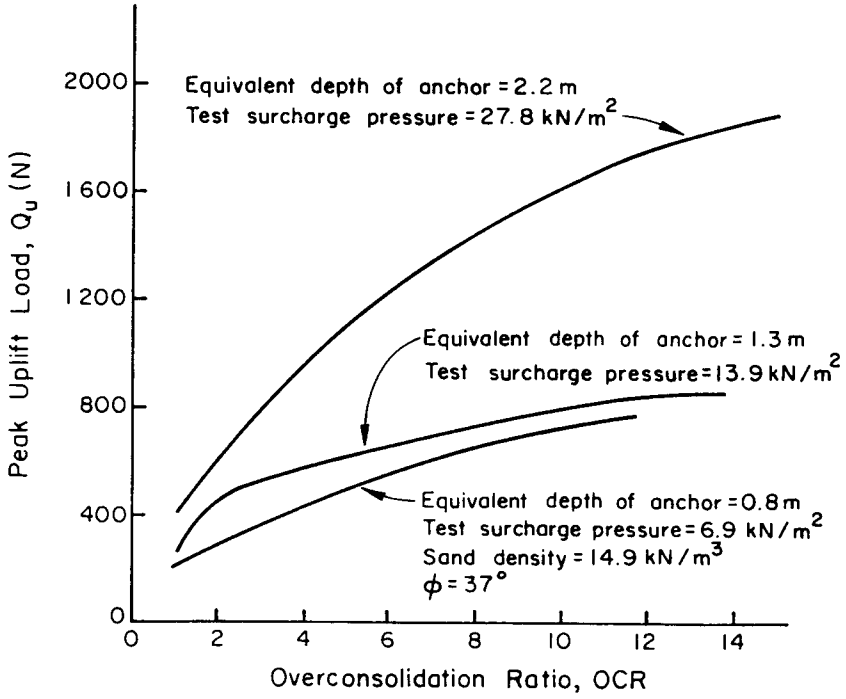

Figure 7-4. Effect of OCR on Peak Uplift Load

Source: Hanna and Carr (16), p. 598.

following, as shown in Figure 7-5. If the backfill is well-compacted, high horizontal stresses are created in the backfill relative to the native soil horizontal stresses, σ_{hn}. The compaction process also densifies a zone within the native soil, imparting a higher horizontal stress to the backfill, σ_{hb}, because the Poisson lateral expansion of the compacted soil can not be resisted fully by the native soil. In this case, failure would be in the native soil. However, if the backfill is placed loosely, the stresses imparted to it will be low, probably at rest or lower. In these cases, failure is likely to occur within the backfill, especially if the native soil is denser. These two cases represent the two extremes previously described.

The effect of backfill stresses has not been considered previously in experimental or analytical studies, because most investigators have used embedded models, which did not involve excavation and subsequent backfilling. Several studies (2, 17, 18) indicated qualitatively the importance of using good backfill material and the improved performance resulting from better compaction. One set of field test results showed that moderate compaction increased the uplift capacity by about 45 percent, while reducing the displacement at which this capacity was mobilized (2). Figure 7-6 presents typical results, which demonstrate clearly the importance of good compaction.

Others have attempted to quantify the term "good compaction" and included backfill density and strength characteristics as variables (19). Although this was an improvement, it still does not account for the stress state.

The level of stress in the backfill seems to be a dominant factor in the behavior of spread foundations, and it is probably responsible for the eventual state of stress around the foundation prior to loading. A comparison between the level of horizontal stress in the native soil and the backfill should indicate where the failure surface forms and which soil properties govern. The soil with the lower horizontal stress will tend to control (13). The above

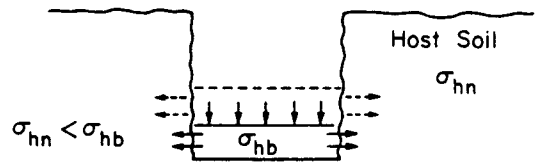

Figure 7-5. Poisson Expansion Because of Backfilling

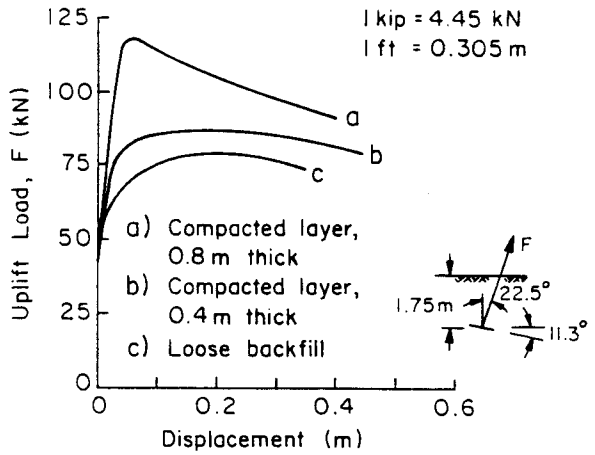

Figure 7-6. Effect of Backfill Compaction on Uplift Load-Displacement

Source: Heikkalä and Laine (2), p. 14.

assessment requires quantitative information on the backfill and native soil stresses. This information is not available in field load test data summaries (e.g., 20). Based on evaluation of the above case histories and several theoretical assumptions, suggested guidelines for the evaluation of the horizontal stress in the backfill have been given, as in Table 7-1 (13). If the backfill is placed loose, the host soil will remain in a relaxed state of stress, while the backfill will be in an active to normally consolidated state of stress. If the backfill is moderately compacted, the stresses in the backfill will be increased, increasing those of the host soil. Finally, if the backfill is very densely compacted, the stress state in the backfill may reach the passive stress limit.

Geometry

Many investigators (e.g., 2, 5, 8, 16) have confirmed the influence of foundation geometry on uplift capacity. Both the depth and plan area of the foundation also influence the location of the failure surface of the foundation.

Depth is particularly important because of the large increase in uplift resistance with increasing depth, as noted in Table 7-2. Although there is agreement on the influence of depth on capacity, there is disagreement on the functional relationship, because many other factors also influence uplift capacity.

The foundation plan shape also influences the uplift resistance, because it

Table 7-1

TENTATIVE GUIDELINES TO EVALUATE HORIZONTAL STRESS IN A BACKFILLED NEAT EXCAVATION

Backfill Compaction	Coefficient of Horizontal Soil Stress, K	
	Host Soil	Backfill
Loose	2/3 K_o	K_a to K_{onc}
Medium	K_o	K_{onc} to 1
Dense	5/4 K_o	1 to K_p

Note: $K_a = \tan^2(45 - \bar{\phi}/2)$; $K_{onc} = 1 - \sin \bar{\phi}$; $K_p = 1/K_a$

Source: Kulhawy (13), p. 15.

Table 7-2

RELATIONSHIPS BETWEEN UPLIFT LOAD AND DEPTH

Investigator	Functional Dependence
Balla (5)	$Q \propto D^3$
Heikkalä and Laine (2)	$Q \propto D^2$ (all other factors fixed)
Hanna and Carr (16)	$Q \propto D$ (loose)

determines the spatial extent of the backfill contributing to capacity. No functional relationships exist that relate the plan area to uplift capacity. In general terms, there seems to be a trend in which uplift capacity increases with increasing foundation perimeter (2, 5).

Construction Method

The construction method alters the soil stress field and may influence the development of the failure mode and uplift capacity. Excavation and backfilling

are used in the field, while embedment has been used for nearly all model laboratory tests. The changes in the stress field resulting from construction have not yet been quantified, largely because relevant field data have been missing.

In theory, the excavation process reduces the level of stress from its in-situ value to one of a relaxed state (13). Consider soil element A in Figure 7-7. Initially, it exists at an in-situ effective horizontal stress, $\bar{\sigma}_{ho}$, given by $\bar{\sigma}_{ho} = K_o\bar{\sigma}_{vo}$. When the soil is excavated, the in-situ stress is removed and the soil element at the excavation interface attains a relaxed state. At this state, the horizontal stress is almost zero. Foundation construction is completed by placing the foundation and backfilling. At this latter stage, the stress field reaches its final state depending upon the applied backfill energy. In particular, the backfill energy near the excavation walls perhaps is most important. Following backfilling, the soil element has a new horizontal stress given by $\bar{\sigma}_{hb} = \Delta\bar{\sigma}_h = K_b\ \bar{\sigma}_{vo}$, in which K_b = horizontal stress coefficient developed by backfilling. This state of stress subsequently is altered during loading.

Embedment has been used in nearly all laboratory studies, in which case the native soil and backfill are placed simultaneously at the same stress state. This procedure does not replicate actual field conditions and does not allow stress changes to occur. However, these results may be used for general comparative purposes. Therefore, this procedure represents only the special case where the backfill is placed at the same density and stress state as the original soil.

Foundation Rigidity

The rigidity of the foundation system may influence the uplift behavior in two different ways. The first is to refer to the backfill-structural element as the

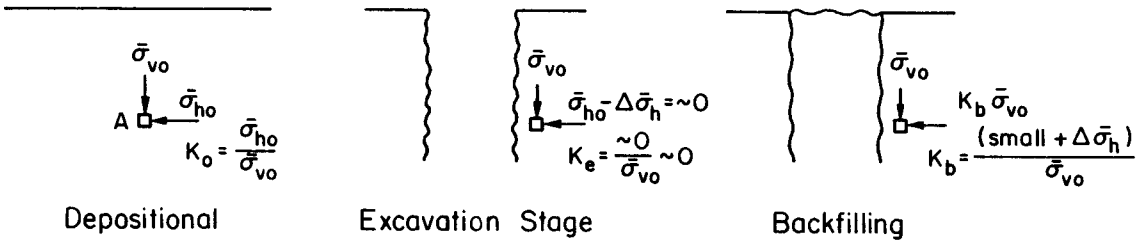

Figure 7-7. Change of Horizontal Stress at Different Stages of Construction

foundation system and compare its stiffness with that of the native soil. The second is to consider the overall effect as the sum of two components: (a) relative stiffness between backfill and native soil, and (b) relative stiffness between the foundation element and backfill. The former considers the influence of the Young's modulus of the native soil, E_{sn}, to that of the backfill-foundation combination, E_t. The latter considers the influence of the ratios of Young's modulus of the backfill, E_b, to that of the structural element, E_f, and of the Young's modulus of the backfill to that of the native soil. The Young's moduli of the soils are functions of the unit weight, $\bar{\gamma}$, angle of friction, $\bar{\phi}$, and confining stress, $\bar{\sigma}_3$. Quantitative correlations between uplift capacity and system rigidity do not exist for either of the two approaches, and the available field load test data (20) do not contain enough information to assess these factors properly. Further data are required to assess the influence of foundation rigidity.

CALCULATION OF UPLIFT CAPACITIES

The important soil properties for the vertical shear model are K_o, $\bar{\gamma}$, and $\bar{\phi}$ for both the backfill and native soil. Geometric parameters include D, B, and P, the foundation perimeter. The geometric properties are obtained easily for the field uplift tests. The soil properties require careful selection. For each grillage site, a best estimate of the soil properties will be given and the uplift capacity will be calculated using the formulation given previously, as implemented in the CUFAD computer program (21). Parametric analyses will be presented showing the sensitivity of the predicted capacities to the soil properties selected.

Hickling Station

The in-situ field tests indicated that the backfill was less dense and had lower strength properties than the native soil. Therefore, the backfill properties should have controlled the uplift behavior of the grillages.

The friction angle profile, $\bar{\phi}(z)$, for the backfill at the Hickling Station site, based on the in-situ test data, was shown in Figure 3-62. The simplified K_o profile was given in Figure 3-64. From these profiles, the subsurface conditions at Hickling Station were divided into four layers for analysis purposes, since the properties varied with depth.

Soil layer 1 extended from the ground surface to a depth of 2 ft (0.61 m), layer

2 went from 2 to 4 ft (0.61 to 1.22 m), layer 3 extended from 4 to 10 ft (1.22 to 3.05 m), and layer 4 extended from 10 to 50 ft (3.05 to 15.2 m). The ground water depth was measured as 15.9 ft (4.85 m). The in-situ data for $\bar{\phi}$ and K_o in the backfill are shown as solid lines in Figure 7-8. The best-estimate layering for $\bar{\phi}$ and K_o at the Hickling Station site also is shown in Figure 7-8. A soil unit weight of 120 pcf (18.9 kN/m^3) was used. A range of values was selected for K/K_o. Since the backfill was looser than the native soil, the ratio of operative to in-situ horizontal stress, K/K_o, was estimated at 0.65 to 0.85. The ratio of interface to backfill soil friction angle was taken as 1.0. Table 7-3 lists the best-estimate soil properties for the No. 4 and No. 84 grillages at the Hickling Station site. An average embedment of 10.5 ft (3.20 m) was used for the No. 4 grillages. The embedment at the No. 84 grillages was taken as 9.3 ft (2.83 m).

Figure 7-9 shows the computed uplift capacities for the Hickling Station grillages, based on the input parameters listed in Table 7-3. Also shown on the figure are the measured (interpreted failure load) capacities and a range of ± 10 percent for the average measured uplift capacities. As seen on the figure, the K/K_o value is important when predicting uplift capacity.

Using the best-estimate of the in-situ $\bar{\phi}$ and K_o values, the K/K_o values necessary to predict capacities within 10 percent of those measured were back-calculated. Table 7-4 lists the required K/K_o values to obtain predicted capacities within ± 10 percent of those measured. For the ground conditions estimated at

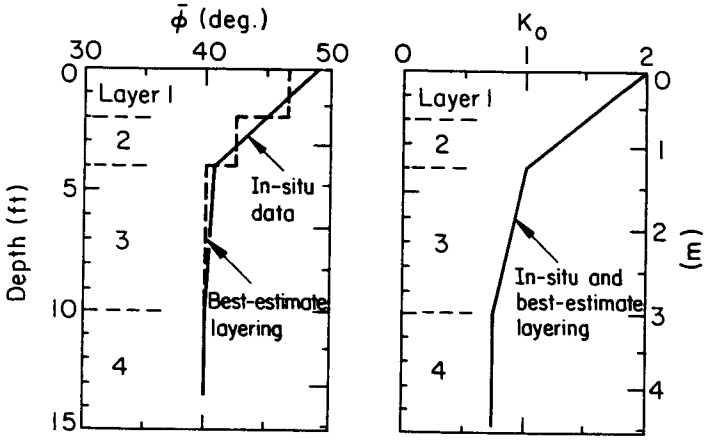

Figure 7-8. In-Situ and Best-Estimate Layering for Backfill $\bar{\phi}$ and K_o, Hickling Station Grillage Set Nos. 4 and 84

Table 7-3

BEST-ESTIMATE SOIL PROPERTIES, HICKLING STATION, GRILLAGE SET NOS. 4 AND 84

Layer	1	2	3	4
Soil type	Gravel	Gravel	Gravel	Gravel
Depth to top (ft)	0	2	4	10
Depth to bottom (ft)	2	4	10	50
Soil unit weight, $\bar{\gamma}$ (pcf)	120	120	120	120
Friction angle, $\bar{\phi}$ (deg)	46.7	42.3	40.0	40.0
Horizontal stress coef., K_o - top	2.00	1.50	1.00	0.75
Horizontal stress coef., K_o - bottom	1.50	1.00	0.75	0.75
Operative/in-situ horizontal stress coefficient, K/K_o	0.65 to 0.85	0.65 to 0.85	0.65 to 0.85	0.65 to 0.85
Interface/soil friction angle, $\delta/\bar{\phi}$	1.0	1.0	1.0	1.0

1 ft = 0.305 m
1 pcf = 0.157 kN/m^3

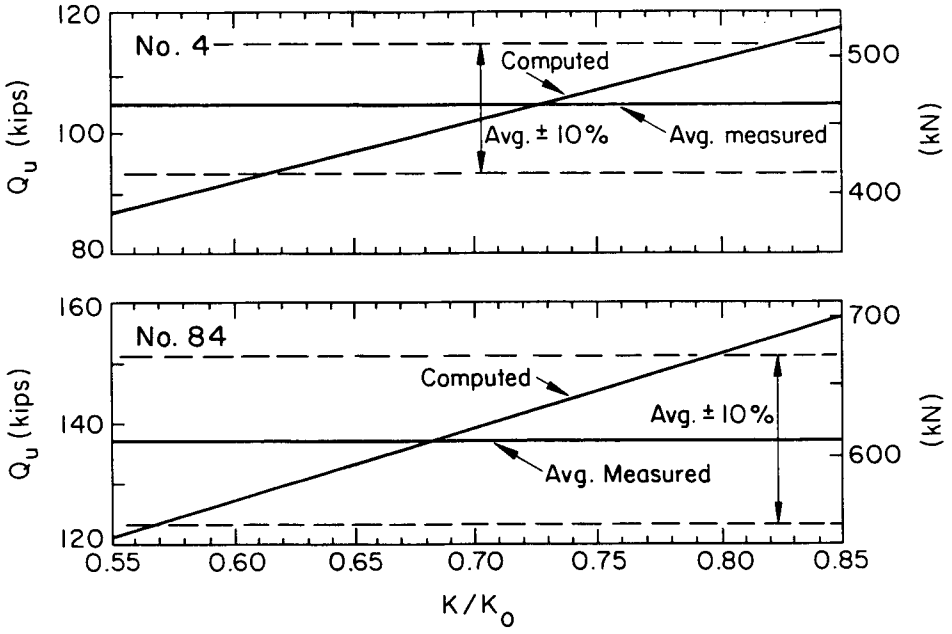

Figure 7-9. Computed and Measured Uplift Capacities Using Best-Estimate Properties, Grillage Set Nos. 4 and 84, Hickling Station

Table 7-4

BACK-CALCULATED K/K_o FOR HICKLING STATION BEST-ESTIMATE LAYER PROPERTIES, GRILLAGE SET NOS. 4 AND 84

Grillage Set	Measured Q_u (kips)			K/K_o Required To Be Within ± 10%
	Average	Range	Average ± 10%	
No. 4	104	104	94 to 114	0.62 to 0.82
No. 84	137	126 to 146	123 to 151	0.57 to 0.80

1 kip = 4.45 kN

Hickling Station, the required K/K_o values range from about 0.6 to 0.8. These values are consistent with the tentative guidelines suggested in Table 7-1 for backfill in the loose to medium density range.

To investigate the sensitivity of the computed uplift capacities on the soil properties, a series of analyses was done for a range of $\bar{\phi}$ and K_o profiles. The $\bar{\phi}$ profiles used are shown in Figure 7-10, and the K_o profiles are shown in Figure 7-11. Note in these figures that there is a letter designation in each profile. These letters will reference the profiles used in the following descriptions.

From the results shown earlier in Figure 7-9 and Table 7-4, the range of K/K_o values for reasonable agreement with the field results ranged from 0.6 to 0.8. Since K/K_o values and in-situ tests indicated slightly denser material at the No. 4 grillages than at the No. 84 grillages, $K/K_o = 0.75$ was selected for the No. 4 grillages, and $K/K_o = 0.70$ was used for the parametric studies for the No. 84 grillages.

Table 7-5 summarizes the results for the various $\bar{\phi}$ and K_o profiles used at the No. 4 grillages. The entries in the table represent the ratio of the computed Q_u to the average measured Q_u from the field tests. For example, with $\bar{\phi}$ profile A and K_o profile A, the computed Q_u is 1.02 times as large as the measured Q_u of 104 kips (463 kN). For all combinations of $\bar{\phi}$ profiles A, B, and C with K_o profiles A, B, and C, the computed Q_u values are within 3 percent of the measured

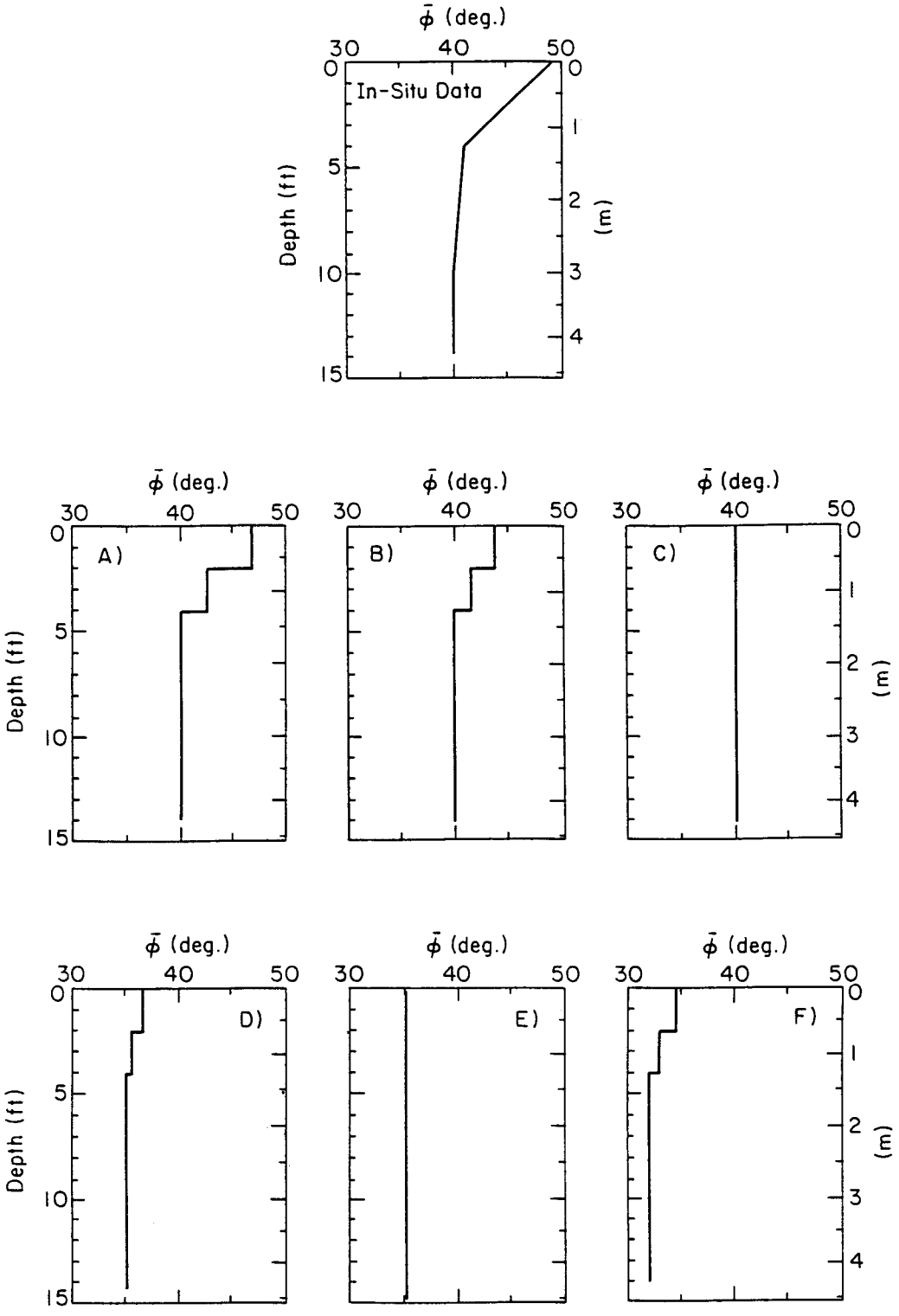

Figure 7-10. $\bar{\phi}$ Profiles Used in Parametric Analyses

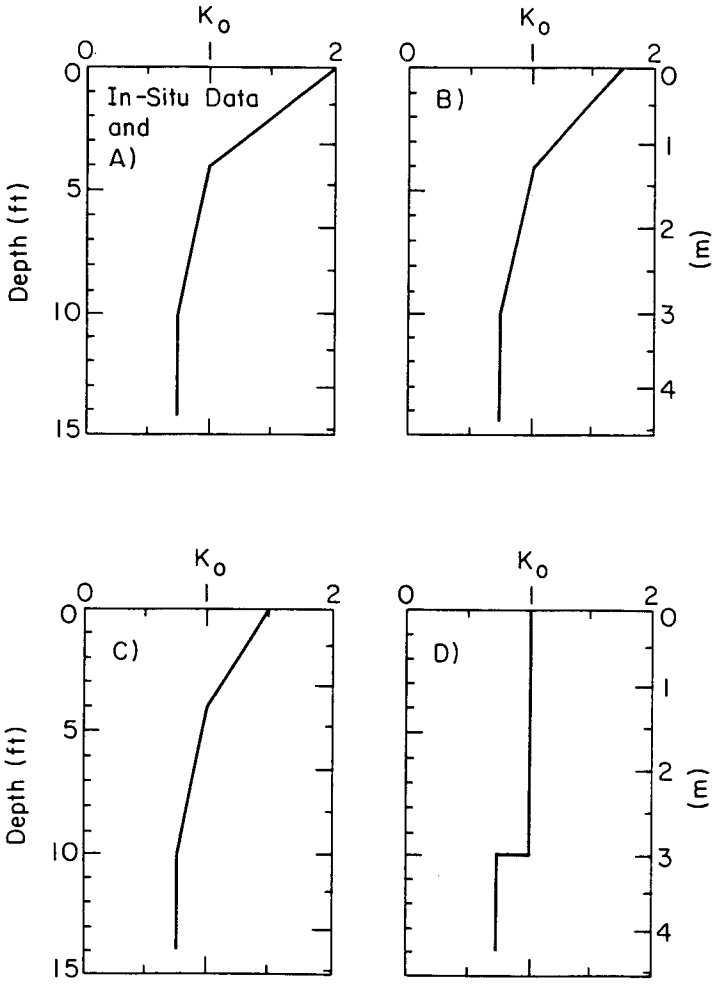

Figure 7-11. K_o Profiles Used in Parametric Analyses

values.

The effect of the reference K/K_o values on the computed capacities for the various soil property profiles can be determined readily from the information given in Table 7-5. The relationship used to determine capacities at other K/K_o values is given by:

$$Q_u^* = [R_Q \cdot Q_u \text{ (measured)} - W_{ref}] \frac{(K/K_o)^*}{(K/K_o)_{ref}} + W_{ref} \qquad (7\text{-}11)$$

in which Q_u^* = computed capacity, R_Q = Q_u (computed)/Q_u (measured) from Table 7-5, Q_u (measured) = measured interpreted failure load, $W_{ref} = \bar{\gamma}DB^2$, $(K/K_o)^*$ =

Table 7-5

RATIO OF COMPUTED TO AVERAGE MEASURED Q_u FOR $\bar{\phi}$ AND K_o PROFILES, K/K_o = 0.75, HICKLING STATION, GRILLAGE SET NO. 4[a]

$\bar{\phi}$ Profile	K_o Profile			
	A	B	C	D
A	1.03	1.02	1.01	0.99
B	1.02	1.01	1.00	0.98
C	1.01	1.00	0.99	0.97
D	0.90	0.89	0.88	0.86
E	0.89	0.88	0.88	0.86
F	0.83	0.83	0.82	0.80

a - $\bar{\gamma}$ = 120 pcf (18.9 kN/m^3)
B = 4.9 ft (1.49 m)
D = 10.5 ft (3.20 m)
Average measured Q_u = 104 kips (463 kN)

alternative value of K/K_o, and $(K/K_o)_{ref}$ = reference K/K_o. For the Hickling Station No. 4 grillages and data given in Table 7-5, the reference values are Q_u (measured) = 104 kips (463 kN), W_{ref} = 30.3 kips (135 kN) for $\bar{\gamma}$ = 120 pcf (18.9 kN/m^3), and $(K/K_o)_{ref}$ = 0.75. For example, the predicted capacity for soil $\bar{\phi}$ profile A and K_o profile A at a K/K_o value of 0.85 would be:

$$Q_u = (1.03 \cdot 104 - 30.3)\frac{0.85}{0.75} + 30.3 = 117 \text{ kips} \quad (7\text{-}12)$$

$$Q_u = (1.03 \cdot 463 - 135)\frac{0.85}{0.75} + 135 = 522 \text{ kN} \quad (7\text{-}13)$$

Table 7-6 lists the ratio of computed to measured Q_u for the various soil $\bar{\phi}$ and K_o values for the Hickling Station No. 84 grillages. For all combinations of $\bar{\phi}$ profiles A, B, and C with K_o profiles A, B, and C, the computed Q_u values are within 4 percent of the average measured value. Capacities at K/K_o values other than 0.7 can be computed using Equation 7-11 with Q_u (measured) = 137 kips (609

Table 7-6

RATIO OF COMPUTED TO AVERAGE MEASURED Q_u FOR $\bar{\phi}$ AND K_o PROFILES, K/K_o = 0.70, HICKLING STATION, GRILLAGE SET NO. 84[a]

	K_o Profile			
$\bar{\phi}$ Profile	A	B	C	D
A	1.02	1.01	1.00	0.97
B	1.01	1.00	0.99	0.97
C	1.00	0.99	0.98	0.96
D	0.90	0.89	0.89	0.87
E	0.90	0.89	0.88	0.87
F	0.85	0.84	0.84	0.82

a - $\bar{\gamma}$ = 120 pcf (18.9 kN/m^3)
B = 7 ft (2.13 m)
D = 9.3 ft (2.83 m)
Average measured Q_u = 137 kips (609 kN)

kN), W_{ref} = 54.7 kips (243 kN) for $\bar{\gamma}$ = 120 pcf (18.9 kN/m^3) and $(K/K_o)_{ref}$ = 0.70.

Other key parameters that have a substantial effect on predicted uplift capacities are the soil unit weight, $\bar{\gamma}$, and the embedment depth, D. Figure 7-12 shows the effect of soil unit weight on the uplift capacities at the Hickling Station No. 4 and No. 84 grillages. The soil unit weights have been normalized by $\bar{\gamma}_{ref}$ = 120 pcf (18.9 kN) to show the relative effects more clearly. The slope of the lines in Figure 7-12 is nearly 1:1, indicating that a 10 percent change in soil unit weight would result in a 10 percent change in the computed uplift capacity. The reference unit weight of 120 pcf (18.9 kN/m^3) is believed to be accurate within 10 percent.

The effects of varying embedment depth are shown in Figure 7-13 for the No. 4 and No. 84 grillages. The lines in Figure 7-13 are at a slope greater than 1:1, indicating a greater percent change in capacity for a given percent change in

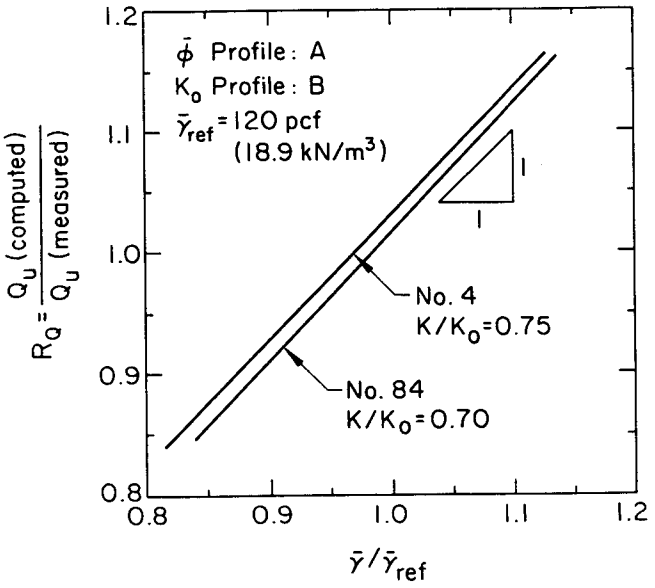

Figure 7-12. Effect of Soil Unit Weight on Computed Uplift Capacity, Hickling Station, Grillage Set Nos. 4 and 84

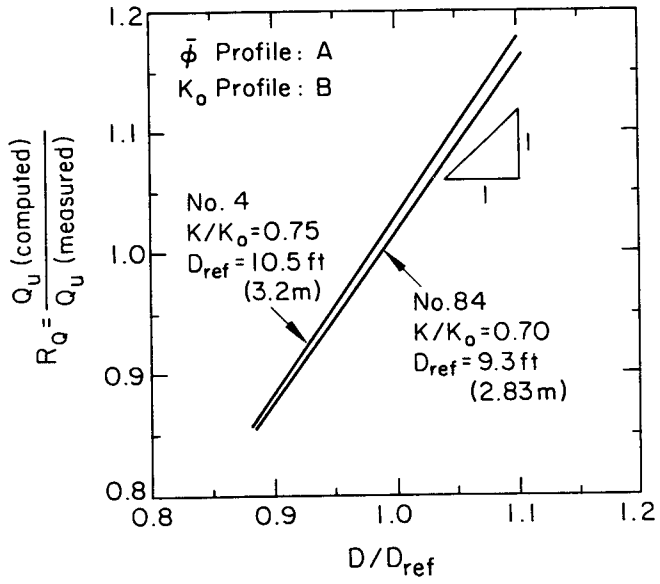

Figure 7-13. Effect of Depth on Computed Uplift Capacity, Hickling Station, Grillage Set Nos. 4 and 84

embedment depth. The reference depths, D_{ref}, used to normalize the depth effects were 9.3 ft (2.83 m) for the No. 84 grillages and 10.5 ft (3.20 m) for the No. 4 grillages. Although the effect of embedment depth is significant, knowledge of the grillage structural details and ground elevation eliminate much of the uncertainty associated with varying depth.

Wyncoop Creek

The lack of the wide range of in-situ test data available for the Wyncoop Creek site makes selection of soil properties more difficult. The best-estimate of properties at the Wyncoop Creek site consist of a uniform $\bar{\phi}$ profile of 40° and uniform K_o profile of 1.0. The limited SPT data indicated $\bar{\phi}$ values of 45° to 50°, but these are thought to be high because of the presence of boulders at the site and their effect on the SPT N values. The K_o = 1.0 value probably is somewhat low, but there are no field data to support a larger value.

Best-estimate soil layer properties for the Wyncoop Creek site are given in Table 7-7. The ground water table was placed at 7 ft (2.13 m) for the comparative analyses, based on field observations. An embedment depth of 7.2 ft (2.19 m) was used to represent the field conditions.

Figure 7-14 shows the computed uplift capacities based on the best-estimate

Table 7-7

BEST-ESTIMATE SOIL PROPERTIES, WYNCOOP CREEK, GRILLAGE SET NO. X2

Layer	1	2	3	4
Soil type	Gravel	Gravel	Gravel	Gravel
Depth to top (ft)	0	2	4	10
Depth to bottom (ft)	2	4	10	50
Soil unit weight, $\bar{\gamma}$ (pcf)	120	120	120	120
Friction angle, $\bar{\phi}$ (deg)	40	40	40	40
Horizontal stress coef., K_o - top	1.00	1.00	1.00	0.75
Horizontal stress coef., K_o - bottom	1.00	1.00	0.75	0.75
Operative/in-situ horizontal stress coefficient, K/K_o	0.65 to 0.85	0.65 to 0.85	0.65 to 0.85	0.65 to 0.85
Interface/soil friction angle, $\delta/\bar{\phi}$	1.0	1.0	1.0	1.0

1 ft = 0.305 m
1 pcf = 0.157 kN/m^3

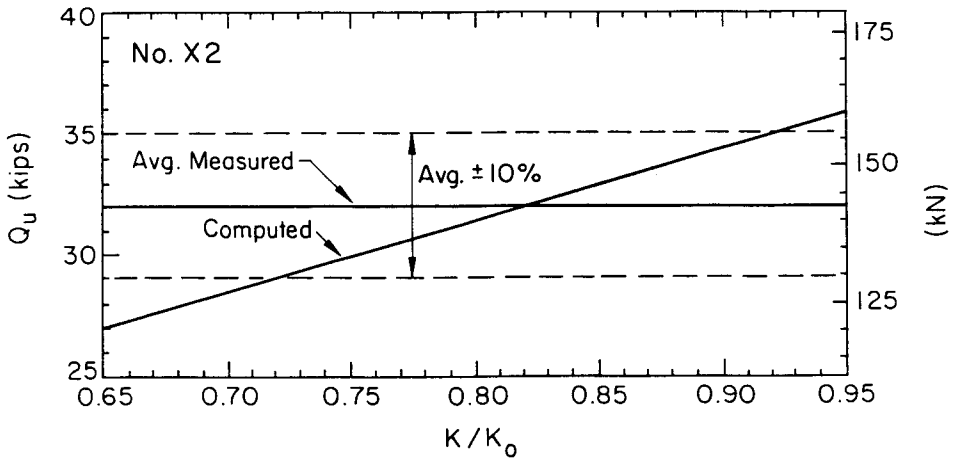

Figure 7-14. Computed and Measured Uplift Capacities Using Best-Estimate Soil Properties, Wyncoop Creek, Grillage Set No. X2

input parameters given in Table 7-7. The average measured value of 32 kips (142 kN) also is shown, with ± 10 percent ranges about the average. K/K_o values of 0.72 to 0.92 result in computed Q_u values within 10 percent of the measured values. Again, this would be representative of backfill that is looser than the native soil.

Parametric analyses similar to those done for the Hickling Station grillages were done for the Wyncoop Creek grillages, using the $\bar{\phi}$ and K_o profiles given in Figures 7-10 and 7-11. Although the soil profiles at Wyncoop Creek were different, the effects of other $\bar{\phi}$ and K_o values are useful in assessing the best-estimate predictions. Table 7-8 gives the ratios of computed to measured uplift capacities for the various $\bar{\phi}$ and K_o profile combinations. A K/K_o value of 0.75 was used for the ratios given in Table 7-8. All combinations of $\bar{\phi}$ profiles A, B, and C with K_o profiles A, B, and C resulted in predicted capacities within 6 percent of the average measured uplift capacity of 32 kips (142 kN). Higher K_o values, such as with K_o profiles A, B, and C, tended to give better agreement than the lower K_o values used in profile D. Also, the friction angle, $\bar{\phi}$, could be larger than 40°, assuming that K/K_o of 0.75 is correct. As with the Hickling Station data, the effects of K/K_o other than 0.75 could be determined using Equation 7-11 with Q_u (measured) = 32 kips (142 kN), W_{ref} = 7.6 kips (34 kN) for $\bar{\gamma}$ = 120 pcf (18.9 kN/m^3), and $(K/K_o)_{ref}$ = 0.75.

Effects of soil unit weight and embedment depth on the computed uplift capacity of the No. X2 grillages at Wyncoop Creek would show trends similar to those

Table 7-8

RATIO OF COMPUTED TO AVERAGE MEASURED Q_u FOR $\bar{\phi}$ AND K_o PROFILES, K/K_o = 0.75, WYNCOOP CREEK, GRILLAGE SET NO. X2[a]

	K_o Profile			
$\bar{\phi}$ Profile	A	B	C	D
A	1.05	-	-	0.97
B	1.03	-	-	0.95
C	1.01	0.99	0.98	0.94
D	0.89	-	-	-
E	0.88	0.87	0.85	0.82
F	-	-	-	-

a - $\bar{\gamma}$ = 120 pcf (18.9 kN/m^3)
D = 7.2 ft (2.19 m)
B = 3 ft (0.91 m)
Average measured Q_u = 32 kips (142 kN)

given for the Hickling Station grillages, as shown in Figures 7-12 and 7-13. However, uncertainties in the Wyncoop Creek soil properties do not warrant further refinement of the predicted capacities.

SUMMARY

The vertical shear model recommended by Kulhawy, et al. (11) gives good accuracy of predicted uplift capacity when used with the appropriate soil properties. The in-situ data were used to develop a range of reasonable properties for both the Hickling Station and Wyncoop Creek grillages. For all of the grillage types, best-estimate properties were based on the in-situ field data. K/K_o values representative of loose to medium dense backfill were consistent with the observed capacities.

The best-estimate values resulted in predicted capacities that were within 10 to 15 percent of the measured uplift capacities. Variations in the $\bar{\phi}$ and K_o profiles as presented previously had relatively minor effects on the computed

uplift capacities. The most important parameter for these computed grillage capacities was the K/K_o value. The K/K_o values representative of the field grillage tests range from about 0.6 to 0.8. Effects of changes in soil unit weight of $\pm$ 10 percent are directly reflected in $\pm$ 10 percent changes in predicted capacity. Variations in embedment depth change the predicted capacities dramatically. However, embedment depth must be considered a known parameter, obtained accurately from simple ground elevation measurements and grillage structural details.

REFERENCES

1. Turner, E. A., "Uplift Resistance of Transmission Tower Footings", Journal of the Power Division, ASCE, Vol. 88, No. PO2, July 1962, pp. 17-33.

2. Heikkalä, K. and Laine, J., "Uplift Resistance of Anchor Plates", Proceedings, 20th Session of the International Conference on Large Electric Systems at High Tension (CIGRE), Vol. 2, Report 217, Paris, June 1964, 14 p.

3. Flucker, R. L. and Teng, W. C., "A Study of Transmission Tower Foundations", Paper 31 CP65-714, IEEE Power Engineering Society Summer Meeting, Detroit, June 1965, 27 p.

4. Mors, H., "Methods of Dimensioning for Uplift Foundations of Transmission Line Towers", Proceedings, 20th Session of the International Conference on Large Electric Systems at High Tension (CIGRE), Vol. 2, Report 210, Paris, June 1964, 15 p.

5. Balla, A., "The Resistance to Breaking Out of Mushroom Foundations for Pylons", Proceedings, 5th International Conference on Soil Mechanics and Foundation Engineering, Vol. 1, Paris, 1961, pp. 569-576.

6. McDonald, H. F., "Uplift Resistance of Caisson Piles in Sand", MSc Thesis, Nova Scotia Technical College, Halifax, 1963 [as referenced in (8)].

7. Bützberger, F., "Individual Foundations of Towers for High Voltage Transmission Lines", Motor-Columbus, Ltd., Switzerland, June 1958, 7 p.

8. Meyerhof, G. G. and Adams, J. I., "The Ultimate Uplift Capacity of Foundations", Canadian Geotechnical Journal, Vol. 5, No. 4, Nov. 1968, pp. 225-244.

9. Mariupolskii, L. G., "The Bearing Capacity of Anchor Foundations", Soil Mechanics and Foundation Engineering, No. 1, Jan.-Feb. 1965, pp. 26-32. (translated from Russian)

10. Vesić, A. S., "Breakout Resistance of Objects Embedded in Ocean Bottom", Journal of the Soil Mechanics and Foundations Division, ASCE, Vol. 97, No. SM9, Sept. 1971, pp. 1183-1205.

11. Kulhawy, F. H., Trautmann, C. H., Beech, J. F., O'Rourke, T. D., McGuire, W., Wood, W. A., and Capano, C., "Transmission Line Structure Foundations for Uplift-Compression Loading", Report EL-2870, Electric Power Research Institute, Palo Alto, Feb. 1983, 412 p.

12. Stewart, J. P. and Kulhawy, F. H., "Behavior of Drilled Shafts in Axial Uplift Loading", Contract Report B-49(5), Niagara Mohawk Power Corporation, Syracuse, Jan. 1980, 261 p. (also Geotechnical Engineering Report 80-2, Cornell University).

13. Kulhawy, F. H., "Uplift Behavior of Shallow Soil Anchors - An Overview", Uplift Behavior of Anchor Foundations in Soil, Ed. S. P. Clemence, ASCE, New York, Oct. 1985, pp. 1-25.

14. Stas, C. V. and Kulhawy, F. H., "Critical Evaluation of Design Methods for Foundations Under Axial Uplift and Compression Loading", Report EL-3771, Electric Power Research Institute, Palo Alto, Nov. 1984, 198 p.

15. Mayne, P. W. and Kulhawy, F. H., "K_o-OCR Relationships in Soil", Journal of the Geotechnical Engineering Division, ASCE, Vol. 108, No. GT6, June 1982, pp. 851-872.

16. Hanna, T. H. and Carr, R. W., "The Loading Behavior of Plate Anchors in Normally and Overconsolidated Sands", Proceedings, 4th Conference on Soil Mechanics and Foundation Engineering, Budapest, 1971, pp. 589-600.

17. Arena, J. K., "Good Backfill - Key to Successful Transmission Tower Footing", Power Engineering, Vol. 66, No. 2, Dec. 1962, pp. 46-48.

18. Taylor, H. and Robinson, K. E., "Guyed Transmission Towers - Design and Performance of Anchors", Proceedings, 21st Canadian Soil Mechanics Conference, Winnipeg, Sept. 1968, 23 p.

19. Ismail, N. F. and Klym, T. W., "Uplift and Lateral Behavior of Earth Grillage Foundations", Paper A78-508-4, IEEE Power Engineering Society Summer Meeting, Los Angeles, July 1978, 7 p.

20. Kulhawy, F. H., O'Rourke, T. D., Stewart, J. P., and Beech, J. F., "Transmission Line Structure Foundations for Uplift-Compression Loading: Load Test Summaries", Report EL-3160, Electric Power Research Institute, Palo Alto, June 1983, 729 p.

21. Trautmann, C. H. and Kulhawy, F. H., "CUFAD - A Computer Program for Compression and Uplift Foundation Analysis and Design", Report EL-4540-CCM, Vol. 16, Electric Power Research Institute, Palo Alto, Oct. 1987, 148 p.

Section 8

SUMMARY AND CONCLUSIONS

This report presents the results of eight grillage foundation uplift tests. The topics addressed include descriptions of the field test sites and steel grillages. Descriptions of the soils were based on both field and laboratory characterizations. The field uplift test methods were reported, along with interpretations of the test results. Analytical models for calculating uplift capacity were presented, and a recommended vertical shear model was used to represent the field performance. Soil properties used to predict capacities were identified, and both best-estimate and parametric prediction studies were performed.

SITE DESCRIPTIONS

Full-scale uplift tests on three geometries of steel grillages were performed at two sites in the Southern Tier of upstate New York. The Hickling Station site was near Corning, NY and the Wyncoop Creek site was near Chemung, NY. At the Hickling Station site, BA structure foundations had base dimensions of 4.75 ft x 5.0 ft (1.45 m x 1.52 m) and an average embedment of 10.5 ft (3.20 m). The Lehigh structure foundation at Hickling Station had base dimensions of 7.0 ft x 7.0 ft (2.13 m x 2.13 m) and an average embedment of 9.3 ft (2.83 m). These foundations had been left in place following a highway relocation project.

The grillages at Wyncoop Creek were from a tangent line section. These grillages had foundation base dimensions of 3 ft x 3 ft (0.91 m x 0.91 m) and average embedments of 7.2 ft (2.19 m). A storm damaged the upper portions of the steel lattice tower, but the grillage foundations were left in place and available for testing.

SOIL TESTING

A variety of in-situ tests were made at the field sites. The range of tests allowed comparisons to be made between correlated properties from each type of test. The soils at the test sites primarily were granular, but they contained substantial percentages of both large cobbles and fines. In general, the native

soil was stiffer and more dense than the backfill material.

Soil profiles of $\bar{\phi}$ and K_o were determined from the in-situ tests. Laboratory testing consisted of index and classification tests, compaction tests, and drained triaxial tests. Estimates of field maximum dry unit weights and optimum moisture contents were determined. Triaxial tests were conducted on specimens with gradations finer than those in-situ, because the in-situ soil had large cobbles. Tests were conducted for a range of soil densities, and the results were used to determine strength parameters. The laboratory strength data correlated well with field borehole shear test data, but the laboratory strength properties were lower than those based on correlations with field SPT and CPT data.

FIELD UPLIFT TESTS

The equipment used to conduct the uplift tests consisted of a reaction beam, spanning the grillage stub and supported on timber cribbing pads. Loads were applied with a hydraulic jack and were measured with both a load cell and hydraulic pressure gage. Stub displacements were measured by optical survey and a dial gage mounted on a reference beam. Ground movements were monitored using arrays of wooden hubs placed near the grillage stubs. The primary measuring systems were the load cell and optical level.

A modified, quick maintained load procedure, with several unload-reload cycles, was used during the uplift tests. Loads were applied at increments of ten percent of the estimated failure loads.

Eight uplift tests were performed, three for each of the two grillage types at Hickling Station and two at the Wyncoop Creek site. The repeatability of the replicate tests at the Hickling Station site was extremely good. Differences in the backbone loading curves of the No. 4 (BA) grillages were indistinguishable. The No. 84 (Lehigh) grillage tests at Hickling Station showed modest differences, but overall the test results were quite similar. Larger differences between test results were measured for the No. X2 grillages at the Wyncoop Creek site. These differences were attributed to the soil conditions, since the soils at Wyncoop Creek contained large boulders and some concrete debris.

Interpreted failure loads and displacements were based on a slope-tangent method. The displacements at one-half the interpreted failure load and at the

failure load were compared with existing data for steel grillages in granular soils. The comparisons pointed out the benefit of applying large displacements during testing to define fully the load-displacement relationship. A revised design recommendation was presented for the displacements of steel grillages in granular soils subjected to uplift loads.

Uplift capacity was characterized by two components, a side resistance uplift capacity factor and a weight capacity factor. The field uplift results indicated that, as D/B increases, more resistance develops from side resistance than from weight of the soil in a prism above the grillage. Predictive equations were presented defining the percentages of capacity from side resistance and weight, as dependent on D/B.

GRILLAGE CAPACITY MODELING

A review of uplift capacity models was given, and a recommended vertical shear model was used to characterize the observed field behavior. Best-estimate soil properties were identified, based on the in-situ test results, and capacity predictions of the three grillage types were made. Important soil properties required for the vertical shear model include $\bar{\phi}$, K_o, and K/K_o, the ratio of operative to in-situ horizontal stress. Since the backfill was less dense than the native soil, K/K_o values were estimated to be between 2/3 and 1, as suggested from previous research.

Capacities computed from the best-estimate soil properties were in good agreement with the interpreted failure loads from the field tests. To investigate sensitivity of the model calculations with varying $\bar{\phi}$ and K_o, a range of realistic soil profiles was established and used in a parametric analysis. For a range of profiles within the bounds derived from the soil testing program, computed capacities were found to be relatively insensitive to both $\bar{\phi}$ and K_o profiles, but they were influenced most by the K/K_o value used for the analysis. The K/K_o values that gave good agreement between measured and predicted response were on the order of 0.7 to 0.8, consistent with the initial estimates based on the results of the in-situ tests.

The field uplift test program identified several important features necessary for validation of analytical and laboratory-scale modeling. Geotechnical property determination is critical to the interpretation of uplift test results. The use of several in-situ tests allowed trends in soil properties to be

identified, as well as verification of properties using alternative measuring techniques. For grillages, large displacements are necessary to define the complete load-displacement curve. Testing with limited displacements results in underprediction of interpreted failure loads and overprediction of displacements at failure.

The vertical shear model, coupled with well-documented geotechnical properties, can be used to predict accurately the uplift capacity of grillage foundations. For grillages in granular soils, the incorporation of side shearing resistance is important. The field test results indicated that, for D/B from 1 to 3, roughly 55 to 80 percent of the uplift capacity is attributable to side resistance, with only 20 to 45 percent of the capacity resulting from soil weight. This result is important when deciding on the allowable loadings that may be imposed from line upgradings and increased tower heights. The use of existing foundations may result in substantial cost savings over new foundations, provided that adequate subsurface exploration and geotechnical data are incorporated into the planning and design stages.

FIELD BORING LOG

BUFFALO DRILLING COMPANY, INC.
955 Niagara Street
Buffalo, New York 14213

Client: Cornell University
Project: In-Situ Testing Program
File No.: 86-142 Boring No.: 4-NE SPT-1

Driller: Darryl Altrogge
Type of Drill Rig: CME-55
Sampling Method: ASTM D1586
Size and Type of Bit: 3-3/4 inch ID augers

Surface Elevation:
Datum:
Location: Hickling Generating Station Site
Date Started: 8/12/86 Completed: 8/12/86

Overburden Samples: Disturbed 5 Undist.
Total Depth of Hole: 9.0 ft.
Depth Drilled into Rock: 0 ft.

Top of Rock Elevation:
Bottom of Hole Elevation:
Ground Water Depth: no water at completion

Depth (ft.)	Blows per .5 ft.		Sample No.	N	% Rec (RQD)	SOIL AND ROCK DESCRIPTION	REMARKS
						Topsoil	
1	6	8	S-1	15	20	Brown, med. dense, SAND and Gravel, dry	S-1: 0-2'
	7	10					
	8	11	S-2	21	50	same as S-1	S-2: 2-4'
	10	7					
5	5	6	S-3	16	25	same as S-1	S-3: 4-6'
	10	14					
	6	7	S-4	12	25	same as S-1	S-4: 6-8'
	5	6					
	5	6	S-5	11	10	same as S-1	S-5: 8-9'
10						Bottom of Hole 9.0 ft.	note 1

Notes: 1.) Encountered top of foundation grid at 9.0 ft.

Sheet No 1 of 1

Figure A-1. SPT Log, Boring 4-NE SPT-1 (Inside), Hickling Station

Appendix A

IN-SITU FIELD DATA

This appendix contains the in-situ field data for both the Hickling Station and Wyncoop Creek sites. Figures A-1 through A-12 are the SPT boring logs for the Hickling Station site. Also included are logs from the boreholes made for the PMTs (Figures A-13 through A-20). The PMT boreholes were advanced using a 3 in. (76 mm) O.D. split-spoon, using a 140 lb (63.6 kg) safety hammer and a drop height of 30 in. (762 mm). Corrected pressure-volume and creep curves from the PMTs are given in Figures A-21 through A-57. A 3 in. (76 mm) diameter, type GA probe with metallic sheaths was used for all the PMTs. The initial probe volume was 122.5 $in.^3$ (790 cm^3). The DCT data from the Hickling Station site were not recorded on log forms and therefore are not given in this appendix.

Figures A-58 through A-61 are the SPT boring logs for the Wyncoop Creek site. The DCT logs are given in Figures A-62 through A-64.

FIELD BORING LOG

BUFFALO DRILLING COMPANY, INC.
955 Niagara Street
Buffalo, New York 14213

Client: Cornell University
Project: In-Situ Testing Program
File No.: 86-142 Boring No.: 4-NW SPT-1

Driller: Keith Danser
Type of Drill Rig: Mobile B-47
Sampling Method: ASTM D1586
Size and Type of Bit: 3-3/4 inch ID augers

Surface Elevation:
Datum:
Location: Hickling Generating Station Site
Date Started: 8/7/86 Completed: 8/7/86

Overburden Samples: Disturbed 10 Undist.
Total Depth of Hole: 20.0 ft.
Depth Drilled into Rock: 0 ft.

Top of Rock Elevation:
Bottom of Hole Elevation:
Ground Water Depth: 16.0 ft.

Depth (ft.)	Blows per .5 ft.		Sample No.	N	% Rec (RQD)	SOIL AND ROCK DESCRIPTION	REMARKS
						Topsoil	
1	4	5	S-1	13	50	Brown, med. dense, SAND and Gravel	S-1: 0-2'
	8	8					
	5	6	S-2	12	50	same as S-1	S-2: 2-4'
	6	5					
5	3	6	S-3	10	25	same as S-1	S-3: 4-6'
	4	4					
	6	10	S-4	15	50	...grade: moist	S-4: 6-8'
	5	8					
	6	6	S-5	13	25	same as S-4	S-5: 8-10'
10	7	12					
	12	6	S-6	12	25	same as S-4	S-6: 10-12'
	6	7					
	11	30	S-7	47	25	...grade: dense, saturated	S-7: 12-14'
	17	10					
15	4	8	S-8	24	50	...grade: med. dense	S-8: 14-16'
	16	22					
	20	17	S-9	47	75	...grade: dense	S-9: 16-18'
	30	47					
	31	31	S-10	81	75	...grade: v. dense, little shale fragments	S-10: 18-20'
20	50	35					
						Bottom of Hole 20.0 ft.	

Notes:
1.) Hole open to 8 ft. after pulling augers.

Sheet No 1 of 1

Figure A-2. SPT Log, Boring 4-NW SPT-1 (Outside), Hickling Station

FIELD BORING LOG

BUFFALO DRILLING COMPANY, INC.
955 Niagara Street
Buffalo, New York 14213

Client Cornell University
Project In-Situ Testing Program
File No. 86-142 Boring No. 4-NW SPT-2

Driller Keith Danser
Type of Drill Rig Mobile B-47
Sampling Method ASTM D1586
Size and Type of Bit 3-3/4 inch ID augers

Surface Elevation
Datum
Location Hickling Generating Station Site
Date Started 8/7/86 Completed 8/7/86

Overburden Samples: Disturbed 5 Undist.
Total Depth of Hole 10.0 ft.
Depth Drilled into Rock 0 ft.

Top of Rock Elevation
Bottom of Hole Elevation
Ground Water Depth no water at completion

Depth (ft.)	Blows per .5 ft.		Sample No.	N	% Rec (RQD)	SOIL AND ROCK DESCRIPTION	REMARKS
						Topsoil	
1	5	10	S-1	22	25	Brown, med. dense,SAND and Gravel	S-1: 0-2'
	12	13					
	7	7	S-2	14	25	same as S-1	S-2: 2-4' note 1
	7	7					
5	4	4	S-3	9	25	same as S-1	S-3: 4-6'
	5	8					
	4	7	S-4	14	25	same as S-1	S-4: 6-8'
	7	7					
	8	8	S-5	26	25	same as S-1	S-5: 8-10'
10	18	15					
						Bottom of Hole 10.0 ft.	

Notes: 1.) Hard augering from 3 to 3.5 ft.

Sheet No 1 of 1

Figure A-3. SPT Log, Boring 4-NW SPT-2 (Inside), Hickling Station

FIELD BORING LOG

BUFFALO DRILLING COMPANY, INC.
955 Niagara Street
Buffalo, New York 14213

Client: Cornell University
Project: In-Situ Testing Program
File No.: 86-142 Boring No.: 4-SE SPT-1

Driller: Keith Danser
Type of Drill Rig: Mobile B-47
Sampling Method: ASTM D1586
Size and Type of Bit: 3-3/4 inch ID augers

Surface Elevation:
Datum:
Location: Hickling Generating Station Site
Date Started: 8/8/86 Completed: 8/8/86

Overburden Samples: Disturbed: 10 Undist.:
Total Depth of Hole: 20.0 ft.
Depth Drilled into Rock: 0 ft.

Top of Rock Elevation:
Bottom of Hole Elevation:
Ground Water Depth: 17.0 ft. at completion

Depth (ft.)	Blows per .5 ft.		Sample No.	N	% Rec (RQD)	SOIL AND ROCK DESCRIPTION	REMARKS
						Topsoil	
1	2	1	S-1	7	10	Brown, loose, SAND and Gravel	S-1: 0-2'
	6	11					
	5	8	S-2	18	25	...grade: med. dense	S-2: 2-4'
	10	10					
5	5	10	S-3	21	50	same as S-2	S-3: 4-6'
	11	8					
	8	7	S-4	15	25	same as S-2	S-4: 6-8'
	8	10					
	5	9	S-5	17	25	same as S-2	S-5: 8-10'
10	8	7					
	6	12	S-6	27	50	...grade: moist	S-6: 10-12'
	15	11					
	37	19	S-7	38	50	...grade: dense	S-7: 12-14'
	19	19					
15	15	27	S-8	56	25	...grade: v. dense, saturated	S-8: 14-16'
	29	17					
	17	14	S-9	26	50	...grade: med. dense	S-9: 16-18'
	12	17					
	9	16	S-10	44	75	...grade: dense	S-10: 18-20'
20	28	34					
						Bottom of Hole 20.0 ft.	

Notes: 1.) Hole open to 9 ft. after pulling augers.

Sheet No 1 of 1

Figure A-4. SPT Log, Boring 4-SE SPT-1 (Outside), Hickling Station

FIELD BORING LOG

BUFFALO DRILLING COMPANY, INC.
955 Niagara Street
Buffalo, New York 14213

Client Cornell University
Project In-Situ Testing Program
File No. 86-142 Boring No. 4-SE SPT-2

Driller Keith Danser
Type of Drill Rig Mobile B-47
Sampling Method ASTM D1586
Size and Type of Bit 3-3/4 inch ID augers

Surface Elevation
Datum
Location Hickling Generating Station Site
Date Started 8/8/86 Completed 8/8/86

Overburden Samples: Disturbed 5 Undist.
Total Depth of Hole 10.0 ft.
Depth Drilled into Rock 0 ft.

Top of Rock Elevation
Bottom of Hole Elevation
Ground Water Depth no water at completion

Depth (ft.)	Blows per .5 ft.		Sample No.	N	% Rec (RQD)	SOIL AND ROCK DESCRIPTION	REMARKS
1	2	3	S-1	7	50	Brown, loose, SAND and Gravel	S-1: 0-2'
	4	7					
	6	6	S-2	9	25	same as S-1	S-2: 2-4'
	3	4					
5	5	5	S-3	11	50	...grade: med. dense	S-3: 4-6'
	6	5					
	6	8	S-4	16	25	same as S-3	S-4: 6-8'
	8	6					
	5	6	S-5	10	0		S-5:8-10' no recovery
10	4	4					
						Bottom of Hole 10.0 ft.	

Notes:

Sheet No 1 of 1

Figure A-5. SPT Log, Boring 4-SE SPT-2 (Inside), Hickling Station

FIELD BORING LOG

BUFFALO DRILLING COMPANY, INC.
955 Niagara Street
Buffalo, New York 14213

Client Cornell University
Project In-Situ Testing Program
File No. 86-142 Boring No. 4-SW SPT-1

Driller Darryl Altrogge
Type of Drill Rig CME-55
Sampling Method ASTM D1586
Size and Type of Bit 3-3/4 inch ID augers

Surface Elevation
Datum
Location Hickling Generating Station Site
Date Started 8/13/86 Completed 8/13/86

Overburden Samples: Disturbed 5 Undist.
Total Depth of Hole 10.0 ft.
Depth Drilled into Rock 0 ft.

Top of Rock Elevation
Bottom of Hole Elevation
Ground Water Depth no water at completion

Depth (ft.)	Blows per .5 ft.		Sample No.	N	% Rec (RQD)	SOIL AND ROCK DESCRIPTION	REMARKS
						Topsoil	
1	4	3	S-1	14	70	Brown, med. dense, SAND and Gravel, dry	S-1: 0-2'
	11	7					
	6	9	S-2	22	25	same as S-1	S-2: 2-4'
	13	10					
5	7	10	S-3	18	10	same as S-1	S-3: 4-6'
	8	10					
	6	4	S-4	11	25	same as S-1	S-4: 6-8'
	7	6					
	10	10	S-5	19	25	same as S-1	S-5: 8-10'
	9	10					
10						Bottom of Hole 10.0 ft.	note 1

Notes: 1.) Encountered top of foundation grid at 9.5 ft.

Sheet No 1 of 1

Figure A-6. SPT Log, Boring 4-SW SPT-1 (Inside), Hickling Station

FIELD BORING LOG

BUFFALO DRILLING COMPANY, INC.
955 Niagara Street
Buffalo, New York 14213

Client: Cornell University
Project: In-Situ Testing Program
File No.: 86-142 Boring No.: 84-NE SPT-1

Driller: Keith Danser
Type of Drill Rig: Mobile B-47
Sampling Method: ASTM D1586
Size and Type of Bit: 3-3/4 inch ID augers

Surface Elevation:
Datum:
Location: Hickling Generating Station Site
Date Started: 8/6/86 Completed: 8/6/86

Overburden Samples: Disturbed: 11 Undist.:
Total Depth of Hole: 22.0 ft.
Depth Drilled into Rock: 0 ft.

Top of Rock Elevation:
Bottom of Hole Elevation:
Ground Water Depth: 15.0 ft. at completion

Depth (ft.)	Blows per .5 ft.		Sample No.	N	% Rec (RQD)	SOIL AND ROCK DESCRIPTION	REMARKS
						Topsoil	
1	3	3	S-1	7	10	Brown, loose, SAND and f/c Gravel, some Silt, dry	S-1: 0-2'
	4	5					
	3	5	S-2	10	10	...grade: moist	S-2: 2-4'
	5	5					
5	4	7	S-3	16	15	...grade: med. dense	S-3: 4-6'
	9	8					
	6	6	S-4	14	15	...grade: wet	S-4: 6-8'
	8	6					
	3	4	S-5	9	15	...grade: loose	S-5: 8-10'
10	5	9					
	3	4	S-6	10	20	...grade: saturated	S-6: 10-12'
	6	9					
	7	11	S-7	38	35	...grade: dense	S-7: 12-14'
	27	25					
15	12	17	S-8	36	50	...grade: tr. Gravel, tr. Silt	S-8: 14-16' note 1
	19	19					
	8	33	S-9	50	10	..grade: and Gravel	S-9: 16-18'
	17	18					
	12	18	S-10	37	10	same as S-9	S-10: 18-20'
20	19	12					
21	5	8	S-11	18	20	...grade: med. dense	S-11: 20-22'
	10	12					
						Bottom of Hole 22.0 ft.	

Notes: 1.) Sand blew up augers 6 inches after sample recovered.

Sheet No 1 of 1

Figure A-7. SPT Log, Boring 84-NE SPT-1 (Outside), Hickling Station

FIELD BORING LOG

BUFFALO DRILLING COMPANY, INC.
955 Niagara Street
Buffalo, New York 14213

Client Cornell University
Project In-Situ Testing Program
File No. 86-142 Boring No. 84-NE SPT-2

Driller Keith Danser
Type of Drill Rig Mobile B-47
Sampling Method ASTM D1586
Size and Type of Bit 3-3/4 inch ID augers

Surface Elevation
Datum
Location Hickling Generating Station Site
Date Started 8/6/86 Completed 8/6/86

Overburden Samples: Disturbed 5 Undist.
Total Depth of Hole 9.0 ft.
Depth Drilled into Rock 0 ft.

Top of Rock Elevation
Bottom of Hole Elevation
Ground Water Depth no water at completion

Depth (ft.)	Blows per .5 ft.		Sample No.	N	% Rec (RQD)	SOIL AND ROCK DESCRIPTION	REMARKS
1	2	2	S-1	4	25		S-1: 0-1'
	10	3	S-2	9	25	Brown, loose, f. Sand, some Silt, some f/c Gravel, damp (Fill)	S-2: 1-3'
	6	7					
	3	5	S-3	9	25	...grade: moist	S-3: 3-5'
5	4	6					
	3	5	S-4	9	23	same as S-3	S-4: 5-7'
	4	5					
	3	4	S-5	10	50	Brown, med. dense, Sand, little f/m Gravel, little Silt, tr. Clay (Fill)	S-5: 7-9'
	6	5					
10						Bottom of Hole 9.0 ft.	

Notes:

Sheet No 1 of 1

Figure A-8. SPT Log, Boring 84-NE SPT-2 (Inside), Hickling Station

FIELD BORING LOG

BUFFALO DRILLING COMPANY, INC.
955 Niagara Street
Buffalo, New York 14213

Client: Cornell University
Project: In-Situ Testing Program
File No.: 86-142 Boring No.: 84-NW SPT-1

Driller: Darryl Altrogge
Type of Drill Rig: CME-55
Sampling Method: ASTM D1586
Size and Type of Bit: 3-3/4 inch ID augers

Surface Elevation:
Datum:
Location: Hickling Generating Station Site
Date Started: 8/12/86 Completed: 8/12/86

Overburden Samples: Disturbed: 5 Undist.:
Total Depth of Hole: 10.0 ft.
Depth Drilled into Rock: 0 ft.

Top of Rock Elevation:
Bottom of Hole Elevation:
Ground Water Depth: no water at completion

Depth (ft.)	Blows per .5 ft.		Sample No.	N	% Rec (RQD)	SOIL AND ROCK DESCRIPTION	REMARKS
1	5	6	S-1	15	10	Topsoil Brown, medium dense, SAND and Gravel, dry	S-1: 0-2'
	9	12					
	4	8	S-2	15	35	same as S-1	S-2: 2-4'
	7	7					
5	5	7	S-3	15	10	same as S-1	S-3: 4-6'
	8	10					
	4	2	S-4	6	25	...grade: loose, moist	S-4: 6-8'
	4	4					
	3	2	S-5	10	10	...grade: saturated	S-5: 8-10'
	8	6					
10						Bottom of Hole 10.0 ft.	

Notes:

Sheet No 1 of 1

Figure A-9. SPT Log, Boring 84-NW SPT-1 (Inside), Hickling Station

FIELD BORING LOG

BUFFALO DRILLING COMPANY, INC.
955 Niagara Street
Buffalo, New York 14213

Client: Cornell University
Project: In-Situ Testing Program
File No.: 86-142 Boring No.: 84-SE SPT-1

Driller: Darryl Altrogge
Type of Drill Rig: CME-55
Sampling Method: ASTM D1586
Size and Type of Bit: 3-3/4 inch ID augers

Surface Elevation:
Datum:
Location: Hickling Generating Station Site
Date Started: 8/12/86 Completed: 8/12/86

Overburden Samples: Disturbed: 5 Undist.:
Total Depth of Hole: 10.0 ft.
Depth Drilled into Rock: 0 ft.

Top of Rock Elevation:
Bottom of Hole Elevation:
Ground Water Depth: no water at completion

Depth (ft.)	Blows per .5 ft.		Sample No.	N	% Rec (RQD)	SOIL AND ROCK DESCRIPTION	REMARKS
1	1	5	S-1	10	0		S-1: 0-2' no recovery
	5	6					
	5	4	S-2	8	50	Brown, loose, SAND and Gravel,dry	S-2: 2-4'
	4	4					
5	6	7	S-3	13	30	...grade; med. dense	S-3: 4-6'
	6	7					
	7	8	S-4	14	25	same as S-3	S-4: 6-8'
	6	4					
	2	2	S-5	5	25	...grade: loose, moist	S-5: 8-10'
	3	6					
10						Bottom of Hole 10.0 ft.	

Notes:

Sheet No 1 of 1

Figure A-10. SPT Log, Boring 84-SE SPT-1 (Inside), Hickling Station

FIELD BORING LOG

BUFFALO DRILLING COMPANY, INC.
955 Niagara Street
Buffalo, New York 14213

Client Cornell University
Project In-Situ Testing Program
File No. 86-142 Boring No. 84-SW SPT-1

Driller Keith Danser
Type of Drill Rig Mobile B-47
Sampling Method ASTM D1586
Size and Type of Bit 3-3/4 inch ID augers

Surface Elevation
Datum
Location Hickling Generating Station Site
Date Started 8/7/86 Completed 8/7/86

Overburden Samples: Disturbed 10 Undist.
Total Depth of Hole 20.0 ft.
Depth Drilled into Rock 0 ft.

Top of Rock Elevation
Bottom of Hole Elevation
Ground Water Depth 15.5 ft. at completion

Depth (ft.)	Blows per .5 ft.		Sample No.	N	% Rec (RQD)	SOIL AND ROCK DESCRIPTION	REMARKS
1	2	4	S-1	10	15	Brown, med. dense, SAND and Gravel	S-1: 0-2'
	6	6					
	13	14	S-2	26	50	same as S-1	S-2: 2-4'
	12	12					
5	6	8	S-3	18	50	same as S-1	S-3: 4-6'
	10	9					
	8	5	S-4	11	50	...grade: moist	S-4: 6-8'
	6	8					
	5	8	S-5	17	25	same as S-4	S-5: 8-10'
	9	11					
10	11	27	S-6	39	25	...grade: dense, saturated	S-6: 10-12'
	12	11					
	8	16	S-7	43	50	same as S-6	S-7: 12-14'
	27	36					
	13	15	S-8	29	25	...grade: med. dense	S-8: 14-16'
15	14	8					
	6	14	S-9	28	25	same as S-8	S-9: 16-18'
	14	13					
	9	9	S-10	31	25	...grade: dense	S-10: 18-20'
20	12	9					

Bottom of Hole 20.0 ft.

Notes: 1.) Hole open to 7 ft. after pulling augers.

Sheet No 1 of 1

Figure A-11. SPT Log, Boring 84-SW SPT-1 (Outside), Hickling Station

FIELD BORING LOG

BUFFALO DRILLING COMPANY, INC.
955 Niagara Street
Buffalo, New York 14213

Client Cornell University
Project In-Situ Testing Program
File No. 86-142 Boring No. 84-SW SPT-2

Driller Keith Danser
Type of Drill Rig Mobile B-47
Sampling Method ASTM D1586
Size and Type of Bit 3-3/4 inch ID augers

Surface Elevation
Datum
Location Hickling Generating Station Site
Date Started 8/7/86 Completed 8/7/86

Overburden Samples: Disturbed 5 Undist.
Total Depth of Hole 8.7 ft.
Depth Drilled into Rock 0 ft.

Top of Rock Elevation
Bottom of Hole Elevation
Ground Water Depth no water at completion

Depth (ft.)	Blows per .5 ft.		Sample No.	N	% Rec (RQD)	SOIL AND ROCK DESCRIPTION	REMARKS
						Topsoil	
1	4	4	S-1	8	5	Brown, loose, SAND and Gravel	S-1: 0-1'
	4	3	S-2	7	50	same as S-1	S-2: 1-3'
	4	4					
	4	5	S-3	11	50	...grade: med. dense	S-3: 3-5'
5	6	5					
	4	4	S-4	7	25	...grade: loose	S-4: 5-7'
	3	5					
	4	0	S-5	1		...grade: v. loose	S-5: 7-8.7'
	1/8"						
10						Bottom of Hole 8.7 ft.	note 1

Notes:
1.) Encountered top of foundation grid at 8.75 ft.
2.) Hole open at 3 ft. 3 inches after pulling augers.
3.) Cone test taken at 7 ft. and 8 ft.

Sheet No 1 of 1

Figure A-12. SPT Log, Boring 84-SW SPT-2 (Inside), Hickling Station

FIELD BORING LOG

BUFFALO DRILLING COMPANY, INC.
955 Niagara Street
Buffalo, New York 14213

Client Cornell University
Project In-Situ Testing Program
File No. 86-142 Boring No. 4-NW PMT-1

Driller Darryl Altrogge
Type of Drill Rig CME-55
Sampling Method ASTM D1586
Size and Type of Bit 3-3/4 inch ID augers

Surface Elevation
Datum
Location Hickling Generating Station Site
Date Started 8/11/86 Completed 8/11/86

Overburden Samples: Disturbed 3 Undist.
Total Depth of Hole 9.0 ft.
Depth Drilled into Rock 0 ft.

Top of Rock Elevation
Bottom of Hole Elevation
Ground Water Depth no water at completion

Depth (ft.)	Blows per .5 ft.		Sample No.	N	% Rec (RQD)	SOIL AND ROCK DESCRIPTION	REMARKS
1	5	8					
	8	9	S-1	17	60	Brown, med. dense, SAND and Gravel	S-1: 0-3'
	12	13					
	13	14					
5	11	9	S-2	20		same as S-1	S-2: 3-6'
	17	21					
	20	15					
	20	9	S-3	29	60	same as S-1	S-3: 6-9'
	13	13					
10						Bottom of Hole 9.0 ft.	

Notes: 1.) Samples obtained using 3 ft. long by 3 in. OD split-spoon sampler.

Sheet No 1 of 1

Figure A-13. 3 in. (76 mm) O.D. Split-Spoon Log, 4-NW PMT-1 (Inside), Hickling Station

FIELD BORING LOG

BUFFALO DRILLING COMPANY, INC.
955 Niagara Street
Buffalo, New York 14213

Client: Cornell University
Project: In-Situ Testing Program
File No.: 86-142 Boring No.: 4-NW PMT-2

Driller: Darryl Altrogge
Type of Drill Rig: CME-55
Sampling Method: ASTM D1586
Size and Type of Bit: 3-3/4 inch ID augers

Surface Elevation:
Datum:
Location: Hickling Generating Station Site
Date Started: 8/11/86 Completed: 8/12/86

Overburden Samples: Disturbed: 5 Undist.:
Total Depth of Hole: 14.0 ft.
Depth Drilled into Rock: 0 ft.

Top of Rock Elevation:
Bottom of Hole Elevation:
Ground Water Depth: no water at completion

Depth (ft.)	Blows per .5 ft.		Sample No.	N	% Rec (RQD)	SOIL AND ROCK DESCRIPTION	REMARKS
1	7	8					
	13	11	S-1	24	65	Brown, med. dense, SAND and Gravel	S-1: 0-3'
	11	10					
	12	13					
5	10	22	S-2	32	65	...grade: dense	S-2: 3-6'
	19	20					
	27	14					
	19	17	S-3	36	60	same as S-2	S-3: 6-9'
	23	14					
10	14	11					
	9	12	S-4	21	30	...grade: med. dense	S-4: 9-12'
	12	21					
	29	40	S-5	78	55	...grade: v. dense	S-5: 12-14'
	38	14					
15						Bottom of Hole 14.0 ft.	

Notes: 1.) S-1 through S-4 obtained using 3 ft. long by 3 in. OD split-spoon sampler.

Sheet No 1 of 1

Figure A-14. 3 in. (76 mm) O.D. Split-Spoon Log, 4-NW PMT-2 (Outside), Hickling Station

FIELD BORING LOG

BUFFALO DRILLING COMPANY, INC.
955 Niagara Street
Buffalo, New York 14213

Client Cornell University
Project In-Situ Testing Program
File No. 86-142 Boring No. 4-SE PMT-1

Driller Darryl Altrogge
Type of Drill Rig CME-55
Sampling Method ASTM D1586
Size and Type of Bit 3-3/4 inch ID augers

Surface Elevation
Datum
Location Hickling Generating Station Site
Date Started 8/11/86 Completed 8/11/86

Overburden Samples: Disturbed 3 Undist.
Total Depth of Hole 9.0 ft.
Depth Drilled into Rock 0 ft.

Top of Rock Elevation
Bottom of Hole Elevation
Ground Water Depth no water at completion

Depth (ft.)	Blows per .5 ft.		Sample No.	N	% Rec (RQD)	SOIL AND ROCK DESCRIPTION	REMARKS
1	3	4					
	4	8	S-1	12	40	Brown, med. dense, SAND and Gravel	S-1: 0-3'
	7	6					
	6	5					
5	7	10	S-2	17	50	same as S-1	S-2: 3-6'
	14	22					
	12	12					
	10	9	S-3	19	60	same as S-1	S-3: 6-9'
	8	8					
10						Bottom of Hole 9.0 ft.	

Notes: 1.) Samples obtained using 3 ft. long by 3 in. OD split-spoon sampler.

Sheet No 1 of 1

Figure A-15. 3 in. (76 mm) O.D. Split-Spoon Log, 4-SE PMT-1 (Inside), Hickling Station

FIELD BORING LOG

BUFFALO DRILLING COMPANY, INC.
955 Niagara Street
Buffalo, New York 14213

Client Cornell University
Project In-Situ Testing Program
File No. 86-142 Boring No. 4-SE PMT-2

Driller Keith Danser
Type of Drill Rig CME-55
Sampling Method ASTM D1586
Size and Type of Bit 3-3/4 inch ID augers

Surface Elevation
Datum
Location Hickling Generating Station Site
Date Started 8/11/86 Completed 8/11/86

Overburden Samples: Disturbed 4 Undist.
Total Depth of Hole 12.0 ft.
Depth Drilled into Rock 0 ft.

Top of Rock Elevation
Bottom of Hole Elevation
Ground Water Depth no water at completion

Depth (ft.)	Blows per .5 ft.		Sample No.	N	% Rec (RQD)	SOIL AND ROCK DESCRIPTION	REMARKS
1	8	16					
	15	17	S-1	32	70	Brown, med. dense, SAND and Gravel	S-1: 0-3'
	14	11					
	10	10					
5	10	13	S-2	23	60	...grade: med. dense	S-2: 3-6'
	24	14					
	18	12					
	10	9	S-3	19	50	same as S-2	S-3: 6-9'
	10	10					
10	10	15					
	14	15	S-4	29		same as S-2	S-4: 9-12'
	17	35					
						Bottom of Hole 12.0 ft.	
15							

Notes: 1.) Samples obtained using 3 ft. long by 3 in. OD sampler. Sheet No 1 of 1

Figure A-16. 3 in. (76 mm) O.D. Split-Spoon Log, 4-SE PMT-2 (Outside), Hickling Station

FIELD BORING LOG

BUFFALO DRILLING COMPANY, INC.
955 Niagara Street
Buffalo, New York 14213

Client Cornell University
Project In-Situ Testing Program
File No. 86-142 Boring No. 84-NE PMT-1

Driller Darryl Altrogge
Type of Drill Rig CME-55
Sampling Method ASTM D1586
Size and Type of Bit 3-3/4 inch ID augers

Surface Elevation
Datum
Location Hickling Generating Station Site
Date Started 8/10/86 Completed 8/10/86

Overburden Samples: Disturbed 3 Undist.
Total Depth of Hole 8.2 ft.
Depth Drilled into Rock 0 ft.

Top of Rock Elevation
Bottom of Hole Elevation
Ground Water Depth no water at completion

Depth (ft.)	Blows per .5 ft.		Sample No.	N	% Rec (RQD)	SOIL AND ROCK DESCRIPTION	REMARKS
1	4	6					
	6	9	S-1	15	60	Brown, med. dense, SAND and Gravel	S-1: 0-3'
	7	7					
	6	8					
5	7	5	S-2	12	60	same as S-1	S-2: 3-6'
	8	7					
	5	8					
	8	7	S-3	15	55	same as S-1	S-3: 6-8.2'
	30/2"					Bottom of Hole 8.2 ft.	
10							

Notes: 1.) Samples obtained using 3 ft. long by 3 in. OD split-spoon samplers.

Sheet No 1 of 1

Figure A-17. 3 in. (76 mm) O.D. Split-Spoon Log, 84-NE PMT-1 (Inside), Hickling Station

FIELD BORING LOG

BUFFALO DRILLING COMPANY, INC.
955 Niagara Street
Buffalo, New York 14213

Client Cornell University
Project In-Situ Testing Program
File No. 86-142 Boring No. 84-NE PMT-2

Driller Darryl Altrogge
Type of Drill Rig CME-55
Sampling Method ASTM D1586
Size and Type of Bit 3-3/4 inch ID augers

Surface Elevation
Datum
Location Hickling Generating Station Site
Date Started 8/10/86 Completed 8/10/86

Overburden Samples: Disturbed 5 Undist.
Total Depth of Hole 14.0 ft.
Depth Drilled into Rock 0 ft.

Top of Rock Elevation
Bottom of Hole Elevation
Ground Water Depth no water at completion

Depth (ft.)	Blows per .5 ft.		Sample No.	N	% Rec (RQD)	SOIL AND ROCK DESCRIPTION	REMARKS
1	7	11					
	11	13	S-1	24	80	Brown, med. dense, SAND and Gravel, dry	S-1: 0-3'
	13	12					
	20	12					
5	13	15	S-2	28	55	same as S-1	S-2: 3-6'
	13	17					
	16	12					
	10	10	S-3	20	25	same as S-1	S-3: 6-9'
	8	8					
	12	8					
10	10	9	S-4	19	55	same as S-1	S-4: 9-12'
	9	11					
	22	20	S-5	42		...grade: dense	S-5: 12-14'
	25	21					
15						Bottom of Hole 14.0 ft.	

Notes: 1.) Samples S-1 through S-4 obtained using 3 ft. long by 3 in. OD split-spoon sampler.

Sheet No 1 of 1

Figure A-18. 3 in. (76 mm) O.D. Split-Spoon Log, 84-NE PMT-2 (Outside), Hickling Station

FIELD BORING LOG

BUFFALO DRILLING COMPANY, INC.
955 Niagara Street
Buffalo, New York 14213

Client Cornell University
Project In-Situ Testing Program
File No. 86-142 Boring No. 84-SW PMT-1

Driller Darryl Altrogge
Type of Drill Rig CME-55
Sampling Method ASTM D1586
Size and Type of Bit 3-3/4 in. ID augers

Surface Elevation
Datum
Location Hickling Generating Station Site
Date Started 8/11/86 Completed 8/11/86

Overburden Samples: Disturbed 3 Undist.
Total Depth of Hole 8.0 ft.
Depth Drilled into Rock 0 ft.

Top of Rock Elevation
Bottom of Hole Elevation
Ground Water Depth no water at completion

Depth (ft.)	Blows per .5 ft.		Sample No.	N	% Rec (RQD)	SOIL AND ROCK DESCRIPTION	REMARKS
1	5	6					
	6	8	S-1	14	70	Brown, med. dense, SAND and Gravel, dry	S-1: 0-3'
	11	9					
	11	11					
5	10	12	S-2	22	65	same as S-1	S-2: 3-6'
	14	18					
	8	6	S-3	17	80	same as S-1	S-3: 6-8'
	11	6					
						Bottom of Hole 8.0 ft.	
10							

Notes: 1.) Samples S-1 and S-2 obtained using 3 ft. long by 3 in. OD split-spoon sampler.

Sheet No 1 of 1

Figure A-19. 3 in. (76 mm) O.D. Split-Spoon Log, 84-SW PMT-1 (Inside), Hickling Station

FIELD BORING LOG

BUFFALO DRILLING COMPANY, INC.
955 Niagara Street
Buffalo, New York 14213

Client Cornell University
Project In-Situ Testing Program
File No. 86-142 Boring No. 84-SW PMT-2

Driller Darryl Altrogge
Type of Drill Rig CME-55
Sampling Method ASTM D1586
Size and Type of Bit 3-3/4 inch ID augers

Surface Elevation
Datum
Location Hickling Generating Station Site
Date Started 8/11/86 Completed 8/11/86

Overburden Samples: Disturbed 5 Undist.
Total Depth of Hole 14.0 ft.
Depth Drilled into Rock 0 ft.

Top of Rock Elevation
Bottom of Hole Elevation
Ground Water Depth no water at completion

Depth (ft.)	Blows per .5 ft.		Sample No.	N	% Rec (RQD)	SOIL AND ROCK DESCRIPTION	REMARKS
1	3	9					
	10	15	S-1	25	90	Brown, med. dense, SAND and Gravel	S-1: 0-3'
	16	14					
	12	13					
5	13	12	S-2	25	55	same as S-1	S-2: 3-6'
	12	11					
	15	9					
	8	8	S-3	16	60	same as S-1	S-3: 6-9'
	10	7					
	12	16					
10	24	23	S-4	47	60	...grade: dense	S-4: 9-12'
	20	13					
	28	37	S-5	70	55	...grade: v. dense	S-5: 12-14'
	33	30					
15						Bottom of Hole 14.0 ft.	

Notes: 1.) Samples S-1 through S-4 obtained using 3 ft. long by 3 in. OD split-spoon sampler.

Sheet No 1 of 1

Figure A-20. 3 in. (76 mm) O.D. Split-Spoon Log, 84-SW PMT-2 (Outside), Hickling Station

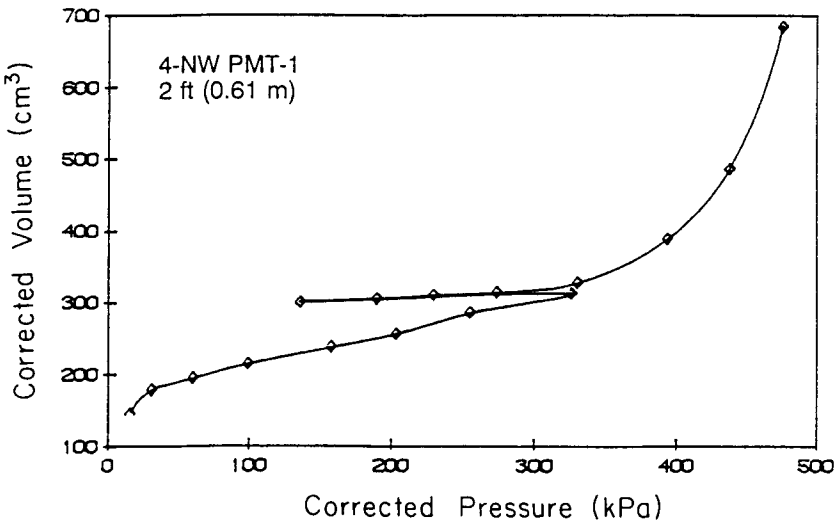

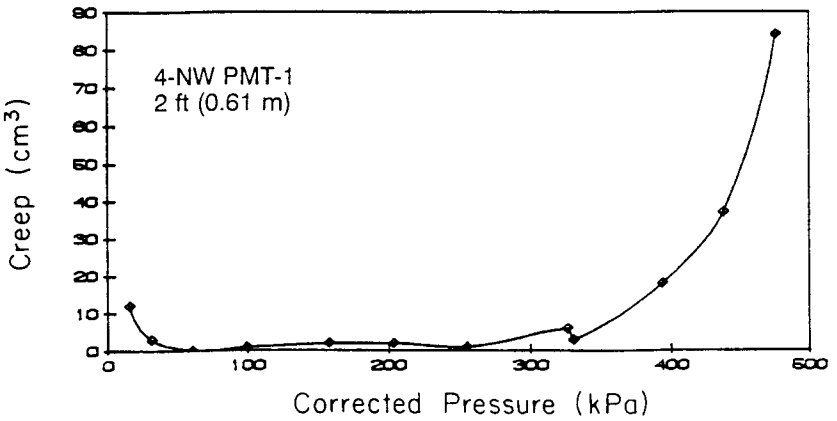

Figure A-21. Corrected Pressure-Volume and Creep Curves, 4-NW PMT-1 (Inside), Hickling Station

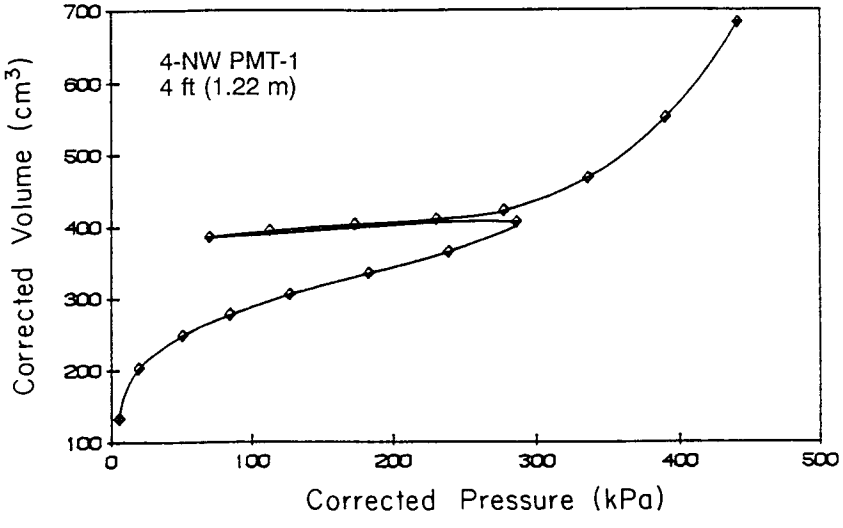

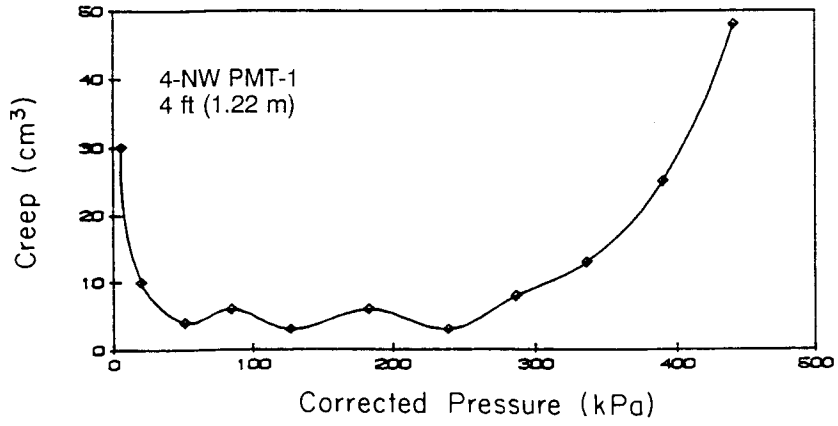

Figure A-22. Corrected Pressure-Volume and Creep Curves, 4-NW PMT-1 (Inside), Hickling Station

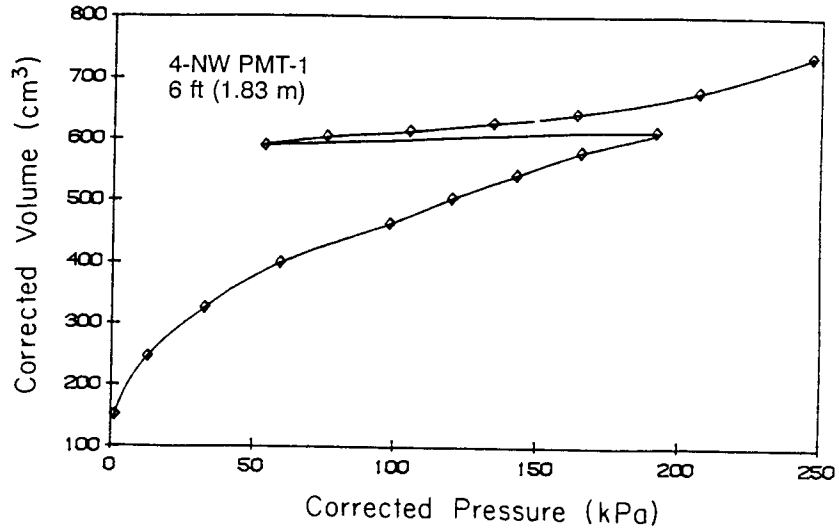

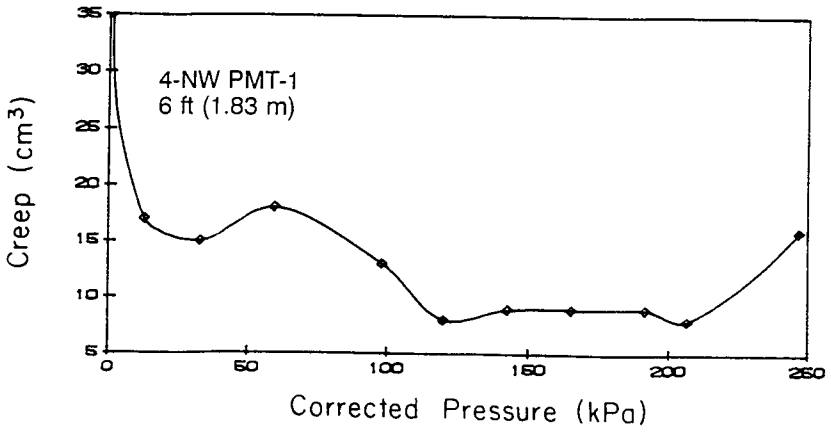

Figure A-23. Corrected Pressure-Volume and Creep Curves, 4-NW PMT-1 (Inside), Hickling Station

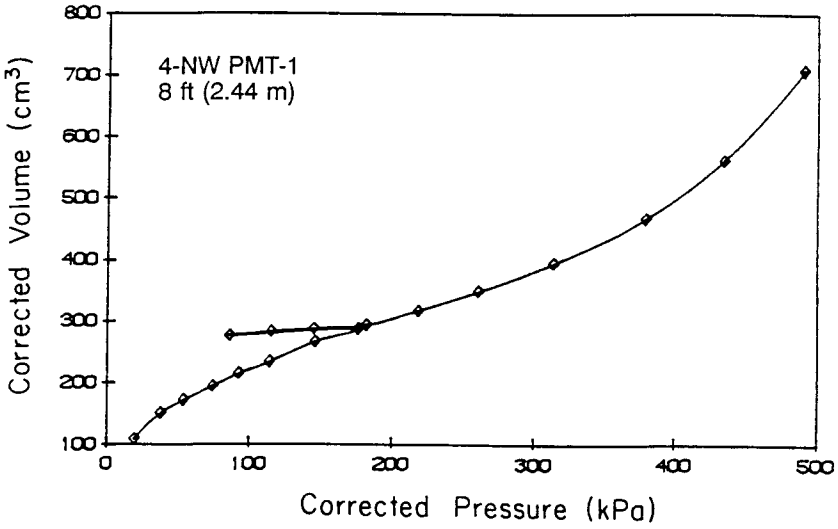

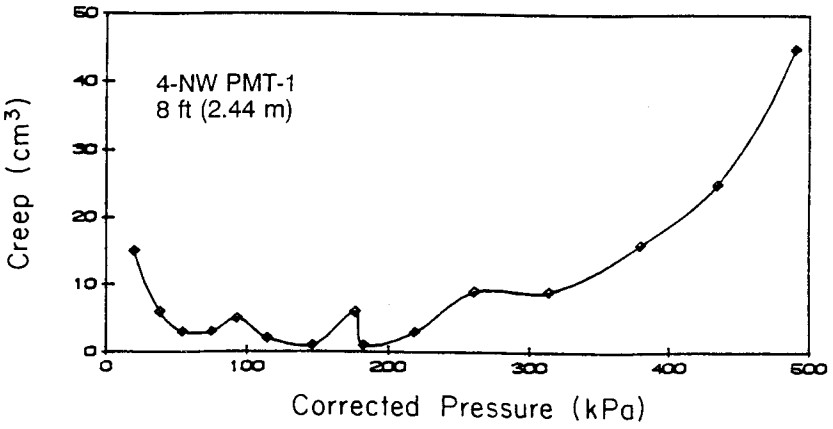

Figure A-24. Corrected Pressure-Volume and Creep Curves, 4-NW PMT-1 (Inside), Hickling Station

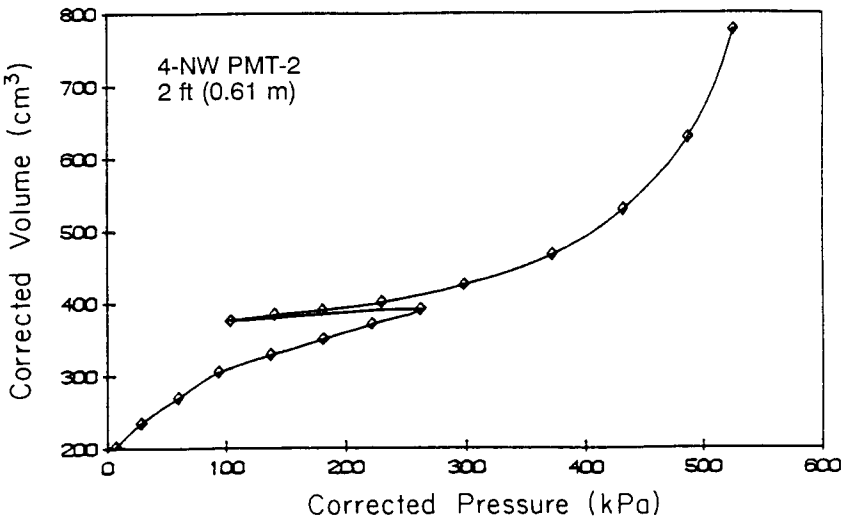

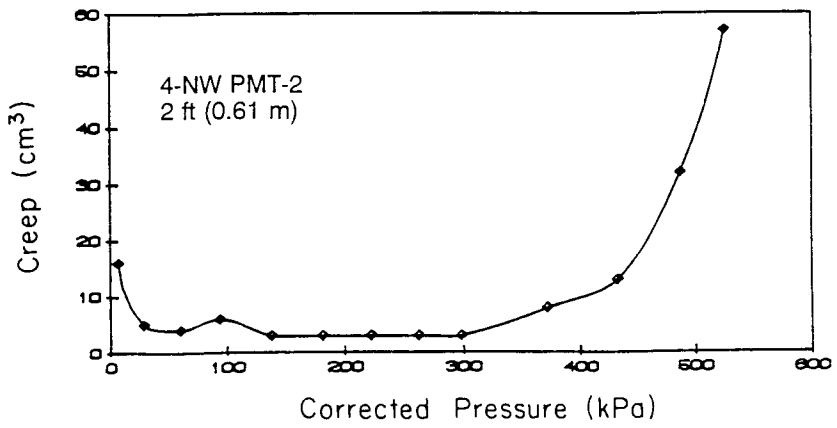

Figure A-25. Corrected Pressure-Volume and Creep Curves, 4-NW PMT-2 (Outside), Hickling Station

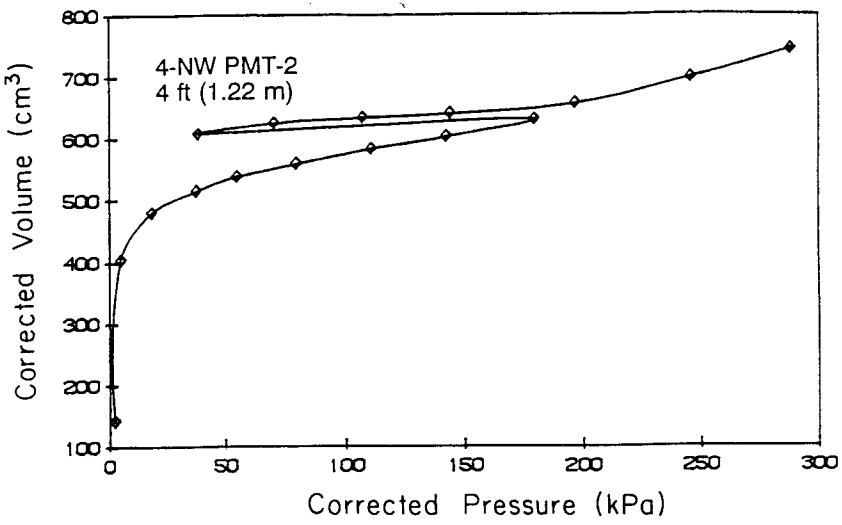

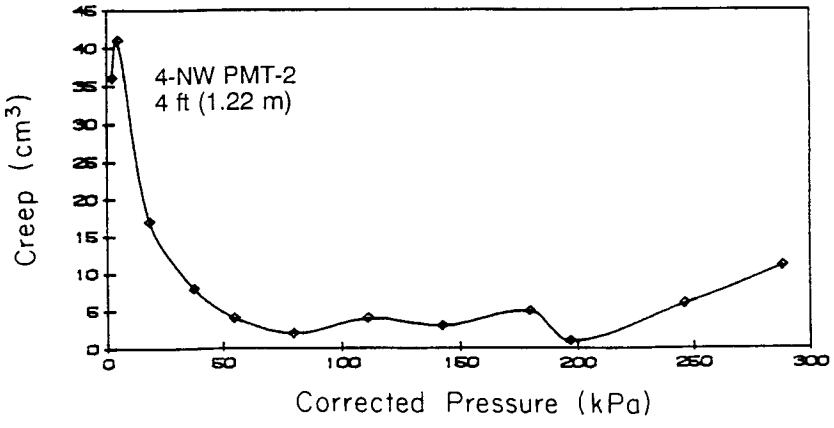

Figure A-26. Corrected Pressure-Volume and Creep Curves, 4-NW PMT-2 (Outside), Hickling Station

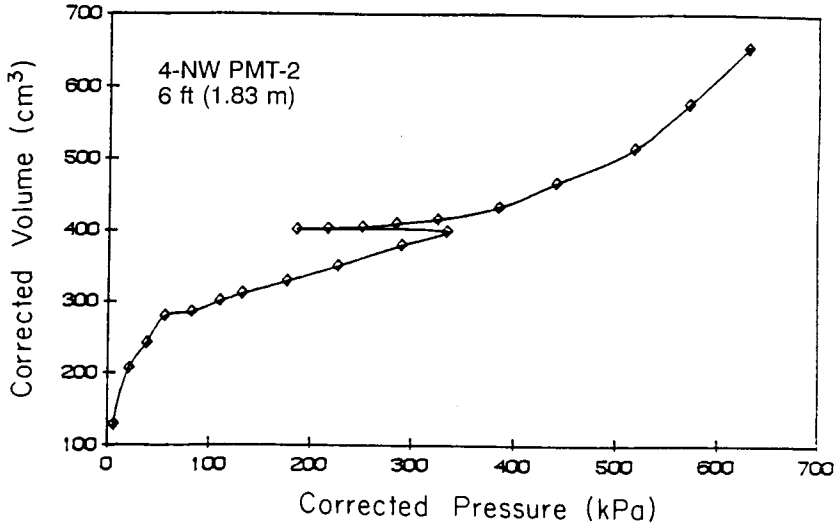

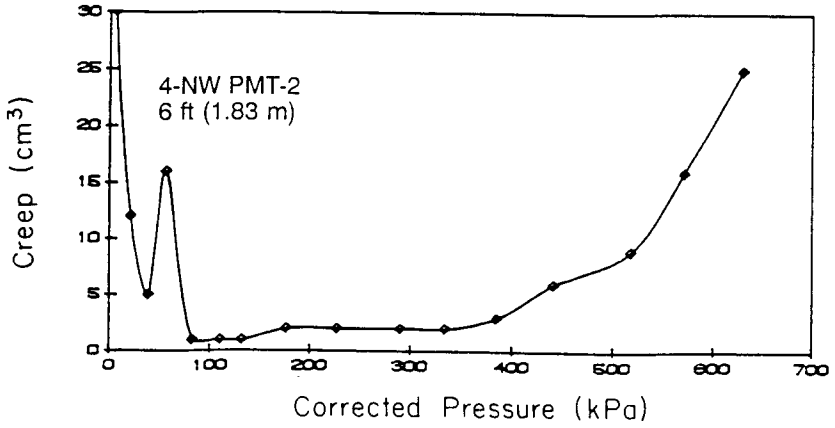

Figure A-27. Corrected Pressure-Volume and Creep Curves, 4-NW PMT-2 (Outside), Hickling Station

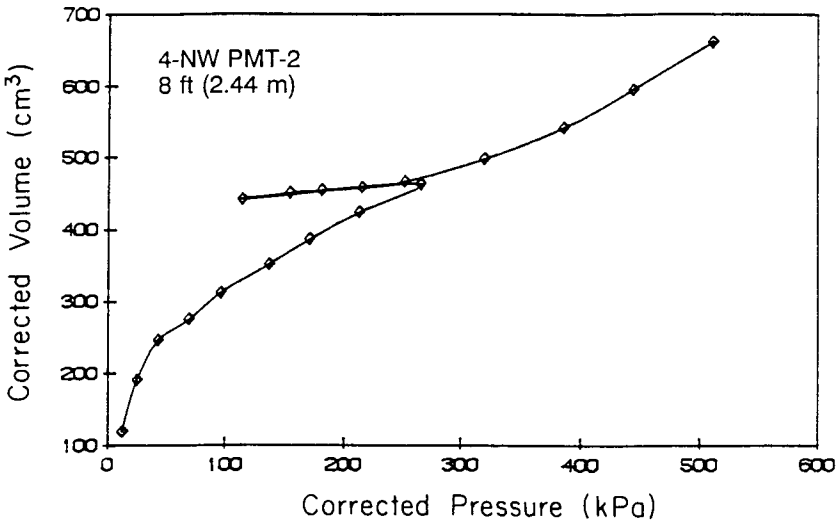

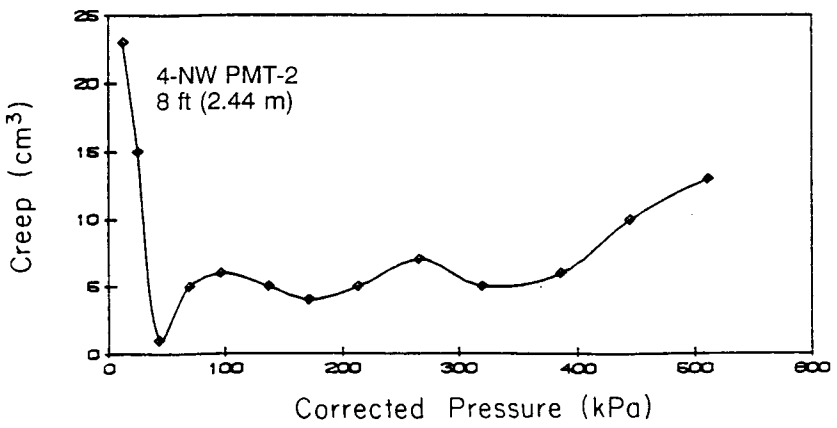

Figure A-28. Corrected Pressure-Volume and Creep Curves, 4-NW PMT-2 (Outside), Hickling Station

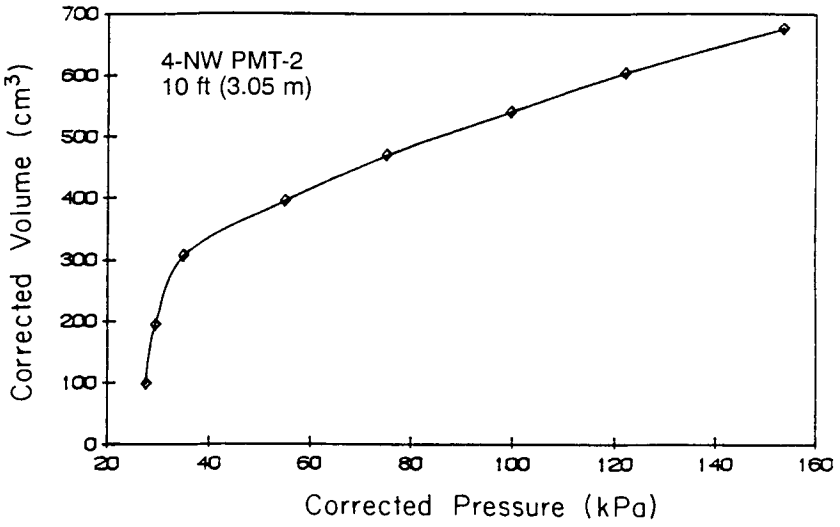

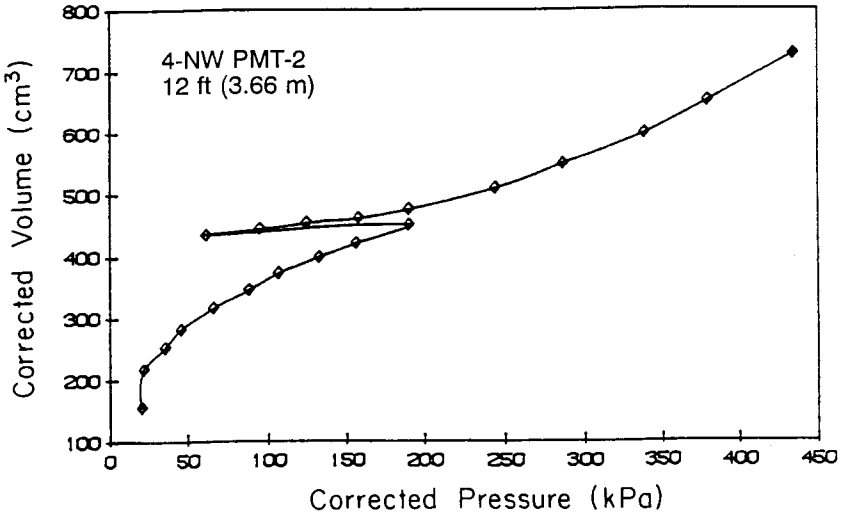

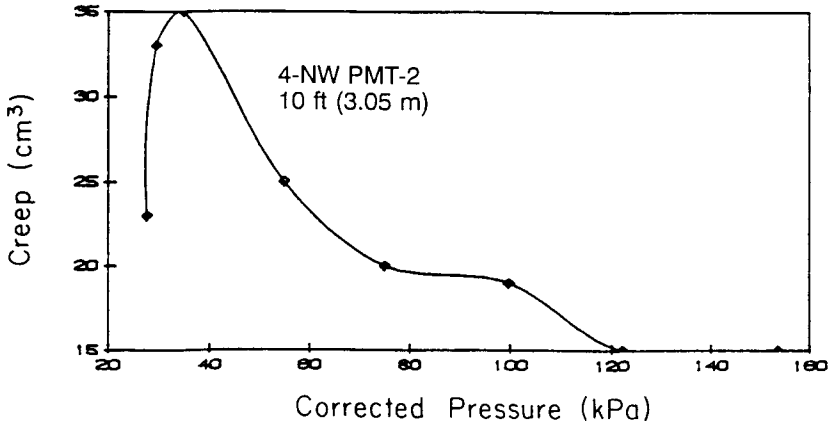

Figure A-29. Corrected Pressure-Volume and Creep Curves, 4-NW PMT-2 (Outside), Hickling Station

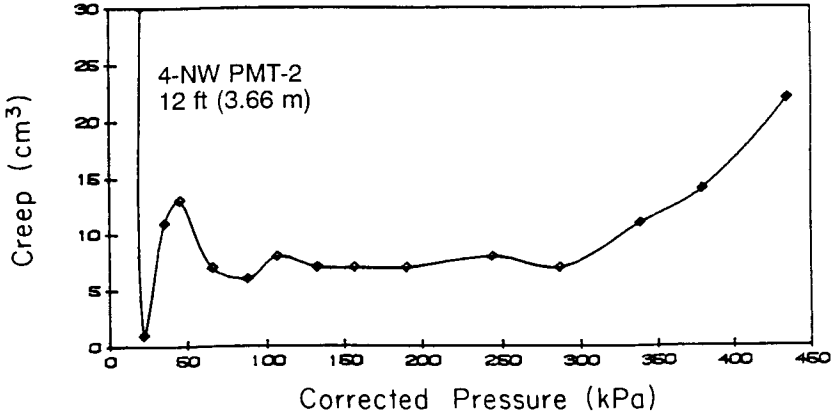

Figure A-30. Corrected Pressure-Volume and Creep Curves, 4-NW PMT-2 (Outside), Hickling Station

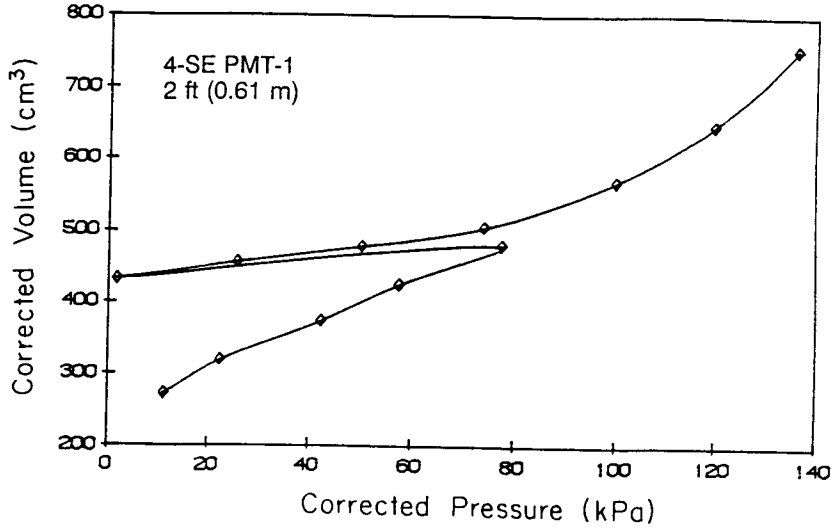

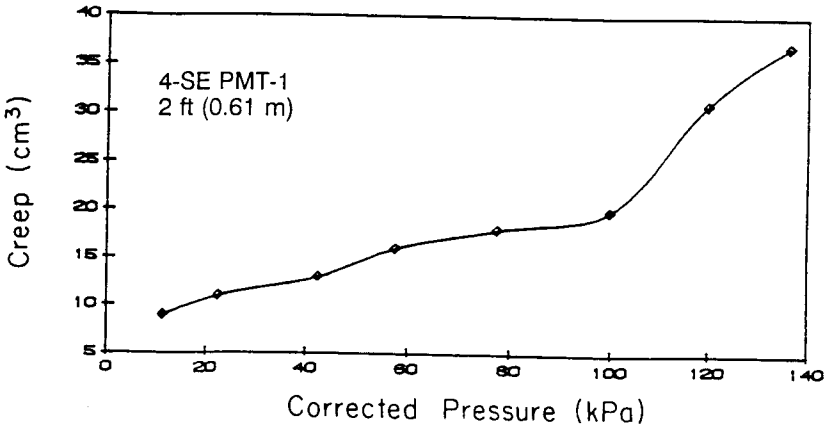

Figure A-31. Corrected Pressure-Volume and Creep Curves, 4-SE PMT-1 (Inside), Hickling Station

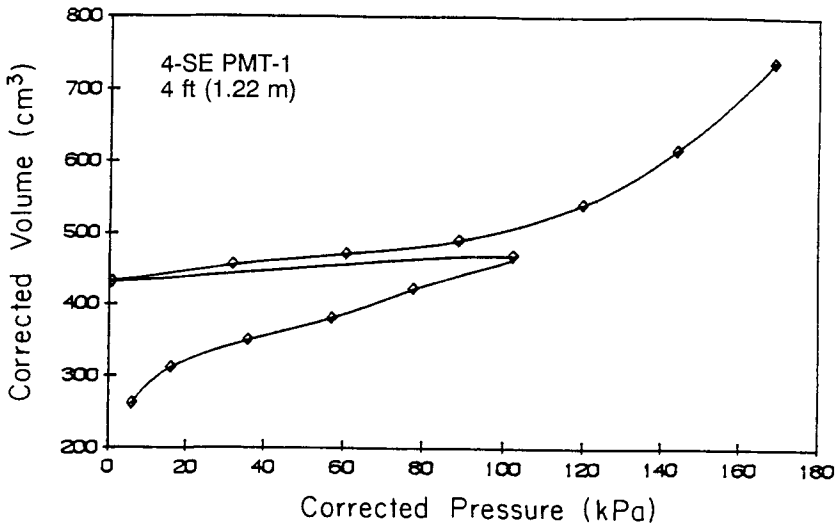

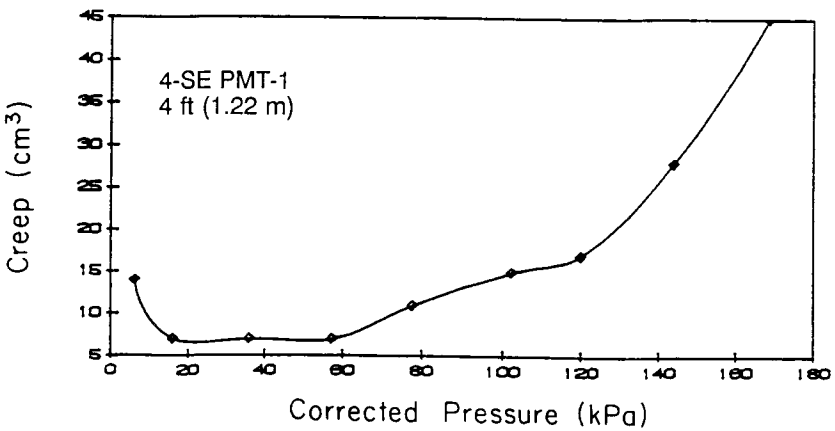

Figure A-32. Corrected Pressure-Volume and Creep Curves, 4-SE PMT-1 (Inside), Hickling Station

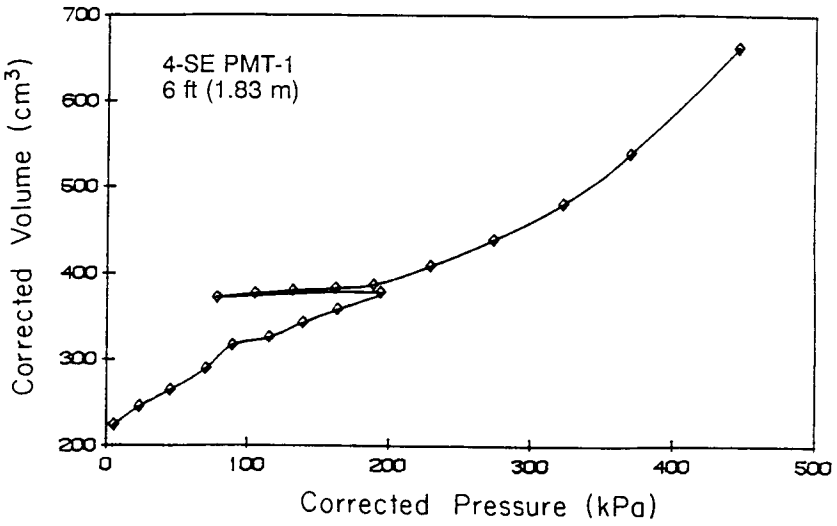

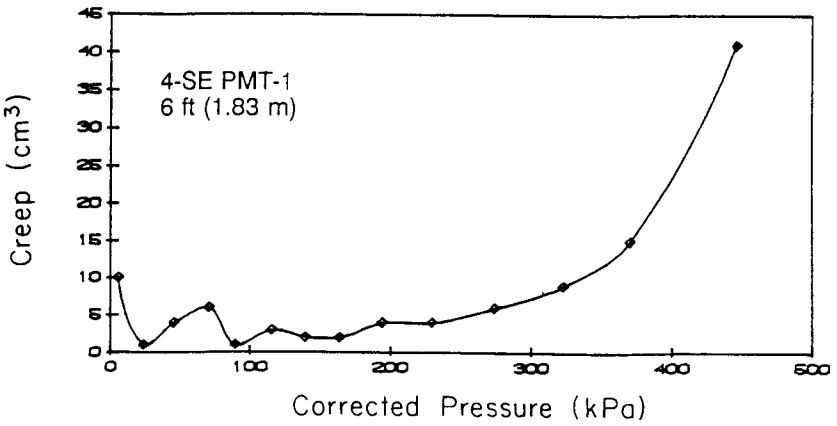

Figure A-33. Corrected Pressure-Volume and Creep Curves, 4-SE PMT-1 (Inside), Hickling Station

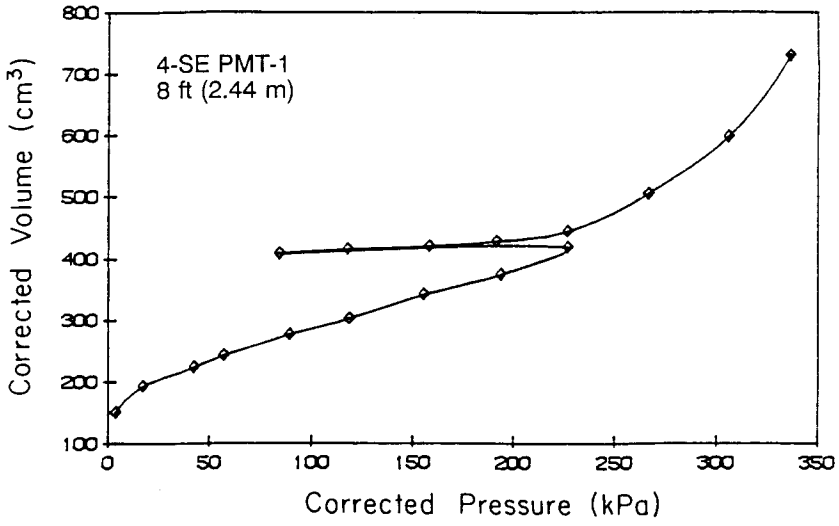

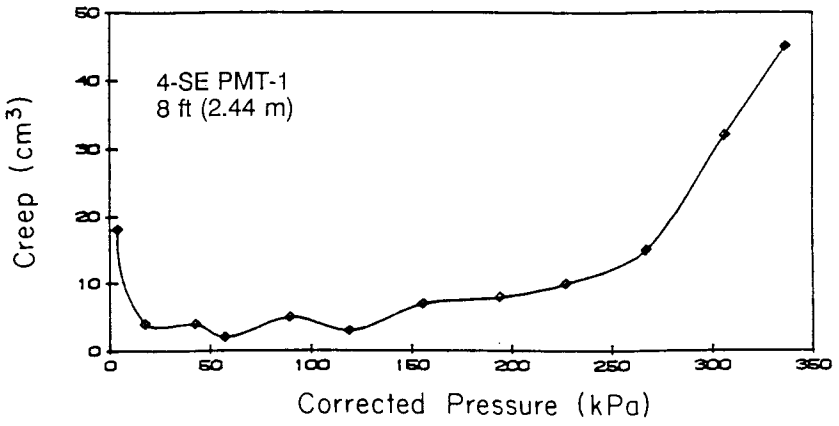

Figure A-34. Corrected Pressure-Volume and Creep Curves, 4-SE PMT-1 (Inside), Hickling Station

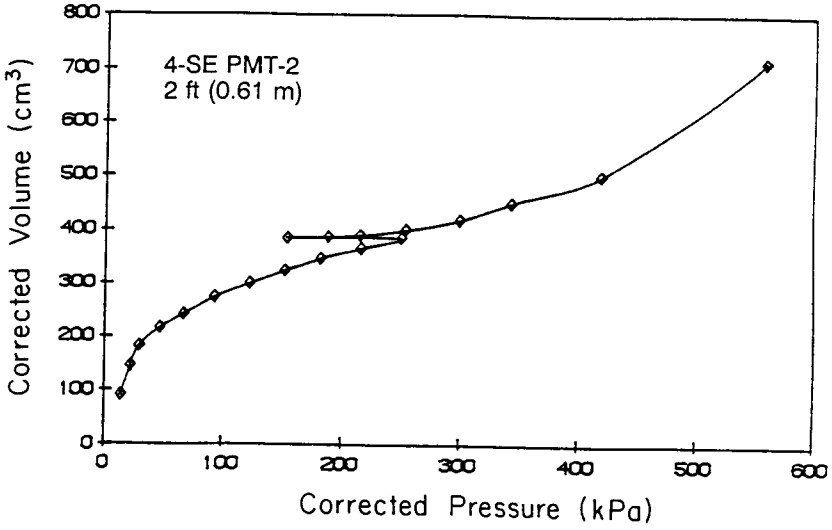

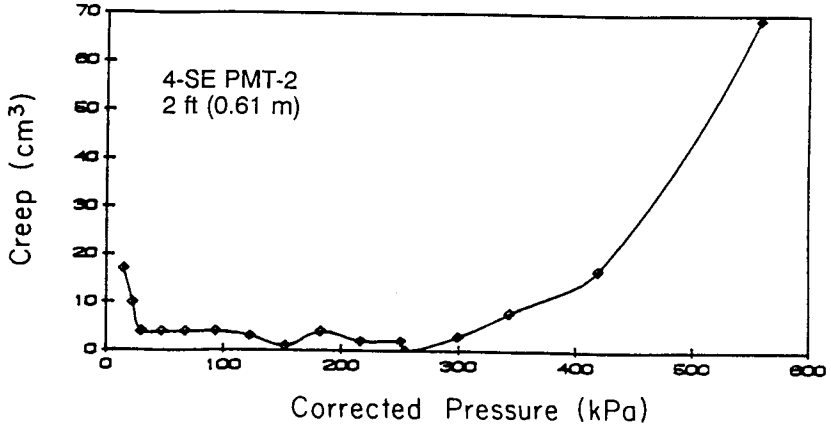

Figure A-35. Corrected Pressure-Volume and Creep Curves, 4-SE PMT-2 (Outside), Hickling Station

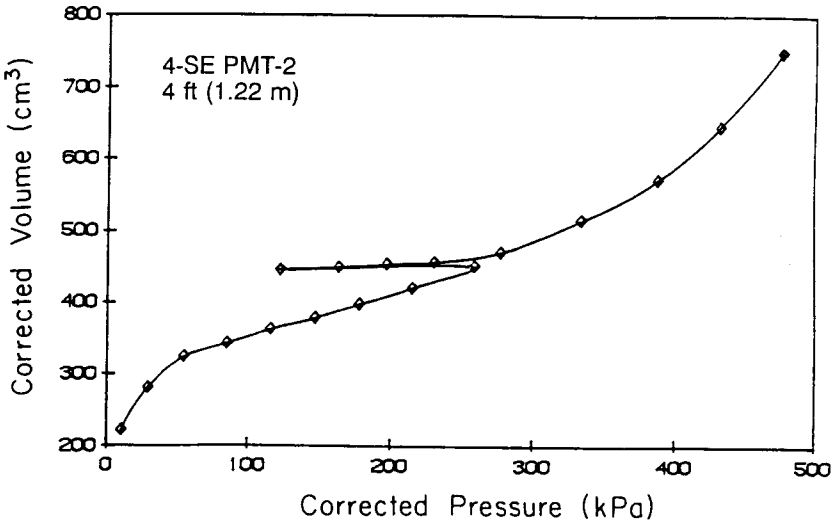

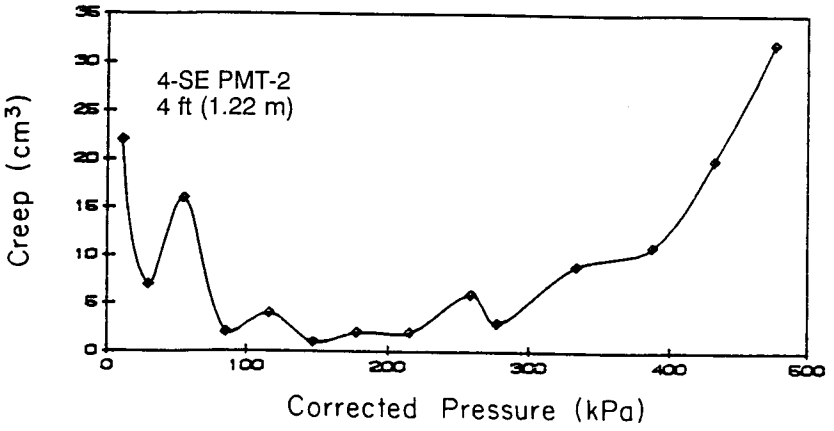

Figure A-36. Corrected Pressure-Volume and Creep Curves, 4-SE PMT-2 (Outside), Hickling Station

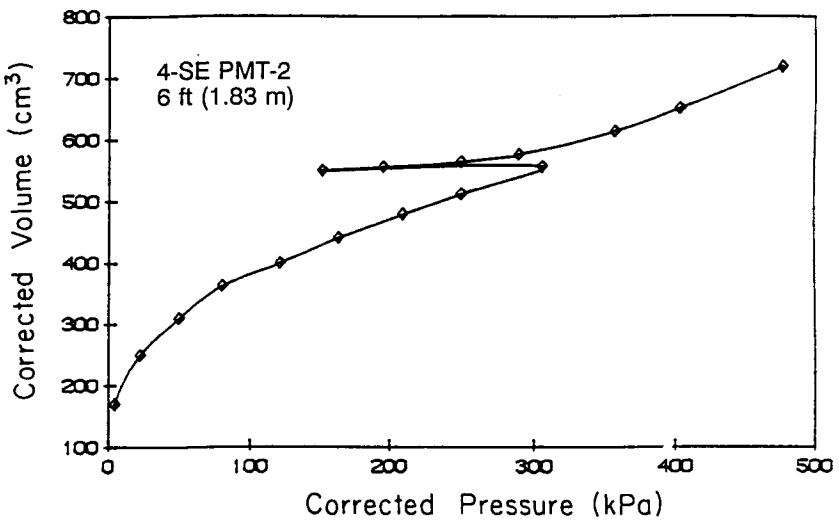

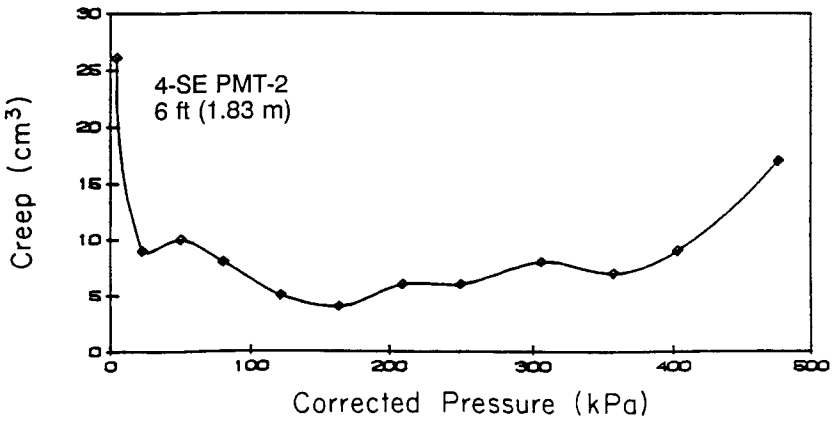

Figure A-37. Corrected Pressure-Volume and Creep Curves, 4-SE PMT-2 (Outside), Hickling Station

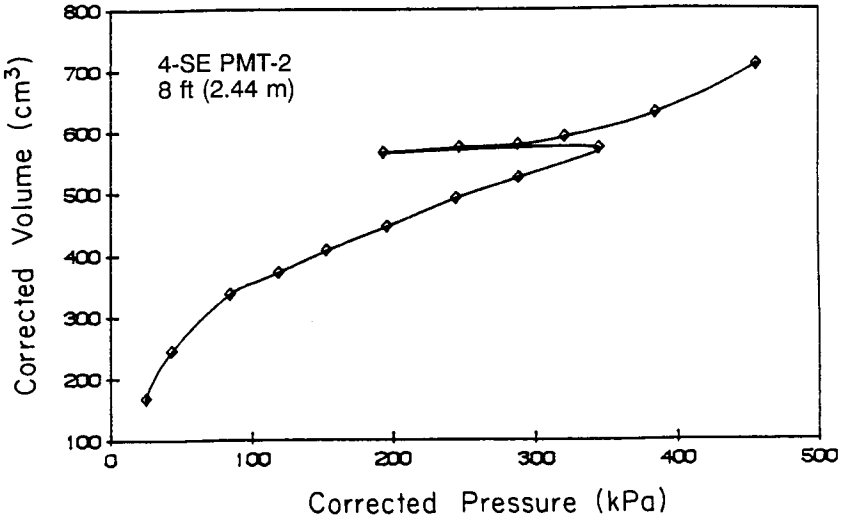

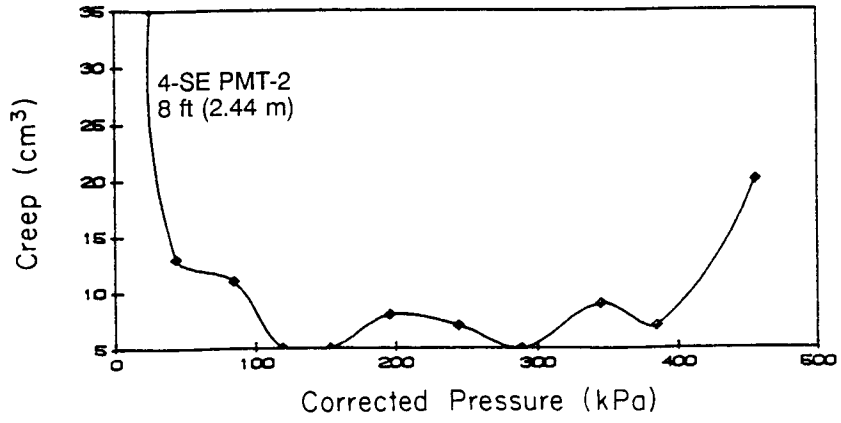

Figure A-38. Corrected Pressure-Volume and Creep Curves, 4-SE PMT-2 (Outside), Hickling Station

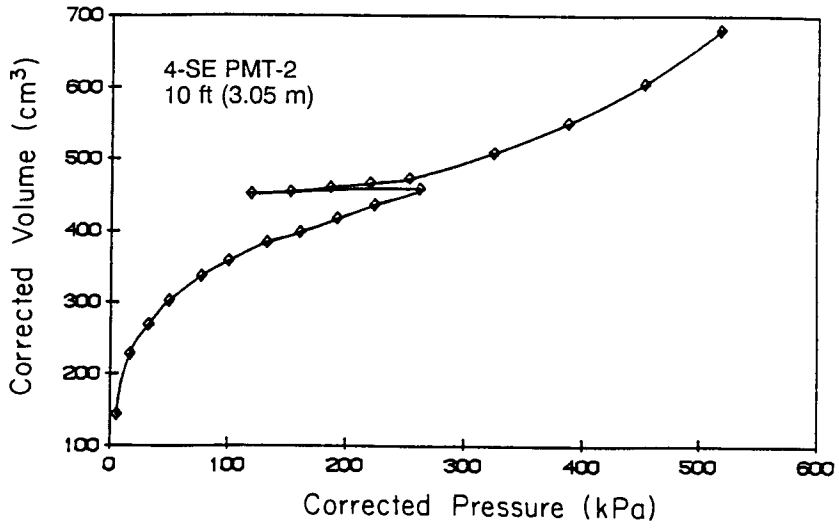

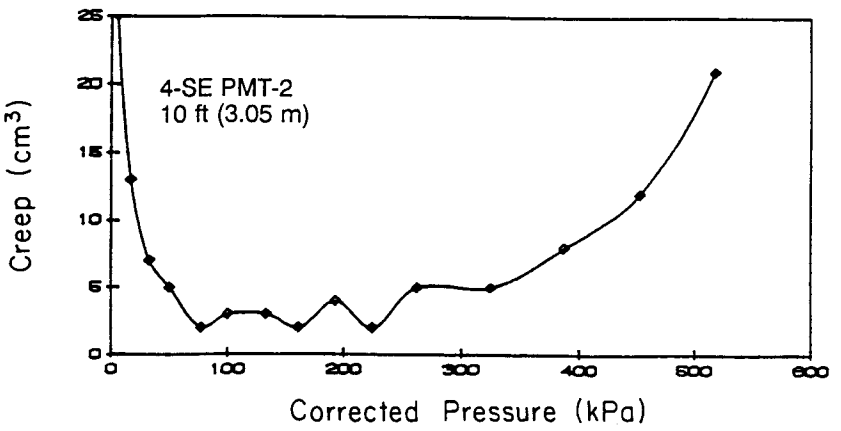

Figure A-39. Corrected Pressure-Volume and Creep Curves, 4-SE PMT-2 (Outside), Hickling Station

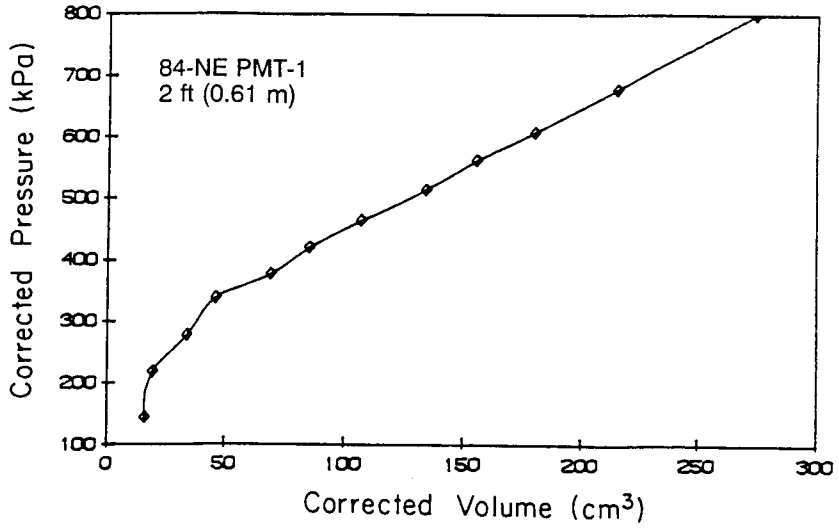

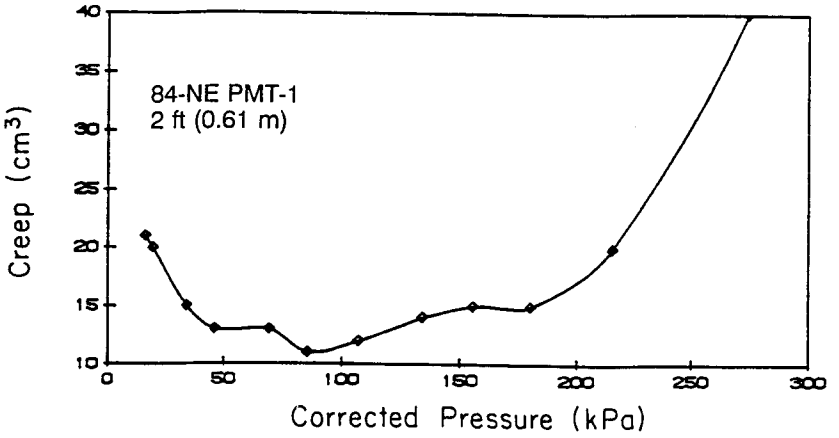

Figure A-40. Corrected Pressure-Volume and Creep Curves, 84-NE PMT-1 (Inside), Hickling Station

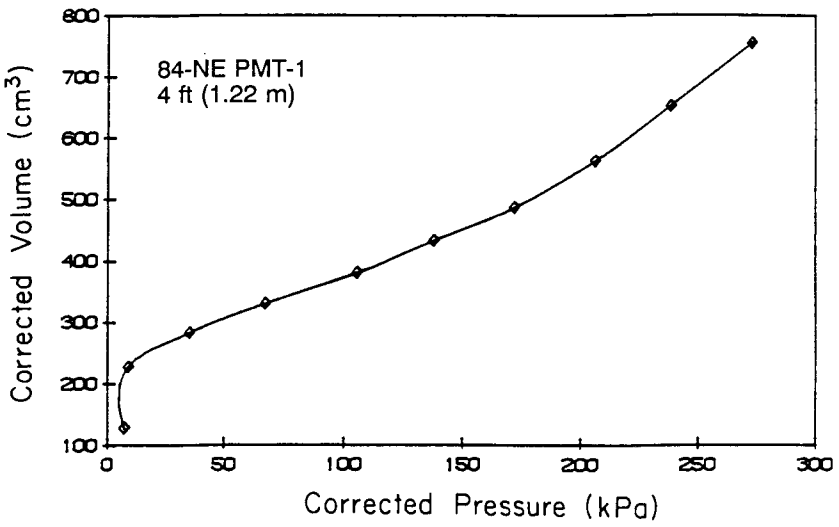

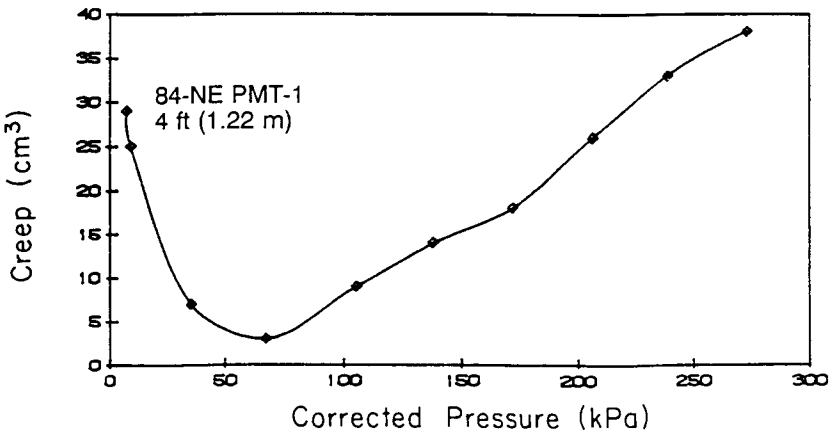

Figure A-41. Corrected Pressure-Volume and Creep Curves, 84-NE PMT-1 (Inside), Hickling Station

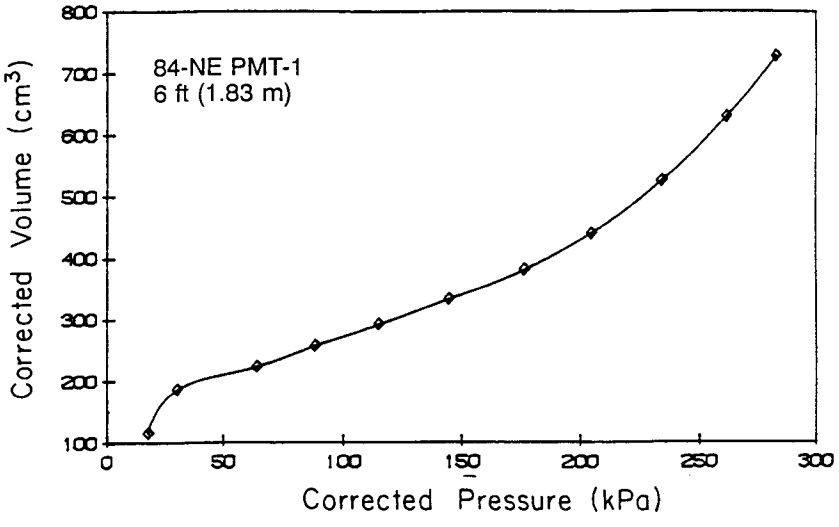

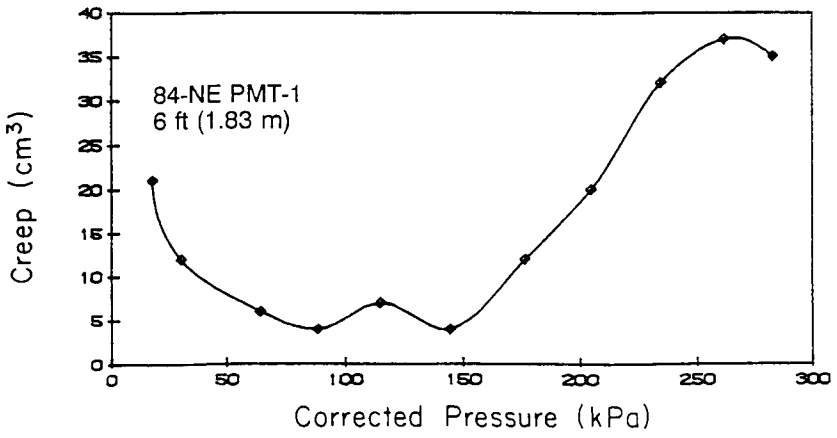

Figure A-42. Corrected Pressure-Volume and Creep Curves, 84-NE PMT-1 (Inside), Hickling Station

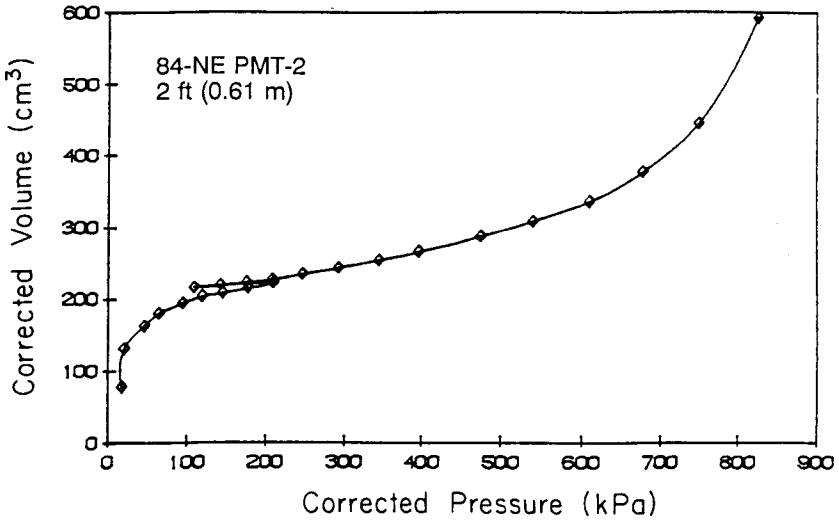

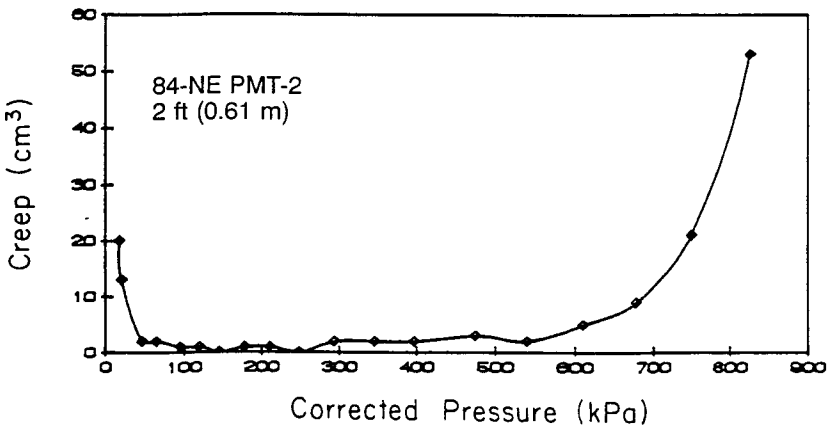

Figure A-43. Corrected Pressure-Volume and Creep Curves, 84-NE PMT-2 (Outside), Hickling Station

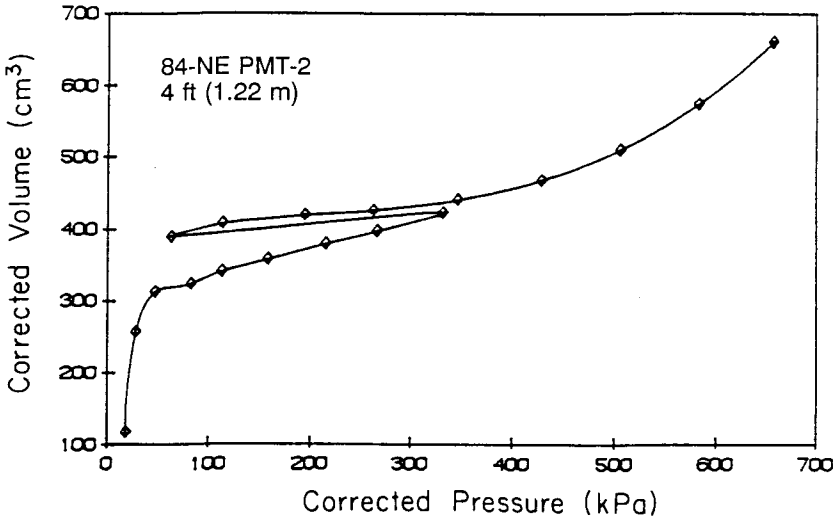

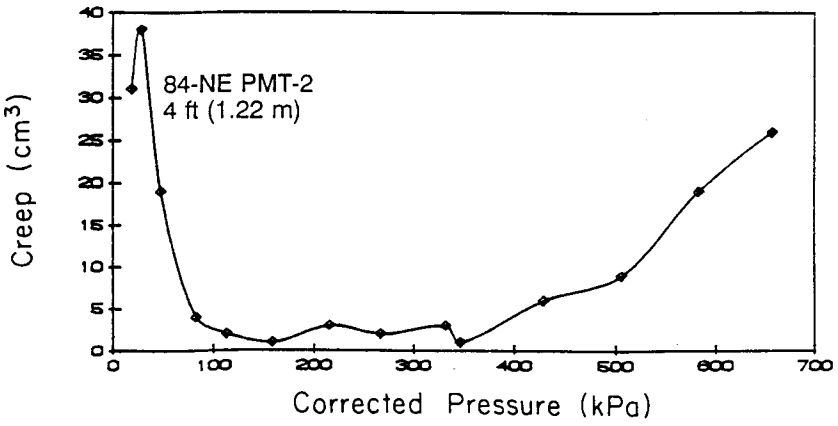

Figure A-44. Corrected Pressure-Volume and Creep Curves, 84-NE PMT-2 (Outside), Hickling Station

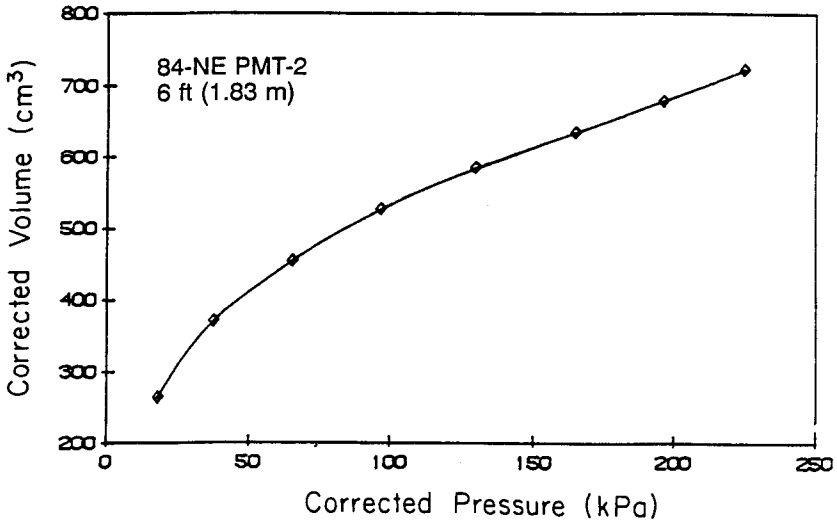

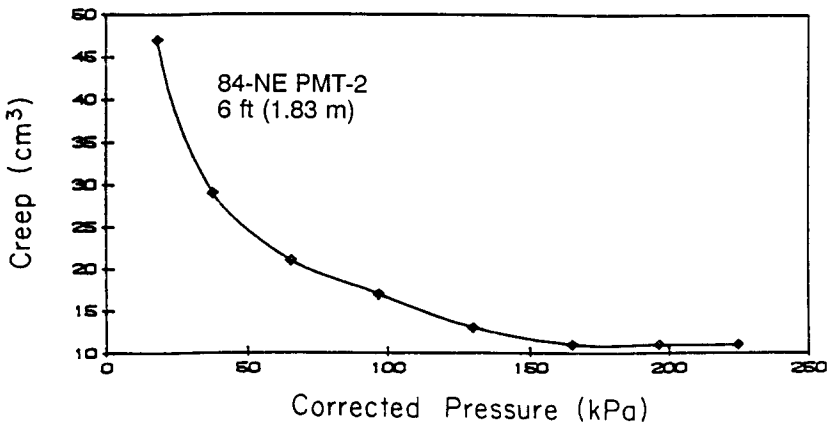

Figure A-45. Corrected Pressure-Volume and Creep Curves, 84-NE PMT-2 (Outside), Hickling Station

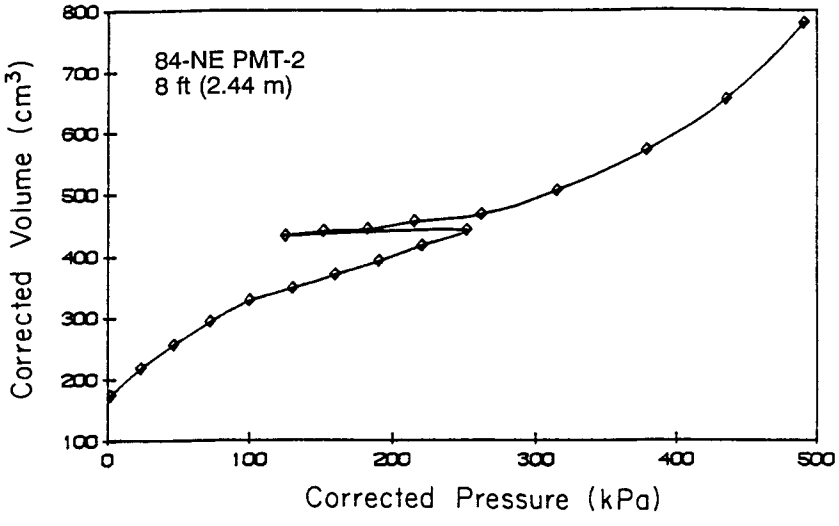

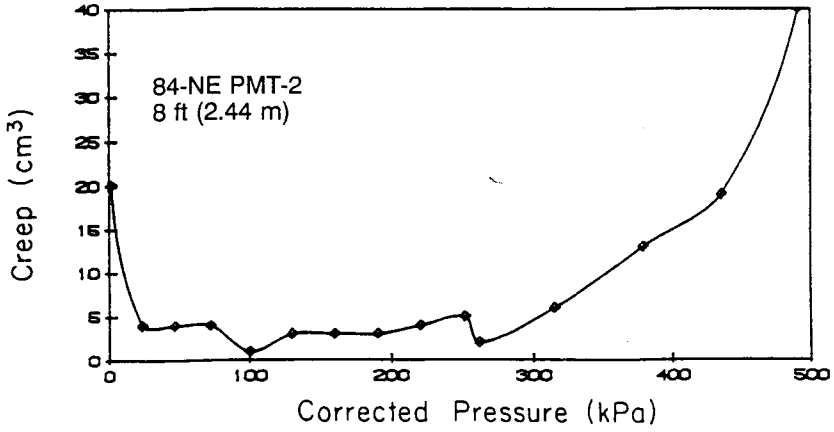

Figure A-46. Corrected Pressure-Volume and Creep Curves, 84-NE PMT-2 (Outside), Hickling Station

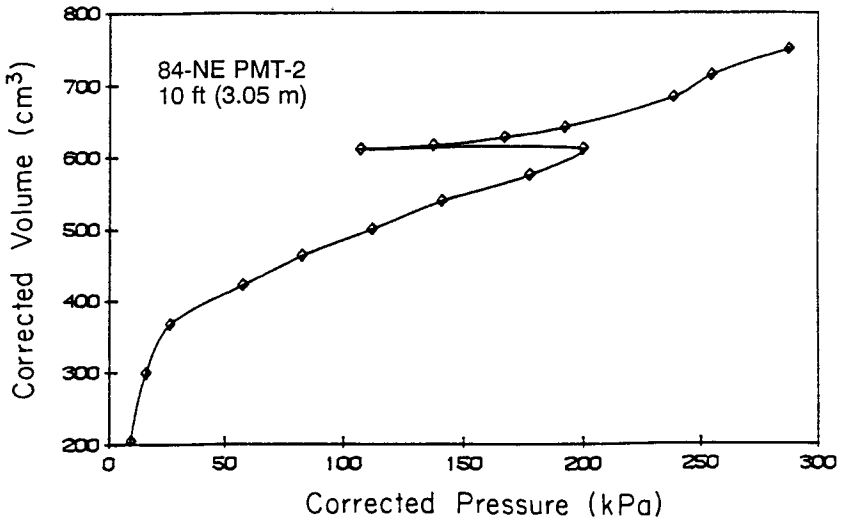

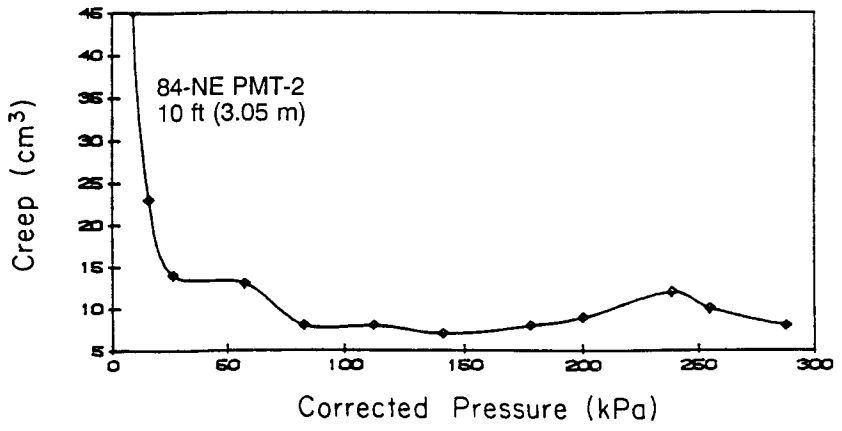

Figure A-47. Corrected Pressure-Volume and Creep Curves, 84-NE PMT-2 (Outside), Hickling Station

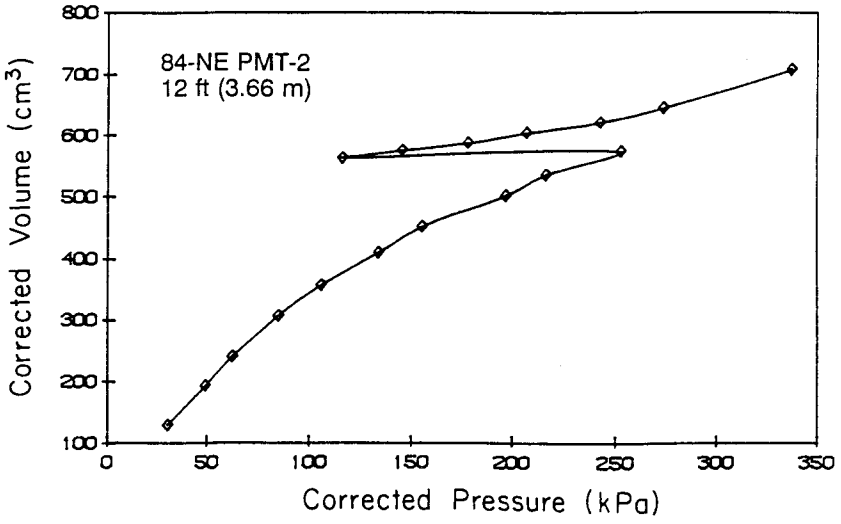

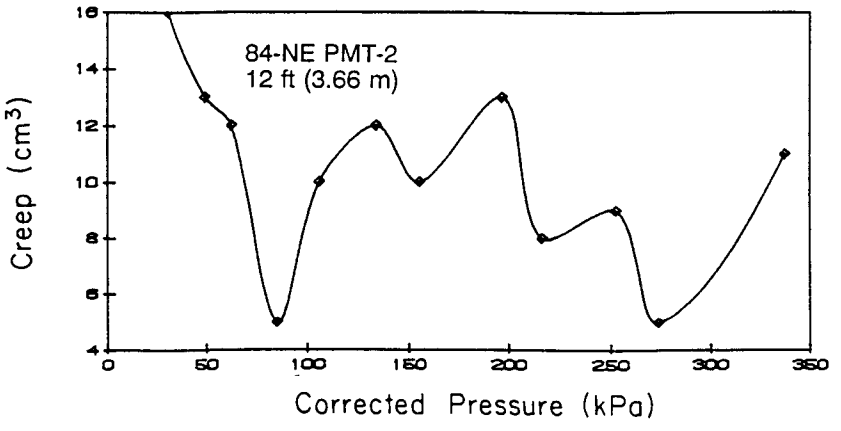

Figure A-48. Corrected Pressure-Volume and Creep Curves, 84-NE PMT-2 (Outside), Hickling Station

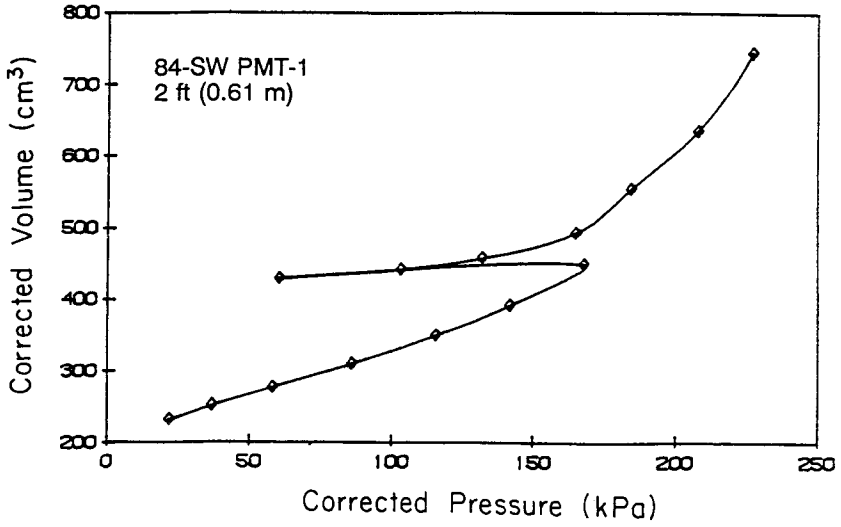

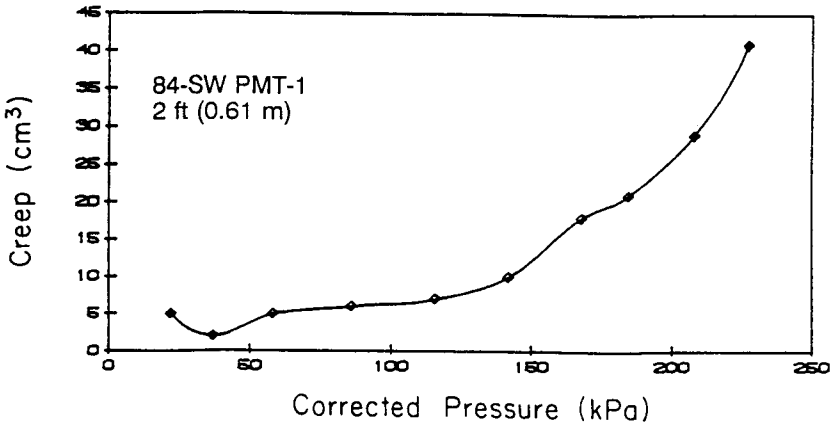

Figure A-49. Corrected Pressure-Volume and Creep Curves, 84-SW PMT-1 (Inside), Hickling Station

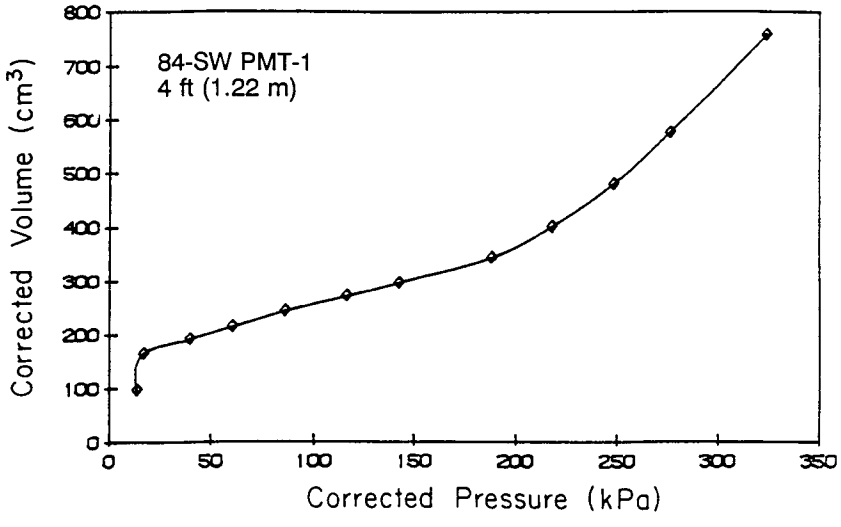

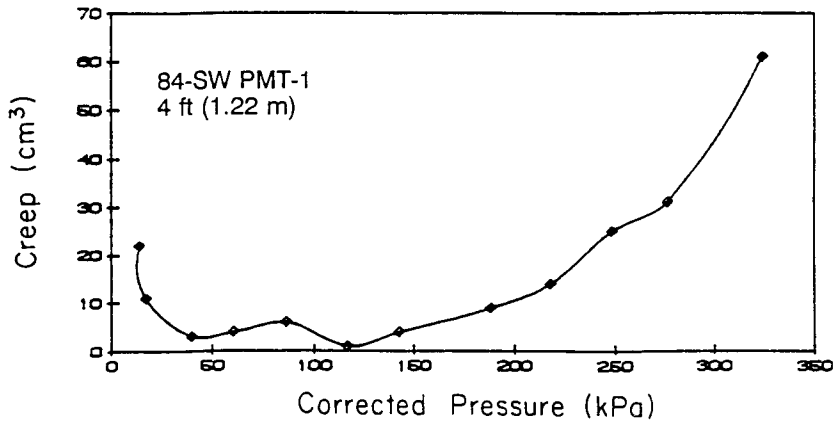

Figure A-50. Corrected Pressure-Volume and Creep Curves, 84-SW PMT-1 (Inside), Hickling Station

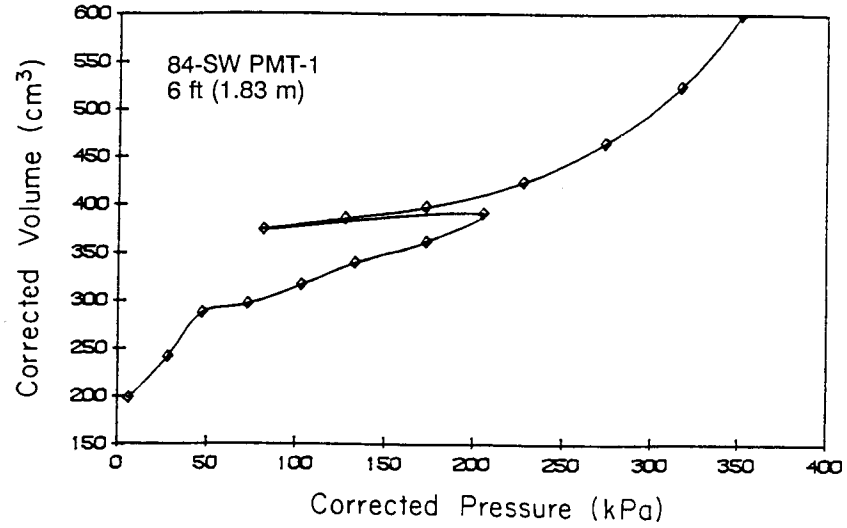

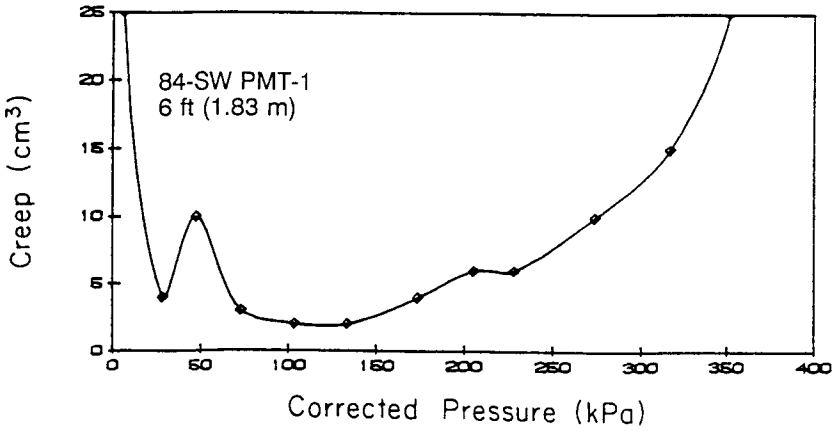

Figure A-51. Corrected Pressure-Volume and Creep Curves, 84-SW PMT-1 (Inside), Hickling Station

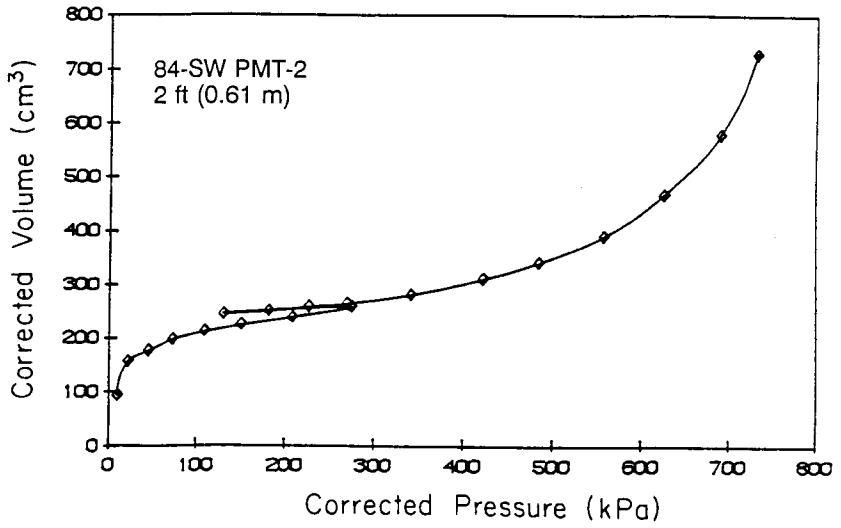

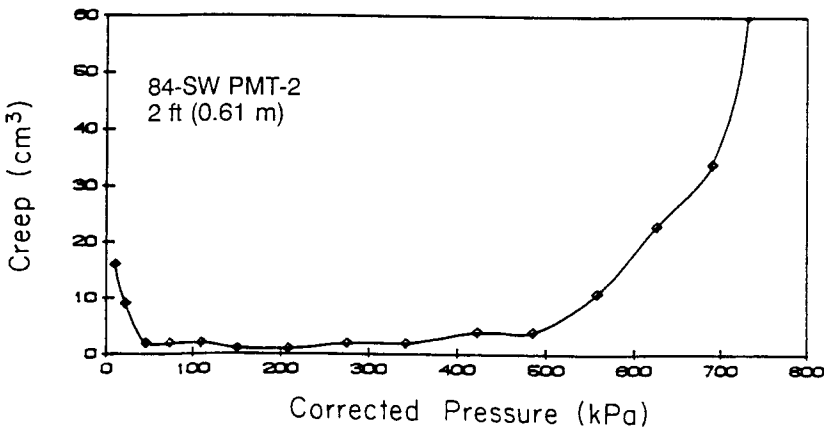

Figure A-52. Corrected Pressure-Volume and Creep Curves, 84-SW PMT-2 (Outside), Hickling Station

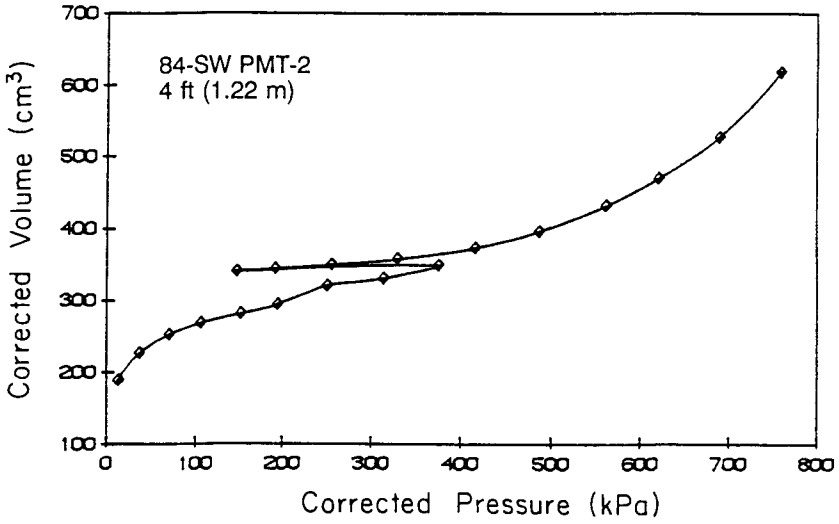

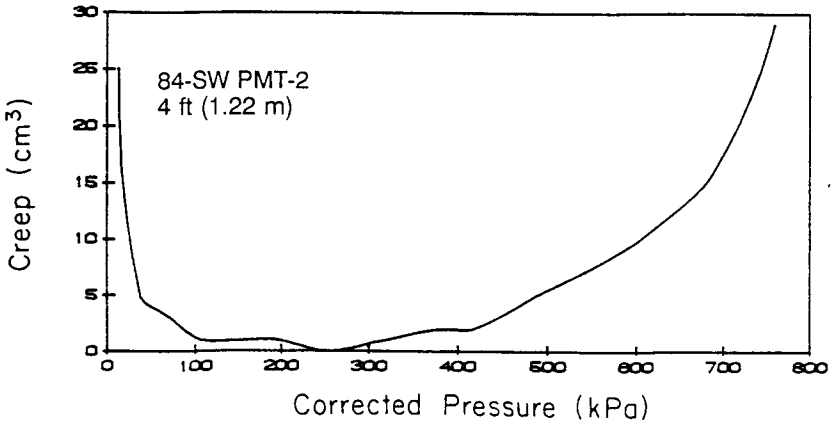

Figure A-53. Corrected Pressure-Volume and Creep Curves, 84-SW PMT-2 (Outside), Hickling Station

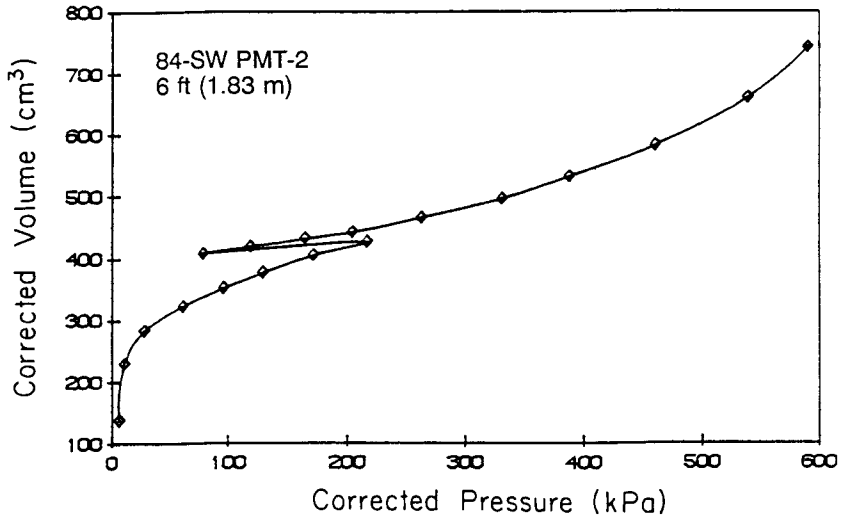

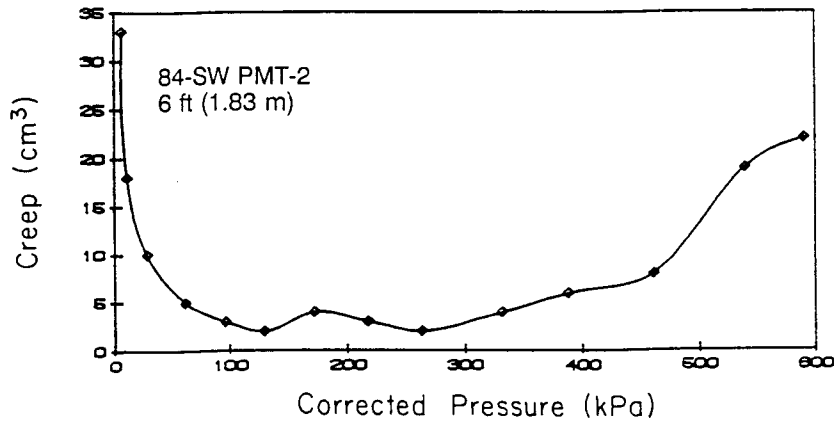

Figure A-54. Corrected Pressure-Volume and Creep Curves, 84-SW PMT-2 (Outside), Hickling Station

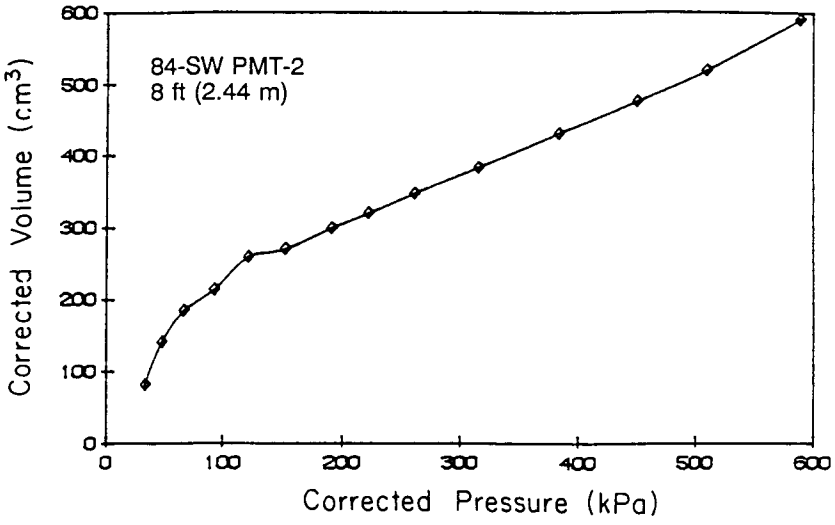

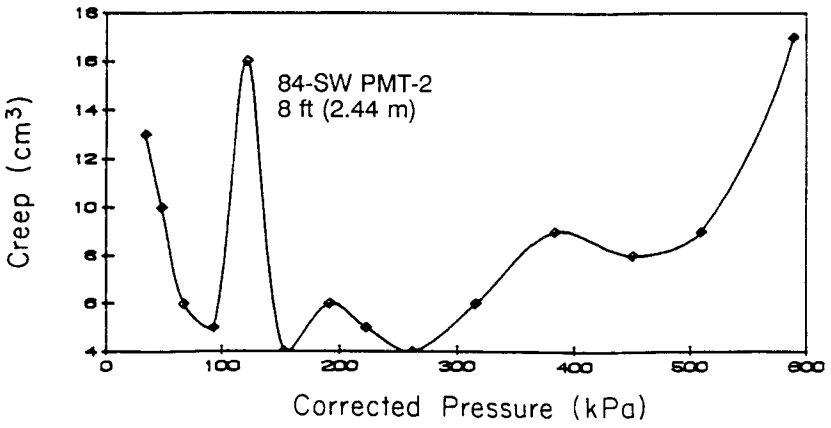

Figure A-55. Corrected Pressure-Volume and Creep Curves, 84-SW PMT-2 (Outside), Hickling Station

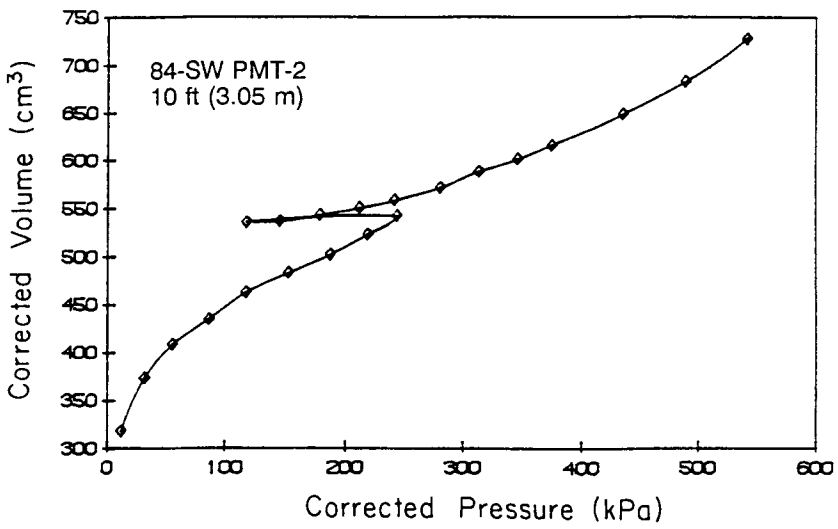

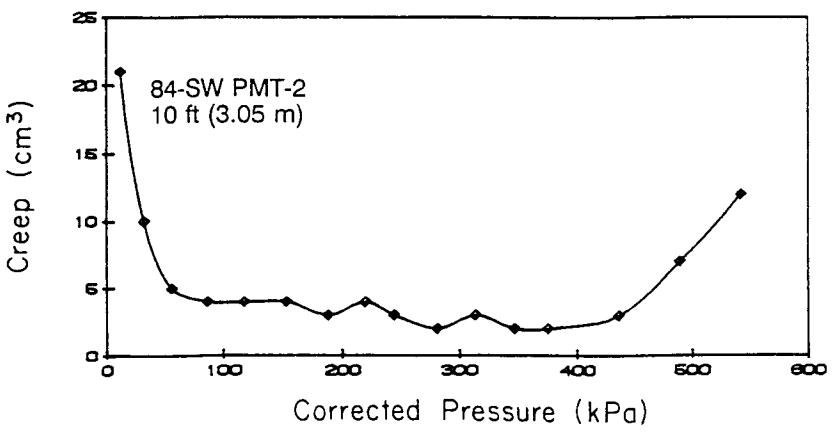

Figure A-56. Corrected Pressure-Volume and Creep Curves, 84-SW PMT-2 (Outside), Hickling Station

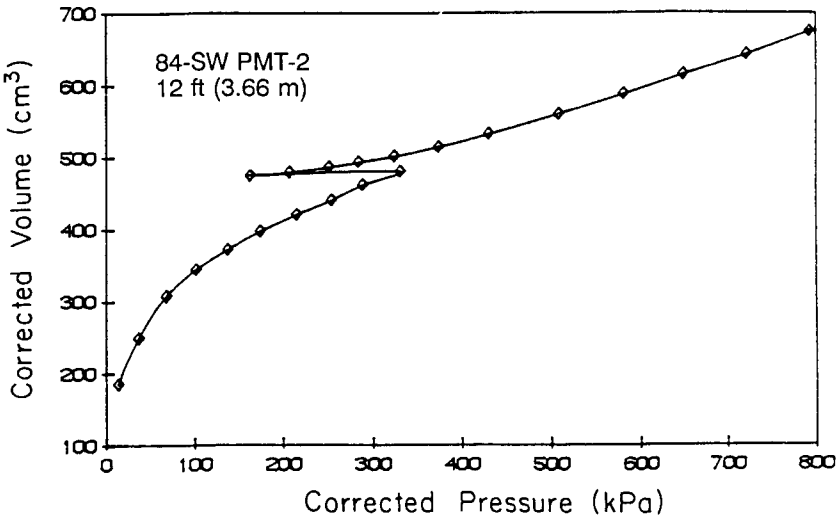

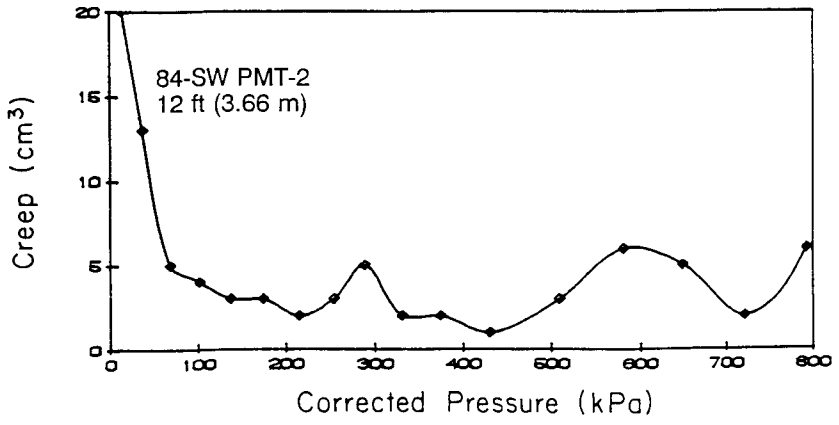

Figure A-57. Corrected Pressure-Volume and Creep Curves, 84-SW PMT-2 (Outside), Hickling Station

FIELD BORING LOG

BUFFALO DRILLING COMPANY, INC.
955 Niagara Street
Buffalo, New York 14213

Client Cornell University
Project In-Situ Testing Program
File No. 86-142 Boring No. X2-NE SPT-1

Driller Keith Danser
Type of Drill Rig CME-55
Sampling Method ASTM D1586
Size and Type of Bit 3-3/4 inch ID augers

Surface Elevation
Datum
Location Wyncoop Creek Site
Date Started 8/13/86 Completed 8/13/86

Overburden Samples: Disturbed 3 Undist.
Total Depth of Hole 6.0 ft.
Depth Drilled into Rock 0 ft.

Top of Rock Elevation
Bottom of Hole Elevation
Ground Water Depth no water at completion

Depth (ft.)	Blows per .5 ft.		Sample No.	N	% Rec (RQD)	SOIL AND ROCK DESCRIPTION	REMARKS
						Topsoil	
1	4	5	S-1	15	10	Brown, med. dense, SAND and Gravel, dry	S-1: 0-2'
	10	11					
	10	13	S-2	29	10	same as S-1	S-2: 2-4'
	16	28					
5	12	21	S-3	38	60	...grade: dense	S-3: 4-6'
	17	33					
						Bottom of Hole 6.0 ft.	
10							

Notes:

Sheet No 1 of 1

Figure A-58. SPT Log, Boring X2-NE SPT-1 (Inside), Wyncoop Creek

FIELD BORING LOG

BUFFALO DRILLING COMPANY, INC.
955 Niagara Street
Buffalo, New York 14213

Client Cornell University
Project In-Situ Testing Program
File No. 86-142 Boring No. X2-NE SPT-2

Driller Keith Danser
Type of Drill Rig CME-55
Sampling Method ASTM D1586
Size and Type of Bit 3-3/4 inch ID augers

Surface Elevation
Datum
Location Wyncoop Creek Site
Date Started 8/13/86 Completed 8/13/86

Overburden Samples: Disturbed 3 Undist.
Total Depth of Hole 5.7 ft.
Depth Drilled into Rock 0 ft.

Top of Rock Elevation
Bottom of Hole Elevation
Ground Water Depth no water at completion

Depth (ft.)	Blows per .5 ft.		Sample No.	N	% Rec (RQD)	SOIL AND ROCK DESCRIPTION	REMARKS
						Topsoil	
1	2	9	S-1	16	25	Brown, med. dense, SAND and Gravel, dry	S-1: 0-2'
	7	5					
	4	7	S-2	11	25	same as S-1	S-2: 2-4'
	4	6					
5	4	14	S-3	28		same as S-1	S-3: 4-6'
	14	31/2"				Bottom of Hole 5.7 ft.	
10							

Notes:

Sheet No 1 of 1

Figure A-59. SPT Log, Boring X2-NE SPT-2 (Outside), Wyncoop Creek

FIELD BORING LOG

BUFFALO DRILLING COMPANY, INC.
955 Niagara Street
Buffalo, New York 14213

Client: Cornell University
Project: In-Situ Testing Program
File No.: 86-142 Boring No.: X2-SW SPT-1

Driller: Keith Danser
Type of Drill Rig: CME-55
Sampling Method: ASTM D1586
Size and Type of Bit: 3-3/4 inch ID augers

Surface Elevation:
Datum:
Location: Wyncoop Creek Site
Date Started: 8/13/86 Completed: 8/13/86

Overburden Samples: Disturbed: 4 Undist.:
Total Depth of Hole: 7.2 ft.
Depth Drilled into Rock: 0 ft.

Top of Rock Elevation:
Bottom of Hole Elevation:
Ground Water Depth: no water at completion

Depth (ft.)	Blows per .5 ft.		Sample No.	N	% Rec (RQD)	SOIL AND ROCK DESCRIPTION	REMARKS
1	6	5	S-1	12	25	Brown, med. dense, SAND and Gravel, dry	S-1: 0-2'
	7	9					
	8	11	S-2	25	10	same as S-1	S-2: 2-4'
	14	14					
5	8	16	S-3	36	50	...grade: dense	S-3: 4-6'
	20	14					
	19	29	S-4	100+	10	...grade: v. dense	S-4: 6-8'
	40/2"					Bottom of Hole 7.2 ft.	
10							

Notes:

Sheet No 1 of 1

Figure A-60. SPT Log, Boring X2-SW SPT-1 (Outside), Wyncoop Creek

FIELD BORING LOG

BUFFALO DRILLING COMPANY, INC.
955 Niagara Street
Buffalo, New York 14213

Client: Cornell University
Project: In-Situ Testing Program
File No.: 86-142 Boring No.: X2-SW SPT-2

Driller: Keith Danser
Type of Drill Rig: CME-55
Sampling Method: ASTM D1586
Size and Type of Bit: 3-3/4 inch ID augers

Surface Elevation:
Datum:
Location: Wyncoop Creek Site
Date Started: 8/13/86 Completed: 8/13/86

Overburden Samples: Disturbed: 3 Undist.:
Total Depth of Hole: 6.0 ft.
Depth Drilled into Rock: 0 ft.

Top of Rock Elevation:
Bottom of Hole Elevation:
Ground Water Depth: no water at completion

Depth (ft.)	Blows per .5 ft.		Sample No.	N	% Rec (RQD)	SOIL AND ROCK DESCRIPTION	REMARKS
1	3	4	S-1	10	20	Brown, med. dense, SAND and Gravel, dry	S-1: 0-2'
	6	9					
	5	6	S-2	11	25	...grade: moist	S-2: 2-4'
	5	4					
5	6	5	S-3	12	10	same as S-2	S-3: 4-6'
	7	4					
						Bottom of Hole 6.0 ft.	
10							

Notes:

Sheet No 1 of 1

Figure A-61. SPT Log, Boring X2-SW SPT-2 (Inside), Wyncoop Creek

FIELD BORING LOG

BUFFALO DRILLING COMPANY, INC.
955 Niagara Street
Buffalo, New York 14213

Client Cornell University
Project In-Situ Testing Program
File No. 86-142 Boring No. X2-NE DCT-1

Driller Keith Danser
Type of Drill Rig CME-55
Sampling Method Drive Cone
Size and Type of Bit

Surface Elevation
Datum
Location Wyncoop Creek Site
Date Started 8/13/86 Completed 8/13/86

Overburden Samples: Disturbed Undist.
Total Depth of Hole 6.0 ft.
Depth Drilled into Rock 0 ft.

Top of Rock Elevation
Bottom of Hole Elevation
Ground Water Depth

Depth (ft.)	Blows per .5 ft.		Sample No.	N	% Rec (RQD)	SOIL AND ROCK DESCRIPTION	REMARKS
1	2	6					
	5	7					
	21	10					
	11	10					
5	7	10					
	8	11					
						Bottom of Hole 6.0 ft.	
10							

Notes: 1.) Blow counts obtained by drive cone method.

Sheet No 1 of 1

Figure A-62. DCT Log, Sounding X2-NE DCT-1 (Inside), Wyncoop Creek

FIELD BORING LOG

BUFFALO DRILLING COMPANY, INC.
955 Niagara Street
Buffalo, New York 14213

Client Cornell University
Project In-Situ Testing Program
File No. 86-142 Boring No. X2-SW DCT-1

Driller Keith Danser
Type of Drill Rig CME-55
Sampling Method Drive Cone
Size and Type of Bit

Surface Elevation
Datum
Location Wyncoop Creek Site
Date Started 8/13/86 Completed 8/13/86

Overburden Samples: Disturbed Undist.
Total Depth of Hole 6.0 ft.
Depth Drilled into Rock 0 ft.

Top of Rock Elevation
Bottom of Hole Elevation
Ground Water Depth

Depth (ft.)	Blows per .5 ft.		Sample No.	N	% Rec (RQD)	SOIL AND ROCK DESCRIPTION	REMARKS
1	2	5					
	5	5					
	3	4					
	4	4					
5	8	6					
	4	13					
						Bottom of Hole 6.0 ft.	
10							

Notes: 1.) Blow counts obtained by drive cone method.

Sheet No 1 of 1

Figure A-63. DCT Log, Sounding X2-SW DCT-1 (Inside), Wyncoop Creek

FIELD BORING LOG

BUFFALO DRILLING COMPANY, INC.
955 Niagara Street
Buffalo, New York 14213

Client Cornell University
Project In-Situ Testing Program
File No. 86-142 Boring No. X2-SW DCT-2

Driller Keith Danser
Type of Drill Rig CME-55
Sampling Method Drive Cone
Size and Type of Bit

Surface Elevation
Datum
Location Wyncoop Creek Site
Date Started 8/13/86 Completed 8/13/86

Overburden Samples: Disturbed Undist.
Total Depth of Hole 4.0 ft.
Depth Drilled into Rock 0 ft.

Top of Rock Elevation
Bottom of Hole Elevation
Ground Water Depth

Depth (ft.)	Blows per .5 ft.		Sample No.	N	% Rec (RQD)	SOIL AND ROCK DESCRIPTION	REMARKS
1	3	6					
	8	10					
	10	11					
	17	25					
5						Bottom of Hole 4.0 ft.	

Notes: 1.) Blow counts obtained by drive cone method.

Sheet No 1 of 1

Figure A-64. DCT Log, Sounding X2-SW DCT-2 (Outside), Wyncoop Creek

Appendix B

STUB LOAD-DISPLACEMENT DATA

This appendix contains the reduced load-displacement data from the eight uplift tests. Summary Tables B-1 through B-8 give the applied loads recorded by both the load cell and hydraulic gage, the vertical displacements obtained by optical survey and dial gage, and the elapsed times since the load was applied and the data were recorded, as well as the time of day.

Table B-1

HICKLING STATION GRILLAGE NO. 4-NW, REDUCED LOADING DATA

Load (kips)		Vertical Disp. (in.)			
Load Cell	Hydraulic Gage	Optical Level	Dial Gage	E.T.[a] (min)	Time of Day
0.0	0.0	0.00	0.000	-	11:05
17.8	18.1	0.04	0.048	10:00	11:15
36.8	35.8	0.12	0.141	10:00	11:29
51.5	49.7	0.25	0.289	10:00	12:00
34.6	32.0	0.24	0.310	10:00	12:20
18.1	16.2	0.18	0.211	10:00	12:37
0.0	0.0	0.07	0.101	10:00	12:52
25.5	22.3	0.14	0.178	10:00	14:17
51.9	48.8	0.32	0.328	10:00	14:32
68.8	66.9	0.72	0.830	10:00	14:49
85.7	83.7	1.54	1.625	14:00	15:07
102.6	101.3	2.88	2.939	14:00	15:28
68.0	63.2	2.87	2.898	10:00	15:46
34.1	28.8	2.58	2.592	10:00	16:00
0.0	0.0	1.14	1.385	10:00	16:15
51.7	48.3	2.32	2.385	10:00	16:36
102.1	99.7	3.84	3.922	10:00	16:56
119.3	118.1	5.86	5.898	14:00	17:20
111.6	112.0	6.16	-	30:00	18:02
121.3	-	8.93	-	18:14	
131.5	-	9.10	-	0:30	
131.8	-	9.25	-	0:30	18:15
132.1	-	9.43	-	0:30	
131.1	-	9.58	-	0:30	18:16
126.9	-	9.61	-	0:30	
124.8	-	9.62	-	0:30	18:17
125.2	-	9.64	-	0:30	
126.3	-	9.66	-	0:30	18:18
124.5	-	9.67	-	0:30	
123.4	-	9.67	-	0:30	18:19
122.6	-	9.68	-	0:30	
122.0	-	9.68	-	0:30	18:20
89.7	83.7	9.58	-	5:00	18:31
62.8	56.9	9.26	-	5:00	18:48
34.3	-	8.35	-	5:00	18:58
0.0	-	5.24	-	5:00	19:09

Note: Axial displacement = vertical displacement/cos 12°.
a - E.T. = Elapsed time since load applied.
1 kip = 4.45 kN
1 in. = 25.4 mm

Table B-2

HICKLING STATION GRILLAGE NO. 4-NE, REDUCED LOADING DATA

Load (kips)		Vertical Disp. (in.)			
Load Cell	Hydraulic Gage	Optical Level	Dial Gage	E.T.[a] (min)	Time of Day
0.0	0.0	0.00	0.000	-	9:17
19.0	17.6	0.02	0.049	10:00	9:32
28.7	27.9	0.08	0.086	10:00	9:48
42.5	43.4	0.16	0.178	10:00	10:02
27.7	22.7	0.12	0.127	10:00	10:17
14.2	8.8	0.06	0.069	10:00	10:32
0.3	0.0	0.01	0.032	10:00	10:49
21.4	19.5	0.08	0.090	10:00	11:02
42.0	43.7	0.17	0.198	10:00	11:18
56.5	58.5	0.43	0.447	10:00	11:33
70.0	72.0	0.84	0.877	16:00	11:55
83.9	86.4	1.52	1.657	16:00	12:16
56.4	53.9	1.44	1.577	10:00	12:30
27.4	22.7	1.24	1.364	10:00	12:44
0.0	0.0	0.52	0.659	10:00	12:58
42.0	44.6	1.21	1.350	10:00	13:18
84.0	88.3	2.08	2.187	16:00	13:32
98.4	104.1	2.99	3.121	16:00	13:57
112.5	118.1	4.44	4.633	16:00	14:26
126.8	132.9	7.75	8.116	16:00	14:54
-	-	7.80	8.158	-	14:55
123.9	128.3	7.80	8.166	1:00	14:56
123.1	127.8	7.80	8.170	1:00	14:57
122.6	126.9	7.80	8.175	1:00	14:58
122.1	126.9	7.81	8.177	1:00	14:59
121.7	126.0	7.81	8.178	1:00	15:00
121.4	125.5	7.81	8.180	1:00	15:01
120.9	125.0	7.81	8.183	2:00	15:03
120.5	124.1	7.82	8.183	2:00	15:05
120.2	123.2	7.82	8.186	2:00	15:07
119.9	123.2	7.82	8.189	2:00	15:09
119.2	122.7	7.82	8.215	6:00	15:15
118.8	122.5	7.82	8.215	5:00	15:20
118.4	121.3	7.82	8.216	5:00	15:25
61.1	56.2	7.55	7.883	10:00	15:41
0.0	0.0	3.96	-	7:30	15:55
63.3	67.4	6.44	-	10:00	16:29
91.0	95.7	7.67	-	7:30	16:35
102.5	-	7.70	-	0:30	
105.9	-	7.90	-	0:30	16:36
107.4	-	8.04	-	0:30	
109.5	-	8.14	-	0:30	16:37
110.3	-	8.29	-	0:30	
115.7	-	8.44	-	0:30	16:38

Table B-2

HICKLING STATION GRILLAGE NO. 4-NE, REDUCED LOADING DATA (Continued)

Load (kips)		Vertical Disp. (in.)			
Load Cell	Hydraulic Gage	Optical Level	Dial Gage	E.T.[a] (min)	Time of Day
122.3	-	-	-	0:30	
123.3	-	8.68	-	0:30	16:39
124.9	-	9.04	-	1:00	16:40
127.6	-	9.29	-	1:00	16:41
130.9	-	9.64	-	1:00	16:42
131.6	-	9.98	-	1:00	16:43
131.8	-	10.26	-	1:00	16:44
135.3	-	10.52	-	1:00	16:45
136.2	-	10.91	-	1:00	16:16
136.2	-	11.28	-	1:00	16:46
136.2	-	11.54	-	1:00	16:47
129.7	-	-	-	1:00	16:48
60.3	55.8	11.36	-	5:00	16:59
0.0	0.0	6.68	-	5:00	17:08

Note: Axial displacement = vertical displacement/cos 12°.
a - E.T. = Elapsed time since load applied.
1 kip = 4.45 kN
1 in. = 25.4 mm

Table B-3

HICKLING STATION GRILLAGE NO. 4-SW, REDUCED LOADING DATA

Load (kips)		Vertical Disp. (in.)			
Load Cell	Hydraulic Gage	Optical Level	Dial Gage	E.T.[a] (min)	Time of Day
0.0	0.0	0.00	0.000	-	9:31
13.8	11.6	0.00	0.009	10:00	9:42
28.4	26.0	0.02	0.053	10:00	9:57
42.4	41.8	0.10	0.120	10:00	10:12
27.7	22.7	0.06	0.079	10:00	10:27
13.7	10.2	0.02	0.046	10:00	10:41
0.8	0.0	0.00	0.015	10:00	10:55
21.6	25.5	0.04	0.058	10:00	11:11
42.5	43.0	0.12	0.120	10:00	11:28
55.9	56.7	0.24	0.264	10:00	11:41
70.2	72.1	0.60	0.668	16:00	12:02
84.4	88.3	1.18	1.258	16:00	12:25
56.3	55.3	1.10	1.203	10:00	12:39
26.9	25.1	0.96	1.041	10:00	12:53
0.0	0.0	0.46	0.515	10:00	13:08
0.0	0.0	0.06	0.515	-	8:40
41.8	40.9	0.88	1.025	10:00	8:53
84.0	89.3	1.56	1.692	10:00	9:10
98.4	105.1	2.33	2.465	16:00	9:32
112.3	121.4	4.13	4.300	16:00	9:55
121.5	128.8	6.71	5.045	8:00	10:10
120.9	127.9	6.72	5.049	0:30	
120.7	127.9	6.72	5.050	0:30	10:11
120.4	127.0	6.73	5.051	0:30	
120.2	126.5	6.73	5.051	0:30	10:12
119.8	126.0	6.73	5.053	1:00	10:13
119.5	125.6	6.74	5.054	1:00	10:14
119.2	125.1	6.74	5.058	1:00	10:15
118.8	124.4	6.74	5.058	2:00	10:17
118.5	123.7	6.74	5.067	2:00	10:19
118.2	123.2	6.74	5.067	2:00	10:21
59.9	50.7	6.40	4.769	5:00	10:38
0.0	0.0	3.82	0.000	5:00	10:49
46.1	46.2	4.90	3.988	10:00	11:15
90.7	91.1	6.40	4.179	10:00	11:31
93.2	97.6	6.44	-	-	11:39
100.7	103.7	6.59	-	0:30	
105.6	109.3	6.82	-	0:30	11:40
112.1	116.3	7.04	-	0:30	
117.0	123.2	7.38	-	0:30	11:41
121.6	127.0	7.66	-	0:30	
123.6	129.7	7.99	-	0:30	11:42
126.4	133.0	8.32	-	0:30	
131.3	137.2	8.58	-	0:30	11:43

Table B-3

HICKLING STATION GRILLAGE NO. 4-SW, REDUCED LOADING DATA (Continued)

Load (kips)		Vertical Disp. (in.)			
Load Cell	Hydraulic Gage	Optical Level	Dial Gage	E.T.[a] (min)	Time of Day
130.4	136.7	8.86	-	0:30	
131.6	137.7	9.23	-	0:30	11:44
135.6	141.8	9.49	-	0:30	
135.5	142.8	9.78	-	0:30	11:45
136.0	142.3	10.13	-	0:30	
136.6	144.2	10.50	-	0:30	11:46
138.9	146.5	10.74	-	0:30	
135.6	-	11.00	-	0:30	11:47
73.6	-	10.84	-	5:00	11:58
0.2	0.0	6.12	-	5:00	12:08

Note: Axial displacement = vertical displacement/cos 12°.
a - E.T. = Elapsed time since load applied.
1 kip = 4.45 kN
1 in. = 25.4 mm

Table B-4

HICKLING STATION GRILLAGE NO. 84-SE, REDUCED LOADING DATA

Load (kips)		Vertical Disp. (in.)			
Load Cell	Hydraulic Gage	Optical Level	Dial Gage	E.T.[a] (min)	Time of Day
0.0	0.0	0.00	0.000	-	10:51
17.2	14.8	0.02	0.019	10:00	11:01
31.4	28.3	0.06	0.070	10:00	11:16
53.3	53.4	0.24	0.186	10:00	11:38
30.7	27.4	0.18	0.178	10:00	11:55
17.3	19.0	0.14	0.134	10:00	12:10
1.0	0.4	0.06	0.066	10:00	12:28
27.5	25.5	0.16	0.125	10:00	12:43
52.0	51.1	0.22	0.189	10:00	12:58
72.5	73.9	0.38	0.311	10:00	13:12
85.2	87.1	0.53	0.420	16:00	13:34
102.1	105.0	0.78	0.599	16:00	13:57
64.7	64.1	0.68	-	10:00	14:11
35.2	32.0	0.55	0.446	10:00	14:27
0.3	0.0	0.32	0.223	10:00	14:42
51.3	51.6	0.55	0.384	10:00	14:59
102.0	106.4	0.90	0.619	10:00	15:18
119.2	125.0	1.25	1.181	16:00	15:41
136.3	143.6	1.93	1.961	16:00	16:03
151.4	159.9	2.94	-	12:00	16:20
0.0	0.0	1.01	-	-	8:45
76.0	77.8	1.79	-	10:00	8:59
153.2	162.2	3.86	-	10:00	9:21
-	-	7.85	-	12:00	9:40
164.8	176.2	7.98	-	-	9:50
163.5	174.8	8.00	-	0:30	
162.0	173.9	8.02	-	0:30	9:51
161.1	173.2	8.02	-	0:30	
160.4	172.5	8.03	-	0:30	9:52
159.8	171.5	8.04	-	0:30	
159.1	171.5	8.04	-	0:30	9:53
158.9	170.1	8.04	-	0:30	
158.6	169.7	8.05	-	0:30	9:54
158.0	169.2	8.05	-	1:00	9:55
157.6	168.8	8.05	-	1:00	9:56
157.1	168.8	8.06	-	1:00	9:57
156.7	168.5	8.06	-	1:00	9:58
156.5	167.8	8.06	-	1:00	9:59
156.2	167.8	8.06	-	1:00	10:00
155.6	166.9	8.06	-	2:00	10:02
155.4	166.9	8.06	-	2:00	10:04
154.9	165.5	8.06	-	2:00	10:06
90.9	93.4	7.50	-	10:00	10:23
0.0	0.0	3.50	-	10:00	10:35

Table B-4

HICKLING STATION GRILLAGE NO. 84-SE, REDUCED LOADING DATA (Continued)

Load (kips)		Vertical Disp. (in.)			
Load Cell	Hydraulic Gage	Optical Level	Dial Gage	E.T.[a] (min)	Time of Day
85.7	92.5	5.41	-	5:00	11:34
156.7	165.5	11.18	-	5:00	11:51
78.0	77.2	10.48	-	5:00	12:00
0.0	0.0	5.48	-	-	12:08

Note: Axial displacement = vertical displacement/cos 15°.
a - E.T. = Elapsed time since load applied.
1 kip = 4.45 kN
1 in. = 25.4 mm

Table B-5

HICKLING STATION GRILLAGE NO. 84-NE, REDUCED LOADING DATA

Load (kips)		Vertical Disp. (in.)			
Load Cell	Hydraulic Gage	Optical Level	Dial Gage	E.T.[a] (min)	Time of Day
0.0	0.0	0.00	0.000	-	10:00
17.3	16.2	0.06	0.006	10:00	10:11
34.6	33.0	0.13	0.133	10:00	10:27
51.4	51.6	0.25	0.299	10:00	10:46
34.2	32.0	0.20	0.265	10:00	11:04
17.0	14.4	0.14	0.215	10:00	11:20
0.1	0.0	0.10	0.129	10:00	11:36
25.6	24.4	0.14	0.221	10:00	13:01
51.0	52.0	0.26	0.358	10:00	13:17
68.4	70.2	0.41	0.528	10:00	13:33
84.8	88.3	0.60	0.749	10:00	13:55
101.9	105.0	0.86	1.093	10:00	14:16
68.9	67.8	0.78	0.993	10:00	14:35
34.8	31.6	0.61	0.796	10:00	14:50
3.6	0.0	0.34	0.459	10:00	15:05
0.0	0.0	0.31	0.459	-	8:36
50.7	55.3	0.58	0.538	10:00	8:46
103.8	112.0	1.07	1.318	10:00	9:14
120.5	129.7	1.62	1.947	16:00	9:39
136.2	144.1	2.71	3.159	16:00	10:03
152.2	162.7	5.05	5.620	16:00	10:29
104.0	106.4	5.05	5.400	10:00	10:53
54.7	57.6	4.24	4.525	10:00	11:03
0.0	0.0	2.04	2.214	10:00	11:21
75.0	77.8	3.41	3.673	-	11:43
82.6	86.4	3.52	-	1:00	11:44
87.1	92.0	3.65	-	1:00	11:45
91.0	95.7	3.78	-	1:00	11:46
96.5	101.8	3.94	-	1:00	11:47
100.5	105.0	4.08	-	1:00	11:48
104.4	109.7	4.20	-	1:00	11:49
109.1	113.9	4.36	-	1:00	11:50
113.2	119.9	4.50	-	1:00	11:51
117.4	124.6	4.62	-	1:00	11:52
121.2	127.8	4.76	-	1:00	11:53
127.0	132.9	5.02	-	2:00	11:55
130.0	137.1	5.11	-	1:00	11:56
134.8	141.3	5.28	-	1:00	11:57
139.3	146.4	5.47	-	1:00	11:58
143.9	151.5	5.68	-	1:00	11:59
147.8	155.7	5.89	-	1:00	12:00
151.6	159.9	6.19	-	1:00	12:01
154.6	162.7	6.44	-	1:00	12:02
156.9	165.5	6.68	-	1:00	12:03

Table B-5

HICKLING STATION GRILLAGE NO. 84-NE, REDUCED LOADING DATA (Continued)

Load (kips)		Vertical Disp. (in.)			
Load Cell	Hydraulic Gage	Optical Level	Dial Gage	E.T.[a] (min)	Time of Day
158.1	167.4	6.80	-	0:30	
158.9	168.3	6.92	-	0:30	12:04
159.4	167.8	7.03	-	0:30	
59.9	169.2	7.14	-	0:30	12:05
160.4	169.7	7.26	-	0:30	
160.7	169.2	7.36	-	0:30	12:06
161.4	170.1	7.46	-	0:30	
162.0	170.1	7.55	-	0:30	12:07
162.6	171.5	7.66	-	0:30	
162.9	171.5	7.76	-	0:30	12:08
162.9	172.0	7.87	-	0:30	
163.1	172.5	7.98	-	0:30	12:09
163.2	172.5	8.08	-	0:30	
163.2	172.5	8.18	-	0:30	12:10
163.7	172.9	8.23	-	0:30	
163.8	173.2	8.34	-	0:30	12:11
164.0	173.4	8.45	-	0:30	
164.5	173.9	8.56	-	0:30	12:12
164.4	173.9	8.66	-	0:30	
164.7	174.3	8.76	-	0:30	12:13
164.8	174.3	8.87	-	0:30	
164.7	173.9	8.98	-	0:30	12:14
160.9	165.0	9.04	-	0:30	
159.8	165.0	9.05	-	0:30	12:15
160.0	165.0	9.06	-	0:30	
160.1	167.4	9.07	-	1:00	12:16
161.1	167.4	9.12	-	1:00	12:17
160.1	165.0	9.15	-	1:00	12:18
152.0	148.8	9.17	-	1:00	12:19
78.3	75.5	8.34	-	10:00	12:31
0.0	0.0	4.40	-	10:00	12:41

Note: Axial displacement = vertical displacement/cos 15°.
a - E.T. = Elapsed time since load applied.
1 kip = 4.45 kN
1 in. = 25.4 mm

Table B-6

HICKLING STATION GRILLAGE NO. 84-SW, REDUCED LOADING DATA

Load (kips)		Vertical Disp. (in.)			
Load Cell	Hydraulic Gage	Optical Level	Dial Gage	E.T.[a] (min)	Time of Day
0.0	0.0	0.00	0.000	-	10:00
16.6	15.8	0.04	0.027	10:00	10:10
34.0	34.4	0.10	0.094	10:00	10:33
51.4	53.0	0.22	0.213	10:00	10:49
33.9	32.5	0.16	0.164	10:00	11:05
17.6	14.4	0.11	0.097	10:00	11:19
0.0	0.0	0.05	0.038	10:00	11:35
25.3	24.8	0.13	0.108	10:00	12:47
51.3	54.8	0.22	0.235	10:00	13:08
68.8	72.0	0.32	0.363	10:00	13:17
85.0	88.8	0.52	0.547	10:00	13:39
101.7	106.9	0.88	0.910	10:00	13:59
68.6	66.9	0.76	0.817	10:00	14:20
34.8	30.2	0.54	0.604	10:00	14:29
0.0	0.0	0.29	0.329	10:00	14:43
0.0	0.0	0.28	0.329	-	8:45
34.3	33.7	0.44	0.496	10:00	8:57
67.7	67.8	0.71	0.809	10:00	9:14
101.8	107.8	1.16	1.264	10:00	9:30
119.4	127.4	1.90	2.003	16:00	9:54
136.5	146.0	3.54	3.738	16:00	10:17
150.8	162.2	6.82	-	-	10:39
148.1	159.0	6.83	-	0:30	
146.7	157.6	6.84	-	0:30	10:40
145.9	156.2	6.84	-	0:30	
145.9	154.3	6.85	-	0:30	10:41
145.0	153.9	6.85	-	0:30	
144.6	153.4	6.85	-	0:30	10:42
144.1	152.9	6.86	-	1:00	10:43
143.8	152.9	6.86	-	0:30	
143.6	152.9	6.86	-	0:30	10:44
143.2	152.0	6.88	-	1:00	10:45
142.9	151.5	6.88	-	1:00	10:46
142.6	151.5	6.88	-	1:00	10:47
142.4	151.1	6.88	-	1:00	10:48
142.2	150.8	6.88	-	1:00	10:49
141.8	149.7	6.88	-	2:00	10:51
141.5	149.7	6.88	-	2:00	10:53
141.2	149.2	6.88	-	2:00	10:55
141.0	149.0	6.89	-	2:00	10:57
140.8	149.0	6.89	-	2:00	10:59
100.1	97.6	6.68	-	5:00	11:12
51.5	48.3	5.35	-	5:00	11:22
0.0	0.0	2.62	-	5:00	11:34

Table B-6

HICKLING STATION GRILLAGE NO. 84-SW, REDUCED LOADING DATA (Continued)

Load (kips)		Vertical Disp. (in.)			
Load Cell	Hydraulic Gage	Optical Level	Dial Gage	E.T.[a] (min)	Time of Day
75.8	83.2	4.52	-	10:00	13:03
99.4	109.2	5.66	-	3:00	13:12
121.1	132.5	6.76	-	3:00	13:15
125.0	136.7	6.82	-	0:30	
128.4	140.4	7.18	-	0:30	13:16
131.8	144.1	7.42	-	0:30	
134.3	146.9	7.64	-	0:30	13:17
139.6	152.9	8.14	-	1:00	13:18
141.3	155.3	8.38	-	0:30	
142.8	156.7	8.64	-	0:30	13:19
144.5	159.9	8.94	-	0:30	
146.3	160.4	8.94	-	0:30	13:20
147.1	162.2	9.67	-	0:30	
146.0	159.0	9.91	-	0:30	13:21
146.0	158.1	10.08	-	0:30	
144.6	155.7	10.19	-	0:30	13:22
141.7	151.1	10.21	-	0:30	
140.8	150.6	10.21	-	0:30	13:23
142.5	153.4	10.26	-	0:30	
141.0	151.1	10.27	-	0:30	13:24
140.3	150.6	10.27	-	0:30	
139.1	149.2	10.28	-	0:30	13:25
139.5	148.8	10.28	-	0:30	
139.2	148.8	10.28	-	0:30	13:26
138.9	147.6	10.28	-	0:30	
140.3	150.6	10.30	-	0:30	13:27
139.7	148.8	10.30	-	0:30	
139.3	148.8	10.30	-	0:30	13:28
139.2	148.8	10.30	-	0:30	
139.0	148.3	10.30	-	0:30	13:29
138.9	146.4	10.30	-	0:30	
138.7	146.9	10.30	-	0:30	13:30
139.3	150.6	10.30	-	0:30	
140.3	149.7	10.31	-	0:30	13:31
141.3	151.1	10.32	-	0:30	
99.4	95.3	10.12	-	5:00	13:47
49.8	42.7	7.98	-	5:00	13:54
0.0	0.0	4.66	-	5:00	14:03

Note: Axial displacement = vertical displacement/cos 15°.
a - E.T. = Elapsed time since load applied.
1 kip = 4.45 kN
1 in. = 25.4 mm

Table B-7

WYNCOOP CREEK GRILLAGE NO. X2-SE, REDUCED LOADING DATA

Load (kips)		Vertical Disp. (in.)			
Load Cell	Hydraulic Gage	Optical Level	Dial Gage	E.T.[a] (min)	Time of Day
0.0	0.0	0.00	0.000	-	12:41
4.0	4.1	0.00	0.046	10:00	12:57
8.0	7.4	0.12	0.186	10:00	13:09
12.1	12.0	0.32	0.418	10:00	13:25
7.9	6.9	0.32	0.400	10:00	13:42
4.2	3.2	0.32	0.354	10:00	13:58
0.6	0.0	0.10	0.116	10:00	14:15
6.4	5.5	0.17	0.331	10:00	14:33
12.4	11.6	0.46	0.520	10:00	14:50
15.9	15.3	0.70	0.751	10:00	15:07
19.8	19.0	1.14	1.206	16:00	15:30
24.0	23.7	1.75	1.864	16:00	15:53
16.2	15.3	1.78	1.894	10:00	16:12
8.6	6.9	1.66	-	10:00	16:21
0.9	0.0	1.06	-	10:00	16:31
0.0	0.0	0.78	1.148	-	8:46
7.7	6.9	1.15	1.522	10:00	8:56
16.1	16.2	1.67	2.053	10:00	9:13
24.3	24.6	2.38	2.768	10:00	9:31
28.2	29.7	3.14	3.513	16:00	9:55
32.3	34.6	4.39	4.806	16:00	10:19
36.3	38.6	6.40	6.798	16:00	10:44
-	-	-	-	8:00	10:57
38.1	41.8	-	-	-	11:01
37.7	40.4	9.38	-	1:00	11:02
37.3	39.9	9.38	-	1:00	11:03
36.8	39.5	9.38	-	1:00	11:04
36.5	39.5	9.40	-	1:00	11:05
36.3	39.0	9.40	-	1:00	11:06
36.2	38.3	9.40	-	1:00	11:07
36.1	38.6	9.40	-	1:00	11:08
24.4	23.2	9.40	-	5:00	11:22
11.9	10.7	8.46	-	5:00	11:33
0.0	0.0	5.20	-	5:00	11:44
20.1	19.5	7.45	-	10:00	13:07
20.0	19.5	7.46	-	-	13:15
22.9	23.7	7.94	-	0:30	
25.3	27.4	8.41	-	0:30	13:16
28.6	30.6	8.89	-	0:30	
32.0	34.8	9.41	-	0:30	13:17
35.6	39.5	10.00	-	0:30	
38.8	43.7	10.58	-	0:30	13:18
41.2	46.5	11.20	-	0:30	
42.9	48.3	11.80	-	0:30	13:19

Table B-7

WYNCOOP CREEK GRILLAGE NO. X2-SE, REDUCED LOADING DATA (Continued)

Load (kips)		Vertical Disp. (in.)			
Load Cell	Hydraulic Gage	Optical Level	Dial Gage	E.T.[a] (min)	Time of Day
43.6	49.2	12.46	-	0:30	
44.4	50.2	13.09	-	0:30	13:20
44.7	47.4	13.67	-	0:30	
44.1	47.4	13.87	-	0:30	13:21
42.8	44.1	14.05	-	0:30	
-	-	14.08	-	0:30	13:22
42.1	43.7	14.08	-	0:30	
41.8	42.3	14.09	-	0:30	13:23
41.1	42.7	14.09	-	2:00	13:25
40.7	41.8	14.09	-	2:00	13:27
40.5	41.8	14.09	-	2:00	13:29
40.3	41.3	14.09	-	2:00	13:31
28.0	26.5	13.98	-	5:00	13:41
14.7	12.0	12.76	-	5:00	13:51
0.0	0.0	7.84	-	5:00	13:56

Note: Axial displacement = vertical displacement/cos 10°.
a - E.T. = Elapsed time since load applied.
1 kip = 4.45 kN
1 in. = 25.4 mm

Table B-8

WYNCOOP CREEK GRILLAGE NO. X2-SW, REDUCED LOADING DATA

Load (kips)		Vertical Disp. (in.)			
Load Cell	Hydraulic Gage	Optical Level	Dial Gage	E.T.[a] (min)	Time of Day
0.0	0.0	0.00	0.000	-	9:10
3.7	1.4	0.02	0.025	10:00	9:20
8.0	6.0	0.17	0.181	10:00	9:34
11.8	11.1	0.64	0.665	10:00	9:50
8.2	6.5	0.61	0.626	10:00	10:05
4.5	2.7	0.53	0.539	10:00	10:21
0.0	0.0	0.11	0.121	10:00	10:36
7.0	4.6	0.41	0.470	10:00	10:53
12.3	11.1	0.74	0.766	10:00	11:08
16.1	15.8	1.08	1.133	10:00	11:23
20.3	20.4	1.76	1.849	16:00	11:46
25.2	25.5	2.65	2.747	16:00	12:08
24.9	25.1	-	2.789	1:00	12:09
24.6	24.4	2.68	2.791	0:30	
24.4	24.4	2.69	2.792	0:30	12:10
24.2	24.1	2.69	2.793	1:00	12:11
24.1	24.1	2.69	2.793	1:00	12:12
23.9	23.7	2.69	2.794	1:00	12:13
23.8	23.7	2.69	2.795	1:00	12:14
16.0	13.4	2.64	2.729	10:00	12:33
9.2	6.9	2.30	2.392	10:00	12:50
0.7	0.0	0.96	1.044	10:00	13:05
8.0	7.4	1.46	1.527	10:00	13:23
15.7	15.8	2.28	2.386	10:00	13:38
24.1	24.6	3.04	3.134	10:00	13:54
27.7	28.3	3.41	3.533	16:00	14:17
31.7	33.4	4.34	4.450	16:00	14:38
36.4	38.1	5.28	5.398	16:00	15:00
40.1	42.3	6.30	6.431	16:00	15:22
44.1	46.5	6.90	7.020	12:00	15:41
43.2	46.0	6.92	7.032	1:00	15:42
42.6	45.5	6.92	7.033	1:00	15:43
42.2	44.6	6.92	7.035	1:00	15:44
41.8	44.4	6.92	7.037	1:00	15:45
41.6	44.1	6.92	7.038	1:00	15:46
41.4	44.1	6.92	7.039	1:00	15:47
41.3	43.9	6.92	7.039	1:00	15:48
41.2	43.7	6.92	7.039	1:00	15:49
41.1	43.7	6.92	7.039	1:00	15:50
41.0	43.7	6.92	7.044	1:00	15:51
-	-	7.97	7.470	12:00	16:05
47.6	51.1	8.08	7.578	-	16:15
46.3	50.6	8.09	7.589	1:00	16:16
45.8	49.7	8.09	7.591	1:00	16:17

Table B-8

WYNCOOP CREEK GRILLAGE NO. X2-SW, REDUCED LOADING DATA (Continued)

Load (kips)		Vertical Disp. (in.)			
Load Cell	Hydraulic Gage	Optical Level	Dial Gage	E.T.[a] (min)	Time of Day
45.5	49.2	8.09	7.592	1:00	16:18
45.0	48.8	8.09	7.594	2:00	16:20
44.8	48.8	8.09	7.596	2:00	16:22
44.4	47.9	8.09	8.211	3:00	16:25
52.5	51.1	8.87	-	4:00	16:35
48.7	49.2	-	-	-	16:39
29.5	28.8	8.78	-	5:00	16:49
0.0	0.0	3.62	-	5:00	17:00
30.1	30.6	7.87	-	5:00	17:18
30.5	31.1	7.92	-	5:00	17:23
36.2	37.6	8.45	-	0:30	
43.9	47.4	8.93	-	0:30	17:24
47.5	51.1	9.41	-	0:30	
53.8	57.6	9.97	-	0:30	17:25
54.1	59.0	10.55	-	0:30	
57.6	62.7	11.15	-	0:30	17:26
56.3	59.5	11.54	-	0:30	
56.3	59.9	11.77	-	0:30	17:28
56.9	59.9	11.98	-	0:30	
57.6	60.4	12.12	-	0:30	17:29
0.0	0.0	5.87	-	5:00	17:51

Note: Axial displacement = vertical displacement/cos 10°.
a - E.T. = Elapsed time since load applied.
1 kip = 4.45 kN
1 in. = 25.4 mm

Appendix C

HUB LOAD-DISPLACEMENT DATA

This appendix contains the reduced data for the ground surface movements for the eight uplift tests. Summary Tables C-1 through C-8 give the change in hub elevation at various applied load levels for each of the hubs surrounding the grillage stub. Hub locations are given in Section 6 for all of the uplift tests.

Table C-1

HICKLING STATION GRILLAGE NO. 4-NW, REDUCED HUB DATA

Load (kips)	Change in Elevation (in.) for Hub Number											
	1	2	3	4	5	6	7	8	9	10	11	12
0.0	0.00	0.00	0.00	0.00	0.00	0.00	0.00	0.00	0.00	-	-	-
17.8	-	-	-	-	-	-	-	-	-	-	-	-
36.8	0.00	0.00	0.00	0.00	0.00	0.00	0.00	0.06	0.00	-	-	-
51.5	0.00	0.06	0.00	0.06	0.00	0.00	0.00	0.12	0.00	-	-	-
34.6	0.00	0.00	0.00	0.00	0.00	0.00	0.00	0.12	0.00	-	-	-
18.1	-0.06	0.00	0.00	0.00	0.00	0.00	-0.06	0.06	0.00	-	-	-
0.0	-0.06	0.00	0.00	0.00	0.00	0.00	-0.06	0.06	0.00	-	-	-
25.5	-0.06	0.00	0.00	0.00	0.00	0.00	-0.06	0.06	0.00	-	-	-
51.9	-0.06	0.12	0.00	0.06	0.00	0.00	-0.06	0.06	0.00	-	-	-
68.8	0.06	0.12	0.00	0.06	0.00	0.00	-0.06	0.06	0.00	-	-	-
85.7	0.06	0.12	0.00	0.12	0.06	0.00	-0.06	0.06	0.06	-	-	-
102.6	0.12	0.12	0.00	0.36	0.06	0.00	0.00	0.12	0.06	-	-	-
68.0	0.06	0.12	0.00	0.24	0.06	0.00	0.00	0.12	0.06	-	-	-
34.1	-0.12	0.12	0.00	0.12	0.00	0.00	-0.06	0.12	0.06	-	-	-
0.0	-0.12	0.00	0.00	-0.06	0.00	0.00	-0.12	0.12	0.00	-	-	-
51.7	0.12	0.00	0.00	0.06	0.00	0.00	-0.06	0.12	0.00	-	-	-
102.1	0.12	0.00	0.06	0.36	0.00	0.00	0.06	0.12	0.00	-	-	-
119.3	0.42	0.12	0.06	0.90	0.06	0.00	0.42	0.12	0.00	-	-	-
111.6	0.48	0.12	0.06	0.90	0.06	0.00	0.42	0.12	0.06	-	-	-
122.0	1.56	0.12	0.06	2.16	0.00	0.00	1.14	0.24	0.06	-	-	-
89.7	1.50	0.30	0.06	1.98	0.06	0.00	1.08	0.18	0.00	-	-	-
62.8	1.14	0.18	0.00	1.80	0.06	-0.06	0.96	0.18	0.00	-	-	-
34.3	0.60	0.06	0.00	1.20	0.06	-0.06	0.48	0.12	0.00	-	-	-
0.0	-0.24	0.00	0.00	0.30	0.06	-0.06	-0.24	0.12	0.00	-	-	-

1 kip = 4.45 kN
1 in. = 25.4 mm

Table C-2

HICKLING STATION GRILLAGE NO. 4-NE, REDUCED HUB DATA

Load (kips)	Change in Elevation (in.) for Hub Number											
	1	2	3	4	5	6	7	8	9	10	11	12
0.0	0.00	0.00	0.00	0.00	0.00	0.00	0.00	0.00	0.00	0.00	0.00	0.00
19.0	0.00	0.00	0.00	0.00	0.06	0.00	0.00	0.00	0.00	0.06	0.06	0.00
28.7	0.06	0.00	0.00	0.06	0.06	0.00	0.00	0.00	0.00	0.06	0.06	0.00
42.5	0.06	0.00	0.00	0.06	0.06	0.00	0.06	0.06	0.00	0.06	0.06	0.00
27.7	0.06	0.00	0.00	0.06	0.06	0.00	0.06	0.00	0.00	0.06	0.06	0.00
14.2	0.06	0.00	0.00	0.06	0.06	0.00	0.00	0.00	0.00	0.06	0.06	0.00
0.3	0.00	0.00	0.00	0.06	0.06	0.00	0.00	0.00	0.00	0.06	0.00	0.00
21.4	0.00	0.00	0.00	0.06	0.06	0.00	0.00	0.00	0.00	0.06	0.00	0.00
42.0	0.00	0.00	0.00	0.06	0.06	0.00	0.06	0.00	0.00	0.06	0.00	0.00
56.5	0.06	0.00	0.00	0.06	0.06	0.00	0.06	0.00	0.00	0.06	0.00	0.00
70.0	0.06	0.00	0.00	0.06	0.06	0.00	0.06	0.06	0.00	0.12	0.06	0.00
83.9	0.12	0.06	0.00	0.12	0.06	0.00	0.18	0.06	0.00	0.12	0.06	0.00
56.4	0.12	0.06	0.00	0.06	0.00	0.00	0.06	0.06	0.00	0.06	0.06	0.00
27.4	0.00	-0.06	0.00	0.00	0.00	0.00	0.06	0.00	0.00	0.06	0.06	0.00
0.0	-0.12	-0.12	0.00	-0.06	-0.06	-0.06	-0.12	-0.06	0.00	-0.06	-0.06	-0.06
42.0	0.00	-0.06	0.00	-0.06	0.00	-0.06	-0.06	-0.06	0.00	0.00	-0.06	-0.06
84.0	0.12	0.06	0.00	0.12	0.06	-0.06	0.12	0.00	0.00	0.12	0.06	0.00
98.4	0.24	0.12	0.00	0.24	0.18	0.00	0.30	0.12	0.00	0.12	0.12	0.00
112.5	0.60	0.36	0.00	0.60	0.18	0.00	0.66	0.42	0.06	0.42	0.24	0.00
118.4	1.86	1.20	0.12	1.92	1.38	0.00	1.92	1.32	0.06	1.20	0.48	0.00
61.1	1.62	1.02	0.06	1.68	1.14	0.00	1.74	1.20	0.00	0.96	0.36	0.00
2.3	-0.42	-0.36	0.00	-0.36	-0.36	-0.06	-0.36	-0.24	0.00	-0.30	-0.18	0.00
63.3	0.00	-0.12	0.00	0.18	-0.06	-0.06	0.36	0.06	0.00	0.00	-0.06	0.00
91.0	0.60	0.24	0.00	0.78	0.42	0.00	0.42	0.06	0.06	0.36	0.06	0.00
129.7	2.88	1.50	0.24	2.94	2.28	0.06	2.82	2.10	0.12	1.68	0.54	0.00
60.3	2.46	1.50	0.06	2.52	1.86	0.00	2.52	1.74	0.00	1.38	0.30	0.00
0.0	-0.48	-0.48	0.00	-0.36	-0.42	-0.06	-0.24	-0.24	0.00	-0.54	-0.30	-0.06

1 kip = 4.45 kN
1 in. = 25.4 mm

Table C-3

HICKLING STATION GRILLAGE NO. 4-SW, REDUCED HUB DATA

Load (kips)	Change in Elevation (in.) for Hub Number											
	1	2	3	4	5	6	7	8	9	10	11	12
0.0	0.00	0.00	0.00	0.00	0.00	0.00	0.00	0.00	0.00	0.00	0.00	0.00
13.8	0.00	0.00	0.00	0.00	0.00	0.00	0.00	0.00	0.00	0.00	0.00	0.00
28.4	0.00	0.00	0.00	0.00	0.00	0.00	0.00	0.00	0.00	0.00	0.00	0.00
42.4	0.00	0.00	0.00	0.00	0.00	0.00	0.00	0.00	0.00	0.00	0.00	0.00
27.7	0.00	0.00	0.00	0.00	0.00	0.00	0.00	0.00	0.00	-0.06	0.00	0.00
13.7	-0.06	0.00	0.00	0.00	0.00	0.00	0.00	0.00	0.00	-0.06	0.00	0.00
0.8	-0.06	0.00	0.00	0.00	0.00	0.00	0.00	0.00	0.00	-0.06	0.00	0.00
21.6	-0.04	0.00	0.00	0.00	0.06	0.00	0.00	0.00	0.00	-0.12	0.00	0.00
42.5	0.00	0.00	0.00	0.00	0.06	0.00	0.00	0.00	0.00	-0.06	0.00	0.00
55.9	0.00	0.00	0.00	0.00	0.06	0.00	0.06	0.00	0.00	-0.06	0.00	0.00
70.2	0.00	0.00	0.00	0.00	0.06	0.00	0.06	0.00	0.00	0.00	0.00	0.00
84.4	0.00	0.00	0.00	0.06	0.06	0.00	0.18	0.00	0.00	0.00	0.00	0.00
56.3	0.00	0.00	-0.06	0.06	0.06	0.00	0.06	0.00	0.00	-0.06	0.00	0.00
26.9	0.00	0.00	-0.06	0.00	0.00	-0.06	0.06	-0.06	0.00	-0.06	-0.12	0.00
0.0	-0.06	0.00	-0.06	-0.12	0.00	-0.06	0.00	-0.12	-0.06	-0.06	-0.12	0.00
0.0	-0.12	-0.06	-0.12	-0.18	-0.06	-0.12	-0.00	-0.12	-0.06	-0.18	-0.12	-0.06
41.8	-0.12	-0.00	-0.12	-0.12	-0.00	-0.06	-0.00	-0.12	-0.06	-0.18	-0.06	-0.06
84.0	-0.00	-0.00	-0.06	-0.00	-0.00	-0.06	0.12	-0.06	-0.06	-0.06	-0.06	-0.06
98.4	-0.00	0.06	-0.06	0.12	0.18	-0.06	0.24	-0.06	-0.00	0.06	-0.06	-0.06
112.3	0.24	0.18	-0.06	0.54	0.42	-0.06	0.60	0.06	-0.00	0.36	0.06	-0.06
118.2	0.72	0.54	-0.06	1.26	0.96	-0.06	1.50	0.36	-0.00	1.02	0.30	-0.06
59.9	0.54	0.30	-0.12	0.96	0.72	-0.12	1.26	0.06	-0.00	0.84	0.12	-0.12
0.0	-0.42	-0.24	-0.18	-0.36	-0.24	-0.12	-0.12	-0.36	-0.06	-0.18	-0.18	-0.12
46.1	-0.42	-0.24	-0.18	-0.30	-0.18	-0.12	-0.00	-0.36	-0.06	-0.06	-0.18	-0.12
90.7	-0.12	-0.06	-0.18	0.30	0.24	-0.12	0.60	-0.18	-0.06	0.36	-0.06	-0.06
135.6	1.62	1.26	0.06	2.46	2.04	-0.00	2.28	0.96	0.06	1.92	0.54	-0.06
73.6	-	-	-	-	-	-	-	-	-	-	-	-
0.2	-0.60	-0.42	-0.18	-0.54	-0.18	-0.12	-0.36	-0.54	-0.06	-0.24	-0.30	-0.06

1 kip = 4.45 kN
1 in. = 25.4 mm

Table C-4

HICKLING STATION GRILLAGE NO. 84-SE, REDUCED HUB DATA

Load (kips)	Change in Elevation (in.) for Hub Number											
	1	2	3	4	5	6	7	8	9	10	11	12
0.0	0.00	0.00	0.00	0.00	0.00	0.00	0.00	0.00	0.00	0.00	0.00	0.00
17.2	0.00	0.00	0.00	0.00	0.00	0.00	0.00	0.00	0.00	0.00	0.00	0.06
31.4	0.00	0.00	0.00	0.00	0.00	0.00	0.00	0.00	0.00	0.00	0.00	0.00
53.3	0.00	0.00	0.00	0.00	0.00	0.00	0.00	0.00	-0.06	0.00	0.00	0.00
30.7	0.00	0.00	-0.06	0.00	0.00	0.00	0.00	0.00	-0.06	0.00	0.00	0.00
17.3	0.00	0.00	-0.06	0.00	0.00	0.00	0.00	0.00	0.00	0.00	0.00	-0.06
1.0	0.00	0.00	-0.06	0.00	0.00	0.00	0.00	0.00	0.00	0.00	0.00	-0.06
27.5	0.00	0.00	-0.06	0.00	0.00	0.00	0.06	0.00	0.00	0.00	0.00	0.00
52.0	0.00	0.00	-0.06	0.00	0.00	0.00	0.06	0.00	-0.06	0.00	0.00	-0.06
72.5	0.06	0.00	-0.06	0.06	0.00	0.00	0.06	0.00	-0.06	0.00	0.00	-0.06
85.2	0.06	0.00	-0.06	0.06	0.00	0.00	0.06	0.00	-0.06	0.00	0.00	-0.06
102.1	0.12	0.06	-0.06	0.12	0.00	0.00	0.06	0.00	-0.06	0.00	0.00	-0.06
64.7	0.06	0.00	-0.06	0.06	-0.06	-0.12	-0.06	-0.06	-0.06	0.00	0.00	-0.06
35.2	0.00	-0.06	-0.12	0.00	-0.06	-0.12	-0.06	-0.12	-0.06	-0.06	-0.06	-0.06
0.3	-0.06	-0.06	-0.12	-0.06	-0.12	-0.12	-0.18	-0.12	-0.06	-0.06	-0.06	-0.06
51.3	0.00	-0.06	-0.12	-0.06	-0.12	-0.12	-0.06	-0.12	-0.06	-0.06	-0.06	-0.12
102.0	0.06	-0.06	-0.12	0.06	-0.06	-0.12	0.00	-0.06	-0.06	-0.06	-0.06	-0.06
119.2	0.18	0.00	-0.12	0.18	0.00	-0.12	0.12	0.00	-0.06	0.12	0.00	-0.12
136.3	0.54	0.18	-0.12	0.42	0.18	-0.12	0.24	0.48	0.00	0.42	0.18	-0.12
0.0	-0.30	-0.42	-0.24	-0.48	-0.54	-0.24	-0.36	-0.48	-0.12	-0.30	-0.18	-0.18
76.0	-0.06	-0.36	-0.24	-0.24	-0.42	-0.24	-0.18	-0.36	-0.18	-0.12	-0.18	-0.18
153.2	1.44	0.72	-0.24	1.26	0.78	-0.18	1.32	0.72	-0.18	1.20	0.42	-0.24
154.9	5.22	4.14	-0.24	5.10	4.32	0.06	4.98	3.96	-0.12	4.62	2.10	-0.18
90.9	4.74	3.66	-0.18	4.56	3.84	-0.18	4.50	3.54	-0.12	4.20	1.74	-0.18
0.0	1.02	0.54	-0.18	0.84	0.36	-0.36	0.96	0.42	-0.18	0.96	0.24	-0.18
85.7	1.98	1.14	-0.12	1.98	1.02	-0.36	1.86	1.08	-0.12	1.74	0.36	-0.24
156.7	-	-	-	-	-	-	-	-	-	-	-	-
78.0	-	-	-	-	-	-	-	-	-	-	-	-
0.0	-	-	-	-	-	-	-	-	-	-	-	-

1 kip = 4.45 kN
1 in. = 25.4 mm

Table C-5

HICKLING STATION GRILLAGE NO. 84-NE, REDUCED HUB DATA

Load (kips)	Change in Elevation (in.) for Hub Number											
	1	2	3	4	5	6	7	8	9	10	11	12
0.0	0.00	0.00	0.00	0.00	0.00	0.00	0.00	0.00	0.00	0.00	0.00	0.00
17.3	0.00	0.00	0.00	0.00	0.06	0.00	0.00	0.00	0.00	0.00	0.00	0.00
34.6	0.00	0.00	0.00	0.00	0.06	0.06	0.00	0.00	0.00	0.00	0.00	0.00
51.4	0.00	0.00	0.00	0.00	0.06	0.06	0.06	0.00	0.00	0.00	0.00	0.00
34.2	0.00	0.00	0.00	0.00	0.06	0.00	0.00	0.00	0.00	0.00	0.00	0.00
17.0	0.00	0.00	0.00	0.00	0.06	0.00	0.00	0.00	0.00	0.00	0.00	0.00
0.1	0.00	0.00	-0.06	0.00	0.00	0.00	0.00	0.00	-0.06	0.00	0.00	0.00
25.6	0.00	0.00	0.00	0.00	0.00	0.00	0.00	0.00	0.00	0.00	0.00	0.00
51.0	0.00	0.00	0.00	0.06	0.00	0.00	0.00	0.00	0.00	0.00	0.00	0.00
68.4	0.00	0.00	0.00	0.06	0.00	0.00	0.00	0.00	0.00	0.00	0.00	0.00
84.8	0.00	0.00	0.00	0.12	0.06	0.00	0.12	0.00	0.00	0.00	0.00	0.00
101.9	0.06	0.06	0.00	0.12	0.06	0.00	0.12	0.00	0.00	0.06	0.00	0.00
68.9	0.00	0.00	-0.06	0.12	0.06	0.00	0.00	-0.06	0.00	0.00	0.00	0.00
34.8	-0.06	0.00	-0.06	0.06	-0.12	0.00	0.00	-0.06	0.00	-0.06	0.00	0.00
3.6	-0.12	-0.06	-0.06	-0.06	-0.06	0.00	-0.12	-0.06	0.00	-0.06	0.00	0.00
0.0	-0.12	-0.06	-0.06	-0.24	-0.12	0.00	-0.06	-0.12	0.00	-0.06	0.00	0.00
50.7	-0.12	-0.06	-0.06	-0.06	-0.12	0.00	-0.12	-0.06	0.00	-0.06	0.00	0.00
103.8	0.00	0.00	-0.06	0.12	0.00	0.00	0.06	0.00	0.00	0.00	0.00	0.00
120.5	0.18	0.12	-0.06	0.30	0.12	0.00	0.18	0.06	0.00	0.18	0.06	0.00
136.2	0.72	0.54	-0.06	0.84	0.54	0.00	0.66	0.24	0.00	0.48	0.24	0.00
152.2	2.16	1.74	0.06	2.46	2.04	0.00	2.10	1.50	0.00	1.62	0.72	0.00
104.0	2.16	1.68	0.00	2.40	1.92	-0.06	2.04	1.38	0.00	1.62	0.66	0.00
54.7	1.38	0.96	-0.06	1.50	1.20	-0.06	1.26	0.72	0.00	0.90	0.30	0.00
0.0	0.58	-0.18	-0.06	-0.24	-0.42	-0.06	-0.24	-0.48	-0.06	-0.06	-0.06	-0.06
152.0	-	-	-	-	-	-	-	-	-	-	-	-
78.3	-	-	-	-	-	-	-	-	-	-	-	-
0.0	0.42	0.12	-0.06	0.48	0.06	-0.06	0.24	-0.12	-0.06	0.30	0.06	-0.06

1 kip = 4.45 kN
1 in. = 25.4 mm

Table C-6

HICKLING STATION GRILLAGE NO. 84-SW, REDUCED HUB DATA

Load (kips)	Change in Elevation (in.) for Hub Number											
	1	2	3	4	5	6	7	8	9	10	11	12
0.0	0.00	0.00	0.00	0.00	0.00	0.00	0.00	0.00	0.00	0.00	0.00	0.00
16.6	0.00	0.00	0.00	0.06	0.12	0.06	0.00	0.00	0.00	0.00	0.00	0.06
34.0	0.00	0.00	0.00	0.06	0.18	0.06	0.00	0.00	0.00	0.00	0.06	0.06
51.4	0.00	0.00	0.00	0.12	0.18	0.06	0.00	0.00	0.00	0.00	0.06	0.06
33.9	0.00	0.00	0.00	0.06	0.18	0.06	0.00	0.00	0.00	0.00	0.06	0.06
17.6	0.00	0.00	0.00	0.00	0.12	0.06	0.00	0.00	0.00	0.00	0.00	0.06
0.0	0.00	0.00	-0.06	0.00	0.12	0.00	0.00	0.00	0.00	0.00	0.00	0.00
25.3	0.00	0.00	-0.06	0.00	0.12	0.00	0.00	0.00	0.00	0.00	0.00	0.00
51.3	0.00	0.00	-0.06	0.06	0.12	0.00	0.00	0.00	0.00	0.00	0.00	0.00
68.8	0.06	0.00	-0.06	0.12	0.12	0.00	0.00	0.00	0.00	0.00	0.00	0.06
85.0	0.06	0.00	-0.06	0.12	0.18	0.00	0.00	0.00	0.00	0.06	0.06	0.18
101.7	0.18	0.06	-0.06	0.24	0.18	0.00	0.12	0.06	0.00	0.06	0.06	0.18
68.6	0.06	0.06	-0.06	0.12	0.18	0.00	0.12	0.06	0.00	0.06	0.00	-0.06
34.8	0.00	-0.06	-0.06	0.06	0.06	0.00	-0.06	-0.06	0.00	0.00	-0.06	0.00
0.0	-0.06	-0.06	-0.06	0.00	0.06	0.00	-0.12	-0.06	0.00	-0.06	-0.06	0.00
0.0	-0.06	-0.06	-0.06	-0.06	0.06	-0.06	-0.18	-0.12	-0.00	-0.12	-0.06	-0.06
34.3	-0.06	-0.06	-0.06	-0.00	0.06	-0.06	-0.12	-0.12	-0.00	-0.00	-0.06	-0.06
67.7	-0.00	-0.06	-0.06	0.06	0.06	-0.06	-0.06	-0.12	-0.00	-0.00	-0.06	-0.06
101.8	0.18	0.06	-0.06	0.30	0.18	-0.06	0.12	-0.00	-0.00	0.06	-0.06	-0.00
119.4	0.54	0.30	-0.06	0.72	0.54	-0.00	0.42	0.30	-0.00	0.36	0.12	-0.00
136.5	1.80	1.26	-0.06	1.98	1.50	-0.00	1.62	1.20	-0.00	1.20	0.42	-0.00
140.8	4.92	3.90	-0.06	5.16	4.62	0.06	4.62	3.72	-0.00	3.54	1.14	-0.00
100.1	4.74	3.72	-0.06	4.98	4.44	-0.00	4.44	3.60	-0.00	3.36	1.08	-0.00
51.5	3.42	2.34	-0.06	3.60	2.94	-0.00	3.12	2.28	-0.00	2.46	0.54	-0.06
0.0	1.02	0.54	-0.06	1.02	0.66	-0.00	0.72	0.36	-0.00	0.72	0.18	-0.06
75.8	2.22	1.20	-0.06	2.34	1.62	0.06	1.86	1.08	-0.00	1.44	0.24	-0.00
141.3	7.68	6.12	-0.06	7.92	7.38	0.06	7.14	5.88	-0.00	5.34	1.56	-0.00
99.4	-	-	-	-	-	-	-	-	-	-	-	-
49.8	-	-	-	-	-	-	-	-	-	-	-	-
0.0	2.28	1.56	-0.06	2.28	1.68	-0.06	1.86	1.08	-0.06	1.80	0.24	-0.00

1 kip = 4.45 kN
1 in. = 25.4 mm

Table C-7

WYNCOOP CREEK GRILLAGE NO. X2-SE, REDUCED HUB DATA

Load (kips)	Change in Elevation (in.) for Hub Number											
	1	2	3	4	5	6	7	8	9	10	11	12
0.0	0.00	0.00	0.00	0.00	0.00	0.00	0.00	0.00	0.00	0.00	0.00	0.00
4.0	0.00	0.00	0.00	0.00	0.00	0.00	0.00	0.00	0.00	0.00	0.06	0.00
8.0	0.00	0.00	0.00	0.00	0.00	0.00	0.00	0.00	0.00	0.00	0.06	0.00
12.1	0.00	0.00	0.00	0.00	0.00	0.00	0.00	0.00	0.00	0.00	0.06	0.00
7.9	0.00	0.00	0.00	0.00	0.00	0.00	0.00	0.00	-0.06	0.00	0.00	0.00
4.2	-0.06	0.00	0.00	0.00	0.00	0.00	-0.06	0.00	-0.12	0.00	0.00	0.00
0.6	-0.06	0.00	0.00	0.00	0.00	-0.06	-0.06	0.00	-0.12	-0.06	-0.06	0.00
6.4	-0.06	0.00	0.00	0.00	0.00	-0.06	-0.06	0.00	-0.12	-0.06	0.00	0.00
12.4	-0.06	0.00	0.00	0.00	0.00	-0.06	-0.06	0.00	-0.12	-0.06	0.06	0.00
15.9	-0.06	0.06	0.06	0.00	0.00	-0.06	0.00	0.00	-0.12	-0.06	0.06	0.00
19.8	0.06	0.06	0.06	0.00	0.00	-0.06	0.00	0.00	-0.12	0.00	0.06	0.00
24.0	0.30	0.06	0.06	0.12	0.06	0.00	0.12	0.00	-0.12	0.06	0.06	0.00
16.2	0.30	0.06	0.06	0.12	0.06	0.00	0.06	0.00	-0.12	0.06	0.00	0.00
8.6	0.24	0.06	0.06	0.06	0.00	0.00	0.06	0.00	-0.12	0.00	0.00	0.00
0.9	0.00	0.00	0.06	-0.06	0.00	0.00	0.06	0.00	-0.18	0.00	0.00	0.00
0.0	-0.12	-0.00	0.06	-0.12	-0.06	-0.00	0.06	-0.00	-0.18	-0.00	-0.00	-0.06
7.7	-0.06	-0.00	0.06	-0.12	-0.06	-0.00	0.06	-0.00	-0.18	-0.00	-0.00	-0.06
16.1	-0.00	-0.00	0.06	-0.06	-0.06	-0.00	0.06	-0.00	-0.18	-0.00	-0.00	-0.06
24.3	0.30	0.06	0.06	0.06	-0.06	-0.00	0.12	-0.00	-0.18	0.12	-0.00	-0.06
28.2	0.66	0.06	0.06	0.30	0.12	-0.00	0.30	-0.00	-0.12	0.30	-0.00	-0.06
32.3	1.38	0.30	0.06	0.90	0.42	-0.00	0.78	0.06	-0.12	0.60	-0.00	-0.06
36.1	2.76	0.66	0.06	1.98	1.02	-0.00	1.80	0.30	-0.12	1.08	0.12	-0.06
40.3	4.86	1.38	0.18	3.90	2.28	-0.00	3.48	0.84	-0.12	2.58	0.24	-0.00
24.4	4.86	1.32	0.06	3.90	2.22	-0.00	3.30	0.72	-0.18	2.52	0.12	-0.06
11.9	3.90	0.72	0.06	3.00	1.38	-0.00	2.70	0.36	-0.18	1.80	0.12	-0.06
0.0	1.02	0.30	0.06	0.54	0.30	-0.06	0.72	0.06	-0.18	0.78	0.06	-0.06
20.1	2.28	0.36	0.06	1.44	0.42	-0.06	1.20	0.12	-0.18	1.08	0.06	-0.06
40.3	7.44	2.40	0.06	6.36	3.90	-0.00	5.64	1.50	-0.18	4.68	0.48	-0.06
28.0	-	-	-	-	-	-	-	-	-	-	-	-
14.7	-	-	-	-	-	-	-	-	-	-	-	-
0.0	1.80	0.42	0.06	1.14	0.60	-0.06	1.32	0.12	-0.18	1.50	-0.00	-0.11

1 kip = 4.45 kN
1 in. = 25.4 mm

Table C-8

WYNCOOP CREEK GRILLAGE NO. X2-SW, REDUCED HUB DATA

Load (kips)	Change in Elevation (in.) for Hub Number											
	1	2	3	4	5	6	7	8	9	10	11	12
0.0	0.00	0.00	0.00	0.00	0.00	0.00	0.00	0.00	0.00	0.00	0.00	0.00
3.7	0.00	0.00	0.00	0.00	0.00	0.00	0.00	0.00	0.00	0.00	0.00	0.00
8.0	0.06	0.06	0.00	0.00	0.00	0.00	0.00	0.00	0.00	0.00	0.00	0.00
11.8	0.12	0.06	0.00	0.00	0.00	0.00	0.00	0.00	0.00	0.00	0.00	0.00
8.2	0.06	0.00	0.00	0.00	0.00	-0.06	0.00	0.00	0.00	0.00	0.00	0.00
4.5	0.06	0.00	0.00	0.00	0.00	-0.06	0.00	0.00	0.00	0.00	0.00	0.00
0.0	0.04	0.00	0.00	-0.06	-0.06	-0.06	-0.06	-0.06	0.00	0.00	-0.06	0.00
7.0	0.00	0.06	0.00	-0.06	0.00	-0.06	0.00	0.00	0.00	0.00	-0.06	0.00
12.3	0.06	0.06	0.00	-0.06	0.00	-0.06	0.00	0.00	0.00	0.00	-0.06	0.00
16.1	0.06	0.06	0.00	0.06	0.00	-0.06	0.00	0.00	0.00	0.00	0.00	0.00
20.3	0.24	0.06	0.00	0.18	0.00	-0.06	0.12	0.06	0.00	0.06	0.00	0.00
23.8	0.48	0.12	0.00	0.66	0.12	-0.06	0.36	0.12	0.00	0.30	0.00	0.00
16.0	0.48	0.06	0.00	0.54	0.06	-0.06	0.36	0.12	0.00	0.24	0.00	-0.06
9.2	0.24	0.00	0.00	0.30	-0.06	-0.12	0.12	0.00	-0.06	0.18	-0.06	-0.12
0.7	-0.18	0.00	0.00	-0.36	-0.12	-0.12	-0.12	0.00	-0.06	0.06	-0.06	-0.12
8.0	-0.18	0.00	0.00	-0.30	-0.12	-0.12	-0.12	0.00	-0.06	0.12	0.00	-0.12
15.7	0.00	0.00	0.00	0.00	-0.12	-0.12	0.00	0.00	-0.06	0.18	0.00	-0.12
24.1	0.36	0.06	0.00	0.12	-0.06	-0.12	0.30	0.06	-0.06	0.36	0.00	-0.12
27.7	0.54	0.12	0.00	0.72	0.06	-0.12	0.48	0.12	-0.06	0.42	0.00	-0.12
31.7	1.08	0.30	0.00	1.32	0.30	-0.12	0.84	0.36	-0.06	0.78	0.00	-0.12
36.4	1.68	0.60	0.00	1.98	0.66	-0.12	1.32	0.72	-0.06	1.14	0.00	-0.12
40.1	2.28	0.84	0.00	2.76	0.96	-0.12	1.86	1.02	-0.06	1.44	0.00	-0.06
41.0	2.64	1.03	0.00	3.18	1.18	-0.12	2.15	1.30	-0.06	1.68	0.00	-0.05
44.4	3.42	0.84	0.00	4.02	1.62	-0.12	2.76	1.74	-0.06	2.10	0.06	0.00
48.7	3.90	1.68	0.00	4.68	1.98	-0.12	3.24	2.04	-0.06	2.34	0.18	0.00
29.5	3.78	1.62	0.00	3.54	1.86	-0.12	3.18	2.04	-0.06	2.34	0.12	0.00
0.0	0.42	0.30	-0.06	0.36	-0.06	-0.12	0.60	0.60	-0.06	1.08	0.00	-0.12
30.1	2.35	0.62	-0.06	3.00	0.66	-0.12	1.91	1.09	-0.06	2.03	0.00	-0.07
57.6	5.26	2.06	0.00	6.24	2.52	-0.12	4.56	3.06	-0.06	3.66	0.50	-0.06
0.0	1.02	0.46	-0.06	1.07	0.14	-0.12	1.19	1.08	-0.06	1.62	0.12	-0.06

1 kip = 4.45 kN
1 in. = 25.4 mm

Appendix D

FIELD TEST PHOTOGRAPHS

This appendix contains photographs from the field uplift tests. Descriptions of the photographs are given below.

Figure	Description
D-1	Overview Showing Stub, and Loading and Reaction Systems, at Grillage No. 84
D-2	Detail of Load Cell, Dywidag Bar, Hydraulic Jack, and Bearing and Angle Plates
D-3	Detail of Stub Connection and Reference Beam with Displacement Measuring System
D-4	Overview of Test Showing Extent of Visible Ground Cracking at Grillage No. 84
D-5	Excavated Grillage No. 84
D-6	Grillage No. 84 Detail Showing Condition of Galvanized Surfaces
D-7	Overview of Wyncoop Creek Test Set-Up
D-8	Wyncoop Creek Test Showing Ground Hubs and Testing System
D-9	Detail of Wyncoop Creek Grillage Showing Condition of Galvanized Surfaces
D-10	Excavation of Wyncoop Creek Grillage Showing Extremely Coarse Backfill

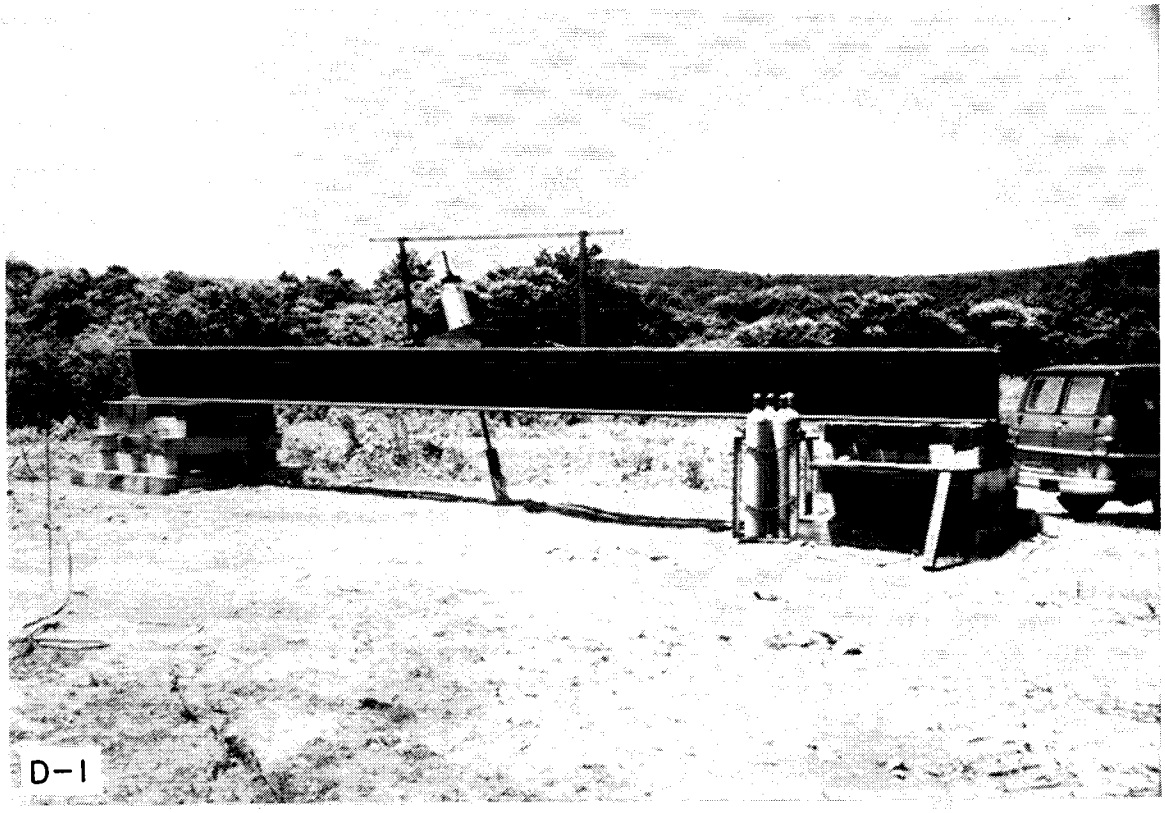

D-1

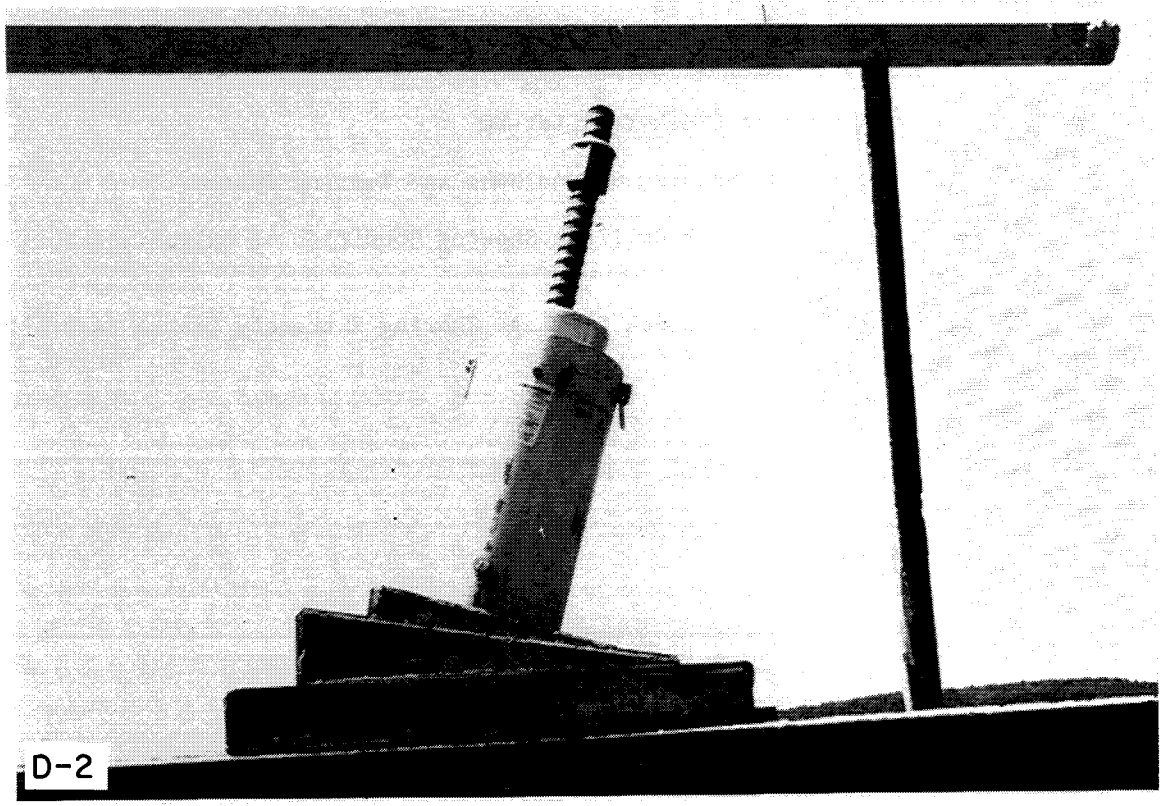

D-2

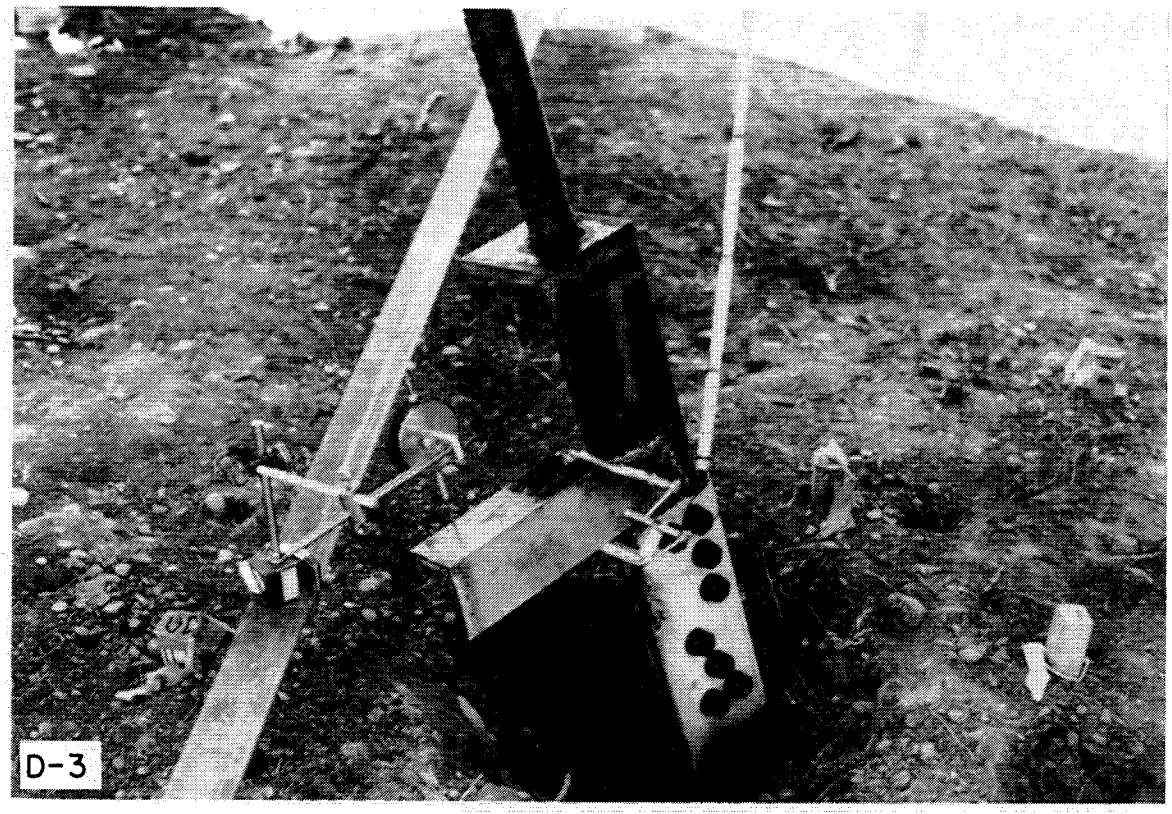
D-3

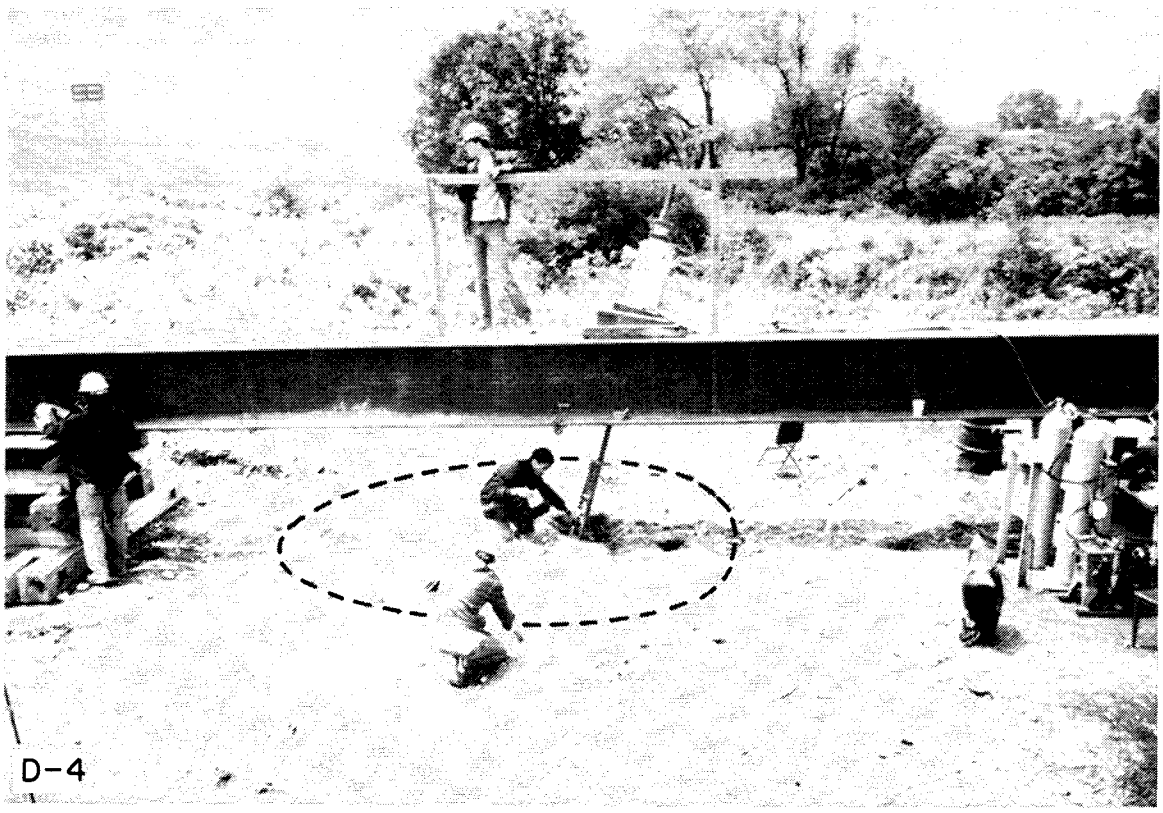
D-4

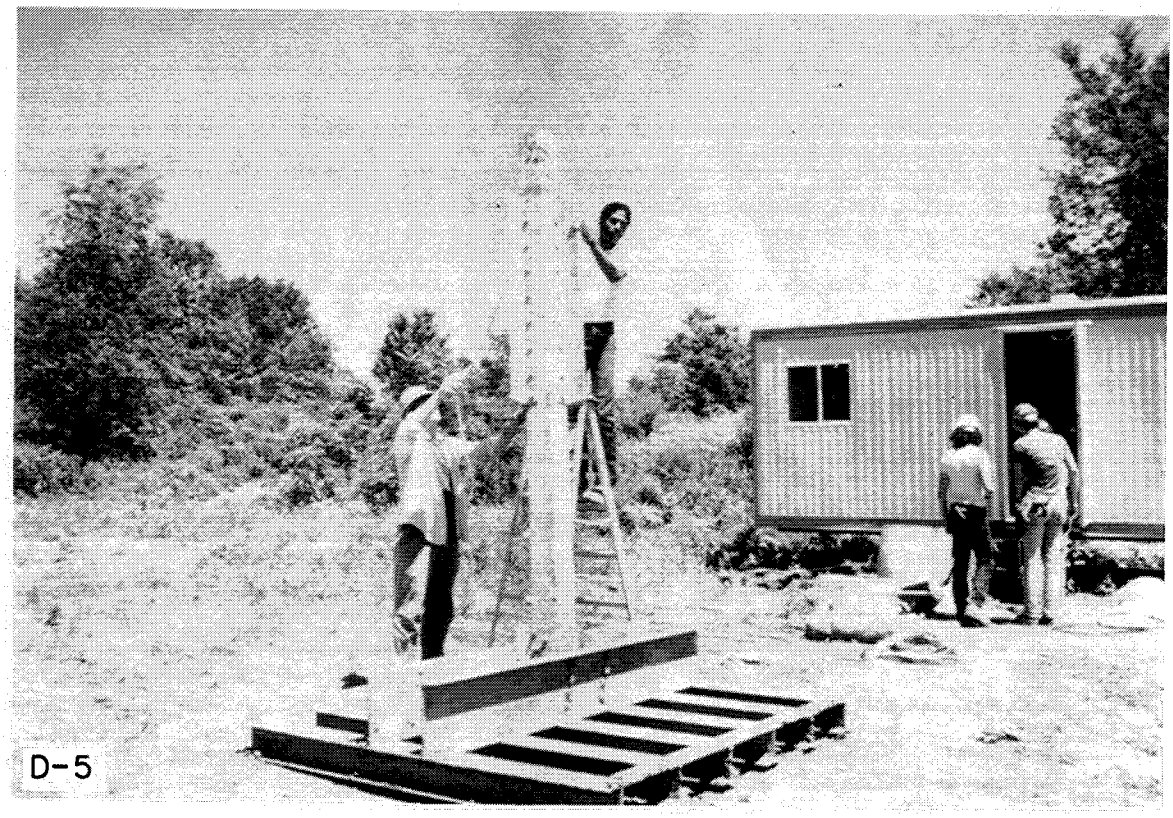

D-5

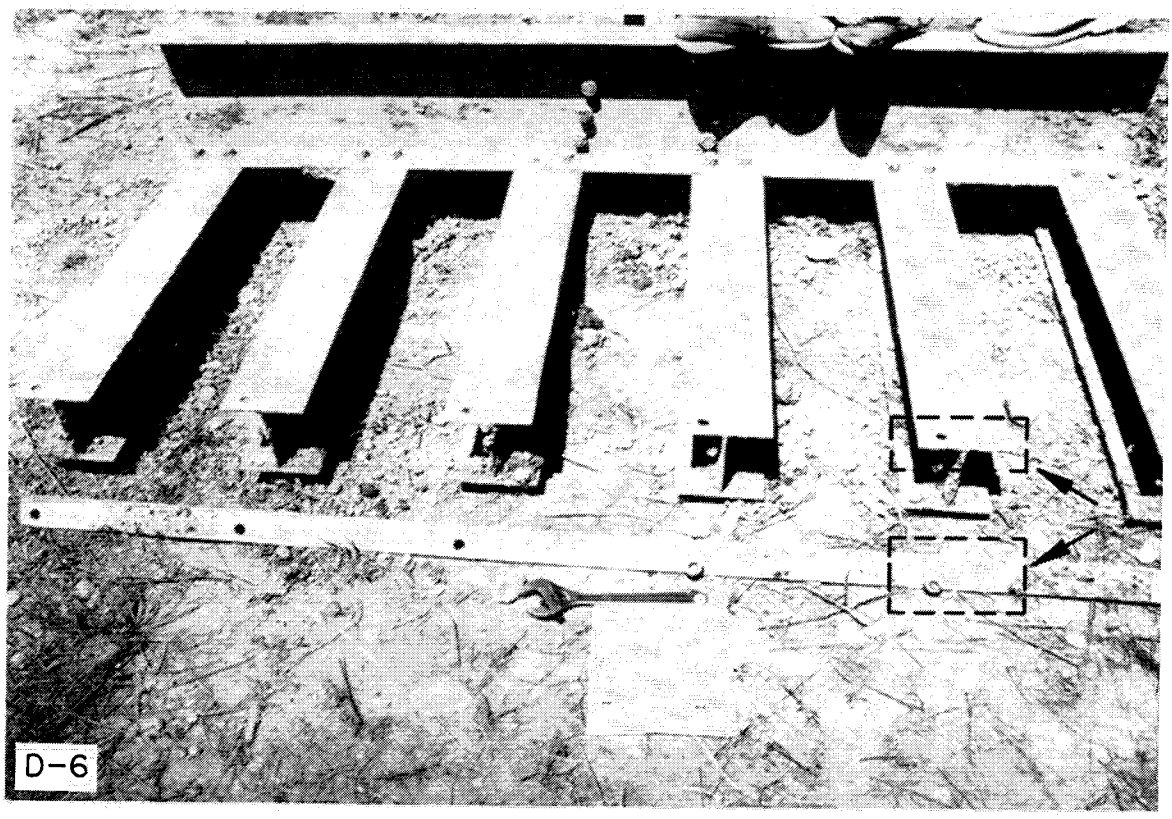

D-6

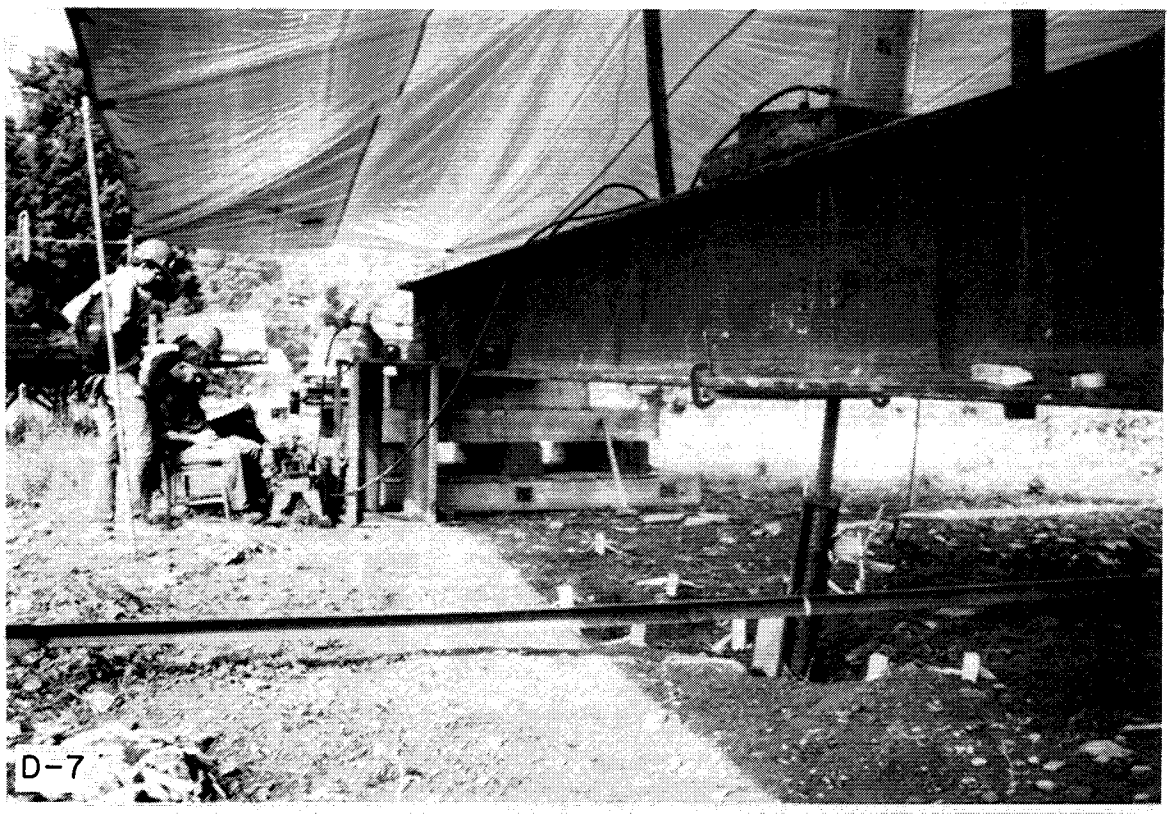

D-7

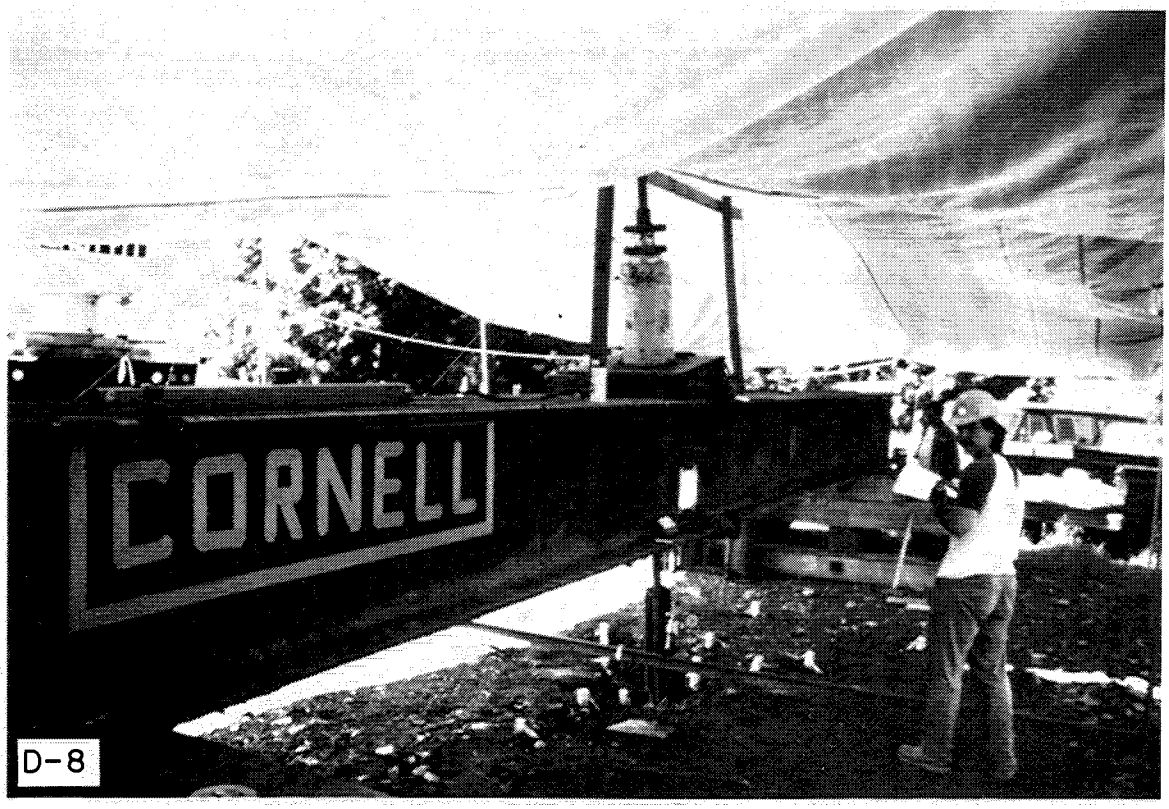

D-8


D-9

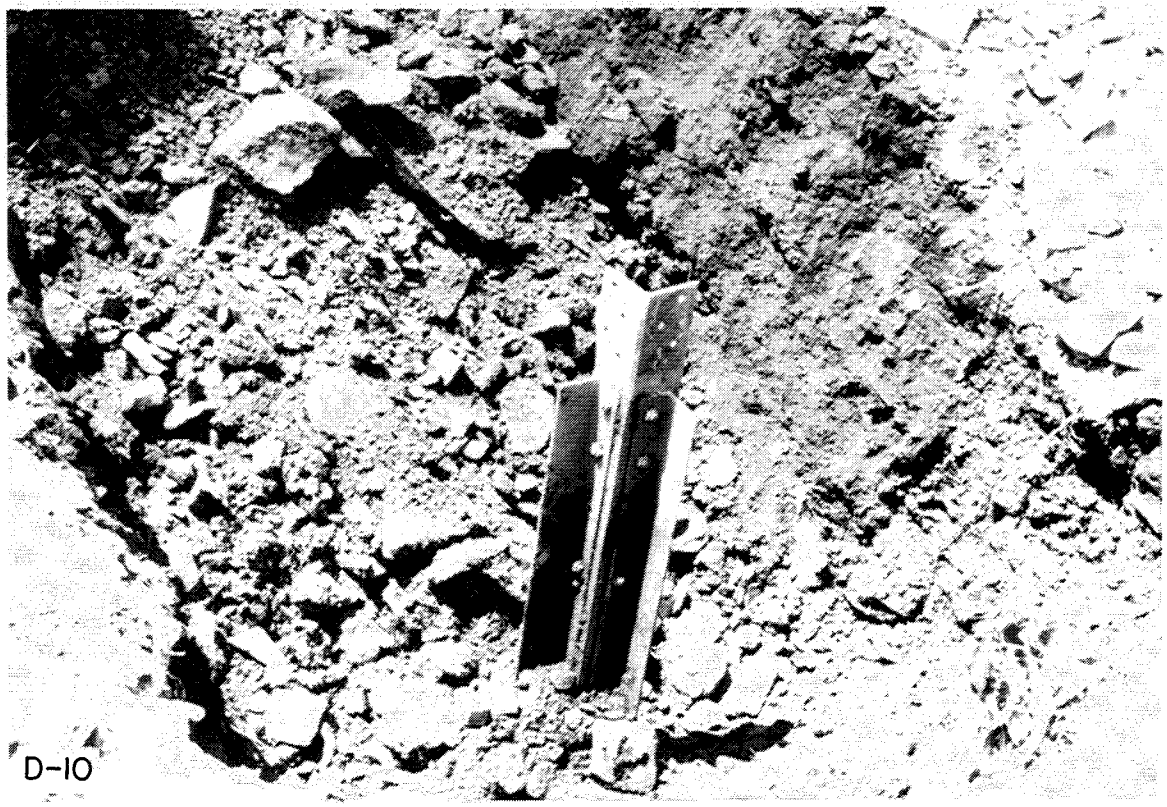
D-10

Appendix E

UNIT CONVERSIONS

Parameter	Measure	Conversions
length	foot (ft)	0.3048 meters (m)
	inch (in)	25.4 millimeters (mm)
mass	pound (lb)	0.4526 kilograms (kg)
force	ton (t)	2000 pounds (lb)
		2 kips (k)
		8.896 kiloNewtons (kN)
stress	atmosphere (atm)	1.058 tons/square foot (tsf)
		2.116 kips/square foot (ksf)
		1.033 kilograms/square centimeter (ksc)
		101.3 kiloNewtons/square meter (kN/m^2)
		101.3 kiloPascals (kPa)
		0.1013 MegaNewtons/square meter (MN/m^2)
		14.70 pounds/square inch (psi)
		1.013 bars
unit weight	pound/cubic foot (pcf) (actually pound-force)	0.157 kiloNewtons/cubic meter (kN/m^3)
density	pound/cubic foot (pcf) (actually pound-mass)	16.02 kilograms/cubic meter (kg/m^3)

Note: 1 atm $\approx$ 1 tsf $\approx$ 2 ksf $\approx$ 1 ksc $\approx$ 100 kN/m^2 $\approx$ 100 kPa $\approx$ 0.1 MN/m^2
$\approx$ 14.7 psi $\approx$ 1 bar
unit weight of water (γ_w) = 62.4 pcf = 9.80 kN/m^3

About EPRI

EPRI creates science and technology solutions for the global energy and energy services industry. U.S. electric utilities established the Electric Power Research Institute in 1973 as a nonprofit research consortium for the benefit of utility members, their customers, and society. Now known simply as EPRI, the company provides a wide range of innovative products and services to more than 1000 energy-related organizations in 40 countries. EPRI's multidisciplinary team of scientists and engineers draws on a worldwide network of technical and business expertise to help solve today's toughest energy and environmental problems.

EPRI. Electrify the World

Printed on recycled paper in the United States of America

EPRI • 3412 Hillview Avenue, Palo Alto, California 94304 • PO Box 10412, Palo Alto, California 94303 • USA
800.313.3774 • 650.855.2121 • askepri@epri.com • www.epri.com